

**Palaeoenvironmental changes in southern Patagonia  
during the Late-glacial and the Holocene: implications  
for forest establishment and climate reconstructions.**

**Claudia A. Mansilla**

**Submitted for the degree of Doctor of Philosophy**

Biological and Environmental Sciences

School of Natural Sciences

University of Stirling

**2015**

**STATEMENT OF ORIGINALITY**

I hereby confirm that the research contained in this thesis is original, has been completed by the author and all work contained herein has not been submitted for any other degree.

All published material has been duly acknowledged and cited.

.....

Claudia A. Mansilla

Date:

## ABSTRACT

Three continuous terrestrial high-resolution palaeoenvironmental records for the Late-glacial and the Holocene have been reconstructed for different ecosystems in Fuego-Patagonia on a longitudinal transect at latitude 53°S. The records describe the nature and extent of environmental and climatic changes inferred from palynological evidence supported by lithostratigraphy, tephrochronology and radiocarbon dating. The environmental changes recorded at the three sites displays a significant degree of synchrony in response to similar large-scale climatic changes. Clear stratigraphical evidence alongside the pollen record indicates a shift to warmer interstadial conditions between c. 14,800 Cal yr BP and 14,400 Cal yrs BP. During the period coeval with ACR the vegetation was dominated by cold resistant dry land herbs such as Poaceae, Asteraceae (Suf. Asteroideae) and *Acaena*, by c. 13,200 Cal yr BP the vegetation changed from the dominance of cold resistant dry land herbs towards more mesic conditions and the expansion of steppe dominated by Poaceae with patches of *Nothofagus* forest. The establishment of the forest and an eastward shift of the forest-steppe ecotone by c. 12,500 Cal yr BP from which a gradual shift from colder to warmer conditions and the relatively stronger influences of the SSWs is inferred. The sequence of Late-glacial environmental changes places Fuego-Patagonia within the new palaeoecological data provided by this study includes “the earliest” evidence for the establishment of subantarctic *Nothofagus* forest during the LGIT in Fuego-Patagonia. During the Early-Holocene two major phases of *Nothofagus* forest expansion were registered between c. 11,700 - 10,500 Cal yr BP and c. 9,500 - 8,200 Cal yr BP. These intervals of expansion of *Nothofagus* forest are separated by an interval of forest contraction in response to lower effective moisture between c. 10,500 - 9,500 Cal yr BP. An intense arid phase is inferred between c. 8,250 Cal yr BP and 6,800 Cal yr BP and probably leading to an increase in the amount of dry fuel available during the mid-Holocene in Fuego-Patagonia leading to the highest fire activity promoted by very weak SSWs at this time. The later Holocene was characterised by an increase in humidity and an inferred intensification of the SSWs.

## GLOSSARY OF TERMS

### Spanish Geographical Names

Canal: Channel

Cabo: Cape

Cordillera: Mountain range

Bahía: Bay

Estancia: Farm or Ranch

Estrecho: Strait

Hambre: Hunger

Isla: Island

Lago: Lake

Punta: Point

Puerto: Port

Región: Region

Río: River

Seno: Sound

Volcán: Volcano

### Abbreviations

ACC: Antarctic circumpolar current

ACR: Antarctic cold reversal

AMS: Accelerator Mass Spectrometry

asl: Above sea level

AVZ: Austral Volcanic Zone

Cal yr BP: Calibrated years before present

(relative to AD 1950)

LIGT: Last Glacial/Interglacial Transition

LGM: Last Glacial Maximum

LPAZ: Local pollen assemblage zone

NPI: North Patagonian Icefield

SPI: South Patagonian Icefield

SSA: Southern South America

SSTs: Sea surface temperatures

SWWs: Southern westerly winds

SVZ: Southern Volcanic zone

TLP: Total Land pollen

YD: Younger Dryas

$\delta^{13}\text{C}_{\text{VPDB}}$  (‰): value for  $^{13}\text{C}$ :  $^{12}\text{C}$  ratio relative to VPDB (for “Vienna PDB”), reported in parts per thousand.

## **ACKNOWLEDGMENTS**

First and foremost my thanks, respect and gratitude go to my supervisor Dr. Robert McCulloch whose help was always on hand, and made the PhD a thoroughly enjoyable experience. I extend my thanks also to Dr. Mary McCulloch who has continually pushed me in the right direction.

The thesis was funded by CONICYT Becas-Chile Scholarship (Gobierno de Chile) and the Quaternary Research Association research fund provided support for fieldwork. The Scottish Alliance for Geoscience, Environment and Society (SAGES) and the Tephra Analytical Unit, School of GeoSciences, The University of Edinburgh provided support for the Electron Microprobe analyses of tephra samples.

I am grateful to Professor Gordon Cook, Scottish Universities Environmental Research Centre and to Dr. Pauline Gulliver, Natural Environmental Research Council Radiocarbon Laboratory, East Kilbride (NERC-RCL: Allocation No.: 1696.0413) for supporting the radiocarbon measurements.

I would like to thank Flavia Morello, Centro de Estudios del Hombre Austral, Instituto de la Patagonia, Universidad de Magallanes, Punta Arenas, for providing support in the field and for ensuring safe transfer of the core samples to Scotland.

I am grateful to the Armada de Chile for logistical support for field work on Isla Dawson. Particular thanks go to the station staff at Puerto Harris, Isla Dawson, and the captains and crews of the LEP-1601 'Ona' and the PSH-77 'Cabrales. I am also grateful to Jim Blakie, Emma Lees and Jonathan Kitchen who assisted with fieldwork on Tierra del Fuego and Isla Dawson.

## TABLE OF CONTENTS

STATEMENT OF ORIGINALITY .....	ii
ABSTRACT .....	iii
GLOSSARY OF TERMS .....	iv
ACKNOWLEDGMENTS .....	v
TABLE OF CONTENTS .....	vi
LIST OF FIGURES .....	x
LIST OF TABLES .....	xvi
<b>CHAPTER 1: Introduction .....</b>	<b>1</b>
1.1 Framework .....	1
1.2 The scope of the research project .....	2
1.3 Objectives .....	3
1.4 Outline .....	4
1.5 Background .....	6
1.5.1 Setting and topography of Patagonia .....	6
1.5.2 Past climatic changes: focus on Fuego-Patagonia (~53°–55°S) .....	11
1.5.3 Glacial records .....	17
1.5.4 Vegetation communities in Fuego-Patagonia .....	18
1.5.5 Past vegetation in Fuego-Patagonia .....	26
1.5.6 Human occupation versus vegetation in central-north of Tierra del Fuego Island ....	28
1.5.7 Past fire activity .....	29
1.6 Summary .....	32
<b>CHAPTER 2: Methodology .....</b>	<b>33</b>
2.1 Study sites .....	33
2.1.1 Rio Grande, Isla Dawson (53°39'37"S, 70°30'27"W, altitude 79m asl.) .....	34
2.1.2 Punta Yartou, Tierra del Fuego (53°51'41"S, 70°08'20"W, altitude 51m asl.) .....	37
2.1.3 Lago Lynch, Tierra del Fuego (53°54'20"S, 69°26'19"W, altitude 165m asl.) .....	40
2.2 Stratigraphy and Loss on ignition (LOI) .....	41
2.3 Tephrochronology .....	42
2.3.1 Visual tephra recognition .....	43
2.3.2 Isolation and preparation of tephra for geochemical analysis .....	43

2.3.3 Geochemical analysis.....	44
2.4 Chronology.....	45
2.4.1 Sediment accumulation rate.....	46
2.4.2 Radiocarbon samples.....	46
2.4.3 BACON: Bayesian age-depth modelling.....	47
2.5 Pollen methodology.....	47
2.5.1 Subsampling.....	47
2.5.2 Pollen preparation.....	48
2.5.3 Taxonomical and morphological fossil pollen classification.....	49
2.6 Pollen stratigraphy.....	54
2.7 Pollen and spore concentrations.....	54
2.8 Pollen preservation.....	55
2.9 Charcoal concentrations.....	58
<b>CHAPTER 3: Results</b> .....	<b>60</b>
3.1 Stratigraphy.....	60
3.1.1 Rio Grande.....	60
3.1.2 Punta Yartou.....	61
3.1.3 Lago Lynch.....	65
3.2 Tephrochronology.....	67
3.2.1 Visual tephra layers.....	67
3.2.2 Cryptotephra layers.....	70
3.3 Chronology.....	77
3.3.1 Rio Grande.....	77
3.3.2 Punta Yartou.....	80
3.3.3 Lago Lynch.....	85
3.4 Pollen stratigraphy.....	87
3.4.1 Rio Grande.....	87
3.4.2 Punta Yartou.....	94
3.4.3 Lago Lynch.....	99
3.5 Pollen concentrations (grains per cm <sup>3</sup> ).....	104
3.5.1 Rio Grande.....	104
3.5.2 Punta Yartou.....	105
3.5.3 Lago Lynch.....	106

3.6 Pollen preservation.....	110
3.6.1 Rio Grande.....	110
3.6.2 Punta Yartou.....	111
3.6.3 Lago Lynch.....	112
3.7 Charcoal concentration.....	114
3.7.1 Rio Grande.....	115
3.7.2 Punta Yartou.....	116
3.7.3 Lago Lynch.....	117
<b>CHAPTER 4: Discussion .....</b>	<b>120</b>
4.1 Rio Grande.....	120
4.1.1 Late-glacial period.....	120
4.1.2 Early-Holocene period.....	124
4.1.3 Mid-Holocene period.....	125
4.1.4 Late-Holocene period.....	127
4.2 Punta Yartou.....	130
4.2.1 Late-glacial period.....	130
4.2.2 Early-Holocene period.....	132
4.2.3 Mid-Holocene period.....	134
4.2.4 Late-Holocene period.....	135
4.3 Lago Lynch.....	137
4.3.1 Late-glacial period.....	137
4.3.2 Early-Holocene period.....	139
4.3.3 Mid-Holocene period.....	141
4.3.4 Late-Holocene period.....	143
<b>CHAPTER 5: Palaeoenvironmental synthesis .....</b>	<b>145</b>
5.1 Palaeoenvironmental reconstruction of Fuego-Patagonia (~53°S) during Last Glacial/Interglacial Transition and Holocene.....	146
5.1.1 Late-glacial period.....	146
5.1.2 Early-Holocene period.....	150
5.1.3 Mid Holocene period.....	153
5.1.4 Late-Holocene period.....	155
5.2 Early establishment of <i>Nothofagus</i> forest at ~53°S.....	157

5.3 Migration of <i>Nothofagus</i> forest, human occupation and past fire activity .....	160
<b>CHAPTER 6: Conclusion.....</b>	<b>165</b>
<b>References .....</b>	<b>171</b>
<b>Appendix .....</b>	<b>183</b>

## LIST OF FIGURES

- Figure 1.1** The location of Fuego-Patagonia (~53° - Figure 1.1 The location of Fuego-Patagonia (~53° – 55°S, dashed rectangle), within the southern hemisphere (adapted from Bentley *et al.*, 2009) ..... 5
- Figure 1.2** The extent of the Last Glacial Maximum (LGM) in Patagonia and the present major ice fields in relation to the present climate (adapted from McCulloch *et al.*, 2000) ..... 8
- Figure 1.3** The location of Southern and Austral Volcanic zones; including the principal source volcanoes for tephra layers found in Fuego-Patagonia: Volcán Hudson (~46°S), Volcán Aguilera (~50°S), Volcán Reclús (~51°S) and Mt Burney (~52°S) ..... 9
- Figure 1.4** Fuego-Patagonia and Late-glacial ice limits in the Estrecho de Magallanes, the present ice fields in the Cordillera Darwin (adapted from McCulloch *et al.*, 2005a) and the vegetation zones of Fuego-Patagonia (adapted from Huber *et al.*, 2004) ..... 10
- Figure 1.5** Summary of Late-glacial palaeoenvironmental records from Fuego-Patagonia and Antarctica a) Glacier advances stages “C” to “E” in the Estrecho de Magallanes (McCulloch *et al.*, 2005a); b) Glacier advances in Seno Skyring (Kilian *et al.*, 2007); c) Alkenone-derived SST record from ~53°S (Caniupán *et al.*, 2011) and d) Deuterium-derived SST from Antarctic continent (Lemieux-Dudon *et al.*, 2010). The blue vertical shading indicates the ACR period and the brown shading the YD period (adapted from Killian and Lamy, 2012)..... 15
- Figure 1.6** a) Correlation model between annual mean 850-hPa zonal wind and precipitation [r(U850, P)], the scale-bar at the bottom is the correlation coefficients; b) Longitudinal profile of terrain elevation (shaded area, scale at left), long-term-mean annual precipitation (black line, scale at left in mm/yr), and the r(U850, P) correlation, averaged between 42°S and 52°S (from Garreaud *et al.*, 2013) ..... 16
- Figure 1.7** The vegetation zones of Fuego-Patagonia (adapted from Huber *et al.*, 2004) and locations named in this study ..... 20
- Figure 1.8** Magellanic moorland; cushion bog plants of *Astelia pumila* and *Donatia fascicularis* and bryophytes such as *Dicronaloma* spp. (©C.A. Mansilla)..... 21
- Figure 1.9** “Evergreen mixed” *Nothofagus* forest dominated by *Nothofagus betuloides* with the presence of *Drimys winteri* (©C.A. Mansilla) ..... 23
- Figure 1.10** Magellanic deciduous forest dominated almost exclusively by the cold-deciduous *Nothofagus pumilio* tree and frequent small green clusters of *Misodendrum* spp. (©C.A. Mansilla)..... 23

<b>Figure 1.11</b> The Fuego-Patagonian steppe landscape (©C.A. Mansilla) .....	<b>24</b>
<b>Figure 1.12</b> Andean vegetation and the timberline of <i>Nothofagus pumilio</i> (©C.A. Mansilla) ..	<b>25</b>
<b>Figure 1.13</b> Terrestrial hunter-gatherer family of Tierra del Fuego (photograph taken by Gusinde 1918) (From Gusinde, 1937) .....	<b>31</b>
<b>Figure 2.1</b> Location of the Rio Grande sample site, Isla Dawson .....	<b>35</b>
<b>Figure 2.2</b> The Rio Grande peat bog within a kettle hole, Isla Dawson (©C.A. Mansilla) .....	<b>36</b>
<b>Figure 2.3</b> The vegetation community dominated by <i>Empetrum rubrum</i> (Ericaceae) and <i>Sphagnum magellanicum</i> moss vegetation in the central part of the peat bog at Rio Grande (©C.A. Mansilla) .....	<b>36</b>
<b>Figure 2.4</b> Location of the Punta Yartou sample site, Tierra del Fuego .....	<b>38</b>
<b>Figure 2.5</b> Close peat-bog where the Punta Yartou core was sampled, Tierra del Fuego (©R.McCulloch) .....	<b>39</b>
<b>Figure 2.6</b> The present vegetation community on the peat bog at Punta Yartou site .....	<b>39</b>
<b>Figure 2.7</b> The location of the Lago Lynch site, Tierra del Fuego (©J. Kitchen).....	<b>41</b>
<b>Figure 2.8</b> An example of a sediment cores were obtained using a Russian D-section corer, this section of the core clearly shows the Vn Reclús tephra layer in the field.....	<b>42</b>
<b>Figure 2.9</b> Four tephra samples mounted on a glass slide prepared for electron microprobe analysis.....	<b>44</b>
<b>Figure 2.10</b> <i>Nothofagus dombeyi</i> “type” and <i>Nothofagus oblique</i> “type” pollen grain (Heusser, 1971) .....	<b>51</b>
<b>Figure 2.11</b> Fresh water algae <i>Pediastrum</i> . a) <i>Pediastrum kawraiskyi</i> (From Waldmann <i>et al.</i> , 2014); b) <i>Pediastrum boryanum</i> (@ C.A.Mansilla).....	<b>53</b>
<b>Figure 2.12</b> The five categories of pollen grain preservation; normal or well preserved, broken, crumpled, corroded and degraded.....	<b>57</b>
<b>Figure 3.1</b> Organic content (Loss on Ignition: LOI <sub>550</sub> %) and tephra layers for the Rio Grande core. Three visible tephra layers found in the core: Mt Burney 2 (B2), Vn Hudson 1 (H1) and	

Vn Reclús 1 (R1) eruptions. The column on the right shows the Local Pollen Assemblage Zones (LPAZs) and the respective subzones ..... 62

**Figure 3.2** *Nothofagus betuloides* leaves: a) an example of the leaves found between 540 cm and 539 cm depth and, between 484 cm and 483 cm depth in Rio Grande sequence, b) a *Nothofagus betuloides* leaf taken from the current forest near the site ..... 63

**Figure 3.3** Organic content (LOI<sub>550</sub>%) and tephra layers for the Punta Yartou core. Six tephra layers found in the cores. Three visible tephra layers: Mt Burney 2 (B2), Vn Hudson 1 (H1) and Vn Reclús 1 (R1) eruptions. Three microtephra layers: Vn Hudson (Hb?), Mt Burney 1 (B1) and Vn Hudson (Ha) eruption, ?= no geochemical analysis. The column on the right shows the Local Pollen Assemblage Zones (LPAZs) and the respective subzones..... 64

**Figure 3.4** Organic content (LOI<sub>550</sub>%) and tephra layers for the Lago Lynch core. Six tephra layers found in the core. Three visible tephra layers: Mt Burney 2 (B2), Vn Hudson 1 (H1) and Vn Reclús 1 (R1) eruptions. Three microtephra layers: Vn Hudson (Hb), Mt Burney 1 (B1) and Vn Hudson (Ha?) eruption, ?= no geochemical analysis. The column on the right shows the Local Pollen Assemblage Zones (LPAZs) and the respective subzones..... 66

**Figure 3.5** Ternary plot of percentage totals of CaO, FeO and K<sub>2</sub>O of individual glass shards for the four volcanic sources identified in Fuego Patagonia (Kilian *et al.*, 2003; Stern, 2008; Heberzetti *et al.*, 2009; Borrromei *et al.*, 2010); the Vn Hudson (~46°S) within the Andean Southern Volcanic Zone (SVZ; 33–46°S): and Mt Burney (~52°S), Vn Reclús (~51°S) and Vn Aguilera (50°S), from the Andean Austral Volcanic Zone (AVZ; 49-55°S)..... 72

**Figure 3.6** Visible tephra layers in chronological order, the thickness and depths are those measured in Punta Yartou core. Tephra layers are: a) Mt Burney 2, b) Vn Hudson 1 and, c) Vn Reclús 1, respectively. The arrows indicate the lower and upper limits of the tephra layers, the blue arrow indicates the depth considered for dating the ash deposition ..... 73

**Figure 3.7** A example of glass shards of 3 visible and 3 cryptotephra layers found in the cores. Visible tephra layers: a) Mt Burney 2 (B2), b) Vn Hudson 1 (H1) and, c) Vn Reclús 1 (R1) eruptions. Cryptotephra layers: d) Vn Hudson “b”, e) Mt Burney 1 (B1) and f) Vn Hudson “a” ..... 75

**Figure 3.8** Ternary plot of percentage totals of CaO, FeO and K<sub>2</sub>O of individual glass shards for the three visible tephra layers found in this study. The diagram shows three distinct groups: Mt Burney (B2) (red circle), Vn Hudson 1 (H1) (green triangle) and Vn Reclús (R1) (blue square) ..... 76

**Figure 3.9** Ternary plot of percentage totals of CaO, FeO and K<sub>2</sub>O of individual glass shard from three Hudson volcano eruptions in this study: Vn Hudson “b” (red circle), Vn Hudson 1 (green triangle) and Vn Hudson “a” (blue square)..... 76

<b>Figure 3.10</b> Ternary plot of percentage totals of CaO, FeO and K <sub>2</sub> O of individual glass shards for two Mt Burney volcanic eruptions found in this study. Mt Burney 2 (red circle), Mt Burney 1 found in Punta Yartou core (green triangle) and Mt Burney 1 (blue square) .....	<b>77</b>
<b>Figure 3.11</b> Accumulation rate, stratigraphy, organic content (LOI <sub>550</sub> %) and, chronology for the Rio Grande core. The age-depth model was constructed using the Bayesian modelling program ‘BACON’ (Blaauw and Christen, 2011). Different colors denote the stratigraphy of Rio Grande core; Grey: bluish clays and silts, Blue: black organic-rich lake sediment, Light blue: laminated lacustrine-mud sediment and yellow: peat. Arrows show: Mt Burney (B2), Vn Hudson (H1) and Vn Reclús (R1).....	<b>80</b>
<b>Figure 3.12</b> Accumulation rate, stratigraphy, organic content (LOI <sub>550</sub> %) and, chronology for the Punta Yartou core. The age-depth model was constructed using the Bayesian modelling program ‘BACON’ (Blaauw and Christen, 2011). Different colors denote the stratigraphy of Rio Grande core; Light blue: laminated lacustrine-mud sediment and Yellow: peat. Arrows show: Mt Burney (B2), Vn Hudson (H1) and Vn Reclús (R1).....	<b>84</b>
<b>Figure 3.13</b> Accumulation rate, stratigraphy, organic content (LOI <sub>550</sub> %) and, chronology for the Lago Lynch core. The age-depth model was constructed using the Bayesian modelling program ‘BACON’ (Blaauw and Christen, 2011). Different colors denote the stratigraphy of Lago Lynch core; Grey: bluish clays and silts, Light blue: laminated lacustrine-mud sediment and Yellow: peat. Arrows show: Mt Burney (B2), Vn Hudson (H1), Mt Burney (B1) and Vn Reclús (R1)..	<b>86</b>
<b>Figure 3.14</b> Rio Grande percentage pollen diagram and charcoal concentration .....	(inside pocket on back cover)
<b>Figure 3.15</b> Summary of percentage pollen diagram for Rio Grande .....	<b>93</b>
<b>Figure 3.16</b> Punta Yartou percentage pollen diagram and charcoal concentration .....	(inside pocket on back cover)
<b>Figure 3.17</b> Summary of percentage pollen diagram for Punta Yartou .....	<b>98</b>
<b>Figure 3.18</b> Lago Lynch percentage pollen diagram and charcoal concentration .....	(inside pocket on back cover)
<b>Figure 3.19</b> Summary of percentage pollen diagram for Lago Lynch .....	<b>103</b>
<b>Figure 3.20</b> Pollen concentrations for Rio Grande.....	<b>107</b>
<b>Figure 3.21</b> Pollen concentrations for Punta Yartou .....	<b>108</b>
<b>Figure 3.22</b> Pollen concentrations for Lago Lynch.....	<b>109</b>

<b>Figure 3.23</b> Pollen preservation for Rio Grande .....	<b>111</b>
<b>Figure 3.24</b> Pollen preservation for Punta Yartou.....	<b>113</b>
<b>Figure 3.25</b> Pollen preservation for Lago Lynch .....	<b>114</b>
<b>Figure 3.26</b> Charcoal concentrations for the Rio Grande, a) micro charcoal, b) macro charcoal and c) total charcoal concentration .....	<b>116</b>
<b>Figure 3.27</b> Charcoal concentrations for the Punta Yartou, a) micro charcoal, b) macro charcoal and c) total charcoal concentration .....	<b>117</b>
<b>Figure 3.28</b> Charcoal concentrations for the Lago Lynch, a) micro charcoal, b) macro charcoal and c) total charcoal concentration .....	<b>118</b>
<b>Figure 4.1</b> Summary of Rio Grande core. a) deuterium record as temperature proxy from ice core (Dome C) (Lemieux-Dudon <i>et al.</i> , 2010); b) organic content; c) accumulation rate; d) percentage <i>Nothofagus</i> ; e) percentage <i>Misodendrum</i> ; f) percentage <i>Drimys</i> ; g) percentage normal pollen preservation; h) charcoal concentrations. Orange shading indicates intervals of warmer and lower effective moisture, light blue shading indicates interval of colder and lower effective moisture, dark blue shading indicates interval of colder and wetter climatic conditions .....	<b>129</b>
<b>Figure 4.2</b> Summary of Punta Yartou core. a) deuterium record as temperature proxy from ice core (Dome C) (Lemieux-Dudon <i>et al.</i> , 2010); b) organic content; c) accumulation rate; d) percentage <i>Nothofagus</i> ; e) percentage <i>Misodendrum</i> ; f) percentage <i>Drimys</i> ; g) percentage normal pollen preservation; h) charcoal concentrations. Orange coloured shading indicates intervals of warmer / lower effective moisture, light blue shading indicates interval of colder / lower, dark blue shading indicates interval of colder / higher effective moisture .....	<b>136</b>
<b>Figure 4.3</b> Summary of Lago Lynch core. a) deuterium record as temperature proxy from ice core (Dome C) (Lemieux <i>et al.</i> , 2010); b) organic content; c) accumulation rate; d) percentage <i>Nothofagus</i> ; e) percentage <i>Misodendrum</i> ; f) percentage <i>Drimys</i> ; g) percentage normal pollen preservation; h) charcoal concentrations. Orange shading indicates intervals of warmer and lower effective moisture, light blue shading indicates interval of colder and lower effective moisture, dark blue shading indicates interval of colder and wetter climatic conditions.....	<b>144</b>
<b>Figure 5.1</b> <i>Nothofagus</i> pollen percentages from b) Rio Grande, c) Punta Yartou and d) Lago Lynch and a) the Antarctic Dome-C deuterium–temperature record (Lemieux <i>et al.</i> , 2010). Black triangle number one and number two show the first and the second phases of human occupation in Tierra del Fuego, respectively. Question mark symbols denotes the gap of evidence in human occupation in Tierra del Fuego. The blue arrows show the establishment of	

*Nothofagus* forest ( $\geq 20\%$ ) in each study sites. Yellow shading indicates intervals of warmer and lower effective moisture, light blue shading indicates interval of colder and lower effective moisture, dark blue shading indicates interval of colder and wetter climatic conditions..... **152**

**Figure 5.2** Potential distributions of *Nothofagus* during the LGM in southern South America. (from Premoli *et al.*, 2010)..... **158**

**Figure 5.3** Charcoal concentrations from a) Rio Grande, b) Punta Yartou and c) Lago Lynch sites. Black triangle number one and number two show the first and the second phases of human occupation in Tierra del Fuego, respectively. The blue arrows show the establishment of *Nothofagus* forest ( $\geq 20\%$ ) in each study sites. Yellow shading indicates intervals of warmer and lower effective moisture, light blue shading indicates interval of colder and lower effective moisture, dark blue shading indicates interval of colder and wetter climatic conditions..... **161**

## LIST OF TABLES

<b>Table 3.1</b> Details of the depths, uncalibrated $^{14}\text{C}$ yr BP maximum ages, calibrated Cal yr BP ages and interpolated ages from the age-depth model for visual and microscopic tephra layers identified at the study sites.....	<b>74</b>
<b>Table 3.2</b> Radiocarbon ages, calibrated age ranges and weighted mean age (WMA) from BACON Bayesian age model for the Rio Grande core.....	<b>79</b>
<b>Table 3.3</b> Radiocarbon ages, calibrated age ranges and weighted mean age (WMA) from BACON Bayesian age model for the Punta Yartou core.....	<b>82</b>
<b>Table 3.4</b> Radiocarbon ages, calibrated age ranges and weighted mean age (WMA) from BACON Bayesian age model for the Lago Lynch core.....	<b>85</b>

# Chapter 1:

# Introduction

## 1.1 Framework.

Southern South America (SSA) plays a key role for palaeoenvironmental and climatic reconstructions at the regional, hemispheric and global scale. SSA is the southernmost and largest landmass outside of the continent of Antarctica. It contains the largest ice-sheets outside the polar regions and also lies athwart the southern westerly winds (SWWs). The SWWs, a zone of storm tracks are a component of the global atmospheric system that have governed the palaeo and modern climate of SSA between  $\sim 30^{\circ}\text{S}$  and  $\sim 60^{\circ}\text{S}$  (Fletcher and Moreno, 2011). Southward migration of the SSWs are accompanied by a synchronous southward shift of the Antarctic Circumpolar Current (ACC) (Lamy *et al.*, 2002), influencing deep-water circulation in the Southern Ocean and recognised as a key factor in global atmospheric  $\text{CO}_2$  variations (Toggweiler *et al.*, 2006; Fletcher and Moreno, 2011) (Figure 1.1). Therefore, SSA represents a key place for understanding the changes in the latitudinal position and strength in the SWWs and to improve knowledge about the complex interactions between the terrestrial, marine and glacial environments of the global climate system.

The Andean cordillera runs longitudinally through SSA. The incidence of the SSWs on the mountains leads to orographic rainfall on the western flanks of the Andes and an enhanced rain shadow on the eastern lee-side. This produces one of the most dramatic west-east precipitation-vegetation gradients in the world from more than 6,000 mm/yr in the west to less than 300

mm/yr in the east (Schneider *et al.*, 2003; Garreaud *et al.*, 2013). The low elevation terrestrial ecotones from forest to steppe are one of the most sensitive ecosystems of the world and where the impact of global climate changes becomes most evident (Myser, 2012). Therefore, in Fuego-Patagonia, the changes in the distribution and abundance of the vegetation in low elevation forest/steppe ecotone (ecological responses) can be linked to large-scale controls by regional and global climate.

In Fuego-Patagonia, the low elevation forest-steppe ecotones are regions that were used by the first inhabitants of SSA. The maritime and terrestrial hunter-gatherer populations were the first inhabitants after the end of the last glaciation and persisted until the beginning of the twentieth century (Gusinde, 1937). The first inhabitants of Fuego-Patagonia were nomads with a low population density and without agricultural development (Mansur and Pique, 2009). These features increase the importance of Fuego-Patagonia as a key place to reconstruct terrestrial palaeoenvironments under low human impacts and to infer climatic conditions during the Late-glacial and the Holocene.

## **1.2 The scope of the research project.**

Despite the key role of SSA in palaeoenvironmental and climatic reconstructions at regional, southern hemisphere and global scales, there are few continuous terrestrial palaeoenvironmental records that have described the responses of vegetation to climatic changes during the Last Glacial/Interglacial Transition (LGIT) (c. 18,000 - 11,500 Cal yr BP) in Fuego-Patagonia (~53°-55°S) (McCulloch and Davies, 2001; Fontana and Bennett, 2012; Markgraf and Huber, 2010; Moreno *et al.*, 2012). Therefore, the timing and extent of vegetation changes during LGIT are presently not well understood.

The high precipitation on the Andean cordillera nourishes the maritime glaciers, ice fields and

temperate rainforest vegetation along and across the Andes (McCulloch, 2010). In Fuego-Patagonia, *Nothofagus* forest (southern beech) has been the dominant vegetation type during the Quaternary and its distribution is highly linked to precipitation gradient. Such changes in precipitation are mainly produced by variations in the latitudinal position and/or intensity of the SWWs. Therefore, variations in the position and/or intensity of the SWWs should be reflected in the vegetation history of Fuego-Patagonia. An eastward shift of the forest-steppe ecotone should suggest an increase in precipitation and a westward shift of the forest-steppe ecotone would indicate a decrease in precipitation. Also, southward/northward migration of the SSWs is accompanied by a synchronous southward/northward shift of the ACC (Lamy *et al.*, 2002). The correlation of high-resolution terrestrial palaeoenvironmental records to deuterium-derived temperature records derived from Antarctic ice cores (Lemieux-Dudon *et al.*, 2010) will improve our understanding of whether climatic changes within the Antarctic domain provoked ecological responses in Fuego-Patagonia.

This study provides new evidence from three deep basin peat-sediment cores that have been sampled along a west-east transect at approximately  $\sim 53^{\circ}\text{S}$  in Fuego-Patagonia. These three cores provide the highest resolution (temporally) and longest/oldest cores of vegetation changes reconstructed from pollen analysis and supported by lithostratigraphy, tephrochronology and radiocarbon dating, during the LGIT and the Holocene from Fuego-Patagonia.

### **1.3 Objectives.**

The aim of this study is to explore the timing and extent of climate-vegetation linkages operating within the Fuego-Patagonia forest/steppe ecotone by identifying the natural variability of ecotone-ecosystems and their responses to large-scale controls of the regional climate in terms of the variations in the intensity of SWWs in Fuego-Patagonia at  $\sim 53^{\circ}\text{S}$ , during the LGIT and the Holocene.

Also, this study will constrain the timing of the migration of subantarctic *Nothofagus* forest during the LGIT in Fuego-Patagonia to provide empirical evidence to test the hypothesis of persistent multiple refugia of *Nothofagus* forest in Fuego-Patagonia during the Last Glacial Maximum (LGM) (Markgraf *et al.*, 1993; Premoli *et al.*, 2010). This study also reconstructs the past vegetation changes during LGIT and Holocene alongside variations in past fire activity to examine the large-scale climate controls during the occupation of Tierra del Fuego by prehistoric peoples.

#### **1.4 Outline.**

This study is organised in 6 chapters; Chapter 1 presents an overview of the importance and relevance of understanding the palaeoenvironmental studies in Fuego-Patagonia, the aims and objectives of this study and a review of the extant knowledge about the palaeoenvironmental and palaeoclimatic reconstruction of Fuego-Patagonia. Chapter 2 describes the methodology employed by this study, including the selection of the study sites, the techniques for the construction of high-resolution pollen cores and supporting evidence derived from the lithostratigraphy, tephrochronology, past fire activity and radiocarbon dating.

The palaeoenvironmental evidence reconstructed by this study is presented in Chapter 3 and organised in three sections related to each study site: Rio Grande, Punta Yartou and Lago Lynch. The order of the sites follows the present west to east precipitation gradient that is reflected in the wetter “mixed evergreen” *Nothofagus* forest in the west, “mixed evergreen-deciduous” *Nothofagus* forest in the central part of the gradient and then “deciduous” *Nothofagus* forest dominated by *Nothofagus pumilio* in eastern drier areas.

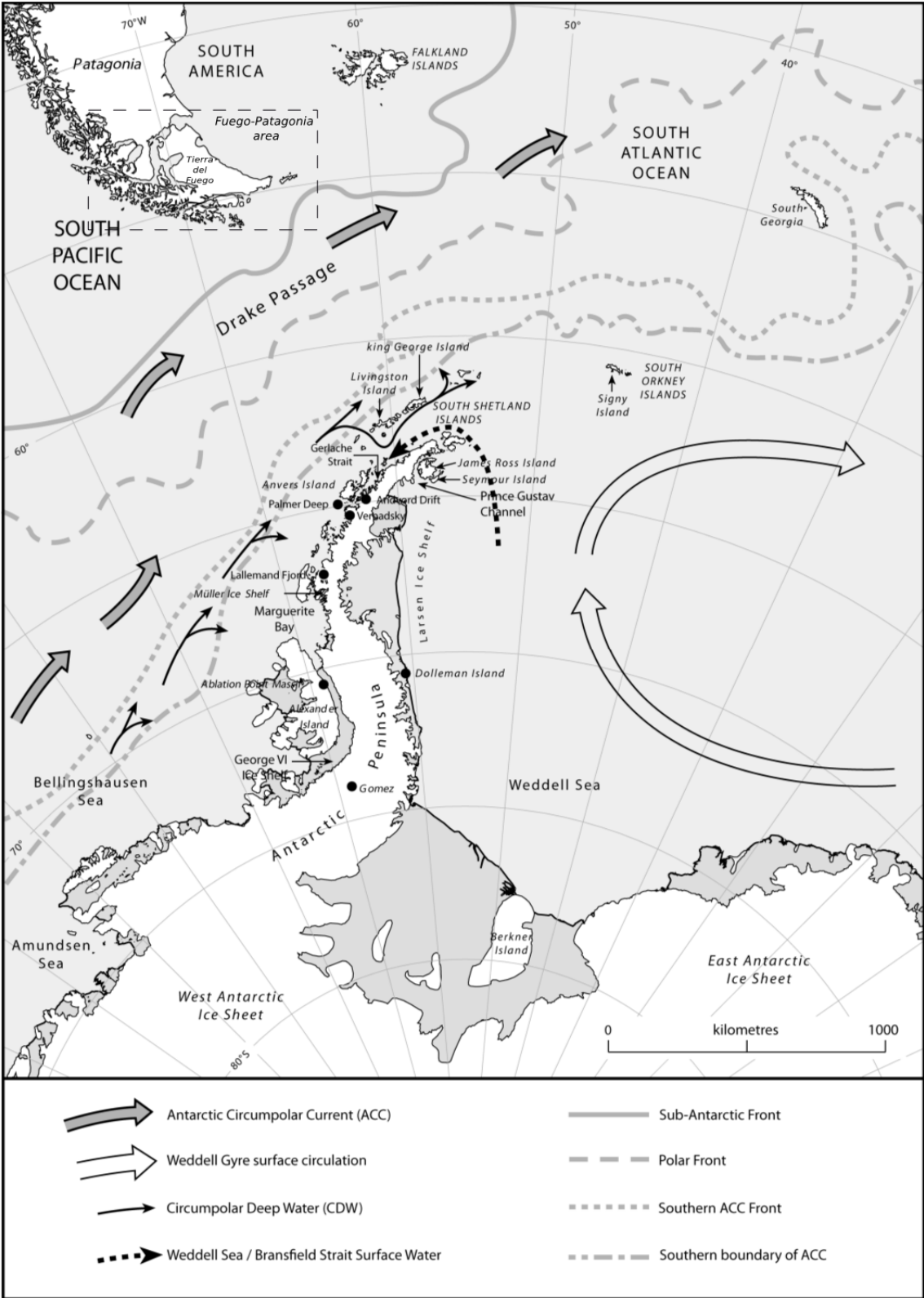


Figure 1.1 The location of Fuego-Patagonia (~53° – 55°S, dashed rectangle), within the southern hemisphere (adapted from Bentley *et. al.*, 2009).

In Chapter 4 the palaeoenvironmental evidence obtained by this study is discussed in relation to each site. The environmental significance for each continuous vegetation core is interpreted in terms of variations in effective moisture during the LGIT and the Holocene and the link between the ecological responses and large-scale controls of the regional climate are discussed.

Chapter 5 provides a synthesis of the three palaeoenvironmental cores and integrates the major findings of this study with those in the literature to produce a new understanding of the sequence of environmental change in Fuego-Patagonia which permits new climatic inferences for regional climatic changes and ecological responses during the LGIT and the Holocene in Fuego-Patagonia and SSA.

Chapter 6 provides a conclusion of this study highlighting the contribution of this study to the knowledge of the sequence of palaeoenvironmental changes in Fuego-Patagonia during the LGIT and the Holocene and its implications and recommendations for future research.

## **1.5 Background.**

### **1.5.1 Setting and topography of Patagonia.**

The Andes follows a north-south direction from  $\sim 27^{\circ}\text{S}$  until approximately  $\sim 52^{\circ}\text{S}$ . From  $\sim 52^{\circ}\text{S}$  to  $\sim 55^{\circ}\text{S}$ , the Andes gradually curve eastwards along the southern extent of Tierra del Fuego, which forms the Cordillera Darwin (Figure 1.2). South of  $\sim 55^{\circ}\text{S}$  the Andes submerge into the sea which forms the  $\sim 1,000$  km wide Paso Drake until they rise again at the Antarctica peninsula (Figure 1.1). The presence of the cold Antarctic continent leads to stronger pressure gradients between the high latitudes and the subtropics of the Southern Hemisphere when compared to the Northern Hemisphere (Aceituno *et al.*, 1993). In consequence, much higher wind speeds are encountered within the west wind zone of the southern hemisphere and the

Andes forms an orographic obstacle leading to an abrupt change of topography and climate across short distances and produces, in the southernmost part of South America, a dramatic west-east precipitation-vegetation gradient (Schneider *et al.*, 2003).

Patagonia can be defined as the territory that lies from  $\sim 37^{\circ}\text{S}$  (Chilean Lake District) to  $\sim 56^{\circ}\text{S}$  (Cabo de Hornos) (Tuhkanen *et al.*, 1990; Rabassa *et al.*, 2008) (Figure 1.2). The Chilean Lake District ( $\sim 37^{\circ}$  -  $42^{\circ}\text{S}$ ) is formed by a complex system of large lake basins running from east - west and from west-east in the Andes foothills. From  $\sim 42^{\circ}\text{S}$  to  $\sim 46^{\circ}\text{S}$  the Andes peaks support many small glaciers. From  $\sim 48^{\circ}\text{S}$  to  $\sim 51^{\circ}\text{S}$  the Andes are covered by the North Patagonian Icefield (NPI) and the larger South Patagonian Icefield (SPI), which are divided narrowly by the Rio Baker  $\sim 49^{\circ}\text{S}$  (Figure 1.2). The Fuego - Patagonia area ( $\sim 53^{\circ}\text{S}$  and  $\sim 55^{\circ}\text{S}$ ) comprises the southernmost part of South America (Figure 1.1). It is separated from the South American continent by the Estrecho de Magallanes (Strait of Magellan)  $\sim 53^{\circ}\text{S}$  and consists of an archipelago, among the biggest islands are; Tierra del Fuego (c. 48,000 km<sup>2</sup>), Isla Santa Inés (c. 4,000 km<sup>2</sup>), Isla Dawson (c. 1,500 km<sup>2</sup>), Isla Clarence (c. 1,100 km<sup>2</sup>) and Isla Navarino (c. 2,500 km<sup>2</sup>) (Figure 1.2).

Patagonia lies within the Andean Southern Volcanic Zone (SVZ;  $\sim 33^{\circ}$  -  $46^{\circ}\text{S}$ ) and Austral Volcanic Zone (AVZ;  $\sim 49^{\circ}$  -  $55^{\circ}\text{S}$ ) and 74 volcanos have been active since the LGM (Global Volcanism Program in Fontijn *et al.*, 2014). The Fuego-Patagonia area has been affected by five known post-glacial large explosive eruptions ( $>1 \text{ km}^3$ ) from four different volcanoes; Volcán Hudson ( $\sim 46^{\circ}\text{S}$ ), Volcán Aguilera ( $\sim 50^{\circ}\text{S}$ ), Volcán Reclús ( $\sim 51^{\circ}\text{S}$ ) and Mt Burney ( $\sim 52^{\circ}\text{S}$ ) (Stern, 2008) (Figure 1.3). The geochemical fingerprinting of tephra layers combined with chronological studies of volcanic events in Fuego-Patagonia area have the potential to allow for more accurate age-depth models of the sediment cores (Kilian *et al.*, 2003; McCulloch and Bentley, 1998; McCulloch *et al.*, 2005a; Stern, 2008; Habertzetti *et al.*, 2009; Borromei *et al.*, 2010; Sagredo *et al.*, 2011; Stern *et al.*, 2011; McCulloch *et al.*, in press; Stern *et al.*, in press).

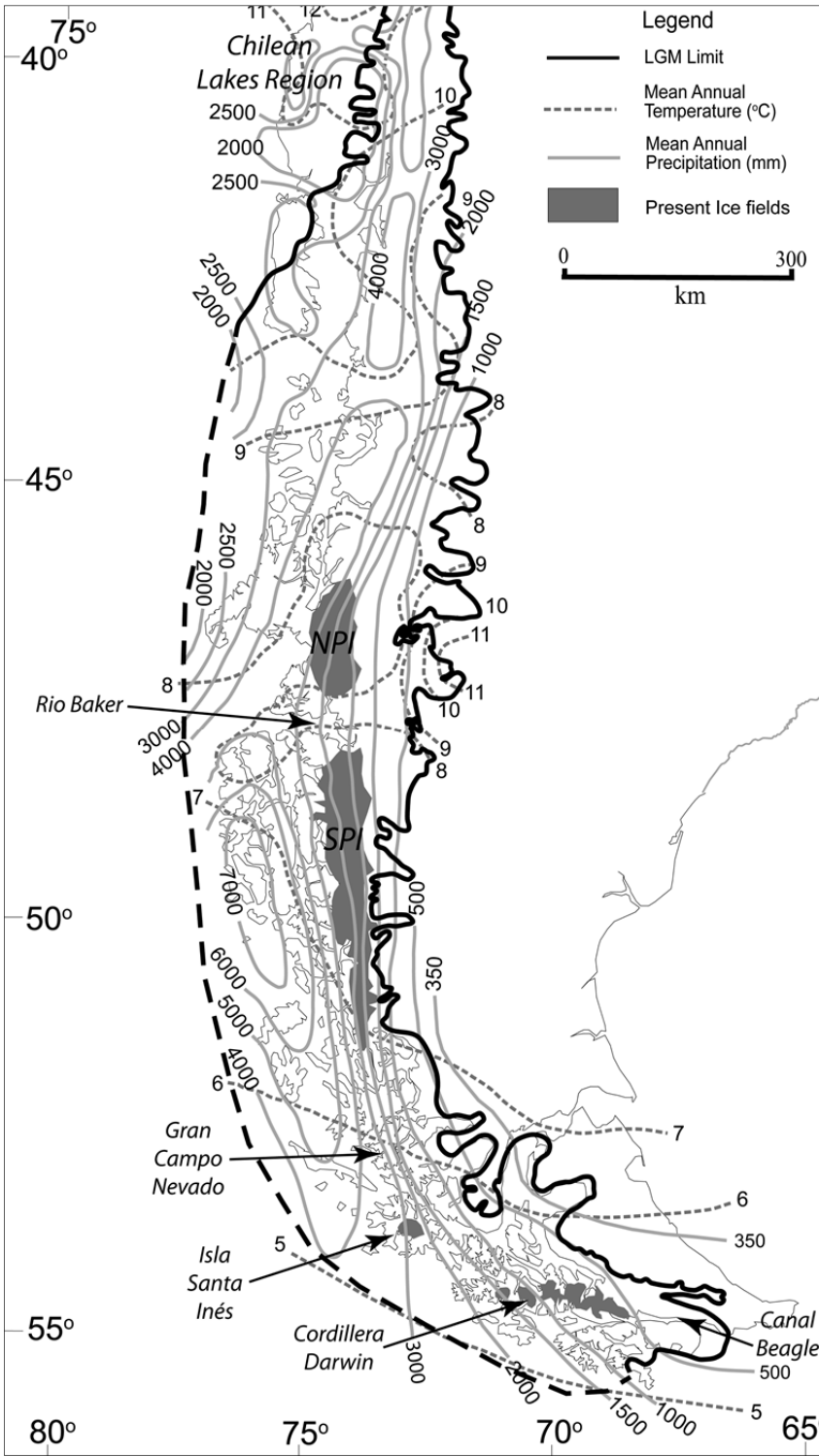


Figure 1.2 The extent of the Last Glacial Maximum (LGM) in Patagonia and the present major ice fields in relation to the present climate (adapted from McCulloch *et al.*, 2000).

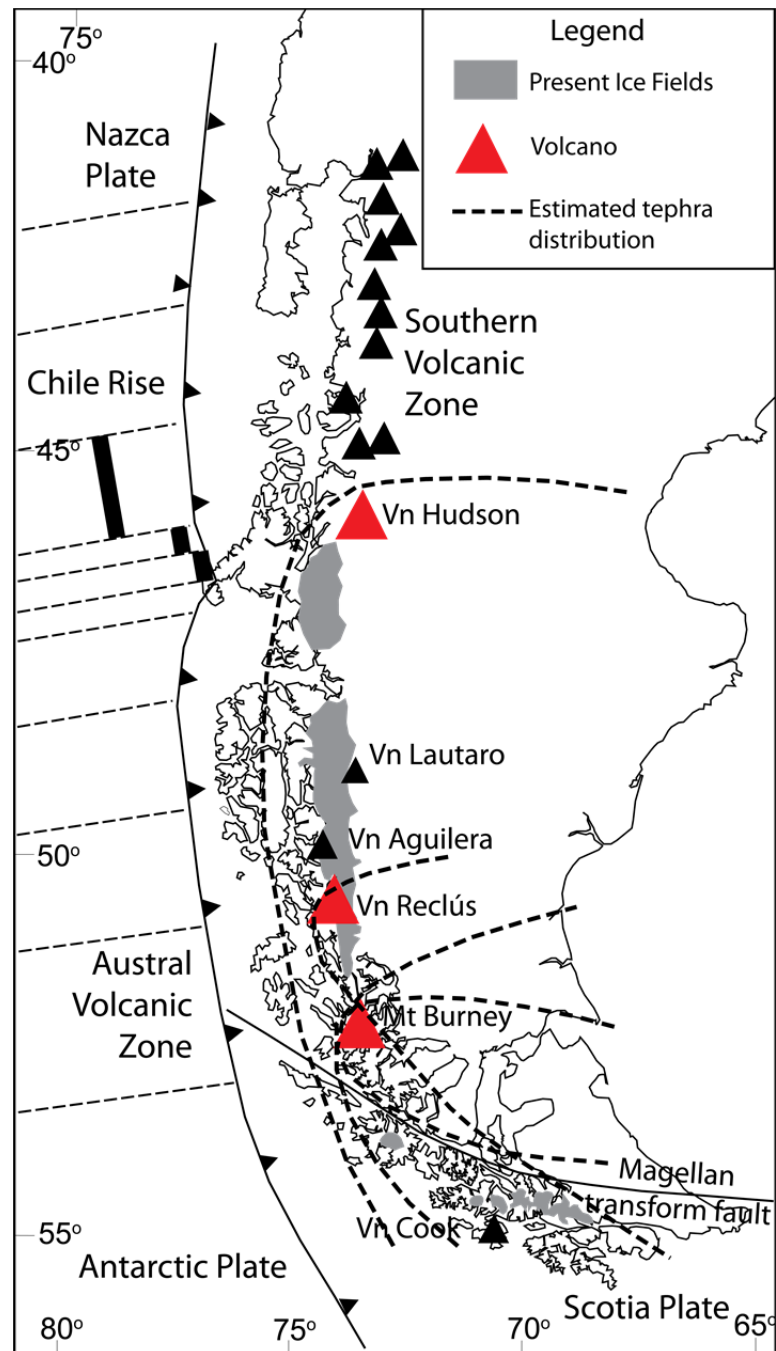


Figure 1.3 The location of Southern and Austral Volcanic zones; including the principal source volcanoes for tephra layers found in Fuego-Patagonia: Volcán Hudson (~46°S), Volcán Aguilera (~50°S), Volcán Reclús (~51°S) and Mt Burney (~52°S).

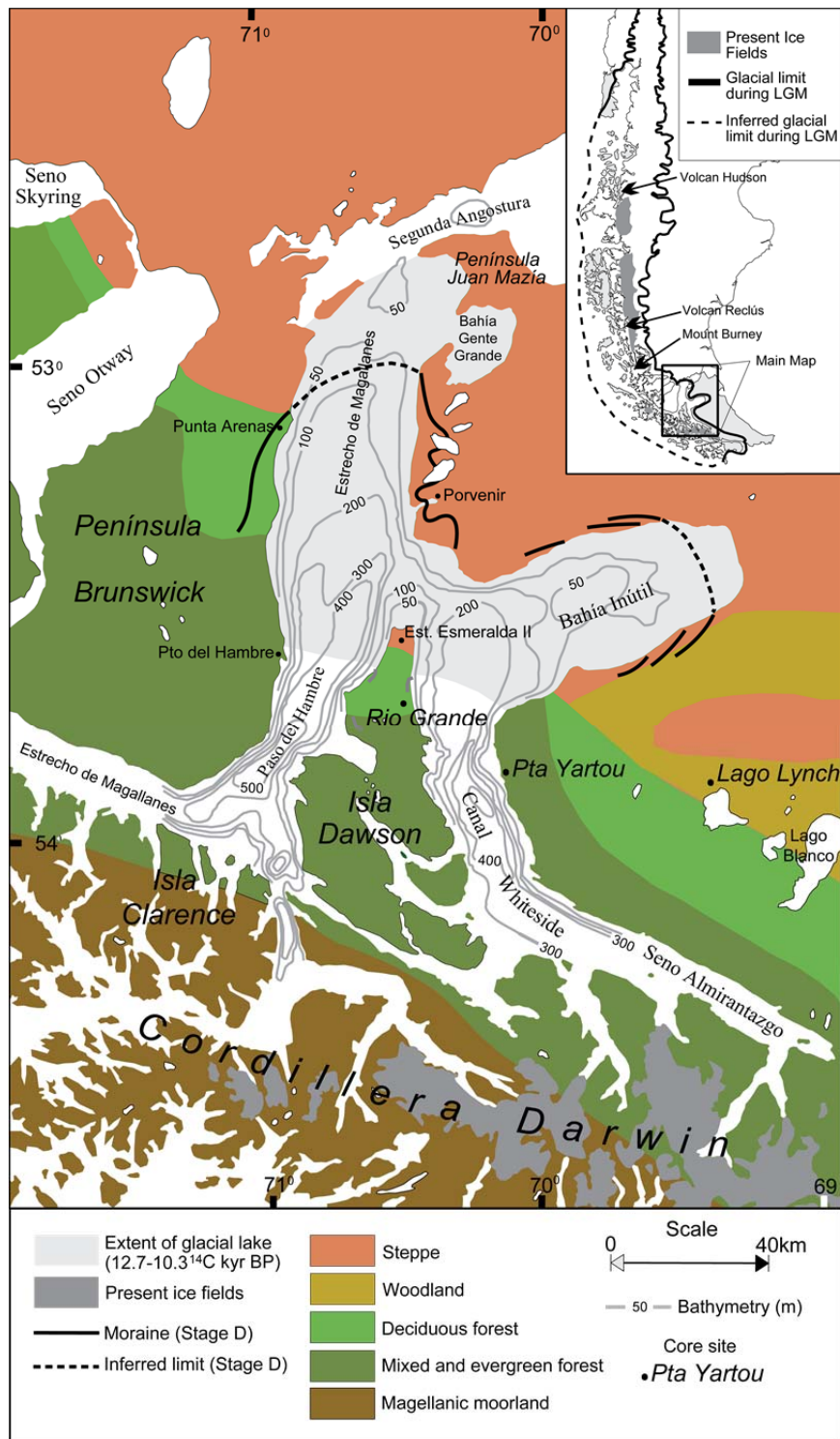


Figure 1.4 Fuego-Patagonia and Late-glacial ice limits in the Estrecho de Magallanes, the present ice fields in the Cordillera Darwin (adapted from McCulloch *et al.*, 2005a) and the vegetation zones of Fuego-Patagonia (adapted from Huber *et al.*, 2004).

However, there is an acute lack of geochemical information for the tephrostratigraphy of SSA during the Late-Glacial and the Holocene and chronological data is often lacking in accuracy and precision which has resulted in the under-used potential of the tephrochronology of Patagonia (Fontijn *et al.*, 2014). There are also few studies that have mentioned the effect of volcanic eruptions on the vegetation of Fuego-Patagonia (Fesq-Martin *et al.*, 2004; Kilian *et al.*, 2006, Fontana and Bennett, 2012). Although these studies mention the potential impact on vegetation causing sustained damage to ecosystems (~2,000 yr) from a volcanic eruption of Mt Burney (B2 at c. 4,400 Cal yr BP) there are no other studies that cover the potential impact of other volcanic eruptions on the vegetation. Therefore, the effects of volcanic eruption on the vegetation need to be studied more in Fuego-Patagonia in order to distinguish between the disturbance effects on the vegetation caused by volcanism and climate change.

### **1.5.2 Past climatic changes: focus on Fuego-Patagonia (~53° - 55°S).**

Palaeoecological and glacial chronological evidence from the Chilean Lake District (~37°S) and the Greenland ice core records suggest that there was climatic synchrony at a millennial-scale between the northern and southern hemispheres during the LGM (Denton *et al.*, 1999; Blunier and Brooks, 2001). However, there appears to be an out-of-phase millennial-scale climate pattern between the northern and southern hemisphere ice core records during the LGM (Blunier and Brooks, 2001; Denton *et al.*, 2010; Lemieux-Dudon *et al.*, 2010). Glacier recession after the LGM began in the northern hemisphere at c. 20,000 yr BP but in Antarctica and the southern oceans the last termination began c. 18,000 yr BP. The causes of this out-of-phase millennial-scale climate pattern may be explained in at least two ways; the first hypothesis invokes the oceanic bipolar seesaw by which weakening of North Atlantic overturning during Heinrich events H1 and the Younger Dryas (YD) reduced the northward ocean heat transport, thereby warming the southern hemisphere. In addition, reduced North Atlantic overturning would have stimulated deep water formation in the southern ocean, further warming the

southern ocean and Antarctica during northern hemisphere stadials. A second hypothesis and complementary mechanism involves a southward shift of the SWWs belt each time that inter tropical convergence zone was pushed toward the southern hemisphere by the spread of winter sea ice over the northern North Atlantic. Such a mechanism would have the advantage of transferring the effects of northern millennial-scale stadial/interstadial events rapidly into the southern hemisphere. The two hypothesized processes likely acted synergistically. For example, the bipolar seesaw facilitated the southward shift of the zonal wind systems by changing sea surface temperature gradients (Denton *et al.*, 2010).

In contrast to the inference of inter hemispheric synchrony drawn from the palaeoenvironmental records from northern Patagonia there is evidence to suggest that during the transition phase between the LGM and the Holocene, Fuego-Patagonia became more under the influence of the Antarctic domain (Sugden *et al.*, 2005). Terrestrial evidence based on dust deposition and glaciological data from the Southern Patagonian Icefield (SPI) at  $\sim 50^{\circ}\text{S}$  during the LGM, show that glaciers expanded more in-phase with Antarctic climate patterns (Kaplan *et al.*, 2008; Sugden *et al.*, 2009). Marine alkenone-derived SST records (MD07/3128) from  $\sim 53^{\circ}\text{S}$  to the west of the Estrecho de Magallanes indicate that the coldest temperatures during the LGM were achieved by c. 18,800 Cal yr BP (Figure 1.5 and 1.7). These colder SST probably reflect a  $\sim 5^{\circ}$  to  $6^{\circ}$  northward shift of the northern margin of the ACC and the SWWs. After c. 18,800 Cal yr BP the alkenone-derived SST record suggests a strong warming of  $\sim 8^{\circ}\text{C}$  (Caniupán *et al.*, 2011) and this is consistent with the warming trend recorded in the Antarctic ice core records (Lemieux-Dudon *et al.*, 2010) (Figure 1.5). Palaeoecological evidence for the LGM and during the last termination at  $\sim 53^{\circ}\text{S}$  is limited as most records are located within the extent of maximum glacier ice cover and so only record the period after the ice retreat after c. 17,700 Cal yr BP from the Estrecho de Magallanes and Bahía Inútil ( $\sim 53^{\circ}\text{S}$ ) (McCulloch *et al.*, 2005b) and c. 18,200 yr BP from Gran Campo Nevado (GCN) ice field and Seno Skyring ( $\sim 53^{\circ}\text{S}$ ) (Kilian *et al.*, 2007).

Palaeoclimatic data and modelling studies of the position and strength of the SSWs during the LGM have not been conclusive (Hulton *et al.*, 2002, Rojas *et al.*, 2009; Sime *et al.*, 2013). However, in broad terms during the LGM, it has been suggested that at c. 21,000 yr BP the core of the SSWs moved northward to  $\sim 45^{\circ}\text{S}$ , leading to moister and cooler conditions in the vicinity of the Chilean Lake District ( $\sim 37^{\circ}\text{S}$ ), which fed the expansion of the Andean glaciers in northern Patagonia (Hulton *et al.*, 2002). One coupled Global Circulation Models (GCM) for the LGM climate in the southern hemisphere concluded that there was no significant shift in the SSWs, but suggested a general weakening, which could have provoked a similar effect during the LGM, leading to cooler and wetter climatic conditions than present in the Chilean Lake District (Rojas *et al.*, 2009).

Terrestrial palaeoenvironmental reconstructions from  $\sim 53^{\circ}$  -  $54^{\circ}\text{S}$  (McCulloch *et al.*, 2000; McCulloch and Davies, 2001; Markgraf and Huber, 2010; Fontana and Bennett, 2012; Moreno *et al.*, 2012) have indicated that concomitant with the Late-glacial warming trend the core of the Westerlies returned to their present position  $\sim 49^{\circ}\text{S}$  and  $\sim 53^{\circ}\text{S}$ . The Late-glacial warming trend recorded in SSA has also been registered in ice core records from the east of Antarctica (Blunier and Brooks, 2001; Lemieux-Dudon *et al.*, 2010). Lemieux-Dudon *et al.*, (2010) propose a new age for the warming recorded in Antarctica during the last deglaciation, with the onset and end dated to c.  $17,900 \pm 300$  Cal yr BP and c.  $14,550 \pm 130$  Cal yr BP respectively. This period was interrupted by a return to colder conditions during the Antarctic Cold Reversal (ACR, c. 14,550 – 12,800 yr BP) (Blunier and Brooks, 2001; Lemieux-Dudon *et al.*, 2010).

The effect of the Antarctic Cold Reversal (ACR) on the palaeoenvironmental record in Fuego-Patagonia ( $\sim 53^{\circ}$  -  $55^{\circ}\text{S}$ ) is poorly understood (McCulloch and Davies 2001; Markgraf and Huber, 2010, Moreno *et al.*, 2012).

However, glacier advances contemporary with the ACR have been documented from across Patagonia: at Lago Buenos Aires (~46°S) (Douglass *et al.*, 2005), Torres del Paine (~51°S) (Garcia *et al.*, 2012), Gran Campo Nevado (~53°S) (Kilian *et al.*, 2007) and Estrecho de Magallanes (~53°S) (McCulloch *et al.*, 2005b) (Figure 1.2 and 1.4). The limited number of palaeoecological records from Fuego-Patagonia that cover the LGIT leads to a big gap in our knowledge about the effect and the timing of the Antarctic influences on the Patagonian vegetation or indeed if we are able to detect the ACR in palaeoecological records as it appears to have been a relatively small-scale Antarctic climatic event.

During the colder and drier Younger Dryas event in the northern hemisphere (YD; c. 12,800–11,700 Cal yr BP) (Rasmussen *et al.*, 2006), the Antarctic ice core temperature record suggests a contrary trend towards warmer climatic conditions (Blunier and Brooks, 2001; Lemieux-Dudon *et al.*, 2010). Within the few marine and terrestrial palaeoenvironmental records from Fuego-Patagonia around 52° - 53°S (Lamy *et al.*, 2010; Harada *et al.*, 2013; Caniupán *et al.*, 2011, 2014) that span the Early-Holocene (c. 12,500 - 8,500 Cal yr BP) the core of the SSWs was stronger and more stable. Thereafter, the SSWs reduced to a moderate intensity until c. 5,000 Cal yr BP and then followed by a further reduction in intensity which led to less precipitation during the Late-Holocene. Contrary to the Fuego-Patagonian evidence, the palaeoclimatic archives from Antarctica and the southern oceans reveal a complex sequence of temperature fluctuations throughout the Holocene (Bentley *et al.*, 2009). It is anticipated that this complex and sometimes contradictory climatic history can be better understood with the aid of high resolution terrestrial palaeoenvironmental records over both latitudinal and longitudinal transects, to identify past latitudinal shifts and changes in the intensity of the SSWs.

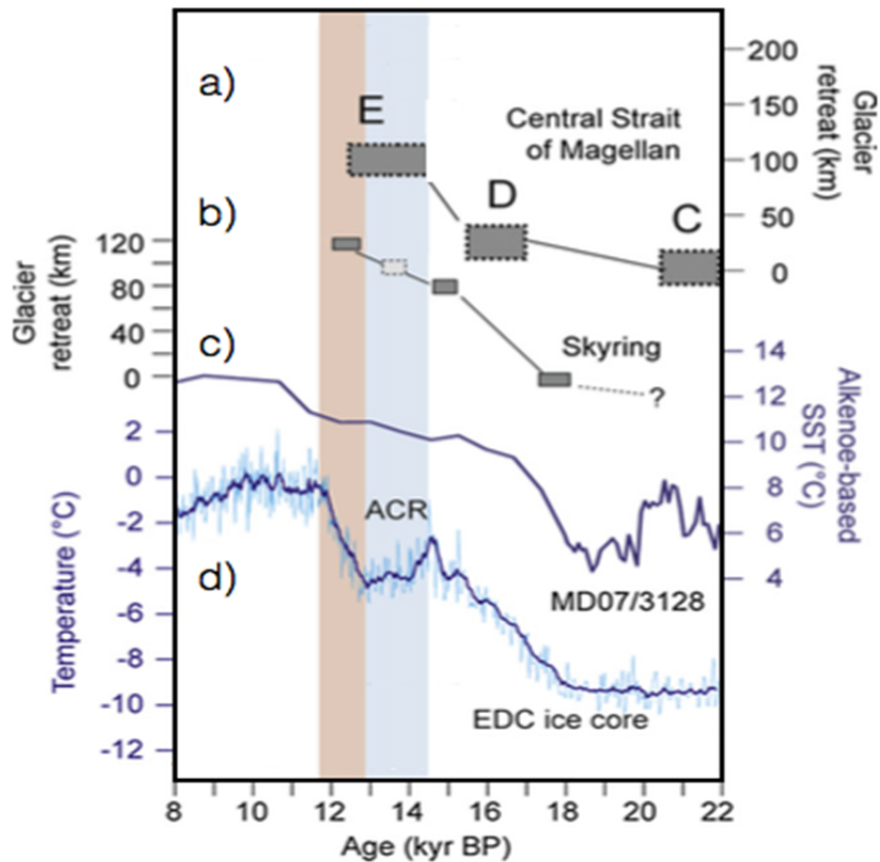


Figure 1.5 Summary of Late-glacial palaeoenvironmental records from Fuego-Patagonia and Antarctica a) Glacier advances stages “C” to “E” in the Estrecho de Magallanes (McCulloch *et al.*, 2005a); b) Glacier advances in Seno Skyring (Kilian *et al.*, 2007); c) Alkenone-derived SST record from  $\sim 53^{\circ}\text{S}$  (Caniupán *et al.*, 2011) and d) Deuterium-derived SST from Antarctic continent (Lemieux-Dudon *et al.*, 2010). The blue vertical shading indicates the ACR period and the brown shading the YD period (adapted from Killian and Lamy, 2012)

The present-day latitudinal position of the SWWs is described as having abnormally high precipitation along the west coast of SSA between  $\sim 30^{\circ}\text{S}$  and  $\sim 55^{\circ}\text{S}$ . The annual variations of the SWWs strength and the associated precipitation have been recorded at a few weather stations within the region (Schneider *et al.*, 2003; Aravena and Luckman, 2009; Garreaud, 2009) and meteorological data has been interpolated from global climate data-sets (Kalnay *et al.*, 1996). The available meteorological data indicates that the highest wind velocities across

SSA occurs between  $\sim 49^{\circ}\text{S}$  and  $\sim 53^{\circ}\text{S}$  and that there is a clear positive correlation between precipitation and SSWs strength at the continental margin and in the Andes (Garreaud *et al.*, 2013) (Figure 1.5). To the east of the Andes the correlation between precipitation and SSWs strength becomes weaker and negative within the eastern steppe region towards the Atlantic coast. The strength of the SSWs and, therefore, the correlation with the precipitation varies with latitude, season, and distance from the Pacific coast (Figure 1.6). During the austral summer, the SSWs contract and the intensity within the core of storm tracks is strengthened and precipitation reaches its maximum along the west coast and on the Andes. During the austral winter, the SSWs form a broader track and are slightly displaced northward, while the core of the storm tracks is relatively weak and the expansion of sea ice forces the polar front to move approximately  $5^{\circ}\text{S}$  of latitude equator wards (Schneider *et al.*, 2003, Lamy *et al.*, 2010).

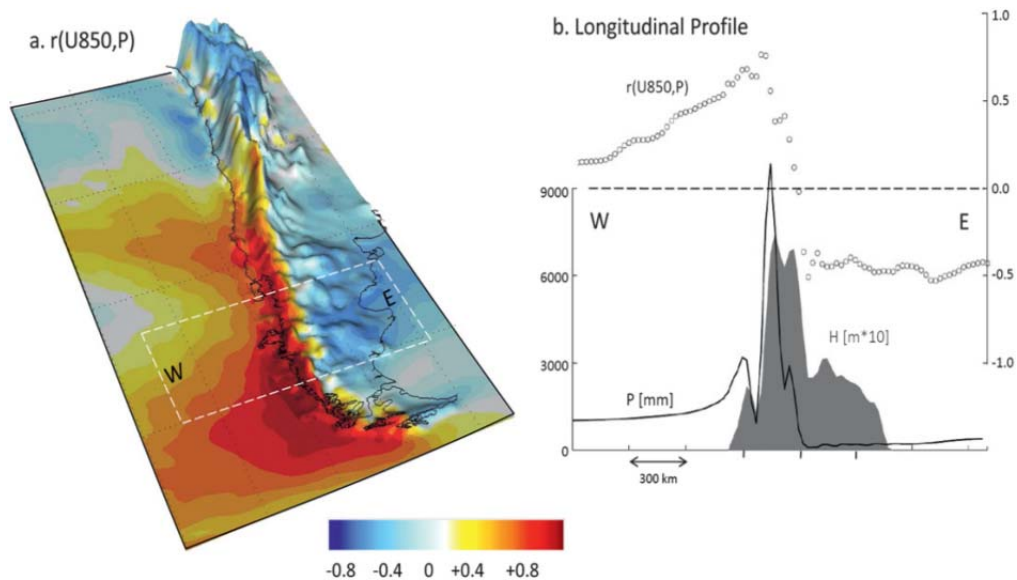


Figure 1.6 a) Correlation model between annual mean 850-hPa zonal wind and precipitation [ $r(\text{U850}, \text{P})$ ], the scale-bar at the bottom is the correlation coefficients; b) Longitudinal profile of terrain elevation (shaded area, scale at left), long-term-mean annual precipitation (black line, scale at left in mm/yr), and the  $r(\text{U850}, \text{P})$  correlation, averaged between  $42^{\circ}\text{S}$  and  $52^{\circ}\text{S}$  (from Garreaud *et al.*, 2013).

### 1.5.3 Glacial records.

Our current understanding of southern hemisphere ocean-atmosphere changes is mainly derived from reconstructions of the glacier fluctuations during the LGIT. The landforms associated with multiple glacial advances in Fuego-Patagonia have been identified as glacial stages A to E and have been mapped in detail (Meglioli, 1992; Clapperton *et al.*, 1995; Benn and Clapperton, 2000; Bentley *et al.*, 2005). The timing of the glacial stages has been constrained by  $^{14}\text{C}$  and cosmogenic isotope dating (Gosse and Phillips, 2001; McCulloch *et al.*, 2005a; Kaplan *et al.*, 2008). Glacial advance stage “A” is prior to the LGM, and the LGM and LGIT advances are represented by glacial stages “B” to “E”. The glacial advance stages B and C have been dated to c. 25,200–23,000 yr BP and c.22,400–20,000 yr BP, respectively (McCulloch *et al.*, 2005a) (Figure 1.4). During the LGM, glacial stages “B” and “C”, in Fuego-Patagonia an extensive glacier flowed from the Cordillera Darwin northward into the Estrecho de Magallanes and formed the moraine limits on the Peninsula Juan Mazia (Bahía Gente Grande), Bahía Inútil, Lago Lynch and Lago Blanco and eastward into Lago Fagnano and the Canal Beagle respectively and, covering most of Tierra del Fuego (Meglioli, 1992; Clapperton *et al.*, 1995; Glasser, 2004). Glacial stage “D” was less extensive than the LGM glacier extent, reaching Bahía Gente Grande and covering most of Bahía Inútil and then retreated sometime before c.17,700 yr BP (McCulloch *et al.*, 2005b). The glacial chronological evidence around the Estrecho de Magallanes is consistent with the glacial behavior to the north of the Estrecho de Magallanes, around Gran Campo Nevado (GCN) and Seno Skyring ( $\sim 53^\circ\text{S}$ ) where moraines were formed between c.17,400 yr BP and c. 18,200 yr BP (Kilian *et al.*, 2007), coeval with the moraine system “D” in the Magallanes strait ( $\sim 53^\circ\text{S}$ ) (McCulloch *et al.*, 2005b) (Figure 1.4). Glacial stage “E” is thought to have occurred between c. 15,300 and c. 11,700 yr BP, prior to the onset of Holocene warming after c. 11,500 yr BP drove the Patagonian ice sheets back to their near-present day limits. Glacial stage “E” has been described on the basis of a suite of evidence for glacial lakes, including raised shorelines and glacial lacustrine sediments deposited

above a key tephra marker (Vn Reclús 1), that suggest the presence of an ice dammed lake in the central section of Magallanes. The moraine limit associated with this stage was thought to be on the northern peninsula of Isla Dawson (McCulloch and Bentley, 1998; McCulloch *et al.*, 2005b). Further evidence for a glacier advance during glacial stage E has been found at around Gran Campo Nevado (GCN) and Seno Skyring (~53°S), where a fast glacier retreat was detected around 15,000 - 14,000 yr BP and slower retreat and glacier fluctuations of limited extent in the fjord channel system northeast of GCN between around 14,000-11,000 yr BP (Kilian *et al.*, 2007) (Figure 1.4). Other authors have also mentioned an initial glacial retreat in the Marinelli Fjord from Seno Almirantazgo (~54°) by ~15,500 Cal yr BP and by ~12,500 Cal yr BP also coeval with glacial stages “E” (Boyd *et al.*, 2008). However, early ages for deglaciation in the western Estrecho de Magallanes at Isla Santa Inés (~53°S) (Fontana and Bennett, 2012) and on the north side of the Cordillera Darwin (~54°S) indicate massive ice collapse that began before c. 18,400 yr BP and which had progressed such that the Magellan glaciers were confined to the interior fjords by c. 16,800 yr BP and without evidence of glacial re-advance after that date (Hall *et al.*, 2013). Thus, the current understanding about the glacier fluctuations around the corresponding glacial stage “E” from c. 15,300 yr BP until the onset of Holocene warming after c. 11,500 yr BP when the region became affected by the Antarctic domain is still unclear and is being investigated further.

#### **1.5.4 Vegetation communities in Fuego-Patagonia.**

During the Quaternary *Nothofagus* forest has been the dominant vegetation in Fuego-Patagonia which may have been able to survive in multiple refugia during the Last Glacial Maximum in Fuego-Patagonia (Markgraf *et al.* 1993; Premoli *et al.*, 2010). The *Nothofagus* genus is included within the Nothofagaceae family with a southern hemisphere distribution. In Fuego-Patagonia there are three species, one evergreen (*Nothofagus betuloides*) and two deciduous (*Nothofagus pumilio* and *Nothofagus antarctica*). The pollen morphological similarities between these

species have prevented species identification and interpretation in the palaeoenvironmental record (Von Post, 1929; Auer *et al.*, 1955; Markgraf and D'Antoni, 1978, Fontana and Bennett, 2012). Therefore, palaeoenvironmental reconstructions include more than one species and are described as *Nothofagus dombeyi* type. To achieve greater clarity in the interpretation of forest dynamics from palaeoenvironmental records it is essential to assess the vegetation assemblage and supporting lithostratigraphical evidence as a whole to ensure ecologically defined and robust interpretations.

The SWWs and the high orographic rainfall along the western flanks of the southern Andes creates a strong rain-shadow to the east of the Andes. The precipitation gradient is reflected in the wetter “mixed evergreen” *Nothofagus* forest in the west (~2,000 mm/yr), “mixed evergreen-deciduous” *Nothofagus* forest in the central part of the precipitation gradient and then “deciduous” *Nothofagus* forest dominated by *Nothofagus pumilio* in the east, in drier areas (~200 - 400 mm/yr) (Figure 1.7). Several studies have classified the vegetation principally into four zones that closely follow the strong west-to-east precipitation gradient: 1) Magellanic moorland; 2) Evergreen *Nothofagus betuloides* forest; 3) Deciduous *Nothofagus* forest; 4) Patagonian steppe and fifth zone that corresponds to high Andes vegetation (Pisano, 1977; Moore, 1983; Boelcke *et al.*, 1985; Tuhkanen *et al.*, 1990) (Figure 1.6).

**Magellanic moorland:** is located in the western areas of Fuego-Patagonia under oceanic influence with high rainfall (>2,000 mm/yr) uniformly distributed throughout the year (Figure 1.2 and 1.7). The temperatures are relatively low with little diurnal and annual variation. The moorland communities have poor drainage and without the presence of permafrost these communities are dominated by cushion bogs of *Astelia pumila* (Asteliaceae) and *Donatia fascicularis* (Donatiaceae) with associated species such as *Drapetes muscosus* (Thymelaeaceae) and *Drosera uniflora* (Droseraceae) (Figure 1.8). In general, the Magellanic moorland is typically treeless or with a sparse population of dwarf trees.

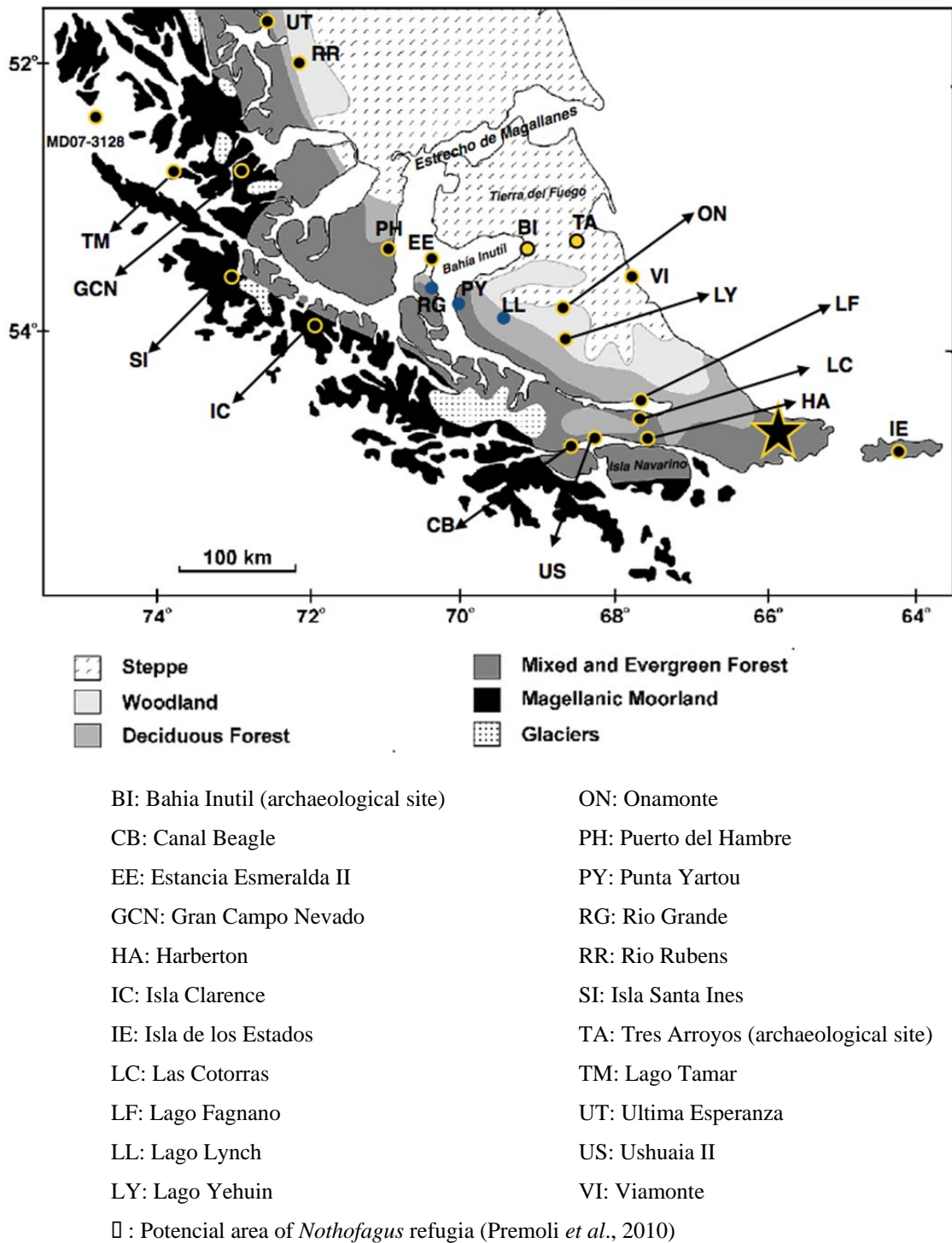


Figure 1.7 The vegetation zones of Fuego-Patagonia (adapted from Huber *et al.*, 2004) and locations named in this study.



Figure 1.8 Magellanic moorland; cushion bog plants of *Astelia pumila* and *Donatia fascicularis* and bryophytes such as *Dicronaloma* spp. (©C.A. Mansilla).

Towards the eastern areas where annual precipitation is between 600 and 1,500 mm/yr, and the vegetation communities depend totally on rainwater resources, peat bogs predominate. The bogs are typically formed by bryophytes such as *Sphagnum magellanicum* (Sphagnaceae) and *Dicronaloma* spp. (Dicranaceae) and are also dominated by low temperature resistant dwarf shrubs and herbs such as *Empetrum rubrum* (Ericaceae) and *Caltha appendiculata* (Ranunculaceae). In drier areas the vegetation assemblage may be also associated with tree species such as *Nothofagus betuloides* (Nothofagaceae), *Drimys winteri* (Winteraceae) and *Pilgerodendron uviferum* (Cupressaceae).

**Evergreen *Nothofagus* forest:** These communities are located in the archipelagic sectors of central and southern Patagonia where the precipitation ranges are between 2,000 and 6,000 mm/yr, and require higher humidity by rain or by poor drainage (Figure 1.2 and 1.7). The “pure” *Nothofagus betuloides* forests can be associated with a dense layer of bryophytes and ferns and fallen logs cover the ground. In zones where the precipitation declines to

approximately 900-2,000 mm/yr and near to the coast (below 200 m a.s.l.) *Nothofagus betuloides* forest can be found with *Drimys winteri* and *Maytenus magellanica* (Celastraceae) (Figure 1.9). In places *Drimys* is co-dominant in forming “mixed evergreen” *Nothofagus* forest dominated by *Nothofagus betuloides*. As rainfall decreases to the east, the forest composition gradually changes and *Nothofagus pumilio* becomes more dominant in the “mixed evergreen-deciduous” forest. The mixed evergreen-deciduous forest can also be dominated by *Nothofagus betuloides* in wetter areas or by *Nothofagus pumilio* in drier areas. This “mixed evergreen-deciduous” *Nothofagus* forest forms a transitional-ecotone community between “evergreen mixed” dominated by *Nothofagus betuloides* and “deciduous” *Nothofagus* forest almost exclusively dominated by *Nothofagus pumilio*. In protected areas along the south side of Bahía Inútil on Tierra del Fuego and towards the entrance of Seno Almirantazgo, remnants of a mixed forest dominated by *Drimys winteri* and *Maytenus magellanica* can be found (Pisano, 1977). This mixed forest existed until 1880 - 1890 after which Europeans cleared many of the trees for firewood and for charcoal production for the goldfields.

**Deciduous *Nothofagus* forest:** This zone is characterised by uniform precipitation between 400 and 800 mm throughout the year. The “deciduous” *Nothofagus* forests (Figure 1.2 and 1.7) are low in diversity and are dominated almost exclusively by the cold-deciduous *Nothofagus pumilio* (Figure 1.10). The plants associated with this deciduous forest are also typical of lower temperatures, such as the shrub taxa *Berberis ilicifolia* and herbaceous plants such as *Ribes magellanicus* (Saxifragaceae). In more mesic areas of this ecotone, *Nothofagus pumilio* is commonly found associated with *Nothofagus antarctica* and the hemi-parasite *Misodendrum* spp. In open and drier areas the principal herbs are Poaceae and shrubs such as *Chiliotrichum diffusum* (Asteraceae, Subfamily Asteroideae), and *Berberis buxifolia* (Berberiaceae).



Figure 1.9 “Evergreen mixed” *Nothofagus* forest dominated by *Nothofagus betuloides* with the presence of *Drimys winteri* (©C.A. Mansilla).



Figure 1.10 Magellanic deciduous forest dominated almost exclusively by the cold-deciduous *Nothofagus pumilio* tree and frequent small green clusters of *Misodendrum* spp. (©C.A. Mansilla).

**Fuego-Patagonian steppe:** This community is located where precipitation is between 200 and 400 mm per year (Figure 1.2 and 1.7). Most of the species found in this community are adapted to minimise water loss, to endure strong winds and low atmospheric humidity. The dominant vegetation comprises members of the Poaceae family (Figure 1.11). In moister, more mesic environments within the Fuego-Patagonian steppe Poaceae is associated with shrubs such as *Chilotrimum diffusum* and herb species such as *Galium fuegianum* (Rubiaceae), *Acaena ovalifolia* (Rosaceae), *Acaena chilensis*, *Anemone multifida* (Ranunculaceae), *Calceolaria* (Calceolariaceae), *Aster vahlii*, (Asteraceae, Asteroideae), *Cerastium arvense* (Caryophyllaceae) and *Gentianella magellanica* (Gentianaceae). In xeric conditions (~200 mm precipitation per year) Poaceae is associated in the lower strata with *Acaena pinnatifida* (Rosaceae), *Acaena platyacantha*, *Acaena poeppigiana*, *Azorella caespitose* (Araliaceae), *Baccharis magellanicum* (Asteraceae, Asteroideae), *Galium fuegianum* (Rubiaceae), *Leucheria* spp. (Asteraceae, Subfamily Mutisioideae), *Nassauvia* spp. (Asteraceae, Subfamily Mutisioideae) and *Taraxacum gilliesi* (Asteraceae, Subfamily Cichorieae).



Figure 1.11 The Fuego-Patagonian steppe landscape (©C.A. Mansilla).

**Andean vegetation:** In general the transition from forest to Andean vegetation in Tierra del Fuego is marked by a rather clear timberline which lies at an average altitude of 500-600m on Tierra del Fuego (Figure 1.2, 1.7 and 1.12). The composition of the high mountain vegetation communities is governed by three principal factors, exposure to wind, availability of water and the physical nature of the substrate (Moore, 1983). The climate is cold and desert-like at high altitudes and the characteristics of the vegetation depends on adjacent ecosystems present on both sides of the Andean cordillera. On the occident side vegetation have more affinity with the isothermal moorland and in the orient side are more similar to the steppe. Sparse vegetation occurs above the *Nothofagus* forests and includes small patches of *Nothofagus pumilio* and/or *Nothofagus antarctica*. On sites in the upper treeline where there is *Nothofagus pumilio* growth and recruitment, tree ring thicknesses have been shown to be positively correlated with temperature and negatively with the precipitation. In contrast *Nothofagus pumilio* low elevation growth is positively correlated with precipitation (Aravena *et al.*, 2002).



Figure 1.12 Andean vegetation and the timberline of *Nothofagus pumilio* (©C.A. Mansilla).

### 1.5.5 Past vegetation in Fuego-Patagonia.

There are few continuous and high resolution fossil pollen records that cover the last c.17,000 Cal yr BP that have investigated the transition from forest to steppe around the Estrecho de Magallanes and Tierra del Fuego (~53°S - 55°S) (McCulloch and Davis, 2001; Huber *et al.*, 2004; Markgraf and Huber, 2010) and around ~52°S (Moreno *et al.*, 2012). These studies have suggested that following the retreat of the Magellan glaciers after the LGM the vegetation rapidly colonised the deglaciated terrain. The early stages of deglaciation appear to have been dominated by *Empetrum* heath-grassland, followed by grassland expansion and establishment of the forest at c. 11,000 Cal yr BP. After c. 11,000 Cal yr BP the grasslands were succeeded by *Nothofagus* woodland which continued until c. 6,000 Cal yr BP. After the Mid-Holocene the character of the woodland changed as it developed into more closed *Nothofagus* forests (McCulloch and Davis, 2001; Huber *et al.*, 2004; Markgraf and Huber, 2010; Moreno *et al.*, 2012). Most of the authors have interpreted the changes in the dominance of *Empetrum* heath-grassland and grassland during the LGIT as due to changes in effective moisture. However, the roles of separate climatic variables, i.e. temperature and humidity that control the establishment and expansion of *Nothofagus* forests are still unclear.

The early continuous presence of *Nothofagus* pollen (>2% Total Land Pollen, TLP) during the LGIT may indicate the regional presence of sparse populations around a site and may support the hypothesis of multiple refugia during the LGM within southern Fuego-Patagonia (south-east of Tierra del Fuego, Markgraf *et al.*, 1993; Premoli *et al.*, 2010) (Figure 1.6). However, the interpretation of the establishment and type of forest from small percentages of *Nothofagus* pollen is not clearly defined. Modern pollen surface spectra from across Fuego-Patagonia suggest the following relationships between the proportions of *Nothofagus* pollen rain and the surrounding woodland ecology: a pollen assemblage may be representative of the forest/steppe ecotone when *Nothofagus* reaches ~20% of the total land pollen (TLP), an open-canopy forest

when *Nothofagus* reaches more than 40% of the TLP and closed forest when *Nothofagus* constitutes more than 63% of the TLP (Burry *et al.*, 2006; Trivi *et al.*, 2006).

Palynological records from Fuego-Patagonia (~52°-55°S) indicate that the establishment of *Nothofagus* forest (~20% of TLP) occurred at c. 11,700 Cal yr BP at Puerto del Hambre (53°36'S, 70°55'W) (McCulloch and Davies, 2001); c. 11,500 Cal yr BP at Ushuaia II (54°47'S, 68°18'W) (Heusser, 1998); c. 11,000 Cal yr BP at Puerto Harberton (54°53'S, 67°10'W) (Markgraf and Huber, 2010); c. 10,500 Cal yr BP on Isla Santa Inés (53°38'S, 72°25'W) (Fontana and Bennett, 2012); c. 8,900 Cal yr BP at Lago Yehuín (54°20'S, 67°45'W) (Markgraf, 1983); c. 8,500 Cal yr BP at Estancia Esmeralda II (53°30'S, 70°35'W) (McCulloch and Davies, 2001); c. 8,500 Cal yrs BP on Isla Clarence (54°12'S, 71°14'W) (Markgraf, 1983) and, c. 5,800 Cal yr BP at Onamonte (53°54'S, 68°57'W) (Heusser, 1993) (Figure 1.6). Three studies have been performed in the wetter areas of Fuego-Patagonia (~52°S, Fesq-Martin *et al.*, 2004; ~53°S, Fontana and Bennett, 2012; ~54°S, Markgraf, 1983) and the current vegetation of those areas is moorland vegetation and woodland dominated by *Nothofagus betuloides*. Around 52°S and to the east of the Gran Campo Nevado (GCN), *Nothofagus* was present continuously in high abundance during the Late-glacial followed by a decline in *Nothofagus* at c. 11,200 Cal yr BP that was related to a re-advance of Gran Campo Nevado icefield with a later re-expansion of evergreen *Nothofagus* forest containing *Drimys* elements (Fesq-Martin *et al.*, 2004). At Isla Santa Inés ~53°S, the Magellanic moorland dominated until 10,500 Cal yr BP after which evergreen *Nothofagus* forest became established in the area, while *Drimys* trees appeared later around 9,500 Cal yr BP (Fontana and Bennett, 2012). Finally, on Isla Clarence (~54°S) *Nothofagus* was established by 8,500 Cal yr BP ~54°S (Markgraf, 1983). In drier areas of Fuego-Patagonia (~53°S) there are very few palaeoenvironmental records and these are limited to studies by Heusser (1993) at Onamonte, Lago Yehuín (Markgraf, 1983) and La Misión (Markgraf, 1980), which are unfortunately not well dated and so comparisons to more recent work are limited (Figure 1.6).

Improving knowledge about the establishment, migration and vegetation changes associated with subantarctic *Nothofagus* forest across Tierra del Fuego are key to reconstructing and better understanding the local and regional climatic records. Presently there is no discernible latitudinal pattern to the timing and expansion of *Nothofagus* forest across Fuego-Patagonia after the Last Glacial Maximum. Identifying the separate climatic variables of temperature or humidity and their control on the colonisation and expansion of *Nothofagus* forests remains problematic. It is anticipated that the construction of well dated palaeoenvironmental records, following a longitudinal west to east transect that includes the different *Nothofagus* ecosystems may advance our understanding of the early colonization and expansion of *Nothofagus* forest after the LGM.

#### **1.5.6 Human occupation versus vegetation in central-north of Tierra del Fuego Island.**

The causal mechanisms for human migration to new territories can be various. However, it is known that there is a strong link between past environments and the process of human occupation (Borrero, 1999, 2011; Morello *et al.*, 2009). During the LGIT in Fuego-Patagonia dramatic regional landscape modifications occurred (e.g. advances and re-advances of glaciers, sea level changes) and the changing vegetation mosaics in response to large-scale climatic influences. The spatial changes in vital resources caused by climatic changes may have provoked a reorganisation of human settlement over the landscape (Borrero, 1999). Therefore, reconstructing the changing patterns of vital resources is important to better understand the patterns of human settlement (Borrero, 2011). The first inhabitants of Tierra del Fuego were the terrestrial hunter–gatherers known as the Selknam (Figure 1.12). These family groups of hunter-gatherers occupied the steppe zone in the north and east parts of Tierra del Fuego and the wooded hillsides, meadows and wide valleys of the central region up to the northern slopes of the Cordillera Darwin. The *Nothofagus* forest was historically an important are source for the

early inhabitants of this region (e.g. used for firewood, for foraging food and to build shelters) (Gusinde, 1937; Piqué and Mansur, 2009). The opportunity for the first inhabitants to migrate from South American continent to Tierra del Fuego after the LGM can be linked to regional-scale landscape modification, between c. 15,570 - 14,490 Cal yr BP and c. 12,840 - 12,570 Cal yr BP. Sea level was approximately 120m lower than present and there was a land bridge between Tierra del Fuego and the SSA mainland. The final separation of Tierra del Fuego from the continent took place some time before c. 12,415 - 11,720 Cal yr BP, with the rise of sea level and the formation of the Estrecho de Magallanes (McCulloch *et al.*, 2005b). Massone (2004) and Morello *et al.* (2012) have identified two main phases of terrestrial human occupation in Tierra del Fuego. The earliest human occupation of Tierra del Fuego at c. 12,840 - 12,570 Cal yr BP has been recorded at the Tres Arroyos “rock-shelter” in the mid-eastern section of Tierra del Fuego and the second phase of human occupation in Tierra del Fuego has been dated at c. 6,290- 6,020 Cal yr BP at the head of Bahía Inútil (Figure 1.6). The reason behind the apparent gap in the record of human occupation between c. 12,570 Cal yr BP and 6,290 Cal yr BP is still unclear. Several hypotheses have been advanced to explain the lack of evidence for human occupation during the Early-Holocene to Mid-Holocene, including local extinction or outward-migration of the earlier Late-Glacial groups (Borrero, 1996; Borrero and McEwan, 1997; Prieto *et al.*, 2013). Harsh environmental conditions and the formation of natural barriers may also have caused independent and discontinuous development of human communities (Morello *et al.*, 2012).

### **1.5.7 Past fire activity.**

In Fuego-Patagonia, both human land use and climate have been invoked to explain the spatial and temporal variations in the occurrence of fire (Heusser, 1994; Markgraf and Anderson, 1994; Huber *et al.*, 2004; Moreno *et al.*, 2009). Records from south of latitude ~53°S have reconstructed the fire history for the last c. 16,000 years (Markgraf, 1993; Heusser, 1994;

Markgraf and Anderson, 1994; Huber *et al.*, 2004; Markgraf and Huber, 2010). The degree of any synchrony in fire activity across Fuego-Patagonia has not been clarified due to the difficulty of separating climatic factors from human factors, as well as the different humidity gradients and ignition sources. However, independent of the type of ignition source (human or lightning), climatic conditions conducive to fire appear to have been a key factor in the spread of fires. The differences in site-specific fire histories may be related to climatic gradients as fire regimes appear to differ along a west to east gradient in effective moisture (Markgraf and Anderson, 1994; Huber *et al.*, 2004; Huber and Markgraf, 2010).

Although increased fire activity appears to be strongly correlated to large-scale climate patterns, Heusser (1987) has suggested fire ignition by pre-historic people as the primary cause behind Late Quaternary fire patterns. He proposed the use of sedimentary charcoal as an indicator for human presence and as a tracer for the migration routes of prehistoric hunter-gatherers (Heusser, 1994). In Fuego-Patagonia few studies have researched the link between climate-vegetation-fire frequency during the LGIT and the Holocene and the interactions between vegetation, fire and climate are still poorly understood. However, palaeoecological research using pollen analysis and fire history have been carried out in SSA (~38° - 55°S), which has had the aim to decipher palaeoenvironmental conditions under which major vegetation changes and fire activity occurred during the Holocene (Huber *et al.*, 2004; Candel *et al.*, 2009; Moreno *et al.*, 2009; Borromei *et al.*, 2010; Huber and Markgraf, 2010). In general terms, the regional pollen and charcoal records from “mixed evergreen-deciduous” and “deciduous” forest zones in Fuego-Patagonia indicate that fire activity was greater than present at c.12,000 Cal yr BP and further increased at c. 9,500 Cal yr BP. Fire activity decreased and became more spatially variable at c. 6,000 Cal yr BP until the present day. Each macroscopic charcoal record is a local reconstruction of fire history (Huber *et al.*, 2004; Candel *et al.*, 2009; Borromei *et al.*, 2010; Huber and Markgraf, 2010). To infer landscape, regional, or larger-scale patterns a network of sites is required and analysed to a similar high standard. In most cases, pollen and charcoal data

from the same cores are used to examine the linkages among climate, vegetation, fire, and sometimes anthropogenic activities in the past. The array of fire-history records along latitudinal and longitudinal gradients through SSA identifies the sensitivity and vulnerability of vegetation to past fire occurrence and the underlying climate and vegetation drivers of fire operating at different spatial and temporal scales.

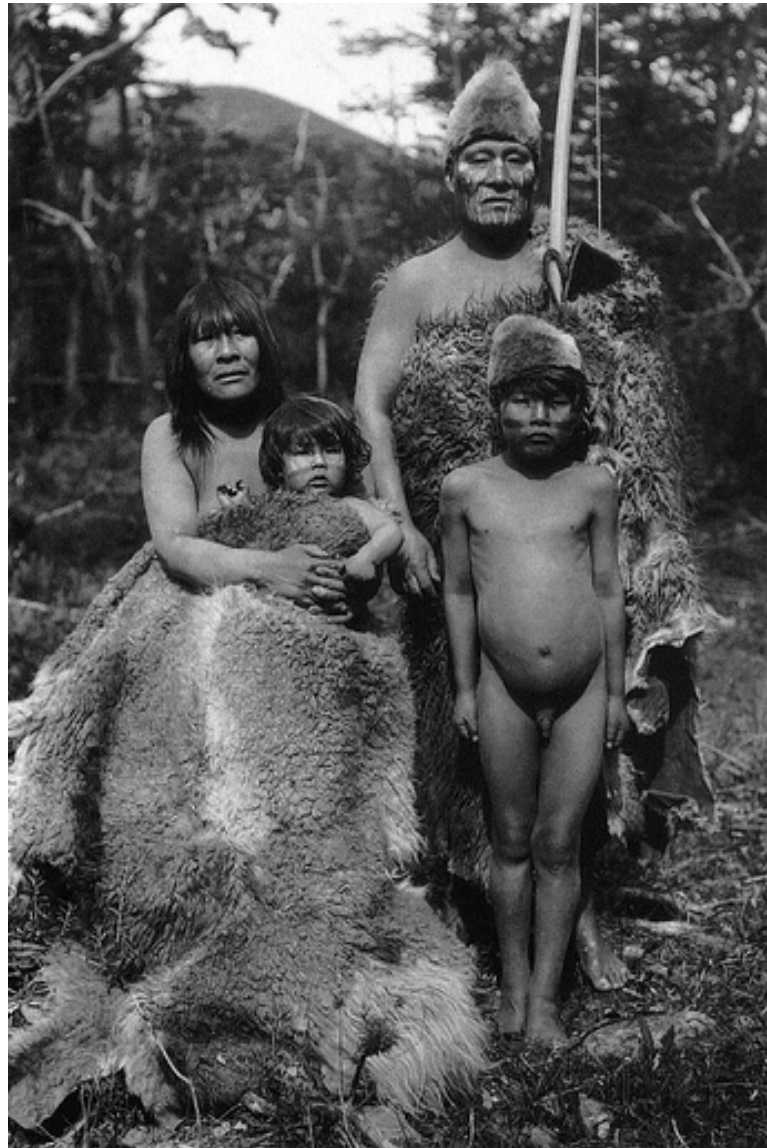


Figure 1.13 Terrestrial hunter-gatherer family of Tierra del Fuego (photograph taken by Gusinde 1918) (From Gusinde, 1937)

## **1.6 Summary.**

Fuego-Patagonia is an ideal region to study environmental changes in the southern hemisphere. The region has the largest extent of ice outside Antarctica due to the distribution of precipitation from the SWWs. The vegetation of Fuego-Patagonia also reflects the precipitation pattern and can be recognised in the pollen rain. The vegetation and ice fields are sensitive to climate changes and to shifts in the distribution of the SWWs. Through the application of pollen analysis, supported by lithostratigraphy, tephrochronology and radiocarbon dating, this study aims to reconstruct the timing and extent of climate-vegetation linkages operating within the Fuego-Patagonian forest/steppe ecotone. It is anticipated that the palaeoenvironmental evidence produced will support inferences regarding variations in the proximity/intensity of the SWWs in Fuego-Patagonia at ~53°S, during the LGIT and the Holocene.

# CHAPTER 2:

## Methodology

This chapter describes the methodology applied in this study. Three high-resolution fossil pollen and charcoal-particle cores were constructed and supported by lithostratigraphy, tephrochronology and radiocarbon dating to achieve the aims of this study. The methodology presented in this chapter is organised by sections following the relative order of the procedures which involved the selection of study sites, methods used to produce the palaeoenvironmental data and how the environmental proxies are presented in the results (Chapter 3).

### **2.1 Study sites.**

The Fuego-Patagonia region is here defined as the geographical area of southern south America that encompass the southernmost part of the South American continent, including Tierra del Fuego (from  $\sim 52^{\circ}\text{S}$  to  $\sim 55^{\circ}\text{S}$ ) (Figure 1.1). The climate of Fuego-Patagonia is influenced mainly by two air masses: sub polar Antarctic air that produces cold, dry stable conditions and, the oceanic southern westerly winds (SWWs) which bring cold, wet and cloudy conditions (Tuhkanen *et al.*, 1990). The predominantly north-south Andean mountain range leads to orographic rainfall, which creates a strong west-east precipitation-vegetation gradient in Fuego-Patagonia ranging from more than 6,000 mm/yr in the west to less than 300 mm/yr in the east (Tuhkanen *et al.*, 1990) (Figure 1.2). The three palaeoenvironmental records in this study were chosen following a longitudinal transect of west-east precipitation-vegetation gradient, reflected

in the present wetter mixed evergreen *Nothofagus* forest in the west to drier deciduous forest in the east (Figure 1.6).

Two fieldwork seasons were carried out; the first during January 2012 on Tierra del Fuego Island (~53°S) and sediment cores were taken from the sites: Punta Yartou and Lago Lynch. The second fieldwork season was carried out in February 2013 and a third core was collected from near to Rio Grande on the north-east coast of Isla Dawson (Figure 1.6).

### **2.1.1 Rio Grande, Isla Dawson (53°39'37"S, 70°30'27"W, altitude 79 m asl).**

Isla Dawson is located between Canal Whiteside and Paso del Hambre in the south-central section of the Estrecho de Magallanes (Figure 1.3). The northern part of Isla Dawson is a low altitude peninsula which rises to ~110 m a.s.l. This peninsula preserves many glacial landforms associated with the retreat of the Magellan glaciers after the Last Glacial Maximum (LGM). The eastern shore of the island is dominated by many elongated mounds oriented east-west, palaeo - meltwater channels and kettle holes now occupied by lakes and bogs (McCulloch and Bentley, 1998). For this palaeoenvironmental study a continuous 750 cm peat sediment core was sampled from a closed peat bog (3 km<sup>2</sup>) within one of the more morphologically defined kettle holes (Figure 2.1)

The vegetation in the central part of the Rio Grande peat bog is characterised by a dominance of *Empetrum rubrum* (Ericaceae) and *Sphagnum magellanicum* moss vegetation (Figure 2.2 and 2.3). This bog community also comprises smaller proportions of *Myrteola nummularia* (Myrtaceae), *Gaultheria pumila* (Ericaceae) and *Tetroncium magellanicum* (Juncaceae). Towards the edges of the peat bog there are wetter conditions and the vegetation community is more dominated by *Marsippospermum* spp. (Juncaceae). A small slope (~5 m) marks the edge of the peat bog and patches of secondary open-canopy mixed-evergreen *Nothofagus betuloides*

forests with low plant diversity surrounds site on the drier ground. The more dominant species associated with evergreen *Nothofagus betuloides* are *Berberis ilicifolia* (Berberidaceae) shrubs and herbs such as *Acaena* spp. This forest is highly modified by logging and other human interventions (e.g. clearance by fire of scrub and woodland for grazing). Due to the poor availability of meteorological records for the region annual rainfall is estimated from precipitation maps produced by Tuhkanen *et al.* (1990) and suggest an annual precipitation of >600 mm/yr evenly distributed throughout the year and mean temperatures in January (austral summer) of 9°C and 1°C in July (austral winter) (Figure 1.2).

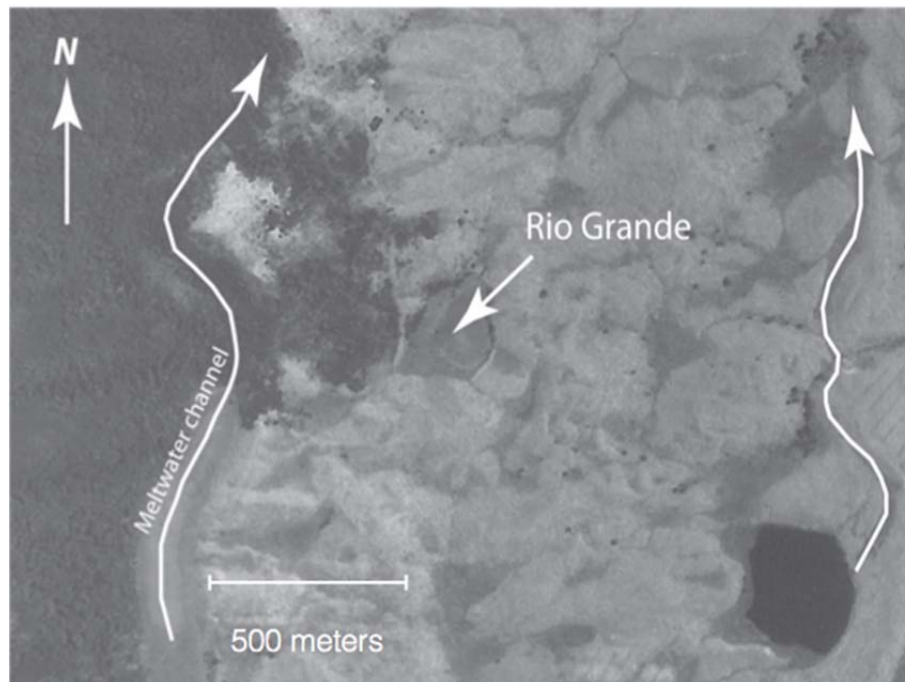


Figure 2.1 Location of the Rio Grande sample site, Isla Dawson.



Figure 2.2 The Rio Grande peat bog within a kettle hole, Isla Dawson (©C.A. Mansilla).



Figure 2.3 The vegetation community dominated by *Empetrum rubrum* (Ericaceae) and *Sphagnum magellanicum* moss vegetation in the central part of the peat bog at Rio Grande (©C.A. Mansilla).

### 2.1.2 Punta Yartou, Tierra del Fuego (53°51'41"S, 70°08'20"W altitude 51 m asl).

The site at Punta Yartou is located on the eastern shore of Canal Whiteside, in the south-western section of Tierra del Fuego (Figure 1.3 and 2.4). This site is located just north of the major fault boundary between the Scotia and American tectonic plates. The north-west to south-east trend of the fault line is expressed through the bedrock peninsula of Punta Yartou. The coastal geomorphology of Fuego-Patagonia has been strongly influenced by glacial fluctuations during the Last Glacial Maximum (LGM) and glacier advances and retreats leading up to the Holocene. The landscape around the study area is dominated by the presence of glacial and glacio-fluvial deposits, glacial landforms, kettle holes, melt-water channels and moraines. The 1,050 cm continuous peat-sediment core was sampled from a deep closed basin (1 km<sup>2</sup>) within a kettle hole within glacial till (Figure 2.5).

The present vegetation at Punta Yartou is characterised by a very wet peat bog dominated by Cyperaceae and lesser amounts of *Sphagnum magellanicum*. There are small dead stands of *Nothofagus betuloides* on the margins of the peat bog, which suggests colonisation of drier-ground tree species in the recent past (Figure 2.5). The small tree diameters (< 15 cm) suggest that the development of the drier phase was relatively short (in the order of decades). The trees did not have fire scars or cut marks and so it is likely that the return of wetter conditions and water saturation probably caused the young trees to die. The current vegetation changes from the centre of the basin to the periphery, beginning with the appearance of *Acaena* spp. and *Gunnera* spp. at the base of the slopes of the basin and higher up on the drier till surfaces *Berberis buxifolia* shrub dominates and the herbs strata is largely *Ribes* spp. and *Adenocaulon* spp. The landscape surrounding the basin is covered by secondary “mixed evergreen-deciduous” forest, dominated by *Nothofagus betuloides* and *Nothofagus pumilio*, and the presence of *Drimys winteri* trees. The forest shows signs of disturbance from logging and fires probably to improve the grazing for cattle. In the more open spaces of the forest *Berberis*

*buxifolia* and *Fuchsia magellanica* shrub can be found. The precipitation at Punta Yartou is estimated from data Tuhkanen *et al.*, (1990) who suggest an oceanic influence with annual precipitation of ~600 mm/yr evenly distributed throughout the year and the mean temperatures in January (austral summer) is 9°C and, 1°C in July (austral winter) (Figure 1.2).



Figure 2.4 Location of the Punta Yartou sample site, Tierra del Fuego.



Figure 2.5 Close peat-bog where the Punta Yartou core was sampled, Tierra del Fuego (©R.McCulloch).

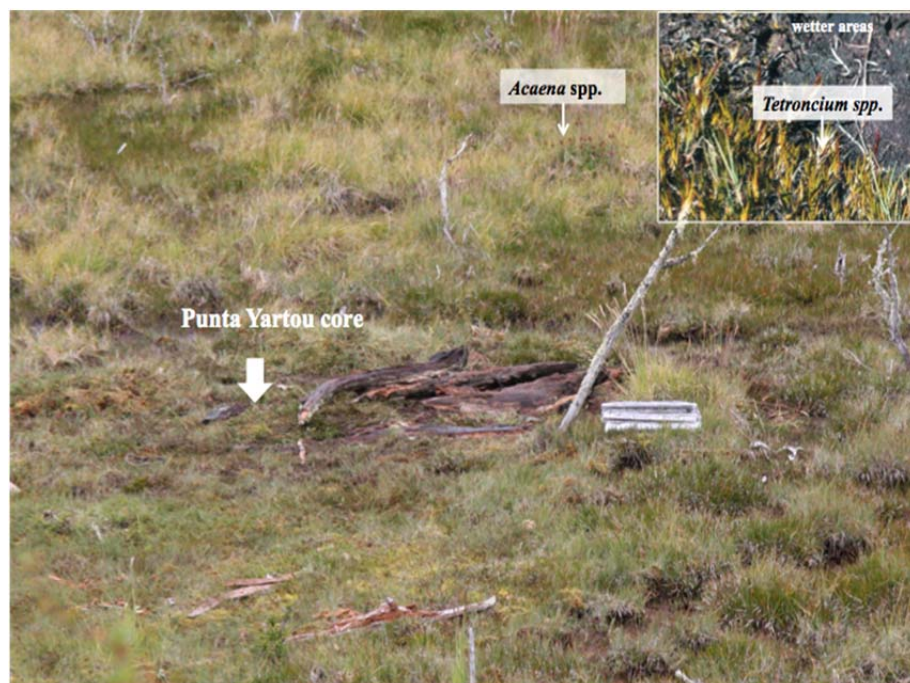


Figure 2.6 The present vegetation community on the peat bog at Punta Yartou site (©R.McCulloch).

### 2.1.3 Lago Lynch, Tierra del Fuego (53°54'20"S, 69°26'19"W, altitude 165 m asl).

Lago Lynch is a large water body in the upper part of the Rio Grande river drainage basin/system (Figure 2.7). The lake surface is about 50 square kilometres. During the LGM advances of small glacier lobes pushed eastwards from Seno Almirantazgo and formed the ice scoured basins of the Lagos Ophidro, Blanco and Lynch (Figure 1.3).

A 950 cm core was sampled from a peat bog located close to Lago Lynch (50 km<sup>2</sup>). The peat bog serves as matrix for a series of small lakes and ponds. This wet peat bog is limited by a distinct frontal moraine (197 m a.s.l.), crossed by the drainage of the Rio Grande river (Figure 2.7). The peat-bog vegetation is dominated by *Sphagnum magellanicum* and in lesser proportions *Tetroncium magellanicum* (Juncaceae). Cyperaceae, *Gaultheria* spp. and *Empetrum rubrum* are scarcely represented. The landscape around the peat bog is covered by primary and secondary *Nothofagus pumilio* “deciduous” forest. The area was in the past century and currently used by forestry enterprises for extensive logging and extraction of wood. This assemblage can be considered as a transition-ecotonal community where forest composition changes gradually from “mixed evergreen-deciduous” forest dominated by *Nothofagus betuloides* (Punta Yartou) to the drier Fuego-Patagonia steppe. The local climate has a continental climatic influence, although the annual precipitation is uniformly distributed throughout the year, with an annual total of ~450 mm. There is a relatively pronounced seasonal difference in temperature, the mean temperature in January (austral summer) is about 9°C and, -3°C in July (austral winter) (Tuhkanen *et al.*, 1990).

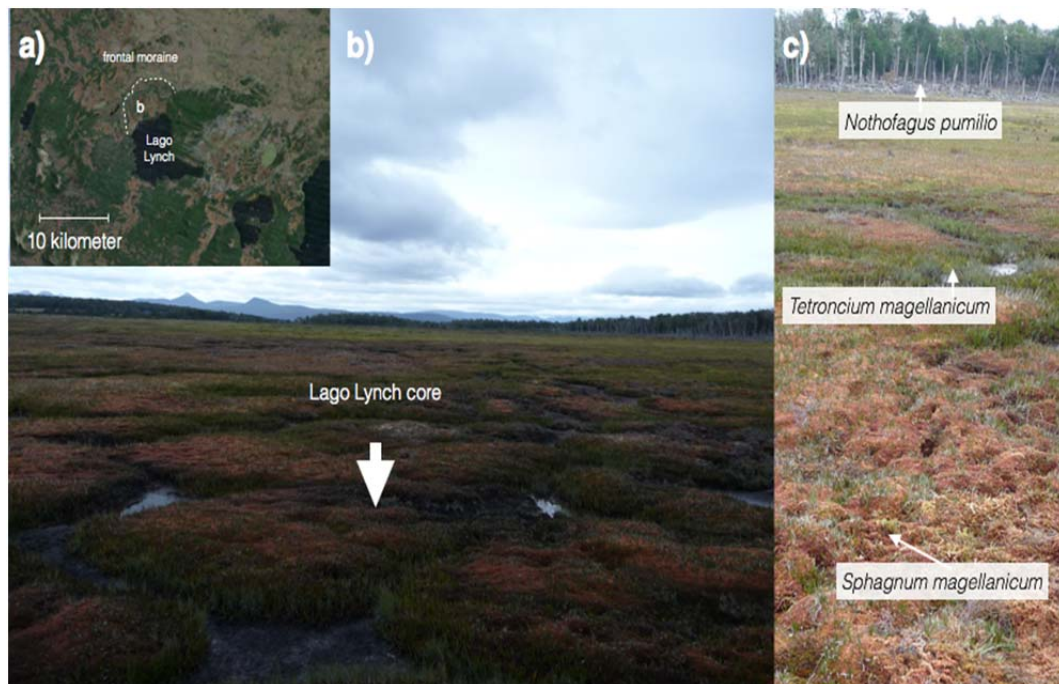


Figure 2.7 The location of the Lago Lynch site, Tierra del Fuego (©J. Kitchen).

## 2.2 Stratigraphy and Loss on ignition (LOI).

The three sediment cores were obtained using a 5.5 cm diameter and 50 cm long Russian corer (Jowsey, 1966) (Figure 2.8). The gross stratigraphic characteristics (e.g. type of sediment, color changes, visual tephra presence) of the sediment cores were noted in the field, each core section was then stored in plastic guttering, sealed in polythene lay-flat tubing, returned to the University of Stirling laboratory and stored at a constant 4°C prior to analysis.

Organic matter content of the sediment was estimated by loss-on-ignition (LOI). The core was sampled at contiguous 2 cm intervals, which were oven-dried for >24 hours at 80°C, to remove water and achieve a stable dry weight. Then, the samples were heated in a muffle furnace for 4 hours at 550°C. The weight percentage organic matter was estimated as the weight loss-on-ignition at 550°C. The weight loss due to combustion is proportional to the amount of organic matter content in each sample.

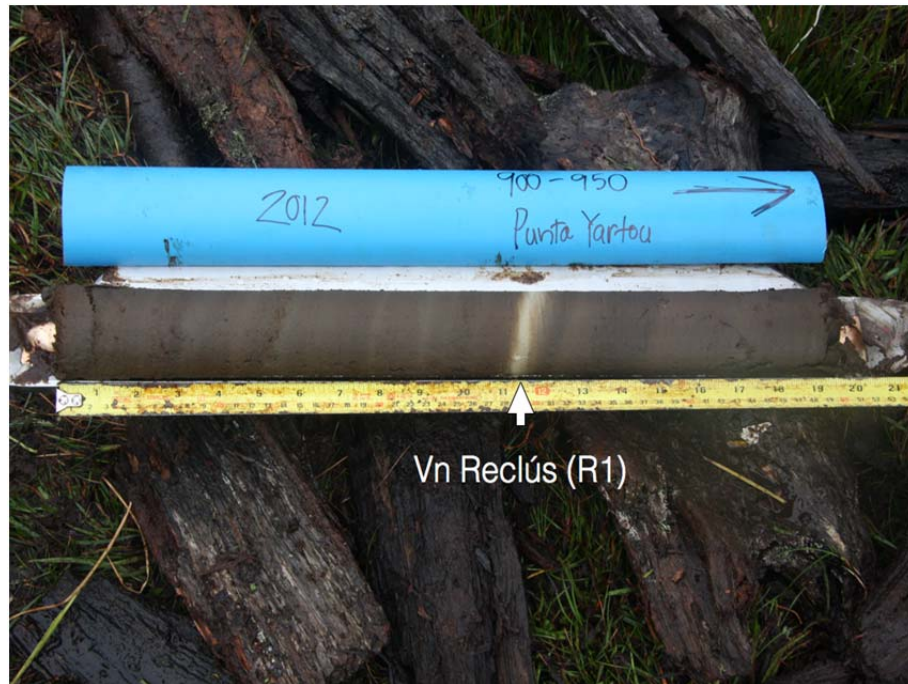


Figure 2.8 An example of a sediment cores obtained using a Russian D-section corer, this section of the core clearly shows the Vn Reclús 1 (R1) tephra layer in the field.

### 2.3 Tephrochronology.

Patagonia lies within the Andean Southern Volcanic Zone (SVZ;  $\sim 33\text{-}46^\circ\text{S}$ ) and Austral Volcanic Zone (AVZ;  $\sim 49\text{-}55^\circ\text{S}$ ) and the Fuego-Patagonia region have been affected by five large-volume ( $>1 \text{ km}^3$ ) explosive eruptions from four different volcanoes; Volcán Hudson ( $\sim 46^\circ\text{S}$ ), Volcán Aguilera ( $\sim 50^\circ\text{S}$ ), Volcán Reclús ( $\sim 51^\circ\text{S}$ ) and Mt Burney ( $\sim 52^\circ\text{S}$ ) (Stern, 2008) (Figure 1.3). Previous geochemical analyses of the tephra layers and geochronological studies of tephra events in Fuego-Patagonia area (Kilian *et al.*, 2003; McCulloch *et al.*, 2005, 2011; Stern, 2008; Heberzetti *et al.*, 2009; Borromei *et al.*, 2010; Sagredo *et al.*, 2011; Stern *et al.*, 2011; Stern in press) have improved the accuracy of the age-depth models of the cores in this study.

### 2.3.1 Visual tephra recognition.

Three macroscopic tephra layers were visually identified in each core in the field (Figure 2.8). Thickness, depth, colour and texture were described. Preliminary descriptions in the field suggests these tephra layers correspond to previously well studied tephras in Fuego Patagonia: Mt Burney 2, Vn Hudson 1 and Vn Reclús 1 (Kilian *et al.*, 2003; McCulloch *et al.*, 2005, 2011; Stern, 2008; Heberzetti *et al.*, 2009; Borromei *et al.*, 2010; Sagredo *et al.*, 2011; Stern *et al.*, 2011; Stern in press). These assumptions were later confirmed by geochemical analysis and radiocarbon dating (Section 3.2.).

### 2.3.2 Isolation and preparation of tephra for geochemical analysis

An acid digestion technique was used to obtain clean sub-samples of the mineral content, free from organic material, suitable for electron microprobe analysis (Dugmore *et al.*, 1992). Contiguous sub-samples of 2 cm<sup>3</sup> sediment were prepared from each core for the section between Mt Burney 2 (B2) and Vn Reclús 1 (R1) tephra layers. This interval was chosen due to previous studies which have identified micro-tephra layers in cores between the B2 and R1 eruptions (Kilian *et al.*, 2003, McCulloch *et al.*, 2005a,b; Stern, 2008). The identification of cryptotephra layers provides further information for building of a more reliable tephrochronology for the study sites. Each sample was placed in an Erlenmeyer conical flask and ~75ml of concentrated Sulphuric acid 98% Standard Laboratory Reagent (SLR) added and simmered at 280°C. After 1 to 2 hours a few drops of Nitric acid S.G. 1.42 68-72% SLR were added until the liquid contents of the flasks turned transparent. The samples were then cooled and distilled water very slowly added. The samples were then left to settle overnight and then the supernatant was drawn off using a pipette and a gentle water vacuum pump to avoid disturbing the settled sediment at the bottom of the flask. The remaining sample was then

transferred to a 50 ml falcon tube and centrifuged at 2,500 rpm for 5 minutes, this procedure was repeated until all the residual acid had been washed from the mineral residue.

### 2.3.3 Geochemical analysis.

The preparation of tephra samples for geochemical analysis by electron microprobe was followed the main steps of the protocols made by Steele and Engwell (2009). Slides were prepared using 600 carborundum powders to produce a frosted surface. This allows the resin to bond properly to the slide. The slide was then ultrasonically cleaned for a few minutes in water and detergent to remove any residual coarse carborundum and degreased using Petroleum spirit (Pet Ether) (Figure 2.9).

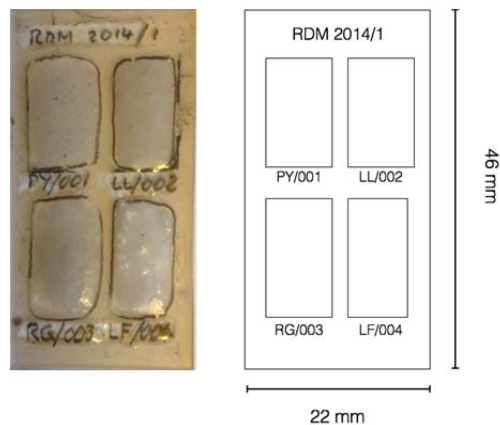


Figure 2.9 Four tephra samples mounted on a glass slide prepared for electron microprobe analysis.

Tephra samples were then placed on the slide and mixed with epoxy resin. The slides-samples were then cured on a hot plate at  $\sim 60^{\circ}\text{C}$  for  $\sim 1$  hour to allow the resin to fully cure.

Slide-samples were ground progressively and carefully to produce a uniform and flat surface. The grinding was made the following grades: 400, 800, 1,200 and finally 2,500 until the sample

thickness was ~0.1 mm. A micrometer was used to monitor sample thicknesses to maintain relative equal sample thicknesses.

Finally, the slide-samples were polished to ~75  $\mu\text{m}$  thickness, using the 6 $\mu\text{m}$  diamond-polishing lap and then the 1  $\mu\text{m}$ -polishing lap for up to 15 minutes each. Then, the samples were put in a slide holder in a beaker of pet-ether and placed in the ultrasonic bath for 5–10 minutes between the 6  $\mu\text{m}$  and 1  $\mu\text{m}$  polishing grades and after the 1  $\mu\text{m}$  polish step. The slides were then checked using a reflected-light microscope to assess the quality of the surface polish before carbon coating the samples prior to electron microprobe analysis (Figure 2.9).

The tephra samples were analysed by electron microprobe at the Tephra Analysis Unit (TAU), at the School of GeoSciences, The University of Edinburgh. A minimum of ten individual glass shards were analysed to geochemically characterise a tephra layer. Ten major elements (Sodium oxide,  $\text{Na}_2\text{O}$ ; Magnesium oxide,  $\text{MgO}$ ; Aluminium oxide,  $\text{Al}_2\text{O}_3$ ; Potassium oxide,  $\text{K}_2\text{O}$ ; Calcium oxide,  $\text{CaO}$ ; Iron oxide,  $\text{FeO}$ ; Silicon dioxide,  $\text{SiO}_2$ ; Phosphorus pentoxide,  $\text{P}_2\text{O}_5$ ; Titanium dioxide,  $\text{TiO}_2$ ; Manganese oxide,  $\text{MnO}$ ) were analysed, with a 3 $\mu\text{m}$  beam operating at 15kv and 2nA during a 20 second analysis period to minimise the volatilisation of the more labile elements (Hayward, 2011).

#### **2.4 Chronology.**

The calendar ages of depths of the sediment cores were obtained from age-depth models constructed from the tephrochronology and radiocarbon age information. The samples for radiocarbon analysis were chosen to constrain specific stratigraphic events within each core, for example, sedimentary changes, changes in the pollen assemblages, charcoal peaks, tephra layers and also the depth intervals between samples to ensure a robust age-depth model.

#### **2.4.1 Sediment accumulation rate.**

The choice of the age-depth model was based on prior knowledge about the sediment deposition rate changes which can suggest a stable or unstable environment in terms of the sediment accumulation for each core through the time (Grimm *et al.*, 2014; Blaauw, 2010). In this study there is the advantage of the presence of the three visual tephra layers in each core which enabled the construction of rudimentary age-depth models to evaluate the presence/absence of significant sediment deposition changes, outlier data and uncertainties. This preliminary work established that the Bayesian age-depth modelling program BACON 2.4 (Blaauw and Christen, 2011) using the southern hemisphere calibration curve 2013 (SHcal13) (Hogg *et al.*, 2013) was most appropriate for age-depth modelling for each sediment core in this study.

#### **2.4.2 Radiocarbon samples.**

The samples for radiocarbon analysis were obtained from bulk sediment and fine plant material; samples were taken from immediate layers (<1 cm) below the event that was considered relevant to date (e.g. tephra layer, significant sedimentary, pollen or charcoal changes). The samples taken from marl, bluish-grey clays or silts, or from low organic material sediment were screened using a 125 µm stainless steel to ensure only plant material was dated (McCulloch *et al.* 2005a). Accelerator Mass Spectrometry (AMS) age estimates were purchased from the Scottish Universities Environmental Research Centre (SUERC), East Kilbride and also supported by the Natural Environment research Council (NERC) radiocarbon facility, East Kilbride. The pre-treatment of samples at both facilities involved the digestion of the samples in 1M HCl (80°C, 8 hours), then washed free from mineral acid using deionised water and then digested in 0.5M KOH (80°C, 2 hours). The sample was then repeatedly washed using deionised water until no further humic acid was extracted. The residue was rinsed free of alkalis, then further digested in 1M HCl (80°C, 2 hours) and then rinsed free of acid, dried and

homogenised. The total carbon of the pre-treated sample was recovered as CO<sub>2</sub> by heating with CuO in a sealed quartz tube. The gas was converted to graphite by Fe/Zn reduction.

### **2.4.3 BACON: Bayesian age-depth modelling.**

Bayesian age-depth modelling software BACON 2.4 (Blaauw and Christen, 2011) using the SH13 calibration curve (Hogg *et al.* 2013) produced the age-depth model for each sediment core in this study. The age-depth model for Rio Grande core was built with 4 AMS radiocarbon dates from bulk organic material and fine plant material, supplemented by the correlation of three previously radiocarbon dated tephra layers (see Section 3.3.1). The Punta Yartou chronology was constrained by 15 AMS radiocarbon dates (from bulk organic material and fine plant material) and three previously published tephra layer radiocarbon ages. Due to preliminary information about the sediment deposition time (yr/cm) changes, the record was divided in two sections at 931cm (see Section 3.3.2). The chronology of Lago Lynch core was built with 5 AMS radiocarbon dates (from bulk organic material) and by the correlation of 4 previously dated tephra layers (see Section 3.3.3).

## **2.5 Pollen methodology.**

The purpose of the pollen sample preparation methods is to produce a sediment residue with high pollen and spore concentrations and to remove as much non-pollen and spore material from the samples. A series of chemical and mechanical standard treatments were used.

### **2.5.1 Subsampling.**

Sediment sub-samples of 1cm<sup>3</sup> were taken at intervals of 4 cm or 8 cm intervals from each core. The criteria used was to aim for sub-centennial resolution for key vegetation community

changes, additional samples were taken when the age control was known for improving the resolution between initial choices of sub-sampling. This strategy resulted in 90, 89 and 89 pollen samples for Rio Grande, Punta Yartou and Lago Lynch cores respectively.

### **2.5.2 Pollen preparation.**

The pollen processing followed was a modified version of the pollen procedures of Moore *et al.*, (1991) and Faegri and Iversen (1989). The basic procedure for fossil pollen preparation is described below:

The 1 cm<sup>3</sup> of sediment was consistently measured by displacement using a 10 ml measuring cylinder, containing 3 ml of Hydrochloric acid (HCL) 10%v/v. This also served to remove carbonates and then the sub-samples were transferred into 10 ml polypropylene centrifuge tubes. A *Lycopodium clavatum* spore tablet of known concentration was added to each sample to enable the estimation of pollen concentrations (Stockmarr, 1971). The absolute abundance of pollen (concentrations) is a useful interpretative tool, complementing the classical pollen percentage presentation technique (Bennett and Willis, 2001). The centrifuge tubes were then centrifuged (2,500 rpm for 5 minutes) and the supernatant decanted. Sodium Hydroxide (NaOH) 10% w/v was added to each samples which was then heated in a hot water bath for ~25 minutes to remove soluble humic acids and then the tubes were centrifuged (2,500 rpm for 5 minutes) and the supernatant decanted.

The samples were sieved through 180 µm stainless steel mesh, to remove coarse debris. A 10 µm nylon sieve mesh was also used to remove material less than 10 µm, predominantly clay particles. The fine sieving also uses large amounts of distilled water and so also helps to wash away the remaining soluble humic acids.

Sub-samples taken from mineral-rich sediment (e.g. glacial sediment such as clays, silts and from mineral-rich lake sediment) were also treated with Hydrofluoric acid (HF) 40% and placed in a boiling hot water baths for approximately 15 minutes. After this each centrifuge tube was balanced with HCL acid 10% prior to being centrifuged, decanted and the supernatant decanted. A further 6ml of HCL acid 10% was added to ensure the removal of any fluorides formed during the silica digestion and to wash away traces of HF acid 40%. Samples were centrifuged and the supernatant decanted.

The cellulose content of pollen was removed by acid hydrolysis. Samples were first dehydrated with 4ml of Acetic acid Glacial >99% SLR, and then the Acetolysis solution of 9 parts of Acetic anhydride acid >97% SLR to 1 part of Sulphuric acid concentrate >98% SLR added. The centrifuge tubes were then placed into a boiling water bath for ~3 minutes. Samples were then centrifuged and the supernatant decanted. Samples were then treated with a Acetic acid Glacial to remove the Acetolysis residues, stirred, centrifuged and the supernatant decanted and then washed with ~7 ml of distilled water, stirred, centrifuged and the supernatant decanted.

The samples were finally dehydrated with ~4 ml of Tert-Butyl Alcohol (TBA) >99% SLR, stirred, centrifuged and the supernatant decanted. This step was repeated twice. Each sub-samples was then transferred to a glass specimen tubes (12 x 50 mm) labeled and ~0.3ml of Silicone oil added. Then the glass specimen tubes were centrifuged and finally, the glass specimen tubes were placed in the Grant Heat Block and heated at 45°C for 12 hours to evaporate the remaining TBA.

### **2.5.3 Taxonomical and morphological fossil pollen classification.**

Pollen grains were counted and identified using an Olympus BX41 light microscope, at 400x magnification. A minimum total of 300 land pollens (TLP) were counted per sample, excluding

Cyperaceae. The pollen and spores were identified using the reference collection made by R. McCulloch (1992) with herbarium material provided by the Departamento de Botánica, Universidad Austral de Chile and supported by photographs of pollen and spores (Heusser, 1971; Villagrán, 1980; Wingenroth and Heusser, 1984; Moore, 1991).

The family taxonomic level was based on the Angiosperm Phylogeny Group (APG III 2009), for the Asteraceae family and the sub-families were based on Panero and Funk (2008) and for genus and species from studies of the native vegetation in Fuego-Patagonia (Moore, 1983; Henríquez *et al.*, 1995). The fossil pollen nomenclature does not have an international standard (Klerk and Joosten, 2007), which can be slightly different among studies. Therefore, this study simplifies the nomenclature following this taxonomical classification:

a) If a complete family produces pollen grains that cannot be morphologically distinguished or a differentiation cannot be made with standard light-microscopy, the group was named by the respective family name (e.g. Amaranthaceae, Apiaceae, Caryophyllaceae).

b) If the pollen grain morphological category is produced by one genus and the species level cannot be identified, the group was named only by the respective genus (e.g. *Acaena*, *Myriophyllum*, *Sphagnum*).

c) If the pollen grain can be morphologically identified at species level, it was named by the respective species (e.g. *Myrteola nummularia*, *Drapetes muscosus*, *Drimys winteri*).

However, further taxonomic distinctions can be made but do not lead to specific genus or species levels and these key taxa are considered below:

*Nothofagus dombeyi* type and *Nothofagus obliqua* type: The genus have very distinctive pollen

grains, are 5–8 porate, rarely 4 or 9 porate and the pollen surface is microechinae (Heusser, 1971). *Nothofagus dombeyi* type includes those species that have distinctively annulate pores. *Nothofagus obliqua* type includes those where the pore appears more as a simple slit in the pollen wall (Figure 2.10). The number of pores that can be found for each *Nothofagus* species varies and although there is a mean number there is too much overlap between species to enable reliable identification below the level of the two types (Heusser, 1971). Therefore, few studies have used the morphological features of *Nothofagus* to define species-specific ecological ranges. A recent exception to this is the study by Fontana and Bennett (2012) who suggest that a shift in the pore numbers of *Nothofagus dombeyi* type pollen during the Holocene indicates a change from *Nothofagus Antarctica* woodland to *Nothofagus betuloides*. However, this work requires independent testing against macrofossil remains of *Nothofagus* to see if it provides reliable information.

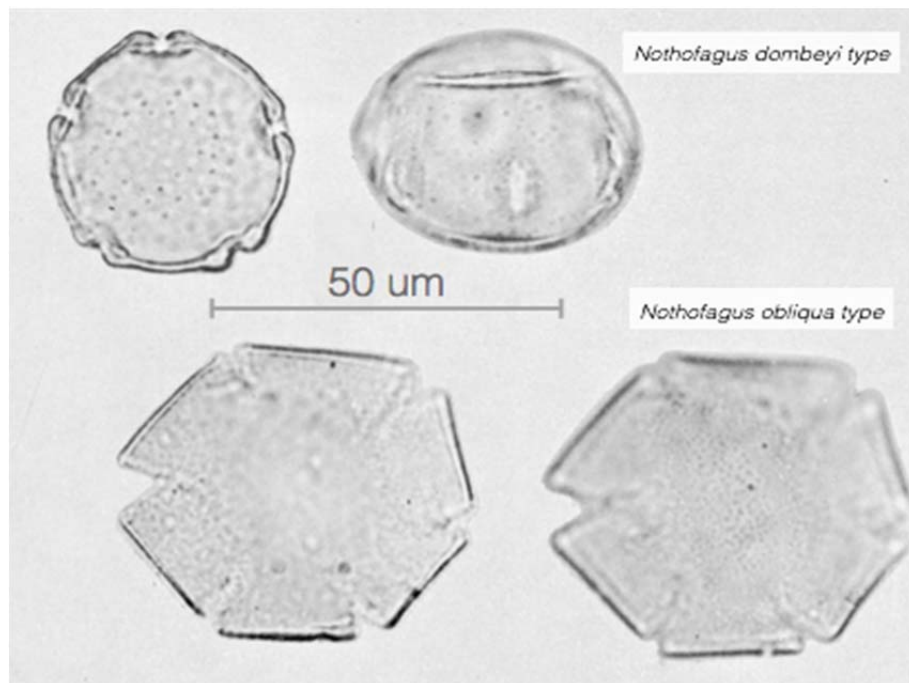


Figure 2.10 *Nothofagus dombeyi* “type” and *Nothofagus oblique* “type” pollen grain (Heusser, 1971).

Pollen recorded as 'unidentified' indicates a terrestrial pollen grain that was highly deteriorated and so although recognized as pollen could not be identified at any level. Also, included in this category are a number of pollen grains that could not be taxonomically identified. These should perhaps have been separated as 'unknown' but they were not present in all the sub-samples and formed less than <1% of the TLP.

Cyperaceae was excluded from the pollen sum, but their percentages were expressed in addition to the TLP sum because sedges can often be a dominant component of the mire vegetation that can lead to the underestimation other taxa in the vegetation assemblage.

Polypodiaceae within the group of Pteridophytes was commonly identified to family level except *Polypodium* and *Lycopodium*.

The genus *Sphagnum* was the only moss that was identified and considered in the interpretation of the assemblage's vegetation. This genus is dominant in peat-bog communities.

The aquatic *Myriophyllum* has been identified in previous palaeoenvironmental studies in Fuego-Patagonia although the ecological meaning of this aquatic at species level is ambiguous. Thus, in this study *Myriophyllum* is interpreted at genus level. Moore (1983) and Heusser (1994) suggest that these aquatic angiosperms grow in clear shallow water and in littoral zones of lakes within humid areas of Patagonia between 0-330 m a.s.l. The present altitudinal distribution of *Myriophyllum* indicates that it grows at a minimum temperature of c. 3°C. More botanical research is required to better understand the ecological range of *Myriophyllum* to support more meaningful interpretations from this taxon.

*Pediastrum* is a genus of fresh water algae (Komárek and Jankovská, 2001). There are few studies from Fuego Patagonia that are concerned with the algal species of *Pediastrum* and its

response to environmental change (Willie *et al.*, 2007; Tell *et al.*, 2011; Waldmann *et al.*, 2014). Recent studies focused on the geographic distribution and biodiversity of the *Pediastrum* in fresh water Patagonian lakes highlight the complexity of the types of water bodies that they inhabit. Additionally, there exists poor understanding of the endemic Patagonian species, e.g. *Pediastrum patagonicum*, which is restricted to cold temperate areas (Tell *et al.*, 2011). The most dominant species found during LGIT are *Pediastrum kawraiskyi* and *Pediastrum boryanum* in Potrok Aike (Willie *et al.*, 2007) and, *P. kawraiskyi* in Lago Fagnano (Waldmann *et al.*, 2014) (Figure 2.11). Both species have very different responses to environmental changes. The high presence of *P. kawraiskyi*, was identified in cold, oligotrophic lake conditions with low productivity (Willie *et al.* 2007; Waldmann *et al.*, 2014). Other studies of lakes from around the world suggest that *P. boryanum* and its varieties are abundant in eutrophic lakes (but not polluted waters) and warmer conditions with higher productivity (Komárek and Jankovská, 2001). In this study *P. boryanum* was the dominant species and other species were not encountered (Figure 2.11).

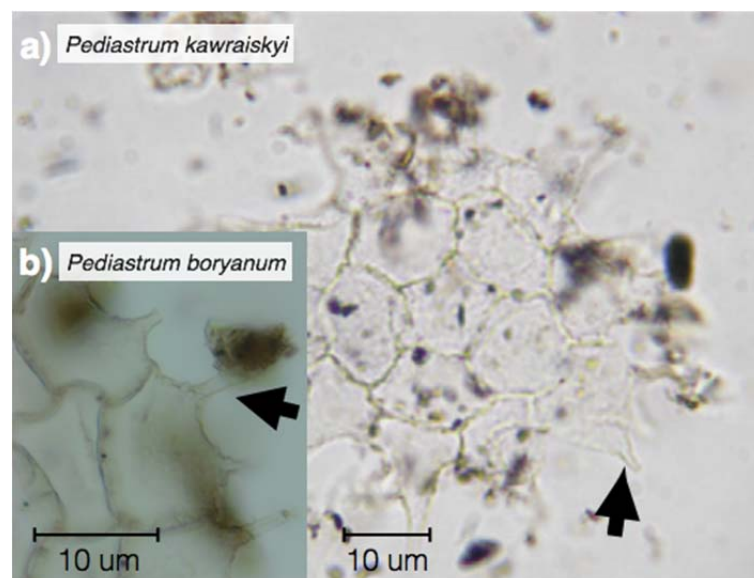


Figure 2.11 Fresh water algae *Pediastrum*. a) *Pediastrum kawraiskyi* (From Waldmann *et al.*, 2014); b) *Pediastrum boryanum* (©C.A.Mansilla).

## 2.6 Pollen stratigraphy.

Pollen and spore diagrams were produced using Tilia and Tilia-Graph software, version 1.7.16 (Grimm, 1987). The Local pollen assemblage zones (LPAZ) were defined using land pollen >2% and stratigraphically constrained incremental sum-of-squares produced cluster analysis (CONISS; Grimm, 1987). All the terrestrial fossil pollen grain, excluding “unidentified” pollen grains and Cyperaceae were included to produce the total land pollen sum (TLP).

The taxa outside of the main sum can vary regionally (Smol *et al.*, 2002). The frequency of each taxa such as Cyperaceae, *Pediastrum* and unidentified pollen grains have been presented as a percentage of the main sum + individual sum (TLP + taxon). Taxa, such as Juncaceae, *Lycopodium*, Polypodiaceae, *Polypodium*, *Sphagnum*, others spores and *Myriophyllum* have been grouped all as “Aquatics and Spores” and the frequency of each taxa have been presented as a percentage of main sum + group sum (TLP+ Aquatics and Spores).

## 2.7 Pollen and spore concentration (grains or spores per cm<sup>3</sup>).

Pollen concentrations were calculated using the method of adding a known quantity of exotic spores (*Lycopodium*) to each sediment sample of 1.0 cm<sup>3</sup> taken from Rio Grande, Punta Yartou and Lago Lynch cores during the laboratory preparation of samples (Stockmarr, 1971). Total pollen concentration values were calculated for all the terrestrial pollen taxa. Selected taxa that contribute the majority of the total pollen concentrations are presented. The following describes the characteristic of some of the trees and shrubs identified in this study:

*Nothofagus dombeyi* type and *Nothofagus obliqua* type: *Nothofagus* is a monoecious genus, the trees possess both male and female flowers but the flowers mature at different times, which is a reproductive strategy that promotes out-crossing via wind dispersal (Veblen *et al.*, 1996). Thus,

the percentage pollen of *Nothofagus dombeyi* type and *Nothofagus obliqua* type can be over-represented in the fossil pollen diagram and the pollen grains can travel long distances from the source areas.

*Misodendrum*: This plant is an exclusive epiphyte and semi-parasitic on the *Nothofagus* genus, whose pollen does not disperse widely and it is mainly abundant on *Nothofagus antarctica* and in more open *Nothofagus* forest or where *Nothofagus* is more stressed (Markgraf *et al.*, 2002). Thus, the presence of this epiphyte in the pollen record can be interpreted as local presence of the forest or the presence of an open *Nothofagus* forest around the study site.

*Drimys winteri*: These trees produce low quantities of large and heavy pollen grains; they are entomophilous in their pollination which leads to their underrepresentation in the modern pollen rain. Thus, the presence of *Drimys winteri* in the fossil pollen diagram can be interpreted as significant of local growth (Villa-Martinez *et al.*, 2012).

Ericaceae: these are dwarf shrubs that are represented in Fuego-Patagonia as *Empetrum rubrum* and the genus *Gaultheria* (Moore, 1983; Henriquez *et al.*, 1995). There are few studies concerning the pollen rain of these taxa. However, the family is predominantly entomophilous in its pollination. Thus, the presence of these taxa in the fossil pollen diagram can be interpreted as local presence, mainly through the colonisation of peat bogs.

## **2.8 Pollen preservation.**

The record of pollen preservation provides a valuable tool that gives additional palaeoenvironmental information, especially in sections of the records sequence where the pollen diversity is low and where major depositional changes happen. However, few studies from Fuego-Patagonia have used this methodology to obtain additional information to assist reconstruction of the past environmental changes (McCulloch and Davies, 2001).

The different characteristic of the structure and ornaments of the pollen exine (the wall) can affect pollen preservation. There is a general tendency e.g. Asteraceae, Amaranthaceae pollen families to have thick and highly ornamented exines and so are potentially better preserved or more resistant to damage. In contrast pollen, such as Cyperaceae and Poaceae have thin and smooth exines and are, therefore, more susceptible to damage.

Pollen preservation data are presented as percentages based on the sum of Total Land Pollen (TLP) sum. The criteria to classify the different type of deterioration are based on Cushing (1967) and Tipping (1987), who classified and distinguished five categories of pollen grain preservation; normal or well preserved, broken, crumpled, corroded and degraded. The normal pollen grains are not damaged, broken pollen have one or more ruptures in the exine, crumpled pollen grains are twisted or folded along more than one axis. Corroded pollen grains have perforations and degraded pollen grains have their exines substantially altered (Cushing, 1967; Tweddle and Edwards, 2010) (Figure 2.12). Many factors can affect the pollen preservation. However, these factors can be grouped into three main categories: mechanical (broken and crumpled) and chemical and biological (corroded and degraded) (Tipping, 1987).

Broken and crumpled pollen are considered to have been damaged by mechanical factors. The first agent that begins to destroy pollen grains, either before or after deposition, tends to be mechanical degradation. After deposition pollen grains can become further abraded by physical factors, including temperature and moisture, which act mechanically to alter the pollen exine (Grill *et al.*, 2007). Also, the broken and crumpled pollen damage have been associated with inwashed inorganic sediments (Birks, 1980; Tipping, 1987) and experimental studies have indicated that repeated phases of wetting and drying can have a significant effect and can lead to both breakage and corrosion (Holloway, 1989; Campbell, 1994) (Figure 2.12).

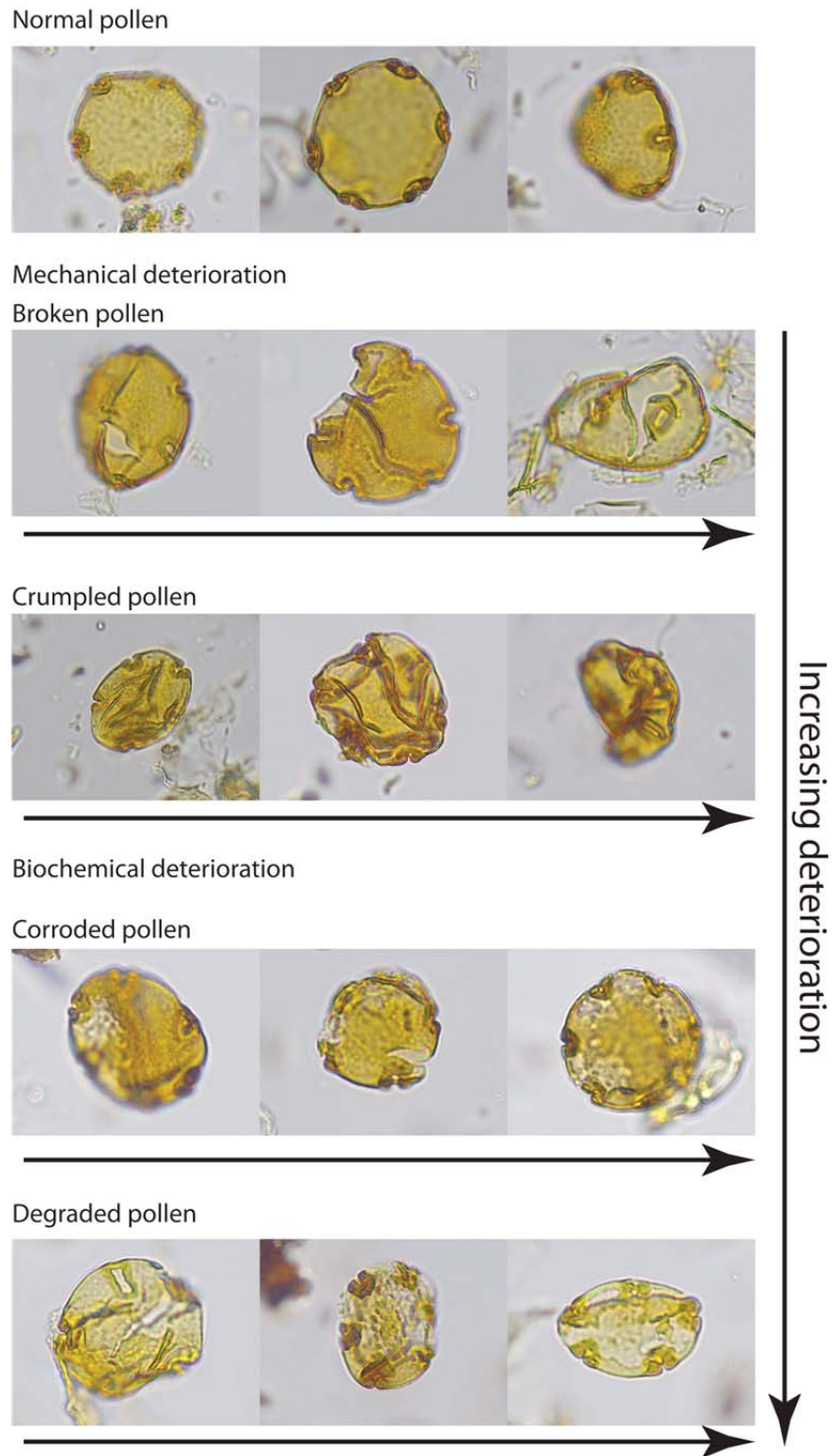


Figure 2.12 The five categories of pollen grain preservation; normal or well preserved, broken, crumpled, corroded and degraded.

Pollen grains are best preserved (i.e normal) in the wetter-acidic and anaerobic conditions of peat bogs and undisturbed lake sediments. Corroded and degraded pollen are considered to have been damaged by biochemical factors operating under more aerobic conditions. They can be caused by chemical oxidation and the actions of bacteria and fungi (Havinga, 1964, 1984). Degraded pollen have been associated mainly with processes that involve higher biological activity (Havinga, 1984) (Figure 2.12).

### **2.9 Charcoal concentration (charcoal particles per cm<sup>3</sup>).**

Charcoal particles were counted and measured alongside the pollen material using an Olympus BX41 light microscope, at 400x magnification. Charcoal particles are visually opaque, angular and usually planar, black fragments. Dark plant fragments can be distinguished from charcoal by applying pressure to the particles, if they fracture under pressure and form smaller angular fragments they tend to be charcoal, whereas plant fragments compress (Whitlock and Larsen, 2001). The mechanisms by which charcoal is produced and dispersed are not comparable with pollination strategies and so the charcoal data is presented as concentrations (particles per cm<sup>3</sup>) estimated using the *Lycopodium* spore tablets.

The charcoal particles were classified in categories by size as micro charcoal: from <25 µm to 100 µm and as macro-charcoal: from 101 µm to 180 µm (Whitlock and Larsen, 2001). Particles >180 µm were removed during the pollen sample preparation and so the macro-charcoal category is of limited value on its own and so this data is grouped with the total micro charcoal concentration. Theoretical models have predicted that particles <100 µm in size travel well beyond 100 m, and very small particles can travel longer distances (regional fires signal). Also, the models suggest that charcoal particles smaller than ~200 µm can be deposited within 6 km from the source (local fires signal) (Whitlock and Larsen, 2001). Therefore, the charcoal concentration data obtained by this study helps to examine regional linkages among past

vegetation changes, variations in the pattern of the distribution of past fire activity, large-scale controls of fire by climate and the timing of occupation of the first inhabitants on Tierra del Fuego.

The methods presented above enabled the reconstruction of the three palaeoenvironmental cores obtained this study: Rio Grande, Punta Yartou and Lago Lynch. The order of the cores follows the west-east precipitation gradient, reflected in the present wetter “mixed-evergreen” *Nothofagus* forest in the west (Rio Grande) to drier “deciduous” forest in the east (Lago Lynch). The pollen analysis was supported by lithostratigraphy, tephrochronology and radiocarbon dating and additional palaeoecological information for each core is presented: pollen concentrations (grains per cm<sup>3</sup>), terrestrial pollen preservation and charcoal concentrations as a proxy of past fire activity. This methodology has enabled the reconstruction of the timing and extent of climate-vegetation linkages operating within the Fuego-Patagonian forest/steppe ecotone presented in Chapter 3, from which we may infer the large-scale controls of climate and the changing proximity/intensity of the SWWs in Fuego-Patagonia.

# CHAPTER 3:

## Results

The results presented in this chapter are organised in sections related to the three-palaeoenvironmental cores obtained by this study: Rio Grande, Punta Yartou and Lago Lynch. The order of the cores follows the west-east vegetation-precipitation gradient, reflected in the present wetter “mixed-evergreen” *Nothofagus* forest in the west (Rio Grande) to drier “deciduous” *Nothofagus* forest in the east (Lago Lynch) (see Section 1.5.4). The stratigraphy of each site is presented first. This then identifies the tephra layers found within each core. The tephrochronology is then reinforced using radiocarbon dating. The resulting chronology is then used to provide robust age-depth models for each core and which is applied to the palaeoenvironmental data. The pollen data is then presented as local pollen assemblage zones constrained by the age-depth models. The pollen data is then supported by additional palaeoenvironmental information for each core: the pollen concentrations (grains per cm<sup>3</sup>), the pollen terrestrial pollen preservation and, finally the charcoal concentrations (particles per cm<sup>3</sup>) as a proxy of past fire activity.

### **3.1 Stratigraphy.**

#### **3.1.1 Rio Grande.**

The Rio Grande core is 750 cm long and was sampled from a closed peat bog (Figure 2.1 and 2.2). Between 750 cm and 645 cm depth, the basal stratigraphy contains bluish-grey clay and

silt. From 645 cm to 550 cm the core sample consists of black organic-rich lake sediment and from 550 cm to 214 cm there is laminated lacustrine-mud. The uppermost section of the sediment core from 214 cm to the surface is characterised by peat. Well-preserved plant fragments, including leaves were found between 540 cm and 539 cm and 484 cm and 483 cm depth. The leaves found are identified as being from the arboreal specie: *Nothofagus betuloides* (Figure 3.2).

The Rio Grande gross stratigraphy estimated from loss-on-ignition at 550°C (LOI<sub>550</sub> %) may be divided into five sections: 1) 750 cm to 645 cm depth is less than 10%, 2) 645 cm to 550 cm the organic content fluctuates between 10% and 62%, 3) 550 cm to 351 cm the organic content oscillates around 20%, 4) 351 cm to 214 cm the organic content increases gradually from ~20% to ~80% and finally, 5) between 214 cm to 0 cm there is high organic content  $\geq 80\%$  (Figure 3.1).

### **3.1.2 Punta Yartou.**

The site at Punta Yartou is a precipitation fed kettle hole, steep sided and near circular and containing 1,098 cm of soft lacustrine sediments and peat (Figure 2.4 and 2.5). Above 1,098 cm to 1,066 cm the basal sediment consists of bluish-grey clays and silts. Between 1,066 cm and 980 cm marl is interbedded with more organic-rich sediment. From 980 cm to 726 cm there is organic-rich lacustrine-mud; the upper boundary at 726 cm marks a shift to peat that continues to the top of the core. From 98 cm the fen peat was too unconsolidated and could not be sampled (Figure 3.3).

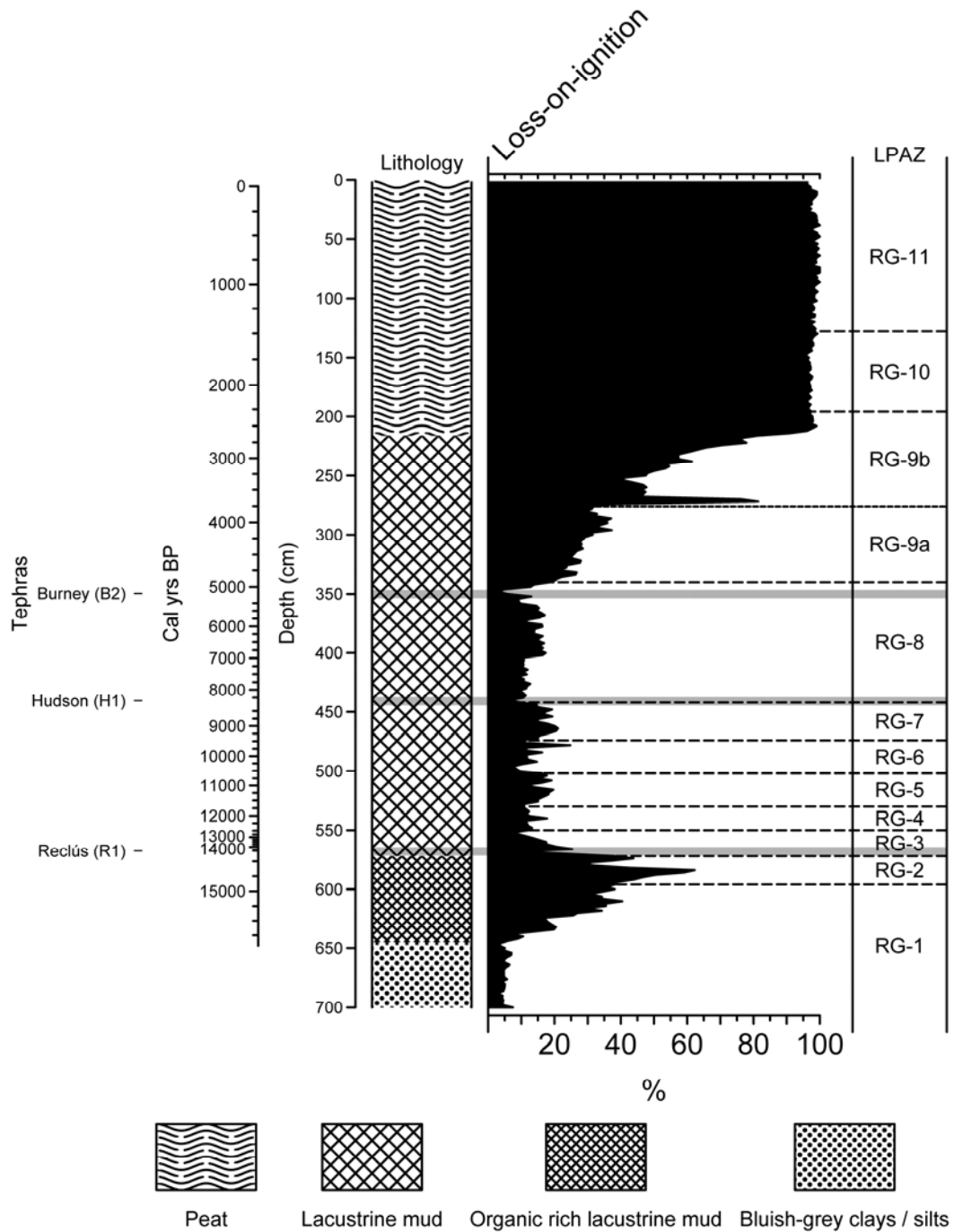


Figure 3.1 Organic content (Loss on Ignition:  $LOI_{550}\%$ ) and tephra layers for the Rio Grande core. Three visible tephra layers found in the core: Mt Burney 2 (B2), Vn Hudson 1 (H1) and Vn Reclús 1 (R1) eruptions. The column on the right shows the Local Pollen Assemblage Zones (LPAZs) and the respective subzones.

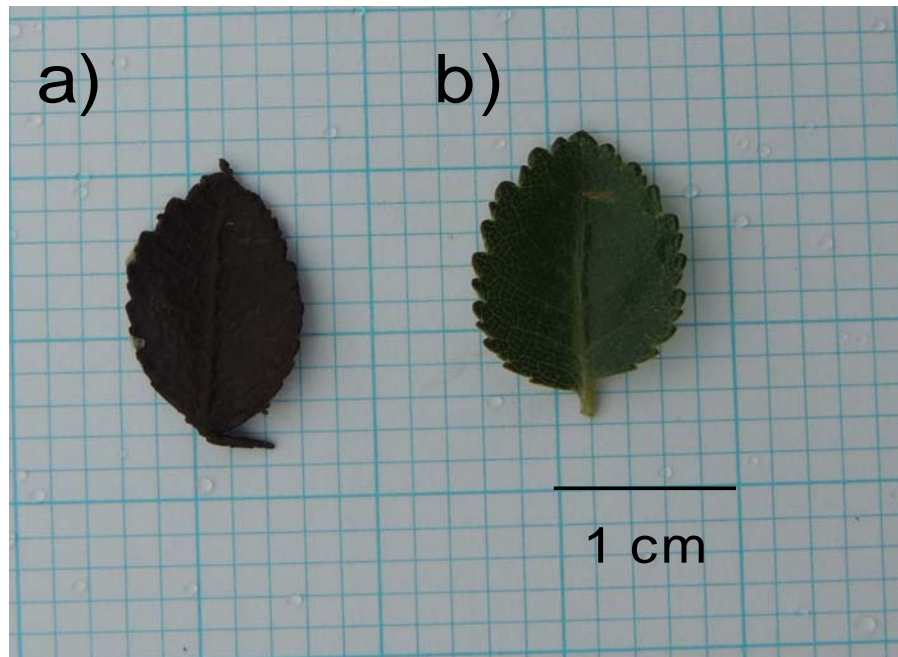


Figure 3.2 *Nothofagus betuloides* leaves: a) an example of the leaves found between 540 cm and 539 cm depth and, between 484 cm and 483 cm depth in Rio Grande sequence, b) a *Nothofagus betuloides* leaf taken from the current forest near the site.

The gross stratigraphy (LOI<sub>550</sub> %) of the Punta Yartou core can be divided into 5 sections: 1) 1,098 cm to 1,066 cm the percentage of organic content is very low, less than 3%, 2) 1,066 cm to 980 cm the organic content increases to ~25%, 3) between 980 cm and 850 cm the organic content continues to increase to values between 25% to 50 %, 4) from 850 cm to 734 cm the organic content fluctuates around 55% and finally, 5) between 734 cm and 98 cm the organic content is consistently between 83% and 100% (Figure 3.3).

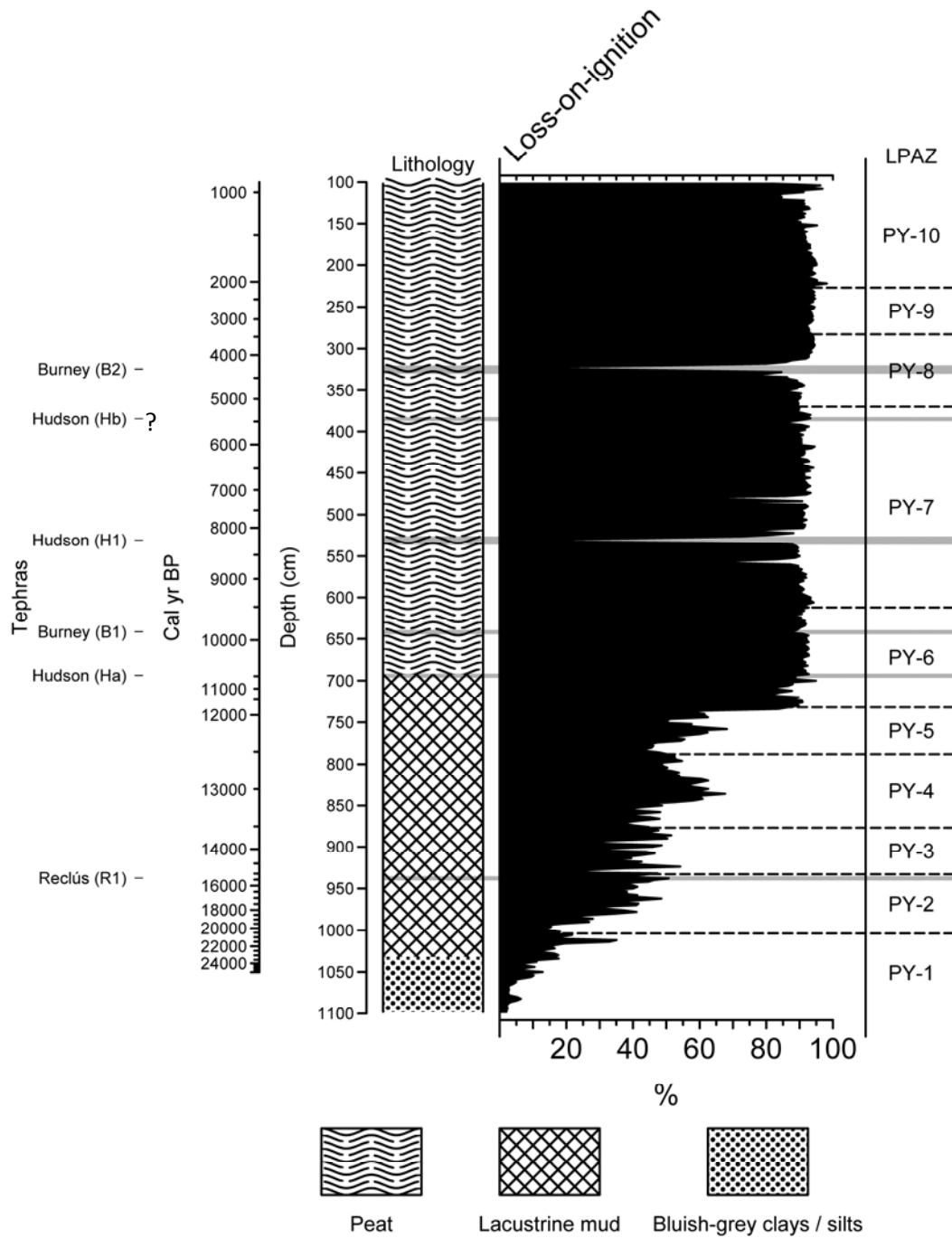


Figure 3.3 Organic content ( $LOI_{50}\%$ ) and tephra layers for the Punta Yartou core. Six tephra layers found in the cores. Three visible tephra layers: Mt Burney 2 (B2), Vn Hudson 1 (H1) and Vn Reclús 1 (R1) eruptions. Three microtephra layers: Vn Hudson (Hb?), Mt Burney 1 (B1) and Vn Hudson (Ha) eruption, ?= no geochemical analysis. The column on the right shows the Local Pollen Assemblage Zones (LPAZs) and the respective subzones.

### 3.1.3 Lago Lynch.

A 450 cm continuous core was obtained from an open peat bog within an area of small lakes and bogs near the larger Lago Lynch (Figure 2.7). From 950 cm to 926 cm the basal sediments consist of a mix of bluish-grey silts and clays including gravel sized clasts. Between 926 cm and 786 cm the sediment is a organic-rich lacustrine-mud; the upper boundary at 786 cm (~80 LOI<sub>550</sub> %) marks a shift to peat. The accumulation of peat continues to the top of the core (550 cm depth) characterised by unhumified and uncompacted *Sphagnum* spp. moss (Figure 3.4). The Russian corer was unable to securely sample the uncompacted *Sphagnum* moss peat between 550 cm and the surface.

The organic content (LOI<sub>550</sub> %) of Lago Lynch core may be divided in 5 sections: 1) between 950 cm and 926 cm the percentage organic content is low, ~5%, 2) between 926 cm and 876 cm the organic content increases to ~20%, 3) from 876 cm to 810 cm the organic content is ~15%, 4) between 810 cm and 786 cm the organic content increases from ~15% to ~80 % indicating the onset of peat accumulation and, 5) between 786 cm and the top of the record (500 cm) the organic content fluctuates from ~80 % to 100% (Figure 3.4).

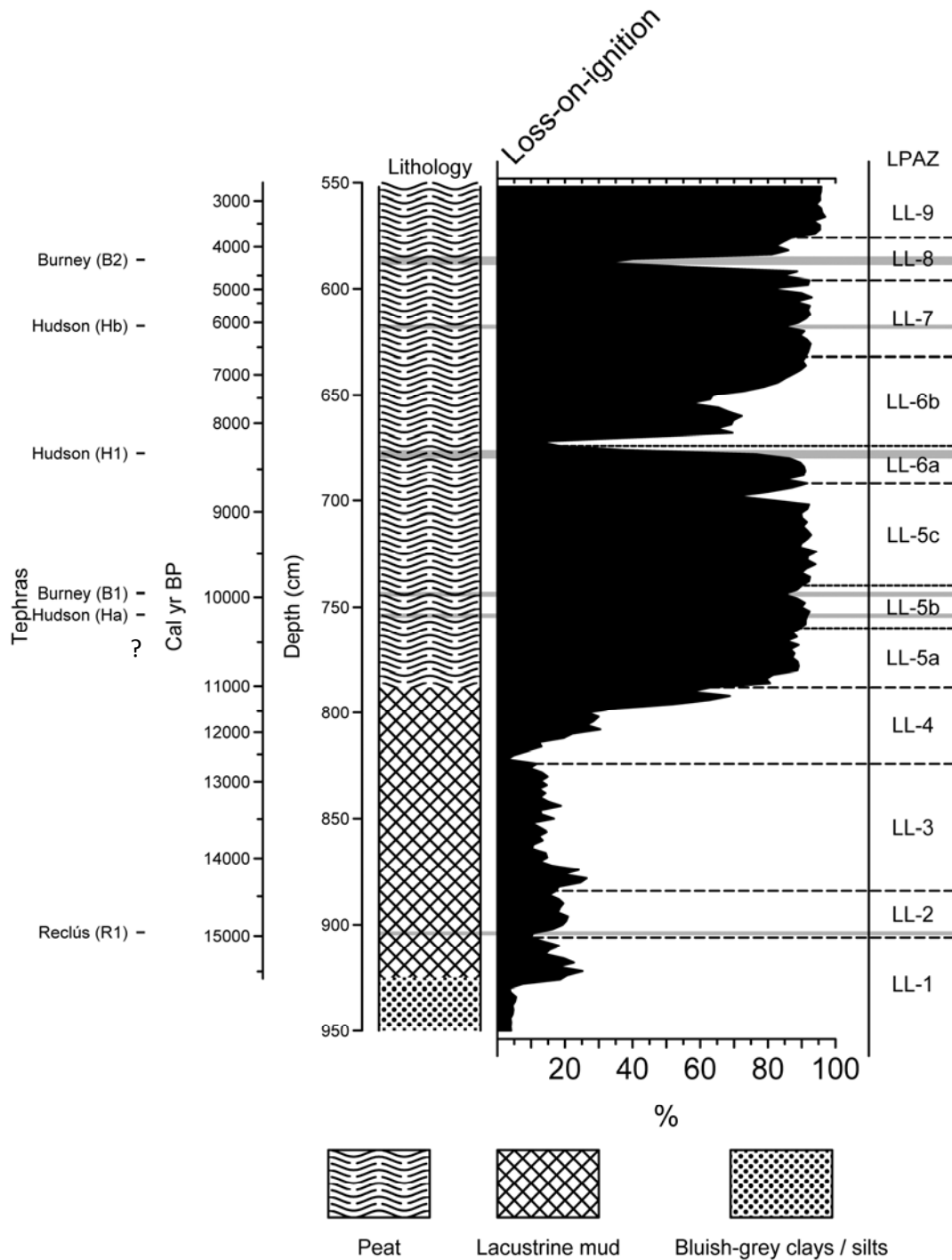


Figure 3.4 Organic content (LOI<sub>550</sub>%) and tephra layers for the Lago Lynch core. Six tephra layers found in the core. Three visible tephra layers: Mt Burney 2 (B2), Vn Hudson 1 (H1) and Vn Reclus (R1) eruptions. Three microtephra layers: Vn Hudson (Hb), Mt Burney 1 (B1) and Vn Hudson (Ha?) eruption, ?= no geochemical analysis. The column on the right shows the Local Pollen Assemblage Zones (LPAZs) and the respective subzones.

### 3.2 Tephrochronology.

In this study three previously identified visible and three cryptotephra layers have been found. Two of the cryptotephra layers have been identified for the first time in the region. The recognition of the tephra layers was initially based on color and texture, shard characteristics and then confirmed using major element geochemical analysis. The geochemical fingerprinting of the tephra layers enabled the correlation of results from this study with previous studies that present  $^{14}\text{C}$  ages for tephra events (Kilian *et al.*, 2003; McCulloch, 1994; McCulloch *et al.*, 2005a and 2005b, 2011; Stern 2008; Heberzetti *et al.*, 2009; Borromei *et al.*, 2010; Sagredo *et al.*, 2011; Stern *et al.*, 2011; Stern *et al.*, in press) and volcanic glass geochemical data (Kilian *et al.*, 2003; Stern, 2008; Heberzetti *et al.*, 2009; Borromei *et al.*, 2010) (Figure 3.5). The tephrochronology constructed by this study is based on six distinct tephra layers that likely originate from three major volcanic sources; volcán Hudson ( $\sim 46^\circ\text{S}$ ) within the Andean Southern Volcanic Zone (SVZ;  $\sim 33^\circ - 46^\circ\text{S}$ ): and Mt Burney ( $\sim 52^\circ\text{S}$ ) and volcán Reclús ( $\sim 51^\circ\text{S}$ ) from the Andean Austral Volcanic Zone (AVZ;  $\sim 49^\circ - 55^\circ\text{S}$ ) (Stern, 2008) (Figure 1.3 and 3.5). The following section describes the six different tephra layers found in the Rio Grande, Punta Yartou and Lago Lynch cores. The visible tephra layers are described first followed by the cryptotephra layers:

#### 3.2.1 Visible tephra layers.

**Mt Burney 2 (B2):** The Mt Burney 2 tephra is a white coarse silt tephra (Figure 3.6a). This tephra is located between 345 cm and 350 cm depth (5 cm) in Rio Grande, from 319 cm to 325 cm (6 cm) depth in Punta Yartou and between 586 cm and 590 cm (4 cm) depth in the Lago Lynch core (Figures 3.2, 3.3 and 3.4; Table 3.1).

The B2 tephra in the Rio Grande core is located within lacustrine mud sediment (Figure 3.1). In the Punta Yartou and Lago Lynch cores the Mt Burney 2 tephra is located within peat sediment (Figure 3.3 and 3.4, respectively). In the three cores the glass shards of B2 tephra are clear and transparent, highly vesicular (Figure 3.7a) and the geochemical analysis suggests the Mt Burney 2 tephra is a rhyolitic deposit, with SiO<sub>2</sub> between 74.7 - 78.1 wt.%, FeO ≤ 1.5 wt.%, K<sub>2</sub>O ≤ 1.7 wt.% and CaO ≤ 1.8 wt.% values (Figure 3.5 and 3.8; Appendix). Figure 3.8 indicates the different geochemical characteristics of the visible tephra layers found in this study: Mt Burney 2, Vn Hudson 1 and Vn Reclús 1.

The maximum radiocarbon age for the Mt Burney 2 tephra layer used in this study is 3,860 ± 50 <sup>14</sup>C yr BP (McCulloch and Davies, 2001) and used for the age-depth models for each core. The calibrated radiocarbon age for the Mt Burney 2 tephra layer is 4,310 - 4,410 Cal yr BP, (using the OxCal 4.2 program; Bronk-Ramsey, 2009) (Table 3.1). The revised age obtained from interpolation from the Punta Yartou (PY) age-depth model is c. 4,170 Cal yr BP (Table 3.1) (see Section 3.3). This age (3,860 ± 50 <sup>14</sup>C yr BP) is consistent with other previous ages reported for this volcanic eruption: >3,520 ± 30 <sup>14</sup>C yr BP (Kilian *et al.*, 2003) and >3,115 ± 100 <sup>14</sup>C yr BP (Stern, 2008).

**Volcán Hudson (H1):** This tephra layer comprises dark olive-green coarse silt material (Figure 3.6b). This tephra is located between 438 cm and 442 cm depth (4 cm) in Rio Grande, from 527 cm to 531 cm depth (4 cm) in Punta Yartou and, between 669 cm and 674 cm depth (5 cm) in the Lago Lynch core (Figures 3.1, 3.3 and 3.4 respectively; Table 3.1).

H1 lies in lake sediment in the Rio Grande core (Figure 3.1) and in the Punta Yartou and Lago Lynch cores the tephra is located within peat (Figure 3.3 and figure 3.4). The H1 glass shards are characterised by their green-brown color and platy structure (Figure 3.7b) and the geochemical data indicates that it is an andesitic tephra, with SiO<sub>2</sub> between 61.6 - 66.4 wt.%,

FeO between 4.0 - 5.7 wt.%, K<sub>2</sub>O between 2.4 - 3.1 wt.%, and CaO between 2.3 - 4.6 wt.%, (Figure 3.5 and 3.8; Appendix). A minimum radiocarbon age for H1 tephra layer used in this study for the age-depth models for each core is  $7,458 \pm 40$  <sup>14</sup>C yr BP (McCulloch *et al.*, in press). The calibrated age for H1 tephra layer is 8,170 - 8,360 Cal yr BP, using the OxCal 4.2 program (Bronk-Ramsey, 2009) and the revised age obtained from interpolation from the Punta Yartou (PY) age-depth model is c. 8,240 Cal yr BP (Table 3.1) (see Section 3.3). This age is consistent with other previous ages reported for this volcanic eruption. A recent review of the radiocarbon ages for the H1 tephra layer provides an average of 8 maximum ages for the H1 tephra of  $7,356 \pm 373$  <sup>14</sup>C yr BP (7,465 - 8,210 Cal yr BP) and an average of 11 minimum ages of  $7,248 \pm 303$  <sup>14</sup>C yr BP (7,460 – 8,645 Cal yr BP) (Stern *et al.*, in press).

**Volcán Reclús (R1):** This tephra layer is a creamy-white- fine silt layer (Figure 3.6c). In the Rio Grande core the R1 tephra is found between 567 cm and 568.5 cm depth (1.5 cm), between 929 cm and 930 cm (1 cm) and, between 903.5 cm and 904.5 cm (1 cm) depth in the Punta Yartou and Lago Lynch cores respectively (Figures 3.1, 3.3 and 3.4; Table 3.1).

The R1 tephra marks the transition from more organic-rich lake sediment to laminated lacustrine-mud in the Rio Grande core (Figure 3.1). In the Punta Yartou and Lago Lynch cores the R1 tephra is located within lacustrine-mud (Figure 3.3 and 3.4). The glass shards of the R1 tephra are clear and transparent and semi-vesicular (Figure 3.7c). The geochemical analyses identify the tephra as a rhyolitic deposit with SiO<sub>2</sub> between 73.9 wt.% and 76.9 wt.%, and values within the range for FeO between 1.0 wt.% and 1.2 wt.%, for K<sub>2</sub>O between 2.3 wt.% and 2.7 wt.%, and for CaO between 1.3 wt.% and 1.6 wt.% (Figure 3.5 and 3.8; Appendix).

The maximum radiocarbon dates for the Vn Reclús 1 tephra layer are:  $12,525 \pm 75$  <sup>14</sup>C yr BP (14,240 - 15,075 Cal yr BP) (McCulloch *et al.*, 2005a) and,  $12,840 \pm 100$  <sup>14</sup>C yr BP (14,910 - 15,660 Cal yr BP) (McCulloch and Bentley, 1998) (Table 3.1). Both radiocarbon ages are used

for the age-depth models for each core in this study. The radiocarbon ages for R1 tephra layer have been re-calibrated using the OxCal 4.2 program (Bronk-Ramsey, 2009) and are consistent with ages for R1 mentioned in previous studies: maximum age  $13,255 \pm 205$   $^{14}\text{C}$  yr BP (15,240 - 16,450 Cal yr BP) (Stern, 1992), minimum age  $12,870 \pm 200$   $^{14}\text{C}$  yr BP (14,450 – 15,965 Cal yr BP) (Stern, 2000) and Sagredo *et al.* (2011) mention an pooled maximum ages of  $12,627 \pm 48$   $^{14}\text{C}$  yr BP (14,620 – 15,185 Cal yr BP) and an pooled minimum ages of  $12,480 \pm 46$   $^{14}\text{C}$  yr BP (14,210 – 14,930 Cal yr BP).

### 3.2.2 Cryptotephra layers.

**Volcán Hudson (Hb):** This cryptotephra has not been previously identified in Fuego-Patagonia. It has been identified in the Lago Lynch core, between 617 cm and 618 cm (Figure 3.3 and Table 3.1) within the peat and has similar characteristics to the visible Hudson tephra layer (H1) with green-brown and platy shards (Figure 3.7d). The tephra-glass geochemical information identifies the tephra as being from an andesitic source with ranges for  $\text{SiO}_2$  between 61.6 wt.% and 65.4 wt.%, FeO between 4.1 wt.% and 5.2 wt.%,  $\text{K}_2\text{O}$  between 2.6 wt.% and 4.6 wt.% and, CaO between 2.4 wt.% and 3.6 wt.% (Figure 3.9; Appendix). The age of this cryptotephra has been estimated to c. 6,130 Cal yr BP at 618 cm by interpolation within the Lago Lynch age-depth model produced using BACON program (see Section 3.3). In the Punta Yartou core a cryptotephra layer was identified at 385 cm depth which has not been geochemically analysed but the age of the tephra layer derived by interpolation within the Punta Yartou age-depth model is c. 5,450 Cal yr BP (Table 3.1).

**Mt Burney 1 (B1):** This cryptotephra has been found in previous work from the northern sector of the Magellan region (Kilian *et al.*, 2003, Stern, 2008) and in this study has been identified for the first time on Tierra del Fuego at Punta Yartou and Lago Lynch between 640 cm and 642 cm and between 740 cm and 742 cm, respectively. The cryptotephra is located within lacustrine-

mud in the Punta Yartou core and within the peat at Lago Lynch (Figure 3.3 and 3.4). The micro-tephra glass-shards are clear and transparent and highly vesicular (Figure 3.7e) and the geochemical data indicate that it is a rhyolitic tephra, with ranges for SiO<sub>2</sub> between 74.8 wt.% and 77.9 wt.%, FeO between 0.8 wt.% and 1.2 wt.%, K<sub>2</sub>O between 1.5–1.7 wt.% and, CaO between 1.2–1.5 wt.% (Figure 3.10; Appendix). The geochemistry of the B1 tephra layer found in the Punta Yartou and Lago Lynch cores is similar in composition to the B2 tephra layer which suggests that Mt Burney is probably the source (Figure 3.10). The B1 tephra layer in the Punta Yartou core has been AMS radiocarbon dated by this study to  $8,870 \pm 35$  <sup>14</sup>C yr BP (9,700 - 10,155 Cal yr BP) (Table 3.1). This age is consistent with previous work that has dated the B1 tephra layer:  $8,520 \pm 70$  <sup>14</sup>C yr BP (Kilian *et al.*, 2003), also Stern (2008; Markgraf Pers. Comm.) suggest ages of  $>8,870 \pm 65$  <sup>14</sup>C yr BP,  $< 8,880 \pm 60$  <sup>14</sup>C yr BP and  $<8,880 \pm 60$  <sup>14</sup>C yr BP.

**Volcán Hudson (Ha):** This micro-tephra has not been encountered before in Fuego-Patagonia. It was found in the Punta Yartou core between 692 cm and 694 cm depth within peat (Figure 3.3, 3.4). These shards have a similar characteristic to the visible Hudson tephra layer (H1), being green-brown with a platy structure (Figure 3.7f) and the geochemical data suggests it is an andesitic glass with ranges of: SiO<sub>2</sub> (59.7–65.1 wt.%), FeO (4.4–5.3 wt.%), K<sub>2</sub>O (2.4–3.0 wt.%) and CaO (2.5-3.6 wt.%) respectively (Appendix) and a comparison with the H1 chemistry suggests Vn Hudson to be the likely source (Figure 3.9). The micro-tephra Ha in the Punta Yartou core has been AMS radiocarbon dated to  $9,288 \pm 44$  <sup>14</sup>C yr BP (10,270 - 10,550 Cal yr BP) (Table 3.1). Although a potential Ha tephra layer has been identified in the Lago Lynch core at 752 - 754 cm depth, a sample has not been geochemically analysed to confirm the correlation and so the AMS radiocarbon date ( $9,288 \pm 44$  <sup>14</sup>C yr BP) for Ha was not incorporated into the Lago Lynch age-depth model. However, the age of the tephra layer derived by interpolation within the Lago Lynch age-depth model is c. 10,200 Cal yr BP (Table 3.1).

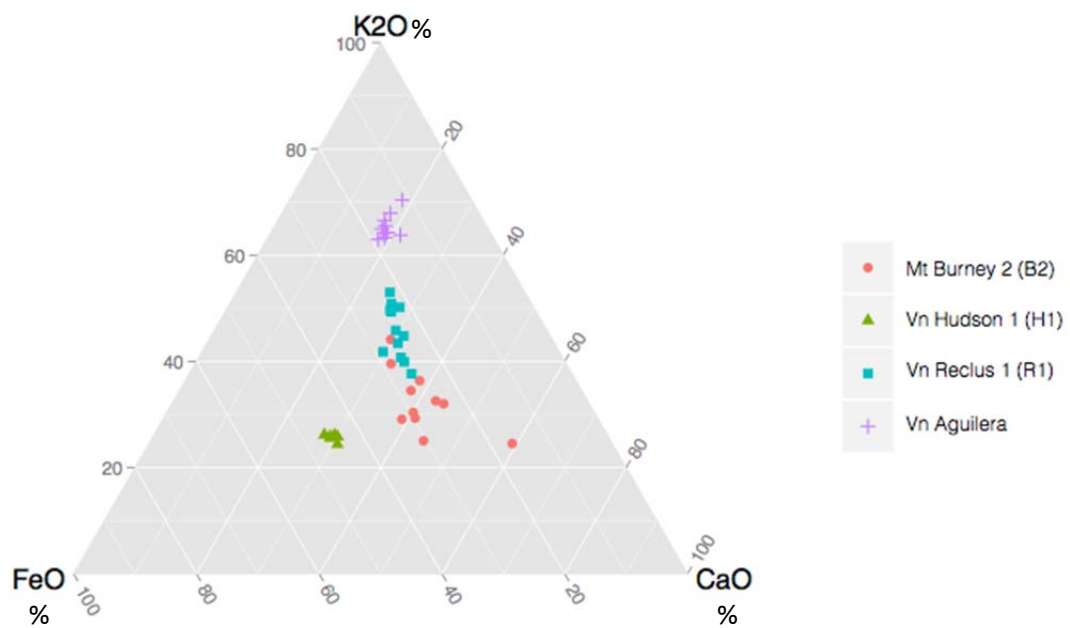


Figure 3.5 Ternary plot of percentage totals of CaO, FeO and K<sub>2</sub>O of individual glass shards for the four volcanic sources identified in Fuego Patagonia (Kilian *et al.*, 2003; Stern, 2008; Heberzetti *et al.*, 2009; Borrromei *et al.*, 2010); the Vn Hudson (~46°S) within the Andean Southern Volcanic Zone (SVZ; 33–46°S): and Mt Burney (~52°S), Vn Reclús (~51°S) and Vn Aguilera (50°S), from the Andean Austral Volcanic Zone (AVZ; 49-55°S).

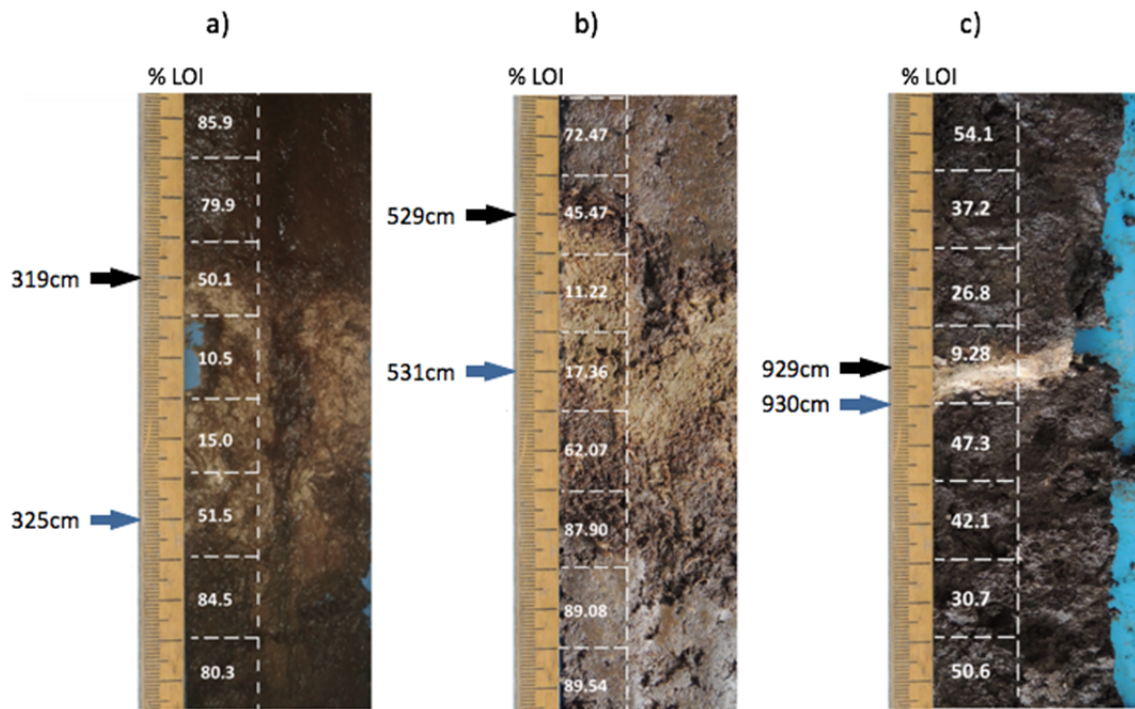


Figure 3.6 Visible tephra layers in chronological order, the thickness and depths are those measured in Punta Yartou core. Tephra layers are: a) Mt Burney 2, b) Vn Hudson 1 and, c) Vn Reclús 1, respectively. The arrows indicate the lower and upper limits of the tephra layers, the blue arrow indicates the depth considered for dating the ash deposition. The values down core indicate the Organic content ( $LOI_{550}\%$ ) for each 2 cm contiguous sample.

Table 3.1 Details of the depths, uncalibrated  $^{14}\text{C}$  yr BP maximum ages, calibrated Cal yr BP ages and interpolated ages from the age-depth model for visual and microscopic tephra layers identified at the study sites.

Tephra	Depth (cm)	Depth (cm) peak of LOI%	AMS age ( $\pm 1\sigma$ ) $^{14}\text{C}$ yr BP	Calibrated age range (95.4%) (Cal yr BP)	Interpolation from age-depth model (Cal yr BP)*	References
B-2 (V) - RG	345 - 350	345 - 350				
B-2 (V) - PY	319 - 325	319-325	3,860 $\pm$ 50	4,313 - 4,413	-	McCulloch and Davies, 2001
B-2 (V) - LL	586 - 590	587 - 589				
H-b ? (C) - PY	-	384 - 385			5,445	This study (Interpolation from PY age-depth model)
H-b (C) - LL	-	617 - 618			6,130	This study (Interpolation from LL age-depth model)
H-1 (V) - RG	438 - 442	438 - 442				
H-1 (V) - PY	527 - 531	527 - 531	7,458 $\pm$ 40* *	8,170 - 8,356	-	McCulloch <i>et al.</i> , press
H-1 (V) - LL	669 - 674	669 - 675				
B-1 (C) - PY	-	640 - 642	8,870 $\pm$ 35	9,700 - 10,153	-	This study
B-1 (C) - LL	-	740 - 742				
H-a (C) - PY	-	692 - 694	9,288 $\pm$ 44	10,268 - 10,550	-	This study
H-a? (C) LL	-	752 - 754	-	-	10,268	This study (Interpolation from LL age-depth model)
R-1 (V) - RG	567 - 568.5	567 - 568				
R-1 (V) - PY	929 - 930	929 - 930	12,525 $\pm$ 75 12,840 $\pm$ 100	14,241 - 15,073 14,908 - 15,661		McCulloch <i>et al.</i> , 2005 McCulloch and Bentley, 1998
R-1 (V) - LL	903.5 - 904.5	904 - 905				

\*WMA at 95% confidence; (V): Visible tephra layer; (C): cryptotephra layer; RG: Rio Grande core; PY: Punta Yartou core; LL: Lago Lynch core; B: Mt Burney; H: Vn Hudson; R: Vn Reclús; ?= no geochemical analysis; \*\*minimum age.

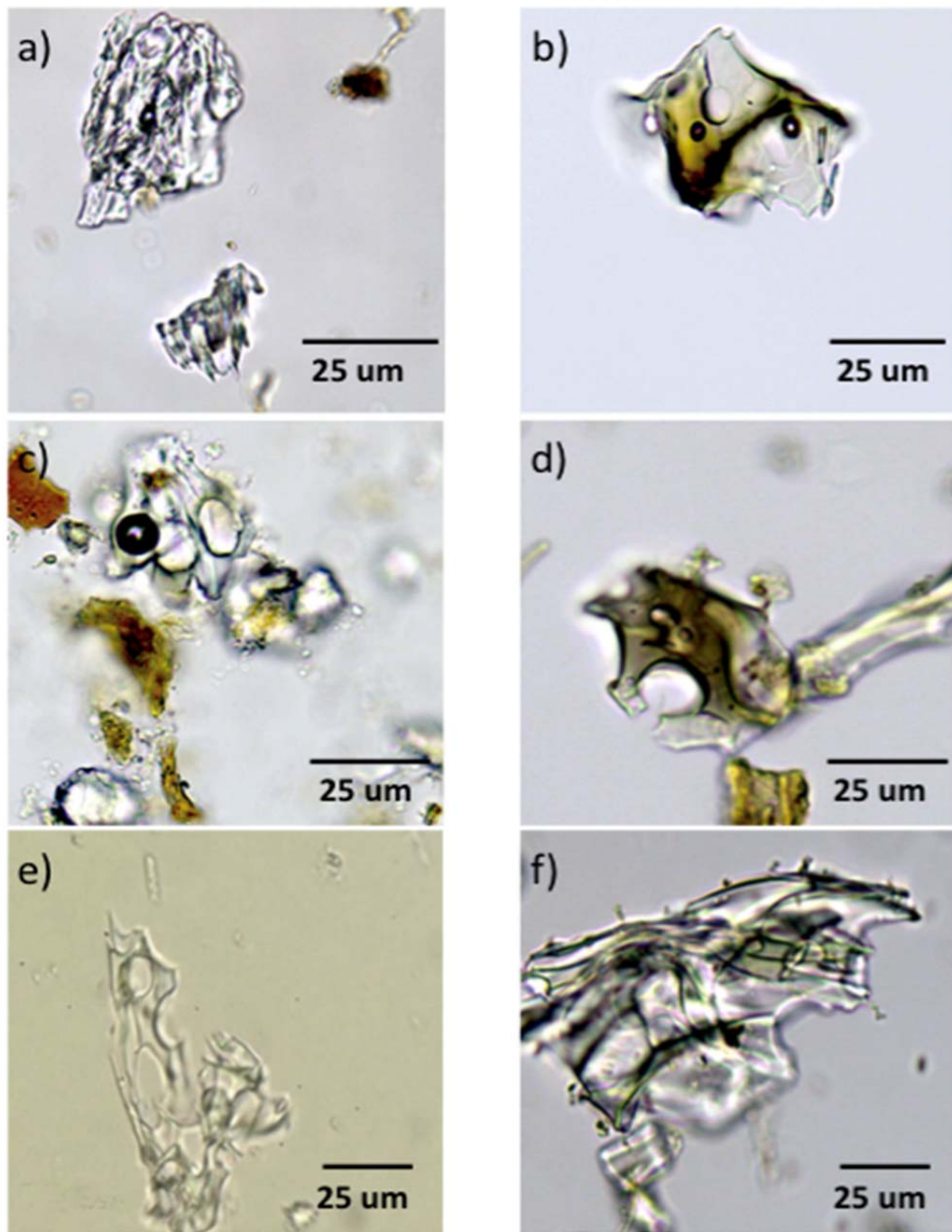


Figure 3.7 A example of glass shards of 3 visible and 3 cryptotephra layers found in the cores. Visible tephra layers: a) Mt Burney 2 (B2), b) Vn Hudson 1 (H1) and, c) Vn Reclús 1 (R1) eruptions. Cryptotephra layers: d) Vn Hudson “b”, e) Mt Burney 1 (B1) and f) Vn Hudson “a”.

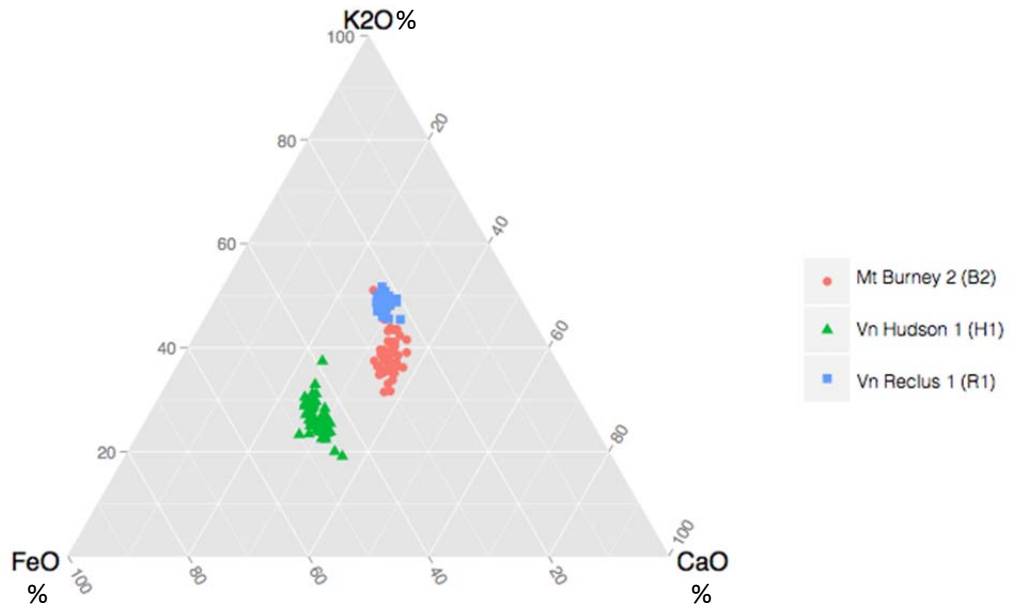


Figure 3.8 Ternary plot of percentage totals of CaO, FeO and K<sub>2</sub>O of individual glass shards for the three visible tephra layers found in this study. The diagram shows three distinct groups: Mt Burney (B2) (red circle), Vn Hudson 1 (H1) (green triangle) and Vn Reclus (R1) (blue square).

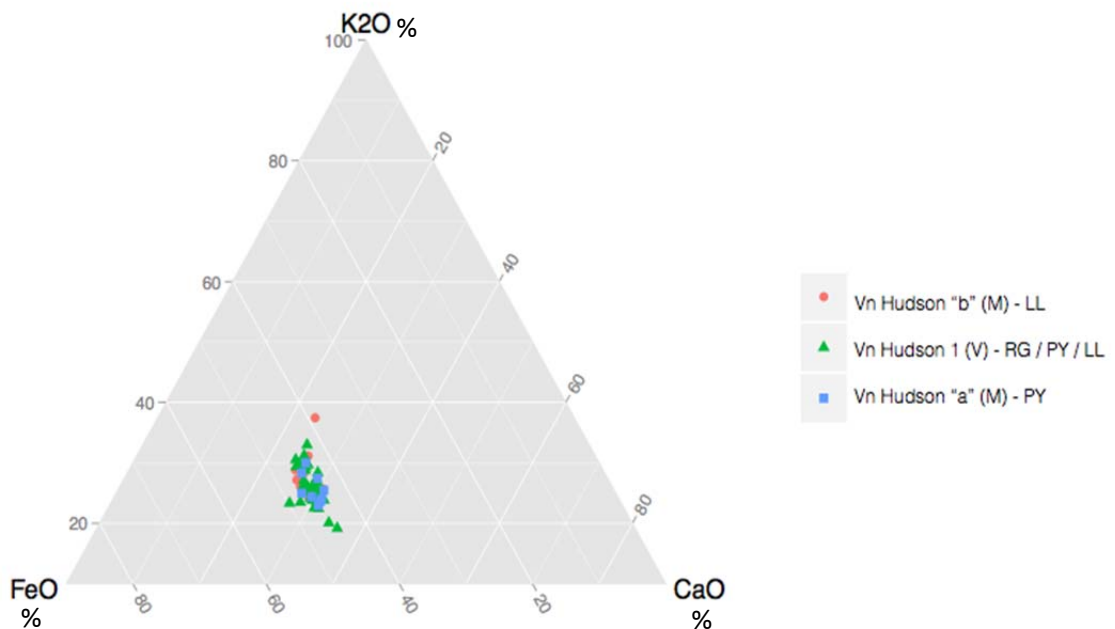


Figure 3.9. Ternary plot of percentage totals of CaO, FeO and K<sub>2</sub>O of individual glass shard from three Hudson volcano eruptions in this study: Vn Hudson "b" (red circle), Vn Hudson 1 (green triangle) and Vn Hudson "a" (blue square).

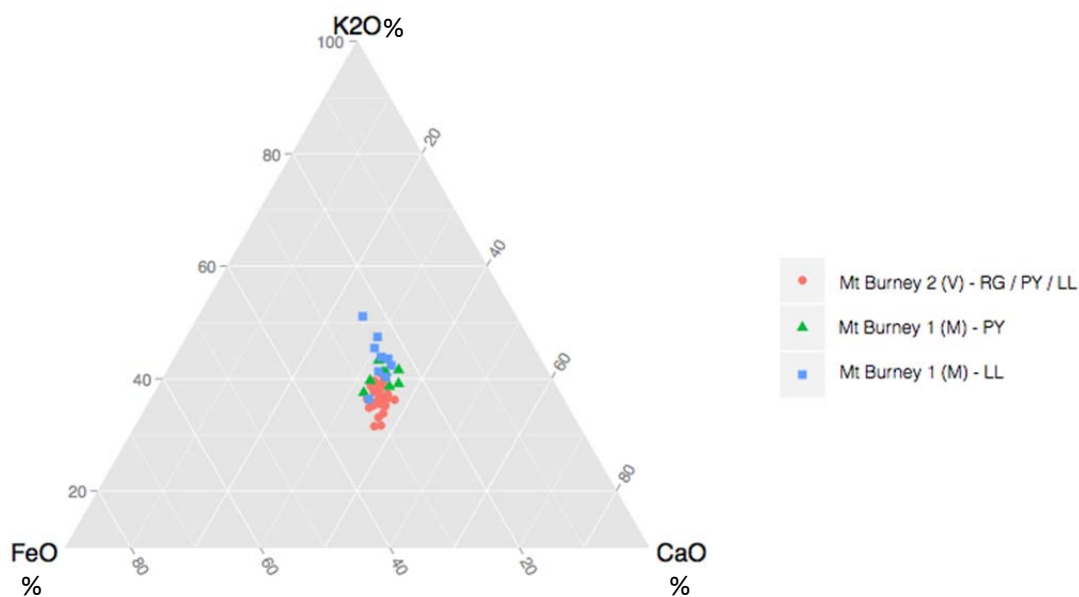


Figure 3.10. Ternary plot of percentage totals of CaO, FeO and K<sub>2</sub>O of individual glass shards for two Mt Burney volcanic eruptions found in this study. Mt Burney 2 (red circle), Mt Burney 1 found in Punta Yartou core (green triangle) and Mt Burney 1 (blue square).

### 3.3 Chronology.

The age-depth models have been constructed to estimate the calendar ages of depths of each sediment core using the radiocarbon samples and the dated tephra layers. The important steps for a robust chronology include the processes of selecting each sample for radiocarbon analysis and how to use the information that is given by each age-depth model. The key steps are described next and the application of the age-depth models to each core.

#### 3.3.1 Rio Grande.

The age-depth model is based on 4 AMS radiocarbon dates from bulk organic material and the published radiocarbon ages for three tephra layers: 1)  $3,860 \pm 50$  <sup>14</sup>C yr BP, the maximum age

for the tephra layer from the Mt Burney 2 (B2) eruption (McCulloch and Davies, 2001), 2)  $7,458 \pm 40$   $^{14}\text{C}$  yr BP, the minimum age for volcán Hudson 1 (H1) (McCulloch *et al.*, press) and, 3) two maximum ages for the Vn Reclús 1 tephra layer  $12,525 \pm 75$   $^{14}\text{C}$  yr BP (McCulloch *et al.*, 2005) and  $12,840 \pm 100$   $^{14}\text{C}$  yr BP (McCulloch and Bentley, 1998) (Table 3.2).

The age-depth model was calculated using the Bayesian age-depth modelling software, BACON (Blaauw and Christen, 2011). The thicknesses of visible tephra layers were excluded from the age-depth model (Table 3.1, and Figure 3.11). The ages interpolated from the model were used with two standard deviations, including the maximum probability of the distribution of each calibration age. The basal age (645 cm) of the Rio Grande sediment core is estimated to be c. 15,870 Cal yr BP. The weighted mean ages (WMA) from Bacon modeling were used to provide the age-depth axis (Cal yr BP) for the pollen diagrams produced using the Tilia Graph program (see Section 3.4).

Figure 3.11 shows that the accumulation rate from 648 cm to 569 cm depth, from c. 15,870 Cal yr BP to c. 14,410 Cal yr BP is relatively high ( $\sim 0.05$  cm/yr) and the sediment deposition is characterised by relatively high organic content ( $\sim 50$  %). This interval of relatively high organic productivity can be linked to conditions more favourable than the previous period when ice was covering the Rio Grande site. This interval is followed by a period between 567 cm and 550 cm depth (c. 14,240 Cal yr BP and c. 12,480 Cal yr BP), characterised by a radiocarbon age plateau, decreasing in organic content to values less than 10 % and low accumulation rates (0.01 cm/yr). Then, between 550 cm and 214 cm depths (c. 12,480 Cal yr BP and c. 5,020 Cal yr BP) the organic content remains at percentages around 20 % and the accumulation rate increases to  $\sim 0.03$  cm/yr and retains moderate values and stabilises through the sequence until c. 5,020 Cal yr BP. From 351 cm to 190 cm depth, (between c. 5,020 Cal yr BP and c. 2,610 Cal yr BP) there is a gradual increase in organic content to around 80 % and the accumulation rate further increase to  $\sim 0.05$  cm/yr, around the same values as that during the interval from 648 cm to 569

cm (c. 15,870 Cal yr BP to c. 14,410 Cal yr BP). The transition from the lake to peat conditions by c. 2,610 Cal yr BP. Finally, after c. 2,610 Cal yr BP the highest values of organic matter (~80%) and accumulation rate (~0.08 cm/yr) in the sequence are found in the Rio Grande core.

Table 3.2 Radiocarbon ages, calibrated age ranges and weighted mean age (WMA) from BACON Bayesian age model for the Rio Grande core.

Laboratory Code	Depth (cm)	Material	<sup>14</sup> C yr BP (1σ)	δ <sup>13</sup> C‰	Calibrated age range (95.4%) Cal yr BP*	Calibrated age range and WMA (Cal yr BP)**
SUERC-55290	125	Organic material bulk	1,594 ± 38	-27.4	1,360 – 1,533	1,335 – 1,554 (1,448)
SUERC-55289	191	Organic material bulk	2,158 ± 35	-26.9	2,005 – 2,300	2,027 – 2,333 (2,201)
Tephra (B2) <sup>1</sup>	351	Organic material bulk	3,860 ± 50	-	4,013 – 4,413	4,180–6,424 (5,020)
Tephra (H1) <sup>2</sup>	443	Organic material bulk	7,458 ± 40	-27.0	8,170 – 8,356	7,301 – 9,377 (8,255)
SUERC-55288	550	Fine plant material	9,425 ± 46	-23.0	10,442 – 10,739	10,553 – 13,961 (12,477)
Tephra (R1) <sup>3</sup>	569	Organic material bulk	12,525 ± 75	-29.2	14,241 – 15,073	13,865–14,629 (14,282)
Tephra (R1) <sup>4</sup>	569	Organic material bulk	12,840 ± 100	-21.2	14,908 – 15,661	13,865–14,629 (14,282)
SUERC-55287	645	Fine plant material	13,223 ± 56	-21.9	15,626 – 16,061	15,523 – 16,143 (15,867)

\* Calibrated age ranges by OxCal 4.2 program (Bronk-Ramsey, 2009) and SH13 curve (Hogg *et al.*, 2013).

\*\* Probability interval of calibrated ages and weighted mean age (WMA) at 95% confidence intervals (Cal yr BP) from BACON (Blaauw and Christen, 2011).

<sup>1</sup> B2 = Mt Burney tephra layer (McCulloch and Davis, 2001).

<sup>2</sup> H1 = Vn Hudson tephra layer (McCulloch *et al.*, in press).

<sup>3</sup> R1 = Vn Reclus tephra layer (McCulloch *et al.*, 2005).

<sup>4</sup> R1 = Vn Reclus tephra layer (McCulloch and Bentley, 1998).

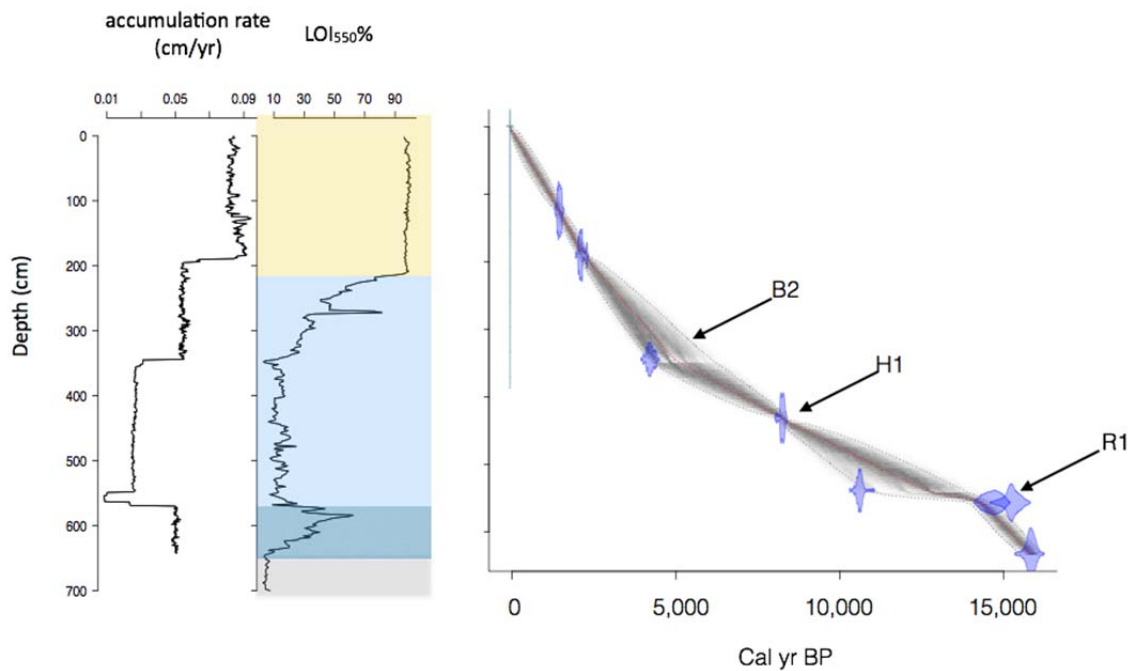


Figure 3.11. Accumulation rate, stratigraphy, organic content (LOI<sub>550</sub>%) and, chronology for the Rio Grande core. The age-depth model was constructed using the Bayesian modelling program ‘BACON’ (Blaauw and Christen, 2011). Different colors denote the stratigraphy of Rio Grande core; Grey: bluish clays and silts, Blue: black organic-rich lake sediment, Light blue: laminated lacustrine-mud sediment and yellow: peat. Arrows show: Mt Burney (B2), Vn Hudson (H1) and Vn Reclús (R1).

### 3.3.2 Punta Yartou.

The chronology of the Punta Yartou core is constrained by 15 AMS radiocarbon dates on bulk organic material and from fine plant material and three previously published tephra layer radiocarbon ages: 1)  $3,860 \pm 50$  <sup>14</sup>C yr BP from Mt Burney (B2) eruption (McCulloch and Davies, 2001), 2)  $7,458 \pm 40$  <sup>14</sup>C yr BP (McCulloch *et al.*, in press) and, 3)  $12,525 \pm 75$  <sup>14</sup>C yr

BP (McCulloch *et al.*, 2005a) and  $12,840 \pm 100$   $^{14}\text{C}$  yr BP from Vn Reclús 1 (McCulloch *et al.*, 2005a) (McCulloch and Bentley, 1998) (Table 3.3).

Bayesian age-depth modelling software, BACON (Blaauw and Christen, 2011) was used to construct a robust age-depth model for the Punta Yartou sediment core. Due to the abrupt sedimentation rate change between 931 cm and 978 cm depth (Figure 3.12) the core was separated into two sections pivoting at 931 cm. This coincides with the Vn Reclús tephra layer. The two-radiocarbon ages for the Vn Reclús tephra were added to make a more robust chronology at the end and beginning of each section, respectively. The thickness of the visible tephra layers, which were likely to be an instantaneous accumulation of sediment have been excluded from the age-depth model (Table 3.2 and Figure 3.12). The weighted mean ages (WMA) from Bacon modeling were used to provide the age-depth axis (Cal yr BP) for the pollen diagrams produced using the Tilia Graph program (see Section 3.4).

The accumulation rate below 931 cm (c. 14,760 Cal yr BP) is very low  $\sim 0.01$  cm/yr and also the organic content is  $\sim 20\%$  (Figure 3.12). Above 931 cm (c. 14,760 - 14,910 Cal yr BP) the accumulation rate increase to  $\sim 0.04$  cm/yr and the sediment deposition is characterised by relatively high organic content ( $> 40\%$ ). A further increase in accumulation rate occurs from 890 cm depth (c. 13,660 Cal yr BP) and the values for organic content increase to  $> 50\%$ , this interval continues until 732 cm depth (c. 11,870 Cal yr BP). The interval between 732 cm and 681 cm depth (from c. 11,870 Cal yr BP to c. 10,310 Cal yr BP) is characterised by a small radiocarbon age plateau (Figure 3.12). However, in this interval the organic content increases to values more than  $80\%$  and remains stable through the sequence until the present. From 681 cm to 573 cm depth (from c. 10,310 Cal yr BP to 8,930 Cal yr BP) the accumulation rate increases to values  $> 0.05$  cm/yr after which the accumulation rate remains stable at  $\geq 0.05$  cm/yr until 220 cm depth (c. 2,000 Cal yr BP). Finally, after c. 2,000 Cal yr BP the highest values of accumulation rate ( $\sim 0.1$  cm/yr) through the sequence are found in the Punta Yartou core.

Table 3.3 Radiocarbon ages, calibrated age ranges and weighted mean age (WMA) from BACON Bayesian age model for the Punta Yartou core.

Laboratory Code	Depth (cm)	Material	$^{14}\text{C}$ yr ( $1\sigma$ )	$\delta^{13}\text{C}\text{‰}$	Calibrated age range (95.4%) Cal yr BP*	Calibrated age range and WMA at 95% confidence (Cal yr BP)**
SUERC-34764	219	Organic material bulk	2,040 ± 35	-27.5	1,844- 2,044	1,852 – 2,269 (1,989)
Tephra (B2) <sup>1</sup>	326	Organic material bulk	3,860 ± 50	-	4,013 – 4,413	4,007 – 4,487 (4,265)
SUERC34759	419	Organic material bulk	5,290 ± 35	-29.1	5,920 – 6,179	5,893 – 6,192 (6,036)
SUERC34758	488	Organic material bulk	6,400 ± 35	-28.0	7,176 – 7,418	7,156 – 7,427 (7,303)
Tephra (H1) <sup>2</sup>	532	-	7,458 ± 40	-27.0	8,170 – 8,356	8,036 – 8,376 (8,237)
SUERC34757	560	Organic material bulk	7,895 ± 35	-29.0	8,542- 8,930	8,519 - 8,948 (8,681)
SUERC34756	598	Organic material bulk	8,345 ± 35	-27.1	9,138 – 9,436	9,106 - 9,452 (9,298)
SUERC347553 Tephra (B1) <sup>3</sup>	642	Organic material bulk	8,870 ± 35	-26.4	9,700 – 10,153	9,664 – 10,137 (9,885)
SUERC493654 Tephra (Ha) <sup>4</sup>	694	Organic material bulk	9,288 ± 44	-26.4	10,268 – 10,550	10,227 – 10,677 (10,448)
SUERC34754	702	Organic material bulk	9,515 ± 35	-24.9	10,581 – 11,067	10,565 – 10,968 (10,716)
SUERC34749	736	Organic material bulk	10,305 ± 35	-25.7	11,809 – 12,361	11,499 – 12,128 (11,912)
SUERC49364	794	Organic material bulk	10,639 ± 47	-26.1	12,433 – 12,673	12,409 – 12,720 (12,587)
SUERC49361	889	Organic material bulk	11,800 ± 45	-26.5	13,465 – 13,725	13,460 – 13,939 (13,641)
Tephra (R1) <sup>5</sup>	931	Organic material bulk	12,525 ± 75	-29.2	14,241 – 15,073	14,267 – 15,171 (14,760)
Tephra (R1) <sup>6</sup>	931	Organic material bulk	12,840 ± 100	-21.2	14,908 – 15,661	14,267 – 15,171 (14,760)
SUERC53159	978	Organic material bulk	14,899 ± 35	-25.5	17,896 – 18,232	17,880 – 18,354 (18,108)
SUERC49360	1039	Fine plant material	19,649 ± 97	-19.1	23,315 – 23,944	23,328 – 24,257 (23,751)
SUERC28041	1054	Fine plant material	21,880 ± 95	-18.5	25,855 – 26,290	25,944 – 27,065 (26,453)
SUERC28515	1054	Fine plant material	22,690 ± 75	-16.6	26,635 – 27,275	25,944 – 27,065 (26,453)

*Footnotes for Table 3.3*

\* Calibrated age ranges by OxCal 4.2 program (Bronk-Ramsey, 2009) and SH13 curve (Hogg *et al.*, 2013).

\*\* Probability interval of calibrated ages and weighted mean age (WMA) at 95% confidence intervals (Cal yr BP) from BACON (Blaauw and Christen, 2011).

<sup>1</sup> B2 = Mt Burney tephra layer (McCulloch and Davis, 2001).

<sup>2</sup> H1 = Vn Hudson tephra layer (McCulloch *et al.*, in press).

<sup>3</sup> B1 = Mt Burney tephra layer (this study).

<sup>4</sup> Ha = Vn Hudson tephra layer (this study).

<sup>5</sup> R1 = Vn Reclus tephra layer (McCulloch *et al.*, 2005a).

<sup>6</sup> R1 = Vn Reclus tephra layer (McCulloch and Bentley, 1998).

The high-resolution chronology for the Punta Yartou core has enabled the testing of the radiocarbon age for the H1 tephra by interpolation using the BACON program. The age-depth model was calculated using the 15 AMS radiocarbon dates and 3 tephra layers ages (see table 3.3). The basal ages from Punta Yartou suggest the area was ice-free sometime before c. 26,450 Cal yr BP (Table 3.3). However, the radiocarbon ages from the lower segment in the chronology (from 931 cm to 1,054 cm) are significantly older than the minimum ages for deglaciation in the region (McCulloch *et al.*, 2000) so it is necessary to interpret the ages for deglaciation provided by this study with caution. This is discussed further in section 4.2 below.

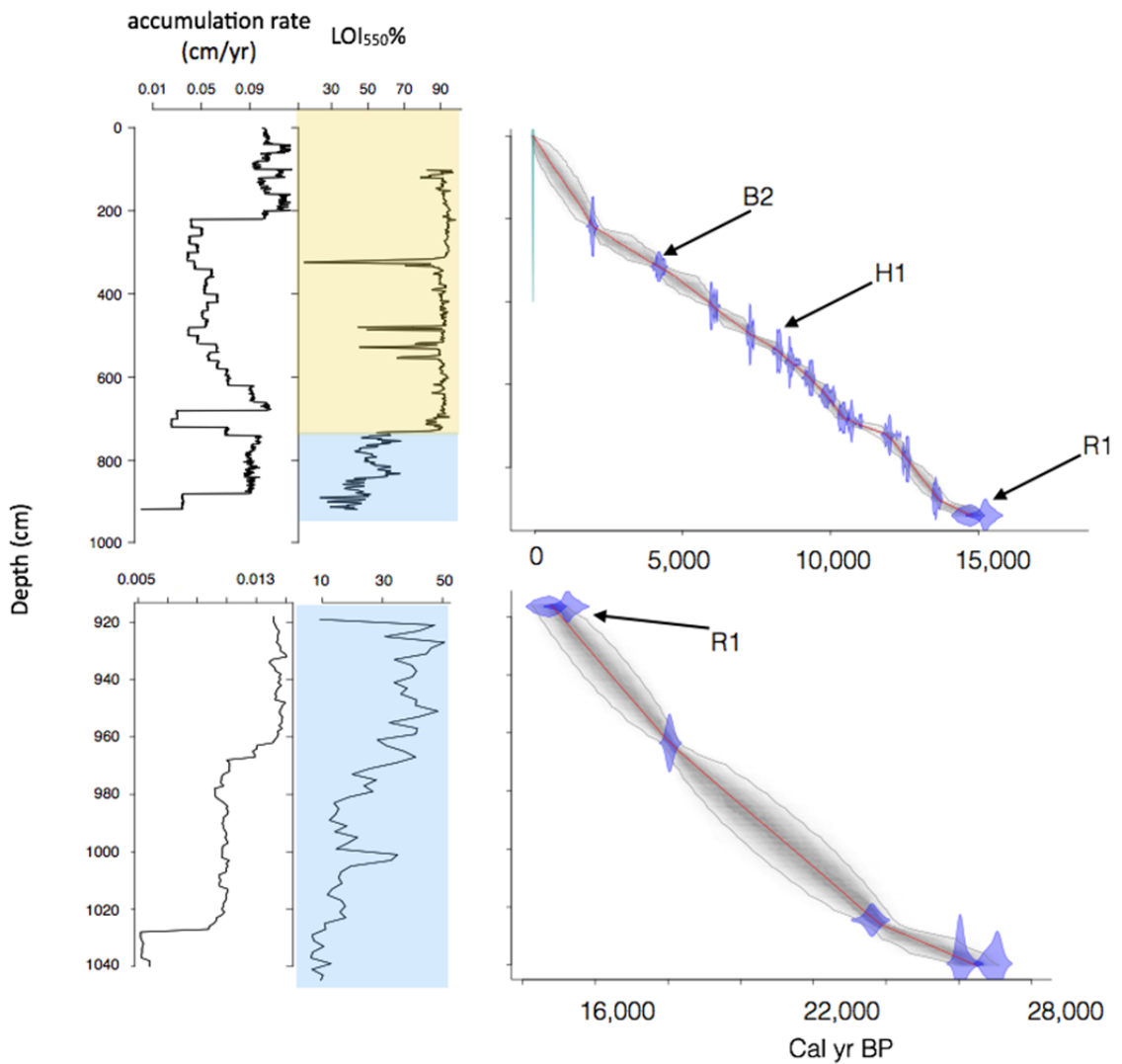


Figure 3.12. Accumulation rate, stratigraphy, organic content ( $LOI_{550\%}$ ) and, chronology for the Punta Yartou core. The age-depth model was constructed using the Bayesian modelling program ‘BACON’ (Blaauw and Christen, 2011). Different colors denote the stratigraphy of Punta Yartou core; Light blue: laminated lacustrine-mud sediment and Yellow: peat. Arrows show: Mt Burney 2 (B2), Vn Hudson 1 (H1) and Vn Reclús 1 (R1).

### 3.3.3 Lago Lynch.

The chronology of the Lago Lynch sediment core was constructed using 5 bulk and fine plant material AMS  $^{14}\text{C}$  dates from organic material and supplemented by tephrochronology based on 3 visible and 1 micro tephra layers from three different volcanoes (the thicknesses of visible tephra layers were excluded from the age-depth model) (Table 3.4). The Bayesian age-depth modelling, using BACON 2.4 (Blaauw and Christen, 2011) and the SH13 calibration curve (Hogg *et al.*, 2013) provides a robust age-depth model for the pollen record from Lago Lynch (Figure 3.13).

Table 3.4 Radiocarbon ages, calibrated age ranges and weighted mean age (WMA) from BACON Bayesian age model for the Lago Lynch core.

Laboratory Code	Depth (cm)	Material	$^{14}\text{C}$ yr ( $1\sigma$ )	$\delta^{13}\text{C}$ ‰	Calibrated age range (95.4%) cal. yr BP*	Calibrated age range and WMA at 95% confidence (cal. yr BP)**
SUERC55284	551	Organic material bulk	$2,555 \pm 36$	-26	2,440 - 2,746	2,441 – 2,757 (2,633)
Tephra (B2) <sup>1</sup>	590	Organic material bulk	$3,860 \pm 50$	-	4,013 - 4,413	4,033 – 4,519 (4,283)
SUERC55283	610	Organic material bulk	$5,026 \pm 39$	-28.5	5,604 - 5,890	5,582 – 5,921 (5,740)
Tephra (H1) <sup>2</sup>	676	Organic material bulk	$7,450 \pm 40$	-	8,170 – 8,356	8,054 – 8,404 (8,259)
Tephra (B1) <sup>3</sup>	743	Organic material bulk	$8,870 \pm 35$	-26.4	9,700 – 10,153	9,689 – 10,208 (9,939)
SUERC55282	788	Organic material bulk	$9,527 \pm 43$	-32.8	10,586 - 11,071	10,712 – 11,244 (11,020)
SUERC55281	824	Organic material bulk	$10,842 \pm 46$	-19.3	12,665 - 12,760	12,386 – 12,882 (12,702)
Tephra (R1) <sup>4</sup>	906	Organic material bulk	$12,525 \pm 75$	-29.2	14,241 - 15,073	14,633 – 15,335 (15,023)
Tephra (R1) <sup>5</sup>	906	Organic material bulk	$12,840 \pm 100$	-21.2	14,908 - 15,661	14,633 – 15,335 (15,023)
SUERC55280	926	Fine plant material	$13,189 \pm 55$	-15.3	15,559 - 16,030	15,220 – 15,949 (15,651)

## Footnotes for Table 3.4

\* Calibrated age ranges by OxCal 4.2 program (Bronk-Ramsey, 2014) and SH13 curve (Hogg *et al.*, 2013).

\*\* Probability interval of calibrated ages and weighted mean age (WMA) at 95% confidence intervals (Cal yr BP) from BACON (Blaauw and Christen, 2011).

<sup>1</sup> B2 = Mt Burney tephra layer (McCulloch and Davis, 2001).

<sup>2</sup> H1 = Vn Hudson tephra layer (McCulloch *et al.*, in press).

<sup>3</sup> B1 = Mt Burney tephra layer (this study).

<sup>4</sup> R1 = Vn Reclus tephra layer (McCulloch *et al.*, 2005).

<sup>5</sup> R1 = Vn Reclus tephra layer (McCulloch and Bentley, 1998).

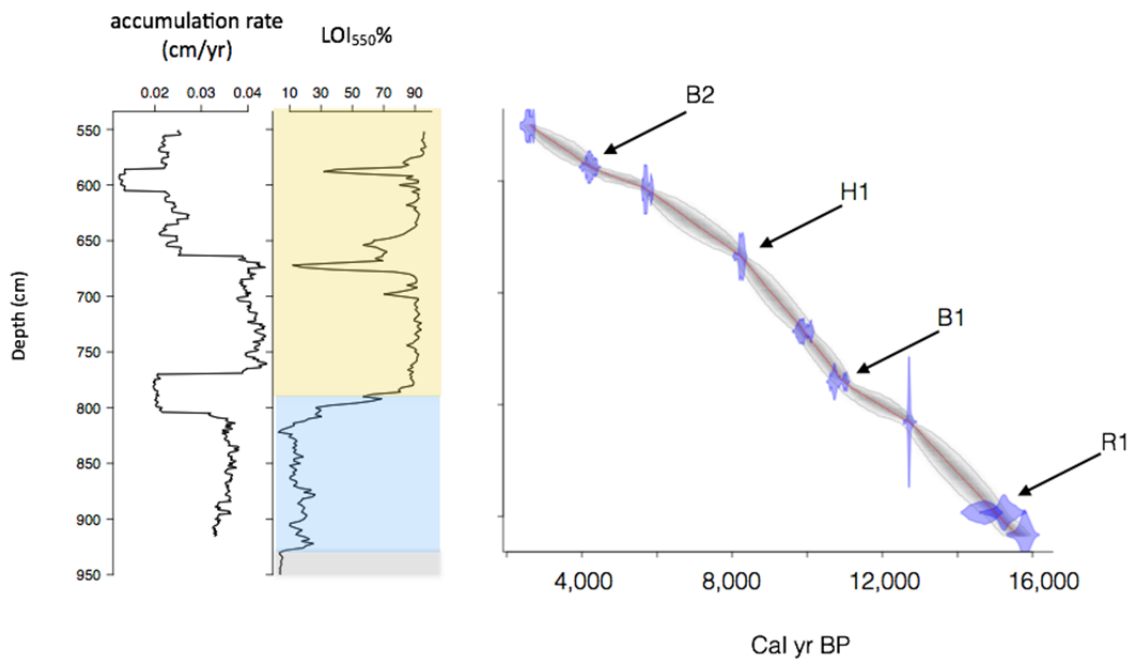


Figure 3.13 Accumulation rate, stratigraphy, organic content (LOI<sub>550</sub>%) and, chronology for the Lago Lynch core. The age-depth model was constructed using the Bayesian modelling program 'BACON' (Blaauw and Christen, 2011). Different colors denote the stratigraphy of Lago Lynch core; Grey: bluish clays and silts, Light blue: laminated lacustrine-mud sediment and Yellow: peat. Arrows show: Mt Burney (B2), Vn Hudson (H1), Mt Burney (B1) and Vn Reclús (R1).

The age of the contact between the basal organic sediment overlying bluish-grey glaciogenic clays and silts at 926 cm is estimated to be c. 15,610 Cal yr BP. The weighted averages of age-depth model derived ages from age-depth modeling were used to provide the age-depth axis (Cal yr BP) for the pollen diagrams produced using the Tilia Graph program (see Section 3.4).

### **3.4 Pollen stratigraphy.**

In order to facilitate the description of the pollen and spore data and to analyse the information in terms of past communities' vegetation changes, the cores were divided into 'local pollen assemblage zones' (LPAZs). The cores have been divided into zones using the CONISS program using the method of incremental sum of squares (Birks and Birks, 1980; Grimm, 1987; Bennett, 1996). Stratigraphically constrained CONISS cluster analysis was performed on the land pollen taxa  $\geq 2$  % and then the suggested LPAZ scheme applied to all (percentage, concentration and preservation) pollen diagrams. The "local pollen assemblage zone" (LPAZ) and its respective subzones are characterised by the most dominant taxa in terms of average percentage in each sub-zone. In this study "trace" presence describes taxa with less than  $\leq 2$  % and continuously represented within an LPAZ. "Virtually" absent describes taxa with less than  $\leq 2$  % and not continuously represented within an LPAZ.

#### **3.4.1 Rio Grande.**

Within the Rio Grande core 11 LPAZs have been defined. Below 640cm there is insufficient pollen abundance to define a vegetation assemblage. The full percentage pollen diagram for the Rio Grande record is shown in figure 3.14 (inside pocket on back cover) and a summary is

shown in figure 3.15, the diagrams encompass the vegetation assemblages from c. 15,870 Cal yr BP to the present.

LPAZ RG-1 (645 - 596 cm; c. 15,870-14,890 Cal yr BP): *Gunnera* – Poaceae – Ericaceae.

The initial pollen assemblage is dominated by herbaceous and shrub taxa such as *Gunnera* (~20%), Poaceae (~19%) and Ericaceae (~18%). *Gunnera* herbs have been recognised as nitrogen-fixers and they can be found currently in recently deglaciated terrains (Pisano, 1977). Herbs, including *Acaena* (~12%), Apiaceae (~12%), Asteraceae (Subf. Asteroideae) (~3%) and moorland elements such as *Drapetes muscosus* (~4%) are also present. The arboreal taxa *Nothofagus dombeyi* type is virtually absent ( $\leq 1\%$ ) and is not continuously found within this zone. Other herbs, such as Amaranthaceae, Asteraceae (Subf. Cichorioideae) and *Dysopsis*, are continually represented but with percentages of  $< 1\%$  for each taxa. There are low proportions of Cyperaceae ( $> 1\%$ ) and Pteridophytes. The aquatic *Myriophyllum* is well represented at ~56% and the freshwater green microalgae *Pediastrum* at ~27%.

LPAZ RG-2 (596 - 572 cm; c. 14,890 - 14,410 Cal yr BP): Poaceae - *Gunnera* - Ericaceae.

This interval is characterised by the same shrub and herbaceous taxa as the previous LPAZ. However, the proportions of each taxa change. Herbs such as Poaceae, *Acaena* and *Drapetes muscosus* increase in percentages to ~37%, ~18.0% and ~6%, respectively. Herbs and shrubs such as *Gunnera* (~16%), Apiaceae (~3%) and Ericaceae (~7%) decrease in percentages, while Asteraceae (Subf. Asteroideae) remain at ~3% of TLP. Others herbs, such as Asteraceae (Subf. Cichorioideae) and Caryophyllaceae, are continuously present throughout the subzone, although with percentages of  $< 1\%$ . Cyperaceae, and the Pteridophytes *Lycopodium* and Polypodiaceae, increase slightly to trace amounts. *Myriophyllum* and *Pediastrum* continue to be abundant reaching the maximum levels of the whole record at ~82% and ~78% respectively.

LPAZ RG-3 (572 - 550 cm; c. 14,410 – 12,480 Cal yr BP): Poaceae - Asteraceae (Subf. Asteroideae) - Ericaceae.

This LPAZ is characterised by increases in Poaceae and Asteraceae (Subf. Asteroideae) to ~62% and ~15%, respectively. There is a rapid drop in the percentage of *Acaena* to ~8% of TLP, while Ericaceae (~5%) and *Gunnera* (~4%) decrease gradually towards the end of this sub zone. Apiaceae and *Drapetes muscosus* decrease in abundance and are virtually absent. *Nothofagus dombeyi* type and Amaranthaceae appear continuously although <1%. Cyperaceae continues to be present in trace amounts. A slight increase in percentages is observed in Polypodiaceae (~3%) and the proportions of *Myriophyllum* and *Pediastrum* rapidly decrease to ~9% and ~22 %, respectively.

LPAZ RG-4 (550 - 530 cm; c. 12,480 - 11,690 Cal yr BP): *Nothofagus dombeyi* type – Poaceae - Asteraceae Subf. Asteroideae.

Within LPAZ RG-4 a layer of *Nothofagus betuloides* leaves was found, and so it is likely that the proportion of *Nothofagus dombeyi* type pollen in this LPAZ corresponds to *Nothofagus betuloides*. This taxa is the main component of hyper-humid sub-Antarctic evergreen forest which requires high humidity by precipitation and/or by poor drainage. Evergreen forest can be found where annual precipitation ranges between 2,000 mm and 6,000 mm. This LPAZ is dominated by a dramatic increase of *Nothofagus dombeyi* type to an average of ~42% TLP. Also, the epiphyte *Misodendrum* (~2%) is continuously present. Poaceae, *Acaena*, Asteraceae (Subf. Asteroideae) and *Gunnera* decrease to ~36%, ~3%, ~6% and trace amounts respectively. Ericaceae remains at ~5%. Pteridophytes such as *Lycopodium* (~3%), Polipodiaceae (~16%) increase in abundance. *Myriophyllum* decreases to trace amounts and proportions of *Pediastrum* increase to ~33%.

LPAZ RG- 5 (530 - 502 cm; c. 11,690 - 10,590 Cal yr BP): *Nothofagus dombeyi* type.

*Nothofagus* is the dominant taxa with an average of ~72% of TLP. *Misodendrum* is virtually absent. Poaceae is substantially reduced to ~17% and herbs such as Asteraceae (Subf. Asteroideae) and Ericaceae decline to ~2 and ~2%, respectively. Other herbs such as *Acaena*, Apiaceae and *Gunnera* are present in traces. Lycopodium and Polypodiaceae ferns decrease in abundance to trace and ~4%, respectively. The percentage of *Myriophyllum* increases to ~7% and *Pediastrum* drops to ~11%.

LPAZ RG- 6 (502 - 474 cm; c. 10,590 - 9,470 Cal yr BP): Poaceae - *Nothofagus dombeyi* type.

Between c. 10,500 - 9,900 Cal yr BP a second layer of *Nothofagus betuloides* leaves are found suggesting that the proportion of *Nothofagus* in this section corresponds to *Nothofagus betuloides* trees. *Nothofagus* decreases to ~40% and *Misodendrum* slightly increases and is present in trace amounts. Pollen grain trees such as *Drimys* and *Maytenus* are virtually absent. Poaceae increases in percentage to ~40% and Ericaceae, Asteraceae (Subf. Asteroideae) and *Acaena*, increase to ~5%, ~5% and ~2% of TPL, respectively. *Gunnera* is present continuously in this LPAZ with percentages less than 1% and Cyperaceae appears in trace amounts. *Lycopodium* and Polypodiaceae increase the percentages to ~3% and ~20%. *Myriophyllum* decreases in abundance and is present in traces amounts. *Pediastrum* increases in percentage to ~41%.

LPAZ RG- 7 (474 - 442cm; c. 9,470 - 8,260 Cal yr BP): *Nothofagus dombeyi* type.

*Nothofagus* increases to ~73% of TLP, while *Misodendrum* is virtually absent. Herbs and shrubs such as Poaceae, Asteraceae (Subf. Asteroideae) and Ericaceae decrease to ~17%, ~2% and

~2% respectively. *Gunnera* and *Littorella* are present in traces amounts. Cyperaceae continues in trace amounts. *Lycopodium* is about ~1% and Polipodiaceae is ~4%, both decrease in abundance. *Myriophyllum* increases in abundance to ~3% and, *Pediastrum* falls to ~14%.

LPAZ RG- 8 (442 - 340 cm; c. 8,260 - 4,930 Cal yr BP): *Nothofagus dombeyi* type – Poaceae.

*Nothofagus dombeyi* type decreases to an average of ~52% in this LPAZ while *Misodendrum* is virtually absent. Trees such as *Drimys* and *Maytenus* are present in trace amounts. Poaceae, Asteraceae (Subf. Asteroideae) and Ericaceae again increase in abundance to ~43%, ~4% and ~3%, respectively. *Acaena* appears with ~3% of TPL and other herbs such as *Gunnera*, Apiaceae and *Littorella* appear in trace amount. *Lycopodium* and Polypodiaceae rise in percentage to ~3% and ~12%, respectively. Both *Myriophyllum* and *Pediastrum* fluctuate from 0 to ~19% and ~1% to ~25% respectively.

LPAZ RG-9 (340 - 196 cm; c. 4,930 - 2,290 Cal yr BP): *Nothofagus dombeyi* type - Poaceae.

LPAZ RG-9a, between 340 cm and 276 cm (c. 4,930 - 3,760 Cal yr BP): *Nothofagus dombeyi* type gradually increases to ~67% towards the upper boundary and *Misodendrum* increases to ~4%. *Drimys* is not continuously present in this sub-zone and the average is less than 1%. Herbaceous taxa such as Poaceae, Asteraceae (Subf. Asteroideae) and *Acaena* decline to ~14%, ~1% and trace amounts, respectively. Ericaceae shrubs decrease to trace amounts. The herb *Rumex magellanicum* appears with an average percentage of 4%. Cyperaceae slightly increases in percentage and is represented in trace amounts. *Lycopodium* and Polypodiaceae decrease in abundance to trace amounts and *Myriophyllum* is virtually absent and the algae *Pediastrum* decreases in percentage to ~6%.

LPAZ RG-9b, between 276 cm and 196 cm (c. 3,760 - 2,290 Cal yr BP): *Nothofagus dombeyi* type is dominant with ~80%. *Misodendrum* decreases slightly in abundance to ~3%. *Drimys* and *Maytenus* are each present at less than 1% and are not continuously represented in this sub-zone. Ericaceae rises in percentage to ~6% and Poaceae decreases to ~7%, while Asteraceae (Subf. Asteroideae) and *Acaena* are also in this sub-LPAZ and persist in trace amounts and ~1%, respectively. Cyperaceae fluctuates from 0 to ~16% and *Lycopodium* and Polypodiaceae remain in trace amounts. The abundance of *Myriophyllum* increases dramatically to ~74% at the beginning of this LPAZ and then gradually disappears by c. 2,610 Cal yr BP (214 cm depth). *Pediastrum* also fluctuates from ~11 to ~2% and then disappears at the same time as *Myriophyllum*.

LPAZ RG-10 (196 - 128 cm; c. 2,290 - 1,480 Cal yr BP): *Nothofagus dombeyi* type – Ericaceae.

This LPAZ is characterised by a decrease in terrestrial plant diversity. *Nothofagus* is dominant with ~49% and *Misodendrum* is virtually absent. The trees *Drimys* and *Maytenus* are each present at less than 1% and are not continuously represented in this LPAZ. This zone is also characterised by a dramatic increase in Ericaceae shrubs to ~48%. Herbs such as Poaceae, *Acaena* and Asteraceae (Subf. Asteroideae) are virtually absent.

LPAZ RG-11 (128 - 0 cm; c. 1,480 Cal yr BP to present day): *Nothofagus dombeyi* type– Ericaceae.

The low terrestrial plant diversity continues in this LPAZ. *Nothofagus* is dominant at ~71% and *Misodendrum* and *Drimys* and *Maytenus* are virtually absent. Poaceae slightly increases in abundance to ~2% and Ericaceae and Asteraceae (Subf. Asteroideae) decrease in abundance to ~25% and traces respectively.

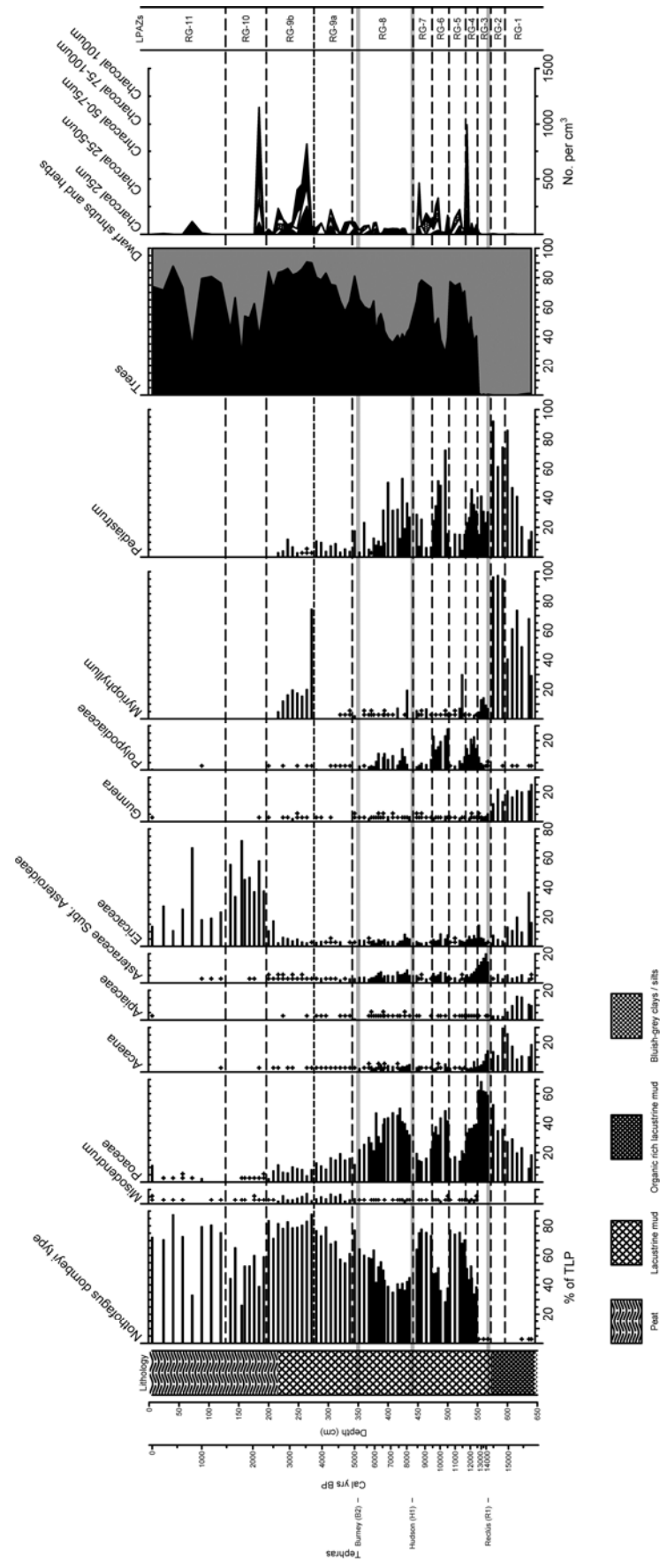


Figure 3.15 Summary of percentage pollen diagram for Rio Grande.

### 3.4.2 Punta Yartou.

Based on a constrained cluster analysis using the CONISS program (Birks and Birks, 1980; Grimm, 1987; Bennett, 1996) ten Local Pollen Assemblage Zones (LPAZs) have been defined in the Punta Yartou core. Samples below 1,032 cm do not contain sufficient total land pollen (TLP) for statistical analysis. The potential freshwater reservoir effect (FRE) below 933 cm (c. 15,050 Cal yr BP) in the Punta Yartou record is discussed in detail in section 4.2 of this study. Therefore, the ages that are included in the LPAZ PY-1 (1,032 - 1,004 cm, c. 23,170 - 20,590 Cal yr BP) and LPAZ PY-2 (1,004 - 933 cm, c. 20,590 - 15,050 Cal yr BP) should be treated with caution. The full percentage pollen diagram for the Punta Yartou record is shown in Figure 3.16 (inside pocket on back cover) and a summary is shown in Figure 3.17. The percentage pollen diagram for Punta Yartou and the LPAZs for the Punta Yartou core are described below:

LPAZ PY-1 (1,032 - 1,004 cm; c. 23,170 - 20,590 Cal yr BP): Ericaceae - *Acaena* - Poaceae.

The basal section is dominated by Ericaceae (~35%) and by herbs, such as *Acaena* (~32%), Poaceae (~18%), *Gunnera* (~3%) and Asteraceae (Subf. Asteroideae) (~3%). Other herbs such as Amaranthaceae and Asteraceae (Tribe Nassauvieae) are present in trace amounts. *Lycopodium* is present in traces. The aquatic plant *Myriophyllum* is virtually absent and the freshwater microalgae *Pediastrum* is present at ~25%.

LPAZ PY-2 (1,004 - 933 cm; c. 20,590 - 15,050 Cal yr BP): *Acaena* - Poaceae.

The pollen assemblage continues to be dominated by the same species as in LPAZ PY-1 but the proportions change; *Acaena*, Poaceae, Asteraceae (Subf. Asteroideae) and Asteraceae (Tribe Nassauvieae) increase to ~36%, ~34%, ~6% and ~6% respectively, while Ericaceae and *Gunnera* decline to ~6% and ~3%, respectively. *Nothofagus* is virtually absent. Other herbs

appear in this LPAZ such as Caryophyllaceae at ~1% and Apiaceae in trace amounts. Cyperaceae is virtually absent. Pteridophytes increase its abundance; *Lycopodium* to ~2% and Polypodiaceae to ~3%. *Myriophyllum* increases in percentage to ~2% and *Pediastrum* fluctuates between ~8% and ~30%.

LPAZ PY-3 (933 – 877 cm; c. 15,050 – 13,520 Cal yr BP): Poaceae - Asteraceae (Subf. Asteroideae).

This interval is dominated by an increase in Poaceae (~41%) and also an increase in Asteraceae (Subf. Asteroideae) (~23%) reaching its maximum value of ~32%, while *Acaena* and *Gunnera* decrease to ~12% and trace amounts respectively. Ericaceae proportions continue to be lower at ~7% and the herbs *Ranunculus* and Caryophyllaceae appear with ~1% and trace amounts, respectively. *Nothofagus* continues to be virtually absent. The abundances of *Lycopodium* (~2%) and Polypodiaceae (~10%) increase in this zone. *Myriophyllum* gradually increases from 0.3% at the beginning of the LPAZ to ~32% toward the upper boundary of the zone. The algae *Pediastrum* increases to ~35%.

LPAZ PY-4 (877 - 788 cm; c. 13,520 - 12,530 Cal yr BP): Poaceae - *Nothofagus dombeyi* type.

The beginning of this LPAZ is characterised by an increase in Poaceae, which reaches its maximum peak of ~71%, while the herbs such as Asteraceae (Subf. Asteroideae) (~15%), *Acaena* (~7%) and Ericaceae (~6%) decrease gradually in abundance towards the upper boundary. At this time *Nothofagus* increases in proportion from ~3% to ~40% and the semi-parasitic plant of *Nothofagus*: *Misodendrum* appears for the first time at 840 cm (c. 13,110 Cal yr BP) in trace amounts. Cyperaceae in this subzone is virtually absent. The Pteridophytes such as *Lycopodium* increase to ~4%, while Polypodiaceae to ~10%. At the beginning, this zone

*Myriophyllum* increases its average to ~28% and *Pediastrum* falls to ~21%, *Myriophyllum* decreasing towards the end to ~17% and, *Pediastrum* increases in proportion to ~50%.

LPAZ PY-5 (788 – 732 cm; c. 12,530 – 11,870 Cal yr BP): *Littorella* - *Nothofagus dombeyi* type.

This interval is characterised by a high percentage of *Littorella* (Plantaginaceae) (~27%). *Nothofagus* also increases with an average of ~28% and *Misodendrum* is present in trace amounts. The herbs such as Poaceae, Asteraceae (Subf. Asteroideae) and *Acaena* decrease to ~30%, ~4% and ~1%, respectively and Ericaceae decreases to around ~2%. Herbs such as *Ranunculus*, Asteraceae (Subf. Cichorioideae) and *Caltha* also remain at abundances of ~2%, ~1% and ~1%, respectively. *Lycopodium* decreases in abundance to ~3% and Polypodiaceae remains at ~8%. *Myriophyllum* continues decreasing to ~6% and *Pediastrum* also decreases in abundance to ~29%.

LPAZ PY- 6 (732 - 612 cm; c. 11,870 - 9,510 Cal yr BP): *Nothofagus dombeyi* type - Poaceae.

The proportions of pollen of *Nothofagus dombeyi* type (~42%) and Poaceae (~37%) increase while *Misodendrum* and *Drimys* are virtually absent. Herbs such as Asteraceae (Subf. Asteroideae) and *Acaena* decrease to ~4% and ~2% respectively. Ericaceae decreases to ~1% and Asteraceae (Subf. Cichorioideae) fluctuates from 0% to ~8%. The abundance of Cyperaceae increases to ~5%. *Lycopodium* and Polypodiaceae increase in abundance to ~6% and ~13%. *Myriophyllum* fluctuates from ~40% to 0% and *Pediastrum* oscillates from 0% to 39%. At 696 cm (c. 10,548 Cal yr BP) the aquatic flora disappears. Between 636 – 612 cm (c. 9,830 – 9,510 Cal yr BP) there is a short interval where there is low terrestrial plant diversity and it is characterised by a drastic increase in Ericaceae abundance reaching a peak of ~50%. *Nothofagus dombeyi* type decreases to ~13%.

LPAZ PY- 7 (612 - 370 cm; c. 9,510 - 5,170 Cal yr BP): Poaceae - *Nothofagus dombeyi* type.

This zone is characterised by high levels of Poaceae with an average of abundance of ~51% and a slight increase of Asteraceae (Subf. Asteroideae) abundance to ~2%. *Nothofagus dombeyi* type has low levels of abundance with an average of ~33% and *Misodendrum* is virtually absent. *Drimys* and *Maytenus* are virtually absent. The herb *Acaena* appears with percentage of ~6%. The shrub Ericaceae decreases to ~3%. Cyperaceae increases its abundance to ~20%. Polypodiaceae retains the percentage to ~7%.

LPAZ PY- 8 (370 - 283 cm; c. 5,170 - 3,440 Cal yr BP): Poaceae - *Nothofagus dombeyi* type – *Drimys*.

This assemblage is characterised by a slight decrease of abundance of *Nothofagus dombeyi* type and Poaceae to ~26% and ~48%, respectively. *Misodendrum* is virtually absent and *Drimys* reaches the highest proportion in the record with ~2%. *Gunnera* fluctuates from ~70% at the beginning of this phase to 0% at the end. The herbs such as *Acaena* decrease in abundance to ~1% and Asteraceae (Subf. Asteroideae) remains at ~2%, while Apiaceae appears with ~3%. Cyperaceae decreases in abundance to ~12%. Polypodiaceae continues decreasing to ~3%.

LPAZ PY- 9 (283 - 227 cm; c. 3,440 - 2,170 Cal yr BP): Ericaceae - *Nothofagus dombeyi* type.

This zone is characterised by low terrestrial plant diversity and by a substantial increase in Ericaceae abundance to ~53%. *Nothofagus* maintains its proportion at ~24%. *Drimys* and *Maytenus* are present in trace amounts. Poaceae fluctuates from ~4% to ~30%.

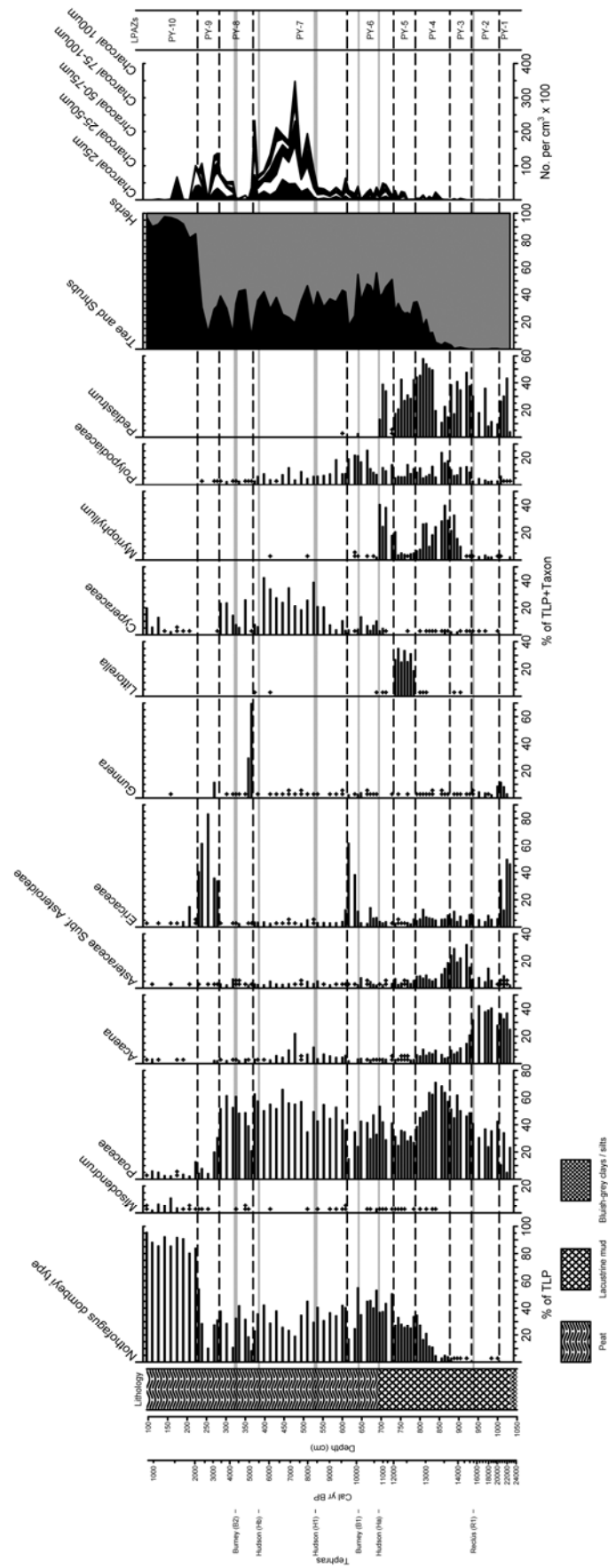


Figure 3.17 Summary of percentage pollen diagram for Punta Yartou.

LPAZ PY- 10 (227 - 98 cm; c. 2,170 - 870 Cal yr BP): *Nothofagus dombeyi* type.

This zone is dominated by *Nothofagus* at ~85% of TLP. *Misodendrum* also correspondingly reaches a maximum of ~3% and *Drimys* and *Maytenus* are virtually absent. Poaceae decreases to an average of ~4%. Ericaceae gradually decreases from ~40 to ~1%. Cyperaceae gradually increases from 0% to ~20%.

### 3.4.3 Lago Lynch.

Based on a cluster analysis of the data using the CONNIS program (Birks and Birks, 1980; Grimm, 1987; Bennett, 1996) nine Local Pollen Assemblage Zones (LPAZ) have been defined in the Lago Lynch core. From samples below 926 cm (c. 15,610 Cal yr BP) there was insufficient total land pollen grain (TLP) concentration to characterise a vegetation assemblage. The full percentage pollen diagram for the Lago Lynch core is shown in Figure 3.18 (inside pocket on back cover) and a summary of percentage pollen diagram for the Lago Lynch is shown in Figure 3.19. The following describes the percentage pollen diagram for Lago Lynch and the LPAZs.

LPAZ LL - 1 (926 - 906cm, c. 15,610 - 15,010 Cal yr BP): Ericaceae - Poaceae - *Acaena*.

The basal section is dominated by Ericaceae (~54%) and herbs such as Poaceae (~20%) and *Acaena* (~10%). Wetland-herbs, such as Ranunculaceae, *Gunnera* and *Caltha* are present at ~8%, ~2% and ~1% of TLP respectively. Herbaceous cover such as Apiaceae and Asteraceae (Subf. Asteroideae) are present in trace amounts. Cyperaceae is represented with ~2% and *Lycopodium* is present in trace amounts. *Myriophyllum* and *Pediastrum* are abundant at ~52% and ~58% respectively.

LPAZ LL - 2 (906 - 884 cm; c. 15,010 - 14,430 Cal yr BP): Ericaceae – Poaceae.

LPAZ LL-2 continues to be dominated by the same species as LPAZ LL-1. However, Ericaceae increases to ~66%, Poaceae slightly decreases in percentage to ~18% and *Acaena* decreases to ~5%. Wet land herbs such as Ranunculaceae, *Gunnera* and *Caltha* are present in traces. Species such as Apiaceae and Asteraceae (Subf. Asteroideae) increase in abundance to ~3% and ~3%. *Nothofagus* appears as trace amounts. Cyperaceae remains at ~1%. The aquatic flora increase: *Myriophyllum* to ~70% and *Pediastrum* to ~67%.

LPAZ LL - 3 (884 - 824 cm; c. 14,430 - 12,710 Cal yr BP): Poaceae – Ericaceae.

This LPAZ is characterised by an increase in the abundance of Poaceae at ~38% and by a decrease of the shrub Ericaceae at ~4%, while *Acaena* remains at ~6%. Ranunculaceae, *Gunnera* and *Caltha* increase slightly in abundance to 1%, ~2% and ~2% respectively and Apiaceae remains at ~3%. Asteraceae (Subf. Asteroideae) remains the abundance to ~3%. At this time *Nothofagus dombeyi* type increases to ~9%. *Myriophyllum* gradually decreases from ~70% to ~4% and *Pediastrum* fluctuates widely from ~87% to ~17%.

LPAZ LL - 4 (824 - 788 cm; c. 12,710 - 11,020 Cal yr BP): *Galium* – *Nothofagus dombeyi* type.

This zone is distinctive due to the significant increase in the percentage of *Galium* to ~11%, a shrub-land/steppe taxon the pollen of which is not dispersal by wind *Nothofagus dombeyi* type also increases to an average of ~50% and *Misodendrum* appears at <1%. Poaceae, *Acaena* and Asteraceae (Subf. Asteroideae) decrease to around ~32%, ~3% and trace amounts respectively. Also Apiaceae appears in trace amounts and *Rumex* at ~2%. Ericaceae maintains its cover at ~4%. Cyperaceae increases to ~4%. *Lycopodium* and Polypodiaceae are present in trace

amounts. *Myriophyllum* continues decreasing to ~2% and *Pediastrum* fluctuates from 17% to ~62%.

LPAZ LL-5 (788 - 692 cm; c. 11,020 - 8,670 Cal yr BP): Poaceae - *Nothofagus dombeyi* type.

LPAZ LL-5a, between 788 cm and 760 cm (c. 11,020 - 10,340 Cal yr BP): this sub-LPAZ is characterised by fluctuations of Poaceae from ~22% to ~62% and *Nothofagus dombeyi* type percentage from ~60% to ~31%. *Misodendrum* is present in traces and *Drimys* is virtually absent. Asteraceae (Subf. Asteroideae) decreases to trace amounts. Cyperaceae increases in abundance to ~14%. *Lycopodium* increases to ~2% and Polypodiaceae and *Sphagnum* persist as trace amounts. At 760 cm (c. 10,340 Cal yr BP) the aquatic flora finally disappears; *Myriophyllum* is already virtually absent and *Pediastrum* gradually decreases from ~10% to 0%.

LPAZ LL-5b, between 760 cm and 740 cm (c. 10,340 - 9,870 Cal yr BP): Poaceae dominates this assemblage with the highest level in the record at ~72% and *Nothofagus dombeyi* type at ~28%. *Acaena* and Ericaceae appear at ~1% and trace amounts respectively. Asteraceae (Subf. Asteroideae) also remains in trace amounts. Cyperaceae increases in abundance slightly reaching ~17% at its maximum. *Lycopodium* remains at ~2% and Polypodiaceae is still present in trace amounts.

LPAZ LL-5c, between 740 cm and 692 cm (c. 9,870 - 8,670 Cal yr BP) In this subzone Poaceae decreases to around 55% and *Nothofagus dombeyi* type increases to ~35%. Ericaceae increases to ~3% and Asteraceae (Subf. Asteroideae) increases in percentage to ~2% and *Acaena* appears at ~1%. Cyperaceae increases and fluctuates from ~3% to ~40%. *Lycopodium* decreases to ~1% and *Sphagnum* fluctuates from 0% to ~38%.

LPAZ LL-6 (692 - 632 cm; c. 8,670 - 6,670 Cal yr BP): *Nothofagus dombeyi* type - Poaceae.

LPAZ LL-6a, between 692 cm and 674 cm (c. 8,670 - 8,220 Cal yr BP): this sub-LPAZ is characterised by an increase in *Nothofagus dombeyi* type to ~40% and a decrease of Poaceae abundance to ~35%. Herbaceous taxa such as Asteraceae (Subf. Asteroideae), Ericaceae and *Acaena* increase to around ~9%, ~6% and ~5%, respectively. The herb Rubiaceae is also present in traces. Cyperaceae increases to ~17% and *Sphagnum* increases in average abundance to ~22%.

LPAZ LL-6b, between 674 cm and 632 cm (c. 8,220 - 6,670 Cal yr BP): Poaceae and *Acaena* increase in percentages to ~40% and ~14% respectively and *Nothofagus dombeyi* type decreases in abundance to ~35%. The herbaceous taxa Asteraceae (Subf. Asteroideae) decreases to ~3% and the shrub Ericaceae to ~5%. The abundance of Cyperaceae drop to around ~5% and *Lycopodium* fern is present with ~2%.

LPAZ LL- 7 (632 - 596 cm; c. 6,670 - 4,660 Cal yr BP): *Nothofagus dombeyi* type - Poaceae.

This subzone is characterised by the dominance of *Nothofagus dombeyi* type at ~55%, while the herbaceous taxa, such as Poaceae and *Acaena* drop in percentage to around ~27% and ~2% respectively. Ericaceae increases to ~10% and Asteraceae (Subf. Asteroideae) remains at around ~3%. Cyperaceae increases again to around ~12%, *Lycopodium* is present in trace amounts and *Sphagnum* fluctuates from 0% to ~39%.

LPAZ LL- 8 (596 - 576 cm; c. 4,660 - 3,790 Cal yr BP): *Nothofagus dombeyi* type - Ericaceae.

*Nothofagus dombeyi* type retains its dominance at ~51% and Ericaceae increases to ~26%. Poaceae correspondingly declines to ~13%. Asteraceae (Subf. Asteroideae) persists at ~3%.

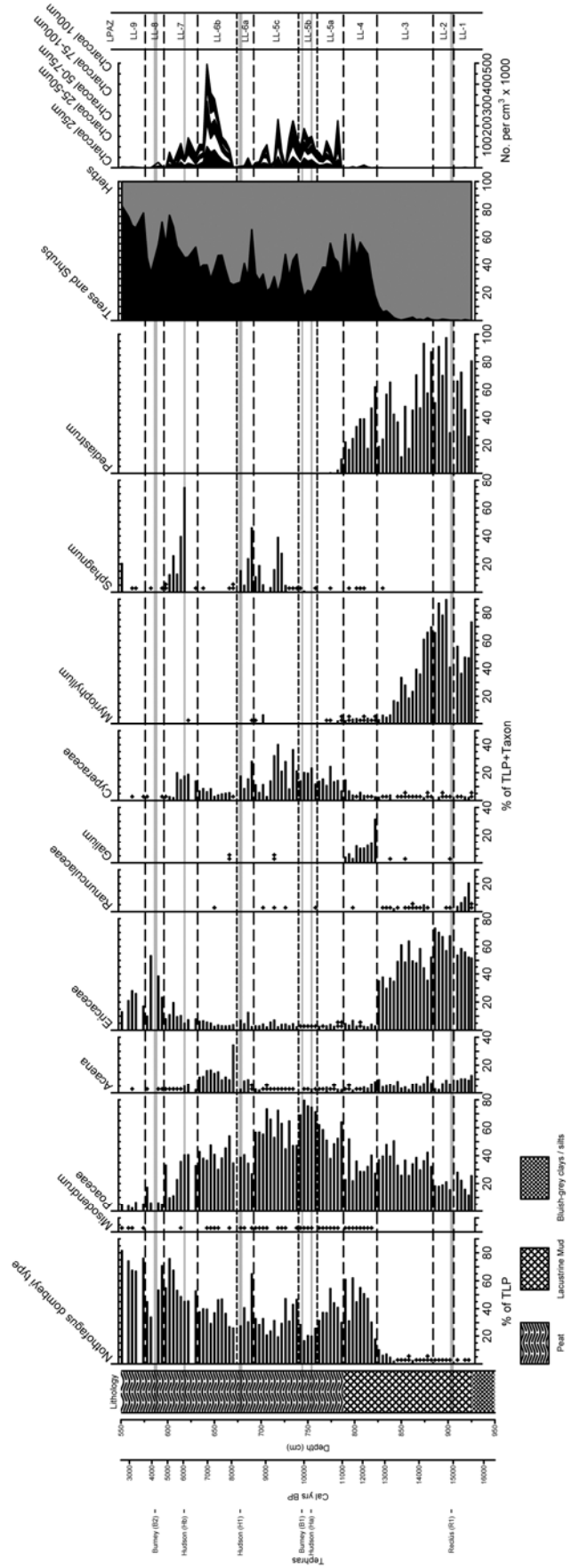


Figure 3.19 Summary of percentage pollen diagram for Lago Lynch.

LPAZ LL- 9 (576 – 550 cm; c. 3,790 - 2,640 Cal yr BP): *Nothofagus dombeyi* type.

*Nothofagus dombeyi* type dominates the profile at ~73% and Ericaceae decreases slightly to ~20% TLP. Poaceae decreases to 4% and Asteraceae (Subf. Asteroideae) decreases to trace amounts.

### 3.5 Pollen concentration (grains per cm<sup>3</sup>).

Pollen concentrations were estimated by adding a known quantity of exotic spores (*Lycopodium clavatum*) to each sediment sample of 1.0cm<sup>3</sup> taken from Rio Grande, Punta Yartou and Lago Lynch cores during sample laboratory preparation (Stockmarr, 1977).

#### 3.5.1 Rio Grande.

The profile of pollen concentrations for selected taxa and the total pollen concentration is shown in Figure 3.20. In the LPAZ RG-1 and RG-2 (c. 15,870 - 14,410 Cal yr BP) there are low total land pollen concentrations (~25 grains per cm<sup>3</sup> x 1,000). However, during LPAZ RG-2 (c. 14,890 - 14,410 Cal yr BP) *Myriophyllum* increases dramatically. During LPAZ RG-3 and RG-4 (c. 14,410 - 10,590 Cal yr BP) the total land pollen concentration increase gradually to moderate values (~50 grains per cm<sup>3</sup> x 1,000) then dramatically rises to peak during LPAZ RG-5 (c. 11,690 - 10,590 Cal yr BP) to ~250 grains per cm<sup>3</sup> x 1,000. The peak is mainly made up from increase in *Nothofagus dombeyi* type pollen concentration. During the following LPAZ RG- 6 (c. 10,590 - 9,470 Cal yr BP) the pollen concentration decreases to moderate values (~50 grains per cm<sup>3</sup> x 1,000). However, during LPAZ RG-7 (c. 9,470 - 8,260 Cal yr BP) again there is a high peak of pollen land concentration mainly contributed by *Nothofagus dombeyi* type (~150 grains per cm<sup>3</sup> x 1,000). The LPAZ RG-8 (c. 8,260 - 4,930 Cal yr BP) is characterised by moderate and stables values of (~50 grains per cm<sup>3</sup> x 1,000). The highest pollen concentration is

found in the interval LPAZ RG-9a (c. 4,930 - 3,760 Cal yr BP) contributed principally by *Nothofagus dombeyi* type, *Misodendron* and Poaceae reaching the total land concentration values of more than 450 grains per  $\text{cm}^3 \times 1000$ . During LPAZ RG-9b (c. 3,760 - 2,290 Cal yr BP) the pollen concentration of *Myriophyllum* increases dramatically to a peak ( $>300$  grains per  $\text{cm}^3 \times 1,000$ ) and then finally disappears by c. 2,610 Cal yr BP.

The Mt Burney B2 (c. 4,400 Cal yr BP) tephra layer marks the transition from LPAZ RG-8 to LPAZ RG-9a, after this boundary a small increase in pollen concentrations mainly contributed by *Galium* and *Rumex* occurs ( $\sim 25$  grains per  $\text{cm}^3 \times 1,000$ ) during a relatively short time ( $\sim 1,000$  yr). Finally, in the LPAZs RG-10 and RG-11 (c. 2,290 Cal yr BP to present day) the total pollen land concentrations appear to fluctuate in both magnitude and frequency of fluctuation mainly, contributed by *Nothofagus* and Ericaceae.

### 3.5.2 Punta Yartou.

The pollen concentrations for the selected taxa and for total pollen land concentrations are shown in Figure 3.21. In LPAZ PY-1, PY-2, PY-3 and PY-4 (c. 23,170 - 12,530 Cal yr BP) the total land pollen concentrations remains low ( $\sim 25$  grains per  $\text{cm}^3 \times 1,000$ ) and then during the LPAZ PY-5 (c. 12,530 - 11,870 Cal yr BP) the pollen concentrations increase to  $\sim 80$  grains per  $\text{cm}^3 \times 1,000$  mainly contributed by *Nothofagus dombeyi* type and *Littorella*. During LPAZ PY-6 and PY-7 (c. 11,870 – 5,170 Cal yr BP), the pollen concentration continues moderate ( $\sim 35$  grains per  $\text{cm}^3 \times 1,000$ ) and relatively stable values throughout the LPAZs. During LPAZ PY- 8 (c. 8,260 - 4,930 Cal yr BP) the pollen concentrations increase ( $\sim 50$  grains per  $\text{cm}^3 \times 1,000$ ) mainly due to the rise in Poaceae. During LPAZ PY-9 (c. 4,930 - 2,290 Cal yr BP) there is a peak in pollen concentrations, mainly contributed by Ericaceae. Finally, during LPAZ PY-10 (c. 2,290 to present day) Ericaceae is replaced by high concentrations, albeit fluctuating of *Nothofagus dombeyi* type.

### 3.5.3 Lago Lynch.

The profile of pollen concentrations for the selected taxa and for total pollen land concentrations is shown in Figure 3.22. During the LPAZ LL-1, LL-2 and LL-3 (c. 15,590 - 12,710 Cal yr BP) the total land pollen concentrations remain low (~25 grains per cm<sup>3</sup> x 1,000) principally made up Ericaceae. Within LPAZ LL-2 (c. 15,010 - 14,430 Cal yr BP) there is a dramatic increase in aquatic taxa, such as *Myriophyllum* and *Pediastrum* (~120 grains per cm<sup>3</sup> x 1,000 and 600 grains per cm<sup>3</sup> x 1,000). In the LPAZ LL-4 (c. 12,710 - 11,020 Cal yr BP) the land pollen concentrations increase and are mainly due to a rise in *Nothofagus dombeyi* type, Poaceae and *Galium* (~100 grains per cm<sup>3</sup> x 1,000). Then during LPAZ LL-5, LL-6 and LL7 and its respective subzones (c. 11,690 - 8,260 Cal yr BP) there were relatively stable levels (~50 grains per cm<sup>3</sup> x 1,000) of pollen land concentrations (c. 11,690 - 8,260 Cal yr BP) contributed by *Nothofagus dombeyi* type and Poaceae. During LPAZ LL-8 (c. 8,260 - 4,930 Cal yr BP) there is a dramatic increase in pollen concentrations (>500 grains per cm<sup>3</sup> x 1,000), which is first due to a rise in Ericaceae and Asteraceae (Subf. Asteroideae), Poaceae, Fabaceae, *Myrteola nummularia* and *Caltha*. Finally, in the LPAZ LL-9 (c. 3,790 - 2,640 Cal yr BP) the pollen concentration decreases to moderate values (~50 grains per cm<sup>3</sup> x 1,000).

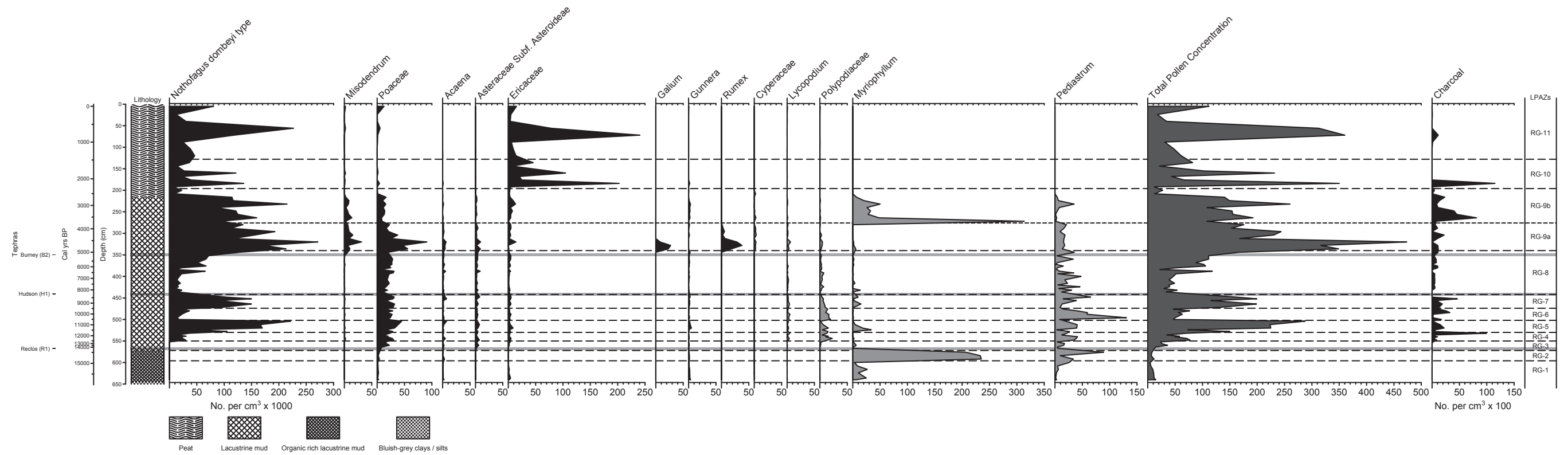


Figure 3.20 Rio Grande: pollen concentrations for selected taxa.

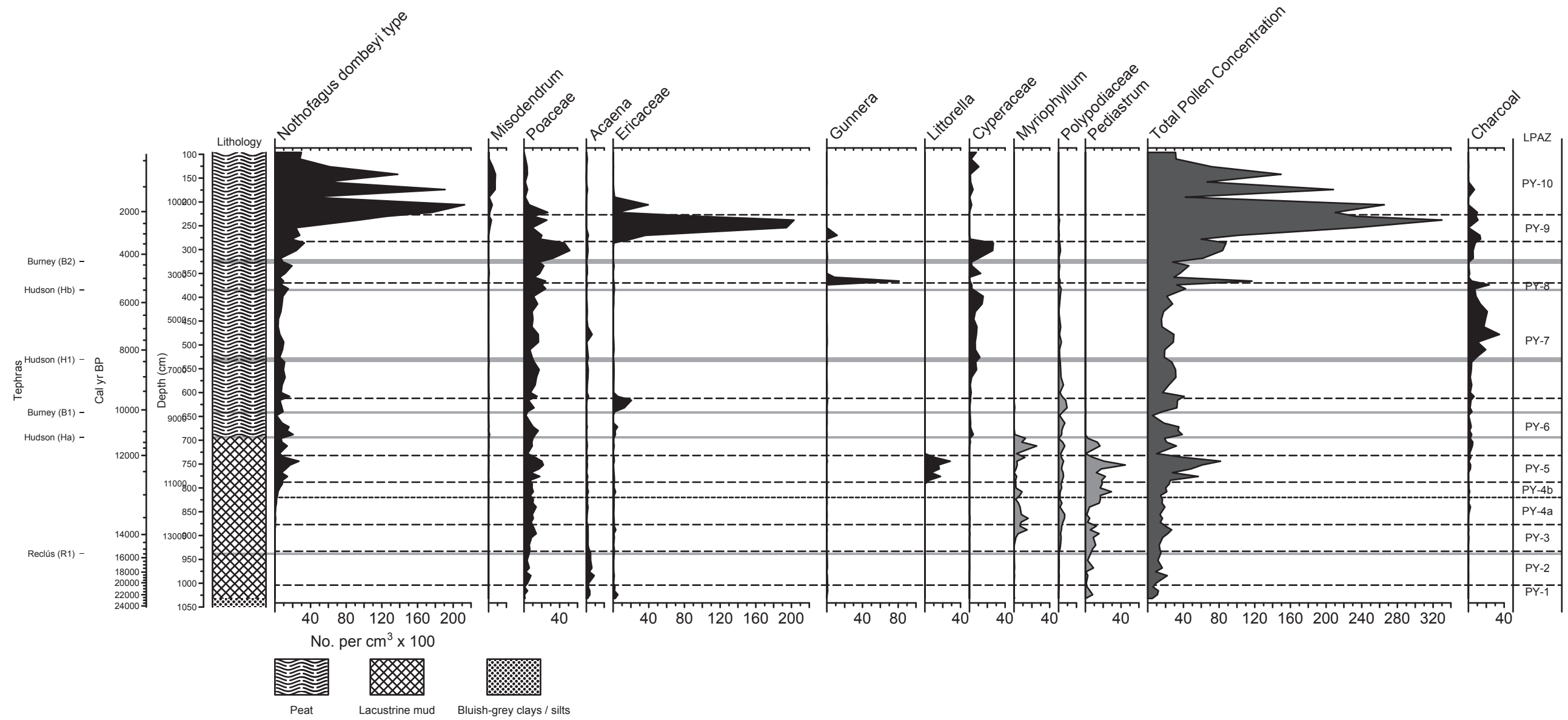


Figure 3.21 Pta Yartou: pollen concentrations for selected taxa.

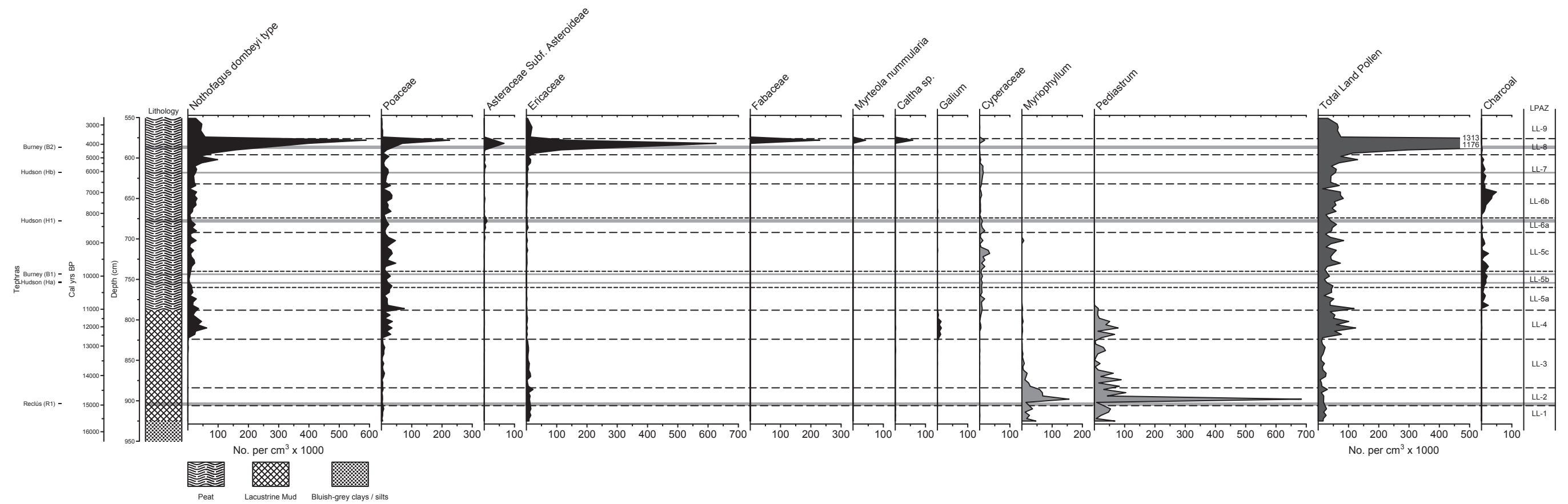


Figure 3.22 Lago Lynch: pollen concentrations for selected taxa.

### 3.6 Pollen preservation.

There were five categories of terrestrial pollen grain preservation used in this study: 1) well preserved or normal, 2) broken, 3) crumpled, 4) corroded and 5) degraded (Cushing, 1967; Tipping 1987). Broken and crumpled pollen grains are considered damaged by mechanical factors, while corroded and degraded pollen grains signify damage to pollen by biochemical factors under more aerobic conditions (see Chapter 2, Section 2.8). The results are expressed as percentages of the TLP and are grouped as normal pollen grains, broken and crumpled pollen grains and, corroded and degraded pollen grains. The preservation data are described by LPAZs.

#### 3.6.1 Rio Grande.

The record of pollen preservation for Rio Grande core is shown in Figure 3.23. In LPAZs RG-1, RG-2 and RG-3 (c. 15,870 - 12,480 Cal yr BP) there are higher proportions (~70%) of normal pollen, while corroded and degraded pollen grains are consistently <25%. Then in LPAZs RG-4, RG-5, RG-6, RG-7 and RG-8 (c. 12,480 - 4,930 Cal yr BP) the proportions of normally preserved pollen decreases and remains relatively stable (~55%) and there is a corresponding increase in the levels of corroded and degraded pollen. During the LPAZ RG-9a (c. 4,930 - 3,760 Cal yr BP) the percentages of well preserved pollen grains reaches their lowest levels in the whole core, (<40%). At the boundary between LPAZ RG-9a and LPAZ RG-9b there is a peak in normal pollen which reaches 80%. This is followed by large fluctuations through LPAZ RG-9b (c. 3,760 - 2,290 Cal yr BP). Finally, during LPAZs RG-10 and RG-11 (c. 2,290 Cal yr BP to present day) the proportion of normally preserved pollen returns to previous higher levels (~70%), correspondingly the crumpled and degraded pollen are very low in proportions (<5% and broken and crumpled reaches to~20%).

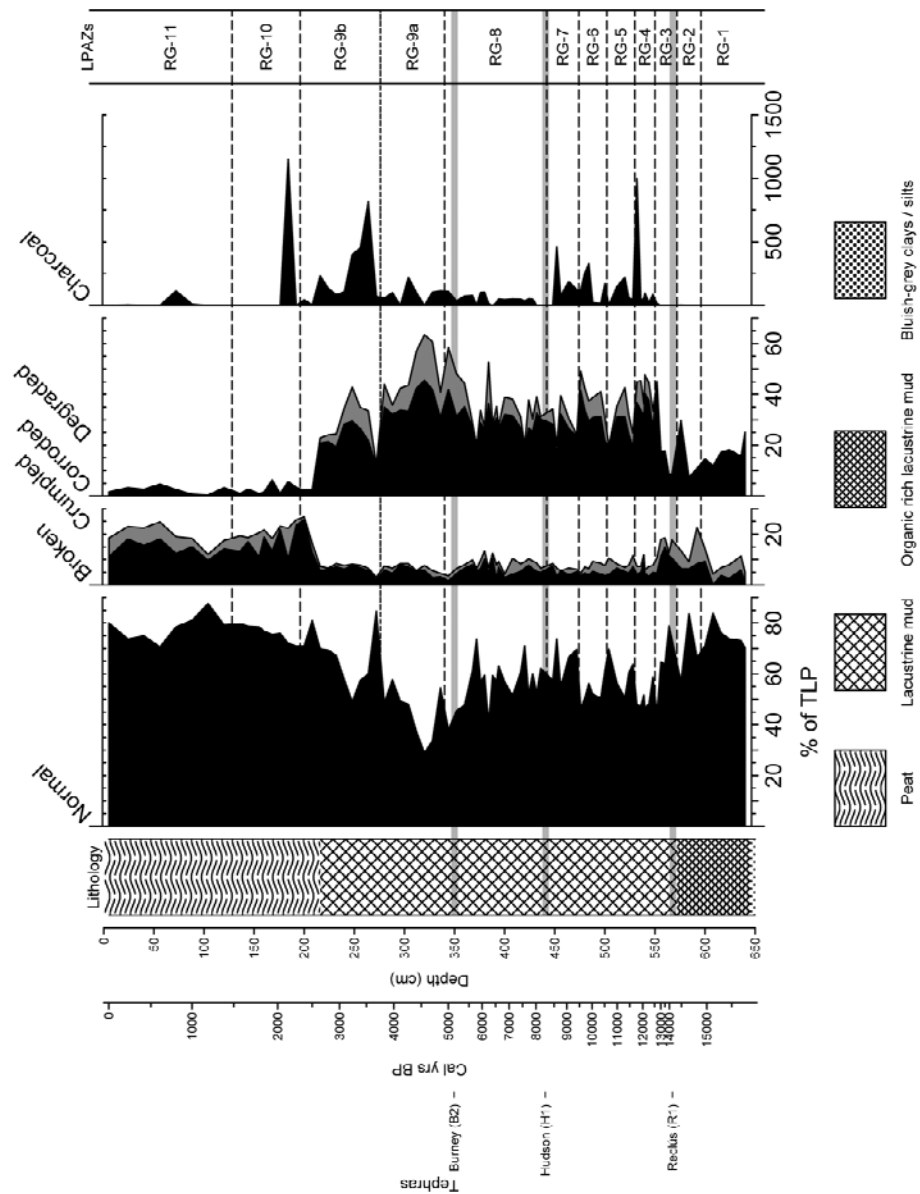


Figure 3.23 Pollen preservation for Rio Grande.

### 3.6.2 Punta Yartou.

The record of pollen preservation for Punta Yartou core is shown in Figure 3.24. The LPAZs PY-1, PY-2, PY-3, PY-4a and b, PY-5 and PY-6 (c. 23,170 - 9,510 Cal yr BP) have high proportions of well preserved (i.e. normal) pollen (~60%) and these levels remain stable through

until c. 9,500 Cal yr BP, coinciding with high levels of charcoal (see Section 3.7). During LPAZ PY-7 (c. 9,510 Cal yr BP) until c. 8,220 Cal yr BP (526 cm depth) the percentage of normal pollen gradually decrease to ~20% and there is a corresponding increase in mainly crumpled pollen (~40%). This is followed by a dramatic decrease of well preserved pollen to <30% and corresponding high proportions of crumpled, corroded and degraded pollen which persist through the LPAZ. During the LPAZs PY-8, PY-9 and until the mid point (174 cm depth) of LPAZ PY-10 (c. 5,170 - 1,580 Cal yr BP) the high percentages of crumpled pollen continues (~45%) while the rest of the categories continue to fluctuate in magnitude during this interval of time. Finally, from c. 1,580 Cal yr BP to the c. 872 Cal yr BP (98 cm depth) in the upper part of LPAZ PY-10 the corroded and degraded pollen increase drastically and there is a reduction in the proportions of crumpled pollen.

### **3.6.3 Lago Lynch.**

The record of pollen preservation for the Lago Lynch core is shown in Figure 3.24. LAPZ LL-1 (c. 15,810 - 15,010 Cal yr BP) evidences high percentages of well-preserved pollen (~60%) and the deteriorated pollen present is mainly corroded and degraded (~20%). During LAPZs LL-2 and LL-3 (c. 15,010 - 12,710 Cal yr BP) the proportions of normal pollen decrease to ~40% and remain at these levels for the remainder of the LPAZ and there is a corresponding increase in crumpled, corroded and degraded pollen. During LPAZ LL-4 (c. 12,710 - 11,020 Cal yr BP) well preserved pollen increases to ~70%, and the deteriorated pollen, principally corroded and degraded, decrease. During the LPAZs LL-5a-c and LL-6a,b and until the mid-point of LPAZ LL-7 (c. 11,020 - 5,920 Cal yr BP) the percentages of normal pollen decrease and fluctuate at ~40% and there is an increase in all the categories of deteriorated pollen. From c. 5,920 Cal yr BP (614 cm depth) into the LPAZ LL-7 to the top of the core 2,640 Cal yr BP (550 cm), there is a dramatic increase in well preserved pollen to 60% corresponding with a decrease in deteriorated pollen, principally degraded pollen.

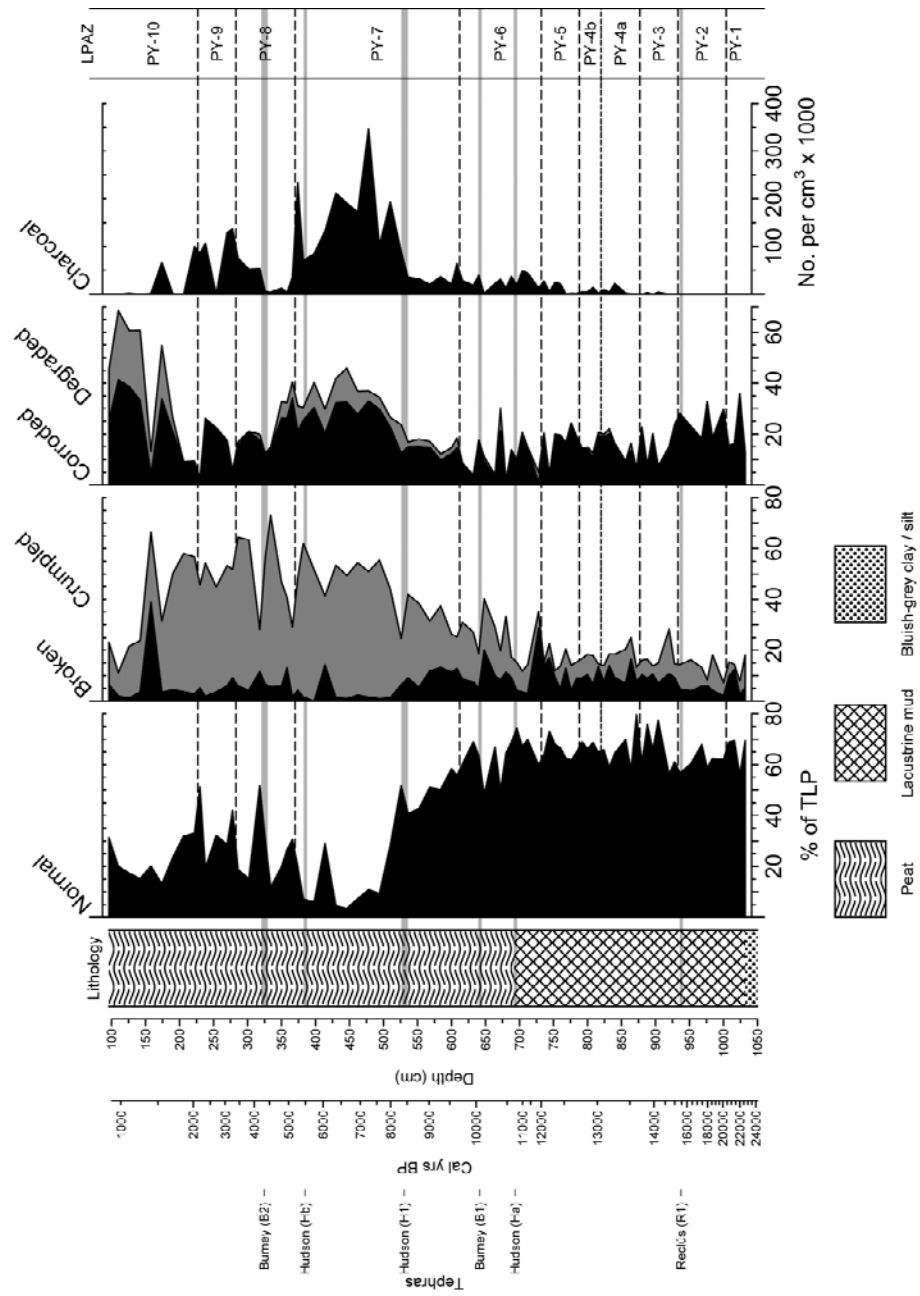


Figure 3.24 Pollen preservation for Punta Yartou.

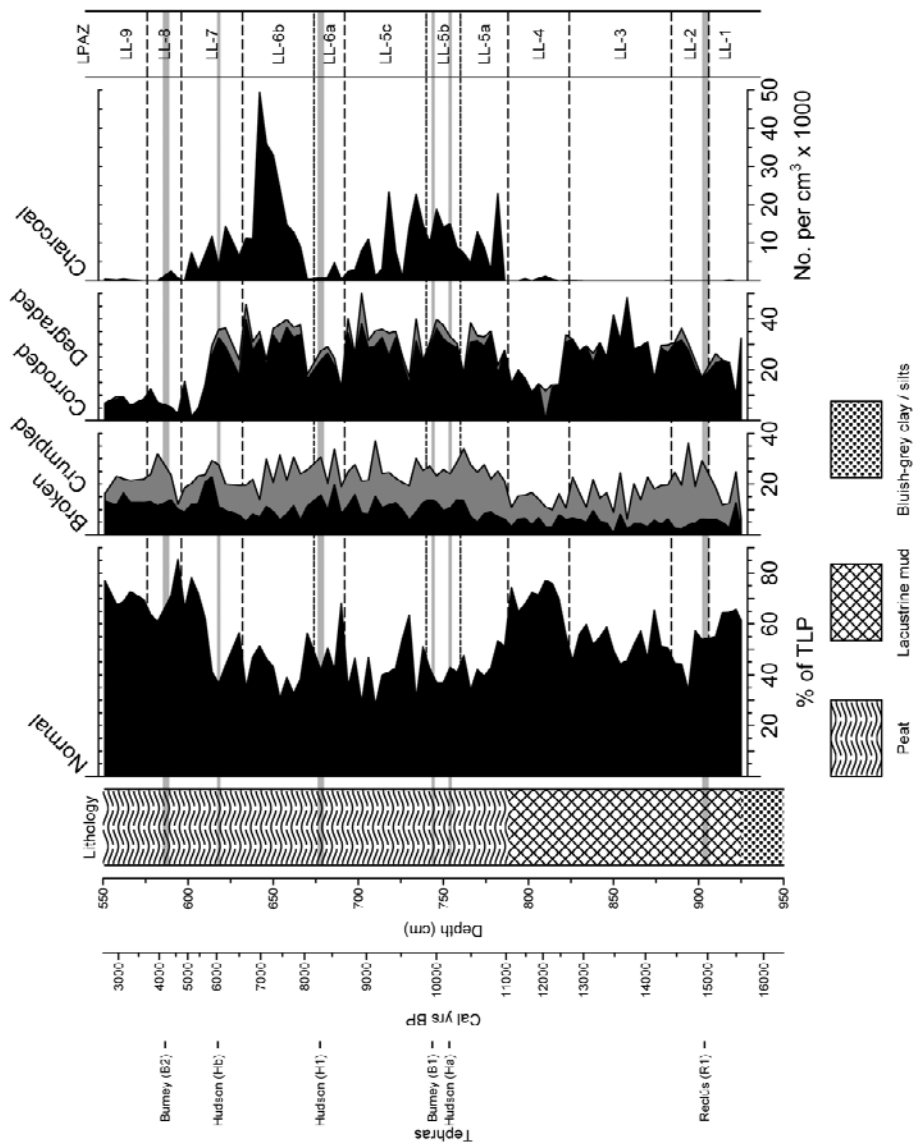


Figure 3.25 Pollen preservation for Lago Lynch.

### 3.7 Charcoal concentration.

The charcoal particles were classified in to categories by size: <25µm, 25 to 50 µm, 50 to 75 µm, 75 to 100 µm and > 100µm up to 180µm (the mesh size of the sieve used in the pollen preparation procedure). The size data was also grouped to provide an estimation of total charcoal concentrations. The charcoal data for each core is described next.

### 3.7.1 Rio Grande.

The Rio Grande core is located to the western end of the precipitation gradient and correspondingly within the wetter ecosystem (evergreen *Nothofagus* forest). Presently, the higher humidity provides an infrequent environment for fire ignition and relatively unfavourable conditions for spreading the fire due to the high fuel moisture content. There is also a lack of evidence of human occupation in this area throughout the Late-glacial and Holocene. Therefore, the charcoal record from Rio Grande is more likely to reflect a regional fire (through long distance charcoal transport) and so larger-scale climate changes rather than variations in local conditions.

Figure 3.26 shows the micro, macro and total charcoal concentrations for the Rio Grande core. The charcoal concentrations for the whole of the core are relatively low ( $< 15,000$  particles per  $\text{cm}^3$ ). Therefore, the results have to be taken with caution to avoid over interpretation of the fire history recorded at the site. The temporal pattern of the particle size distributions of the charcoal particles have relatively similar characteristics among categories (micro and macro charcoal) in terms of the past fire activity; a relatively continuous presence of charcoal particles is found from the early Holocene to the late Holocene (c. 12,610 - 2,120 Cal yr BP). There is also a small peak of charcoal within the interval between c. 1,000 Cal yr BP and c. 804 Cal yr BP. Overall, two significant phases of past fire activity in the Rio Grande core can be identified; 1) from 11,770 Cal yr BP to 8,600 Cal yr BP and, 2) from 3,540 Cal yr BP to 2,120 Cal yr BP.

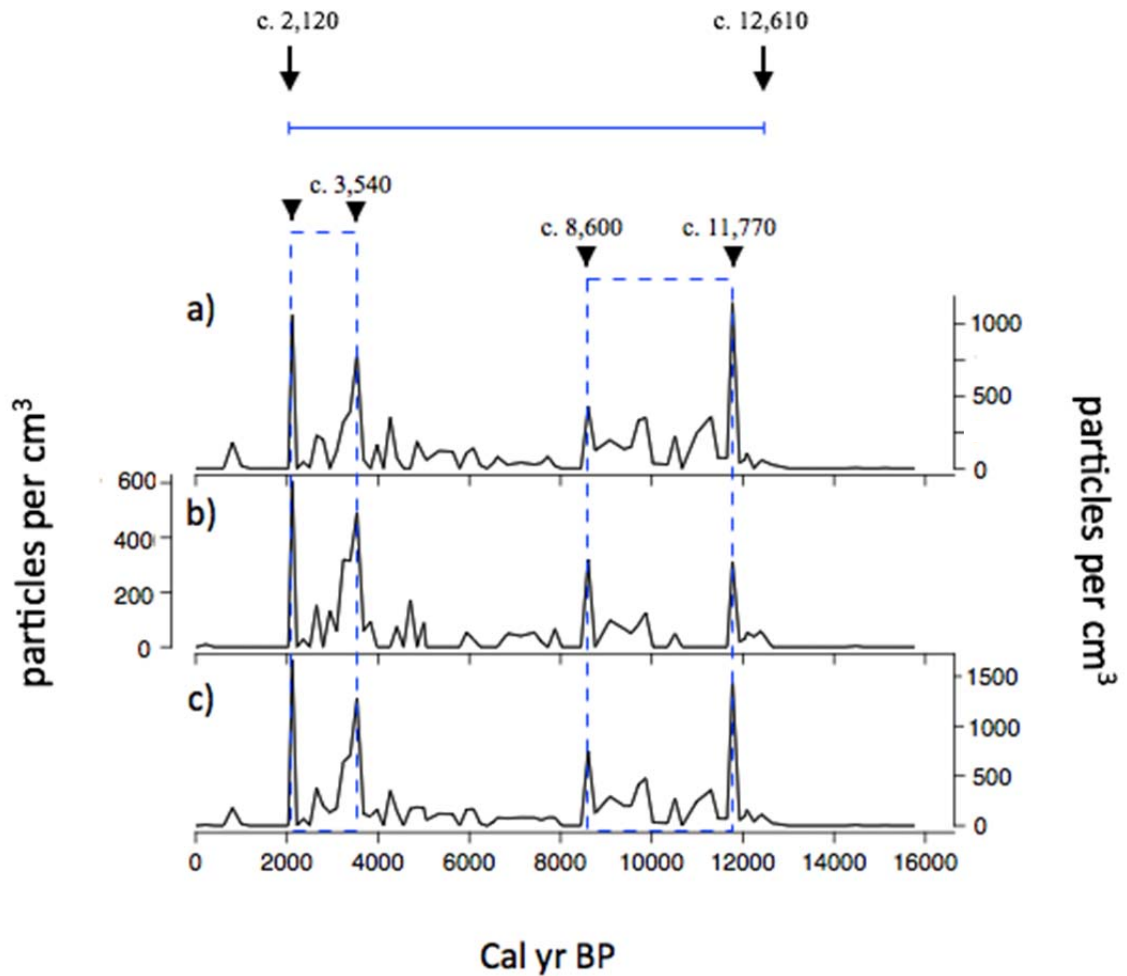


Figure 3.26 Charcoal concentrations for the Rio Grande, a) micro charcoal, b) macro charcoal and c) total charcoal concentration.

### 3.7.2 Punta Yartou.

Figure 3.27 shows the charcoal record for Punta Yartou. The micro charcoal particle concentrations and the macro charcoal particle concentrations have relatively similar distribution patterns and relative changes in term of abundance. The data indicates a continuous presence of charcoal particles from c. 13,640 Cal yr BP to c. 1,130 Cal yr BP. From c. 13,640 Cal yr BP charcoal first appears but remains consistently low in concentrations until c. 12,400 Cal yr BP (<6,000 particles per cm<sup>3</sup>). After c. 12,400 Cal yr BP there is a small increase in

charcoal concentrations ( $\sim 6,000$  particles per  $\text{cm}^3$ ) which persists until 8,220 Cal yr BP. After this time the charcoal concentrations substantially increase ( $\sim 30,000$  particles per  $\text{cm}^3$ ) and high charcoal concentrations continue to c. 5,240 Cal yr BP. There follows an interval of lower charcoal concentration from c. 5,240 Cal yr BP to c. 4,270 Cal yr BP. From c. 4,270 Cal yr BP the charcoal concentrations increase and fluctuate until c. 1,130 Cal yr BP with two periods during which charcoal is virtually absent at c. 2,760 Cal yr BP and c. 1,860 Cal yr BP. Two intervals of increased fire activity can be identified at: 1) c. 8,220 Cal yr BP to c. 5,240 Cal yr BP and, 2) c. 4,270 Cal yr BP to c. 1,130 Cal yr BP.

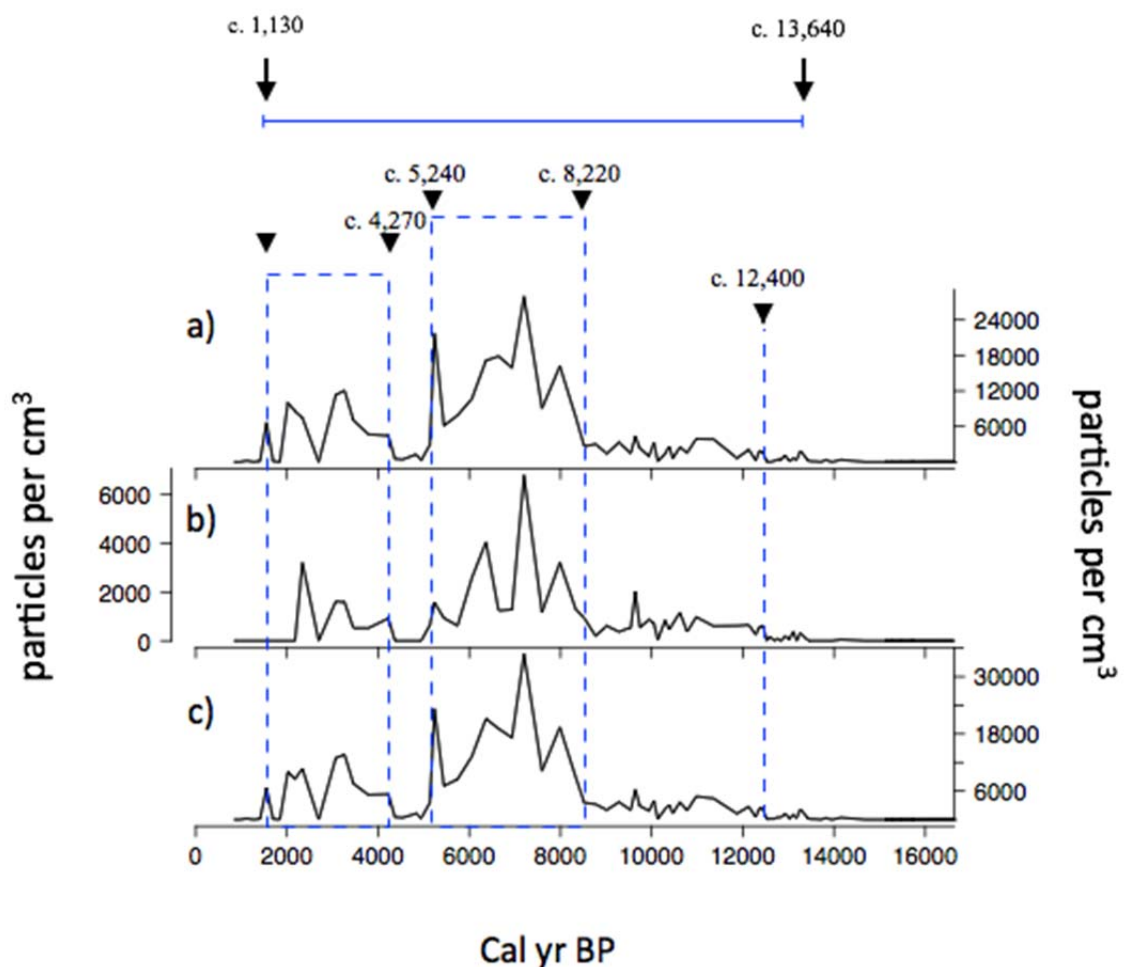


Figure 3.27 Charcoal concentrations for the Punta Yartou, a) micro charcoal, b) macro charcoal and c) total charcoal concentration.

### 3.7.3 Lago Lynch.

Figure 3.28 presents the micro, macro and total charcoal concentration for the Lago Lynch. There is a relatively continuous presence of charcoal particles beginning at c. 12,930 Cal yr BP which persists to the top of the core c. 2,640 Cal yr BP (550 cm depth). From c. 12,930 Cal yr BP the charcoal concentration first appears but remains at low concentrations (<1,000 particles per  $\text{cm}^3$ ) until c. 12,230 Cal yr BP. From c. 12,230 Cal yr BP it is possible to see a small increase in concentration ( $\sim 1,000$  particles per  $\text{cm}^3$ ) which continues until c. 10,870 Cal yr BP. Overall, two intervals of past fire activity can be identified: 1) c. 10,870 Cal yr BP to c. 8,920 Cal yr BP and, 2) c. 8,100 Cal yr BP to c. 5,130 Cal yr BP.

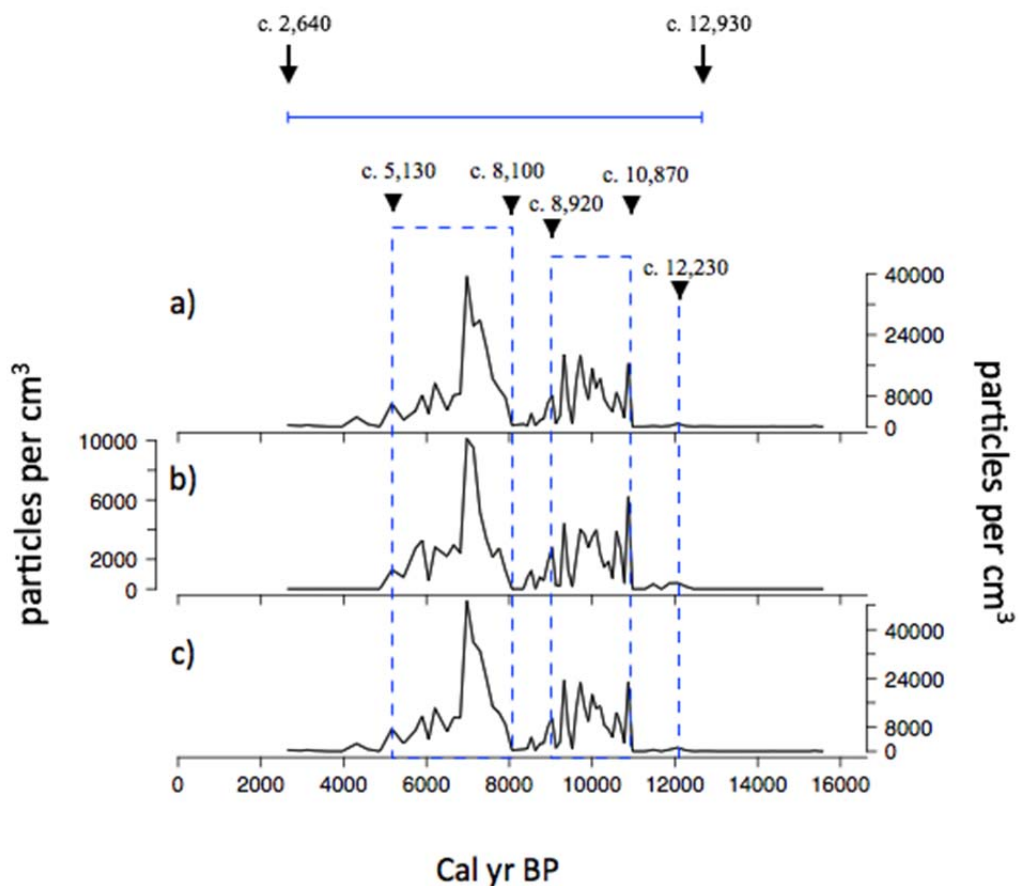


Figure 3.28 Charcoal concentrations for the Lago Lynch, a) micro charcoal, b) macro charcoal and c) total charcoal concentration.

Chapter 3 has presented the palaeoecological results supported by stratigraphical analyses and constrained by rigorous age-depth modelling based on radiocarbon ages and an expanded tephrochronology for Fuego-Patagonia. The three temporally high-resolution cores, including the record from Punta Yartou which is now one of the best resolved records in the region, will now provide the foundation for a robust reconstruction of environmental and climatic changes during the LGIT and the Holocene (Chapter 4).

# CHAPTER 4:

## Discussion

The high sensitivity and resolution of the three palaeoenvironmental cores obtained by this study and the strong positive correlation between the Patagonian precipitation and the SWWs (Garreaud *et al.*, 2013) have enabled shifts of the forest/steppe ecotone to be reconstructed. This reconstruction allows us to evaluate the link between ecological responses and large-scale controls of the effective moisture changes at millennial/centennial scales during the Last Glacial/Interglacial Transition (LGIT) and the Holocene in Fuego-Patagonia.

This discussion is organised according to each study site. Figure 1.6 shows the order of the study sites, Rio Grande, Punta Yartou and Lago Lynch, following the natural strong west-east climatic and vegetation gradient in Fuego-Patagonia, ranging from the more humid forest to drier vegetation communities. All the palaeoenvironmental evidence for each study site is organised chronologically following the intervals of time referred to as the Late-glacial, early Holocene, mid-Holocene and late Holocene period respectively.

### **4.1 Rio Grande.**

#### **4.1.1 Late-glacial period.**

The climatic warming that led to the retreat of the Magellan glaciers after Glacial stage D (c. 17,700 yr BP) from the Estrecho de Magallanes and Bahía Inútil (~53°S) (McCulloch *et al.*,

2005a) and after c. 18,200 yr BP from the Gran Campo Nevado (GCN) ice field and Seno Skyring (~53°S) (Kilian *et al.*, 2007) resulted in the Rio Grande area being ice-free sometime before c. 15,850 Cal yr BP (Figure 1.4 and 3.11; Table 3.2). After c. 15,850 Cal yr BP accumulation of organic lacustrine sediments began in the kettle-hole (~40% LOI<sub>550</sub> %) at a relatively high accumulation rate (~0.05 cm/yr) (Figure 3.11 and 4.1). This period of relatively high organic productivity after the ice retreated likely reflects the increase in temperature and/or precipitation in the region; conditions that were more favourable than during Glacial stage D.

The shift to more favourable climatic conditions in the region is also inferred from the development of the vegetation around Rio Grande after c. 15,850 Cal yr BP (Figure 3.14 and 3.15). The vegetation was dominated by pioneer plant species such as *Gunnera*, Poaceae and Ericaceae that are typical of post-glacial environments. Andean plant taxa, such as the herb Apiaceae (*Azorella* sp.) and more humid tolerant vegetation such as Amaranthaceae and the cushion-forming plant *Drapetes* are present and the high levels of well-preserved pollen (~75%) suggests the persistence of colder and wetter conditions during this period (Figure 3.14, 3.15 and 4.1). The lower pollen concentrations are more indicative of the pioneer nature of the surrounding vegetation at this time (Figure 3.20) and perhaps the continuation of relatively cold conditions during this early phase of the Late-glacial period. In summary, the Rio Grande pollen core suggests that the climate, although relatively humid, remained colder than present but warmer than the previous glacial period. This pattern is represented in other pollen records from Fuego-Patagonia (McCulloch and Davies, 2001; Markgraf and Huber, 2010).

Between c. 14,880 Cal yr BP and c. 14,410 Cal yr BP the pollen assemblage of the same shrub and herbaceous taxa as the previous period continues. However, the proportion of the species changes indicating a shift in vegetation patterns. There is a particular increase in grassland taxa such as Poaceae (~37%) and *Acaena* (~18%). Other more mesic herb taxa such as Amaranthaceae and the pioneer plants such as *Gunnera* and Ericaceae decrease. The spread of

the aquatic plant *Myriophyllum* (~82%) reaches its maximum level in the whole record and this was likely due to a decrease in the level of the lake increasing the extent of suitable habitat for relatively shallow rooting aquatics. This evidence suggests a reduction in effective moisture in comparison to the previous interval. However, the continuation of well-preserved pollen suggests that this reduction in effective moisture was subtle and did not result in a major drying out of the site (Figure 3.23 and 4.1). The high level of *Pediastrum* (~78%) may suggest an increase in bio-productivity in the lake probably caused by an increase in temperature. The increase in bio-productivity is also suggested by the increase in organic matter to ~50% (Figure 3.11 and 4.1) Therefore, overall the evidence from this interval (c. 14,880 - 14,410 Cal yr BP) suggests that humidity levels may have been largely unchanged but the reduction in effective moisture was caused by an increase in relative temperature. Furthermore, the Rio Grande provides for the first time stratigraphical evidence alongside the pollen record of vegetation change that supports the inference of a shift to warmer interstadial conditions between c. 14,880 and c. 14,410 Cal yr BP.

Between c. 14,410 Cal yr BP and c. 12,470 Cal yr BP organic content decreases to values of less than 10% and there are lower accumulation rates (~0.01 cm/yr) (Figure 3.11 and 4.1). This decrease in organic content and accumulation rate suggests a shift to less favourable climatic conditions, either a decrease in temperature and/or precipitation leading to lower biological productivity in the lake. The deterioration in climatic conditions is also inferred from an increase in cold resistant dryland herbs such as Poaceae (~62%) and Asteraceae (Subf. Asteroideae) (~15%) and a dramatic decrease in moorland plants, such as *Drapetes*, suggesting less effective moisture to support bog vegetation (Figure 3.14). Also, *Pediastrum* dramatically decreases suggesting less eutrophic lake conditions and decreased bio-productivity (Komárek and Jankovská, 2001) and *Myriophyllum* decreases dramatically. This could indicate a deepening in the lake level and a corresponding reduction in the spatial extent of shallow water suitable for such aquatic flora. However, the reduction of the surrounding moorland plants and

the increase in cold resistant dryland herbs points to the more likely lowering of temperature and decrease in effective moisture leading to the loss of *Myriophyllum* (Figure 3.14, 3.15 and 4.1). This period of colder less productive conditions recorded at Rio Grande is coeval with decreasing temperatures recorded in Antarctic ice cores during the Antarctic Cold Reversal (ACR, 14,550 - 12,800 yr BP) (Blunier and Brook 2001; Lemieux-Dudon *et al.*, 2010) (Figure 4.1).

After c. 13,470 Cal yr BP *Pediastrum* recovered suggesting a return to more eutrophic lake conditions and by c. 12,610 Cal yr BP charcoal first appears in the Rio Grande which probably suggests a shift to warmer and drier conditions. This warming phase is contemporary with the end of the colder climatic conditions identified in the Antarctic ice core records (Blunier and Brook 2001; Lemieux-Dudon *et al.*, 2010). Palaeoenvironmental evidence for an equivalent ACR event in Patagonia has to date been ambiguous (McCulloch and Davies, 2001; Markgraf and Huber, 2010; Moreno *et al.*, 2012) and so the Rio Grande record provides stronger evidence for an ecological response to climatic cooling in southern South America coeval with the ACR.

During the interval between c. 12,470 Cal yr BP and c. 11,690 Cal yr BP there was a dramatic increase in the percentage of *Nothofagus dombeyi* type (~42%). The presence of macrofossil leaves of *Nothofagus betuloides* and the presence of its epiphyte *Misodendrum*, indicate the establishment of an open-canopy *Nothofagus betuloides* forest around the site while the dry land herbs such as Poaceae, *Acaena* and Asteraceae (Subf. Asteroideae) markedly declined. This vegetation change suggests a significant shift to warmer and more humid conditions. Also, the increases in proportion of *Pediastrum*, organic matter (~20%) and in the accumulation rate (~0.03 cm/yr) indicate an increase in the biological productivity and more eutrophic lakes conditions due to more favourable climatic conditions (Figure 3.11 and 4.1). The relatively warmer and more humid conditions recorded in Rio Grande represent the termination of the Late-glacial period and the start of the Holocene. This warmer period recorded at Rio Grande is

relatively coeval with the colder and drier climatic conditions experienced in the northern hemisphere during the Younger Dryas (YD; c. 12,800 - 11,700 yr BP) (Rasmussen *et al.*, 2006). The Rio Grande palaeoenvironmental record reinforces the evidence for a substantial lead of ~770 yrs in the warming of the southern hemisphere in comparison to the northern hemisphere (Blunier and Brook, 2001; Lemieux-Dudon *et al.*, 2010).

#### 4.1.2 Early- period.

During the Early Holocene the Rio Grande core reveals two major phases of *Nothofagus* forest expansion between: 1) c. 11,690 Cal yr BP and c. 10,590 Cal yr BP and 2) c. 9,470 Cal yr BP and c. 8,250 Cal yr BP. These intervals of expansion of *Nothofagus* forest are separated by an interval of forest contraction and a corresponding expansion of a grassland community that suggests a westward shift in the steppe/forest ecotone between c. 10,590 Cal yr BP and c. 9,470 Cal yr BP. Both intervals of forest expansion are likely close-canopy evergreen *Nothofagus betuloides* forest, *Nothofagus dombeyi* type is the dominant taxon at >70% of TLP, while Poaceae, Asteraceae (Subf. Asteroideae), *Acaena* and the shrub Ericaceae dramatically decrease in percentage. This suggests a shift to higher levels of effective moisture during the intervals between c. 11,690 Cal yr BP and c. 10,590 Cal yr BP and between c. 9,470 Cal yr BP and c. 8,260 Cal yr BP. Increases in the percentages of the aquatic *Myriophyllum* also occurred during these warmer and more humid intervals marked by the expansion of evergreen *Nothofagus* forest.

Between c. 10,590 Cal yr BP and c. 9,470 Cal yr BP there was an expansion of the grassland dominated by dry land herbs such as Poaceae, Asteraceae (Suf. Asteroideae) and *Acaena*. The evergreen forest, probably dominated by *Nothofagus betuloides* (a community located where annual precipitation ranges between 2,000 mm and 6,000 mm), is replaced by a more open-canopy evergreen *Nothofagus* forest indicated by the presence of temperate forest elements such

as *Drimys* and *Maytenus* trees (mixed evergreen forest) that require lower rainfall ranges between 900-2,000 mm/yr. From this evidence a shift to lower levels of effective moisture is inferred. However, it is not clear if this decrease in effective moisture during the interval between c. 10,590 Cal yr BP and c. 9,470 Cal yr BP was triggered by a decrease in precipitation and/or increase in temperature. This period of decreased effective moisture found in Rio Grande is likely part of a wider regional signal that has been identified previously by McCulloch and Davies (2001) who inferred an intense arid phase between c. 10,700 Cal yr BP and c. 9,550 Cal yr BP based on pollen and diatoms evidence from Puerto del Hambre (~53°S).

#### 4.1.3 Mid-Holocene period.

Between c. 8,260 Cal yr BP and c. 4,930 Cal yr BP the vegetation assemblage is characterised by a dramatic decrease in *Nothofagus dombeyi* type (~53%). *Drimys* and *Maytenus* are also present, while Poaceae, Asteraceae (Subf. Asteroideae) and *Acaena* increase in percentages, denoting the expansion of grassland steppe in the area and relatively lower levels of effective moisture (Figure 3.14). However, at the same time fire activity reaches its most quiescent phase of the entire Holocene (Figure 3.16, 3.26 and 4.1) (see Section 5.3).

Within the interval c. 8,260 Cal yr BP and c. 4,930 Cal yr BP two episodes of climatic conditions can be inferred: 1) from c. 8,250 Cal yr BP to c. 6,980 Cal yr BP and 2) from c. 6,980 Cal yr BP to c. 4,920 Cal yr BP. Between c. 8,260 Cal yr BP and c. 6,980 Cal yr BP there was a dramatic westward shift in the forest/steppe ecotone, from closed-canopy evergreen *Nothofagus* forest to steppe dominated by Poaceae and Asteraceae (Subf. Asteroideae) (Figure 3.14, 3.15 and 4.1). This is further supported by the decrease in organic matter to ~10% and an increase in *Pediastrum* that suggests there was a dramatic decrease in effective moisture leading to lower organic productivity likely triggered by an increase in temperature and/or decrease in precipitation (Figure 3.11 and 4.1) Between c. 6,980 Cal yr BP and c. 4,930 Cal yr BP there was

a gradual increase of *Nothofagus dombeyi* type (~70%) also accompanied by a slight increase in organic matter to ~20% and a decrease in *Pediastrum* (Figure 3.16 and 4.1). These suggest a change to more mesic and less warm climatic conditions that led to the establishment of a more closed-canopy *Nothofagus* forest in the area. This evidence is highly consistent with the warmer and drier climatic conditions between c. 8,000 Cal yr BP and c. 6,500 Cal yr BP followed by cold and wet environmental conditions reconstructed from pollen and diatom analysis at La Cotorra mire ~54°S (Borromei *et al.*, 2010).

Between c. 4,930 Cal yr BP and c. 3,750 Cal yr BP *Nothofagus dombeyi* type proportions are maintained at ~70% together with a gradual increase in organic content to more than ~80% and an increase in the accumulation rate (~0.05 cm/yr) to values similar to the interstadial (c. 15,860 to c. 14,410 Cal yr BP) during the Late-glacial period (Figure 3.11 and 4.1). The evidence suggests that effective moisture levels increased between c. 4,920 and 3,730 Cal yr BP. However, *Misodendrum* is well represented and the prevalence of this epiphytic parasite and the lower proportions of well-preserved pollen (mainly corroded and degraded pollen) (Figure 3.23 and 4.1) suggest that the *Nothofagus* forest was probably under more stress and living near its critical ecological range, probably caused by a reduction in temperature. Also, the charcoal concentrations were virtually absent or very low suggesting that this was a period of relatively wetter and colder climatic conditions (Figure 4.1). Further evidence for Neo-glacial climatic cooling between c. 4,500 Cal yr BP and c. 3,800 Cal yr BP has been obtained from bulk organic geochemistry analysis from Lago Fagnano ~55°S (Moy *et al.* 2011), pollen and marine mollusca from Canal Beagle ~54°S (Candel *et al.*, 2009), proxy-derived SSTs from ~53°S (Lamy *et al.*, 2010; Harada *et al.*, 2013; Caniupán *et al.*, 2014).

#### 4.1.4 Late-Holocene period.

Between c. 3,750 Cal yr BP and c. 2,290 Cal yr BP a closed-canopy of *Nothofagus* forest developed around Rio Grande, however, the persistence of *Misodendrum* well represented suggest that the *Nothofagus* forest was still under relative stress conditions, it is not clear if this stress was caused by a decrease in precipitation and/or increase in temperature. However, between c. 3,530 Cal yr BP and c. 2,110 Cal yr BP there were higher charcoal concentrations at Rio Grande suggesting an increase in the availability of drier fuel due to drier conditions. The higher proportions of *Myriophyllum* suggests a shallowing of the lake and this taxon finally disappeared by c. 2,610 Cal yr BP (80% LOI<sub>550</sub>) at the transition from a lake to a peat bog. The switch in the hydrological conditions in the kettle-hole is typical of a gradual hydrosereal succession (autogenic process). However, it is likely that the shallowing of the lake and transition to peat bog was accelerated by the decrease in effective moisture produced by relatively warmer and drier climatic conditions. This is consistent with a period of reduced humidity between c. 3,500 yr BP and c. 2,500 yr BP recorded in a high-resolution study of stalagmites at ~53°S (Schimpf *et al.*, 2011). The transition from the lake to peat conditions by c. 2,610 Cal yr BP (80% LOI<sub>550</sub>) coincides with an increase in accumulation rate (~0.08 cm/yr) although this increase is more likely to be due to less compaction of the upper sediments (peat) (Figure 3.11). Also, the lower proportion of well-preserved pollen and increase in mainly broken and crumpled grains may indicate repeated phases of wetting and drying (Holloway, 1989; Campbell and Campbell, 1994).

Between c. 2,290 Cal yr BP and the present the surrounding *Nothofagus* forest appears to have undergone large magnitude and high frequency fluctuations probably in response to significant variability in the effective moisture levels in the Rio Grande area. The episodes of reduced and more open-canopy *Nothofagus* forest are coupled with the colonisation of the peat bog by

Ericaceae heath facilitated by a decrease in effective moisture; the highest peak of Ericaceae is at c. 1,700 Cal yr BP (Figure 3.14 and 4.1).

During the last c. 1,400 Cal yr BP, the surrounding vegetation was likely closed-canopy evergreen *Nothofagus* forest which is inferred from the virtual absence of *Drimys* and *Maytenus* trees and the low proportion of *Misodendrum* from which more temperate and humid climatic conditions are inferred. Although there was a brief interruption marked by a dramatic decrease in *Nothofagus* along with an increase in Ericaceae and a small peak of charcoal at c. 800 Cal yr BP this was likely due to a brief period of reduced effective moisture. After c. 224 Cal yr BP and towards the present there was a slight decrease in *Nothofagus* forest. It is not clear if this decrease in the presence of *Nothofagus* forest after c. 224 Cal yr BP is driven by climate changes or by the impact of European settlement. Decreases and fluctuations in *Nothofagus* forest within the region during the last c. 2,000 Cal yr BP have also been registered in palaeoenvironmental records from Lago Cipreses (~51°S) (Moreno *et al.*, 2014), Isla Santa Inés (~53°S) (Fontana and Bennett, 2012), Estrecho de Magallanes (~53°S) (Caniupán *et al.*, 2014), Lago Yehuin (~54°S) (Markgraf, 1983) and Las Cotorras (~54°S) (Borromei *et al.*, 2010). The occurrence of the high climatic variability at these sites to the north, east and south-west respectively of Rio Grande suggests that the period of high variability in levels of effective moisture during the last c. 2,000 Cal yr BP was a substantial regional, rather than local, climatic signal and corroborates the sensitivity of the Rio Grande site for identifying climatic changes.

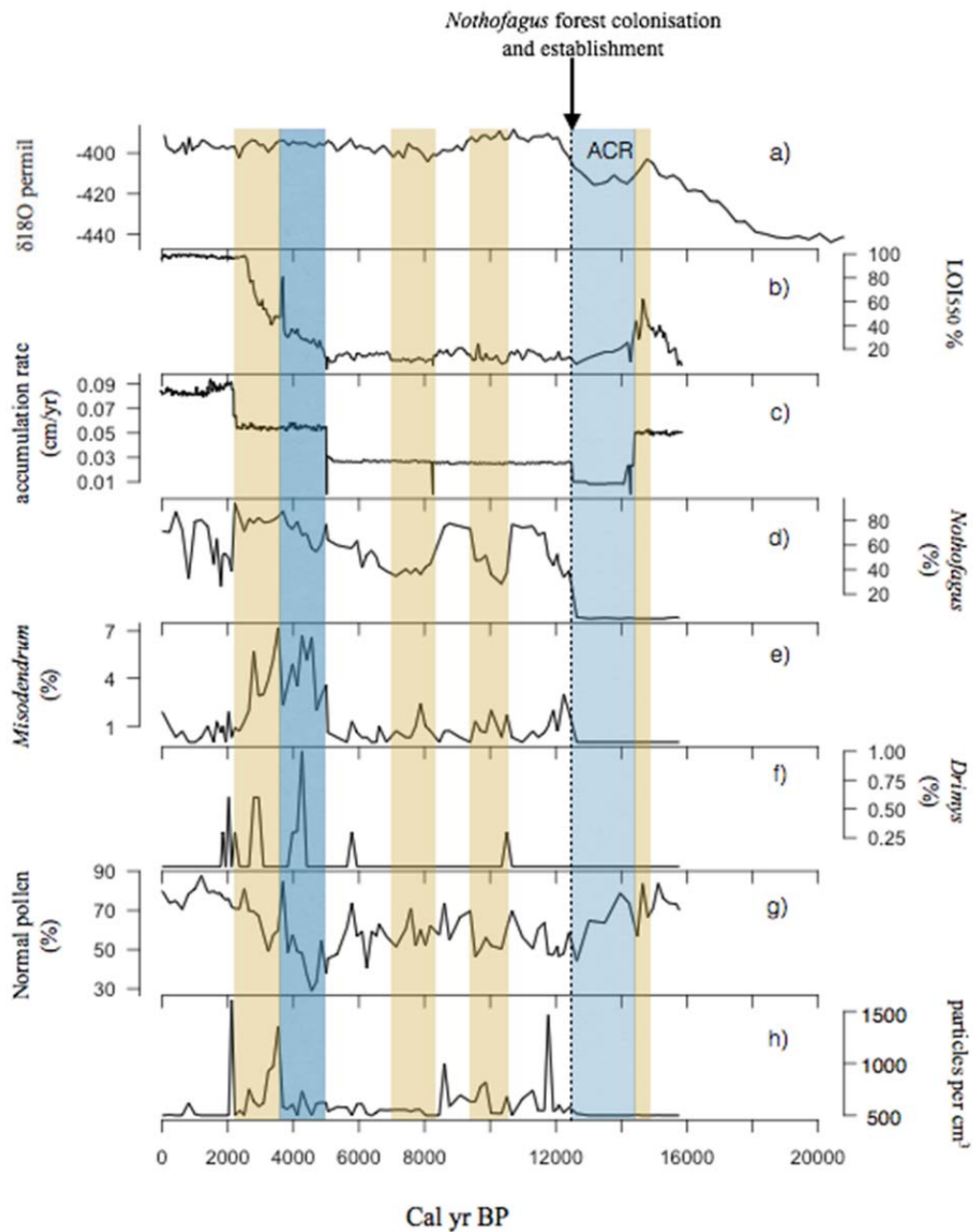


Figure 4.1 Summary of Rio Grande core. a) deuterium record as temperature proxy from ice core (Dome C) (Lemieux-Dudon *et al.*, 2010); b) organic content; c) accumulation rate; d) percentage *Nothofagus*; e) percentage *Misodendrum*; f) percentage *Drimys*; g) percentage normal pollen preservation; h) charcoal concentrations. Orange shading indicates intervals of warmer and lower effective moisture, light blue shading indicates interval of colder and lower effective moisture, dark blue shading indicates interval of colder and wetter climatic conditions.

## 4.2 Punta Yartou.

### 4.2.1 Late-glacial period.

The bluish-grey clays and silts at the base of the Punta Yartou core (below 1,066cm) were likely deposited within the kettle hole following the retreat of a major glacier advance in the Estrecho de Magallanes (Figure 1.3). The basal ages from Punta Yartou suggest that the area was ice-free sometime before c. 26,280 Cal yr BP (Figure 3.12; Table 3.3). However, Punta Yartou lies well within the limits of Glacial Stages B and C (LGM) and Glacial Stage D (> 17,700 Cal yrs BP) (Bentley *et al.*, 2005; McCulloch *et al.*, 2005b) (see Section 1.5.3). The lithostratigraphy of the core from Punta Yartou indicates the continuous accumulation of lacustrine sediments overlain by peat (Figure 3.12) and there is no evidence of the site having been over-ridden by glacial ice. The presence of Tertiary Lignite within the glacial clays found at the base of cores around the Estrecho de Magallanes is known to be a source of radiocarbon error (Heusser, 1999; McCulloch *et al.*, 2005a; Moy *et al.*, 2011). However, the basal samples from Punta Yartou were sieved to remove the fine mineral component and acid-base treatment was used to remove soluble carbonates so that only plant fibres were dated. Therefore, the effect of infinite aged carbon from Lignite is unlikely. At the base of the core there are carbonate rich sediment layers (marl), which suggests the potential for a freshwater reservoir effect (FRE) with older carbon drawn up by aquatic flora. The plant fibres dated yielded  $\delta^{13}\text{C}$  values between 19.1‰ and 16.3‰ (Table 3.3) which indicates that the plants were probably aquatics and so the uptake of ‘old’ carbon from the water column may be a source of error. Examples of FREs are typically of the order of 400  $^{14}\text{C}$  years although FREs of between 0 and c. 6,000  $^{14}\text{C}$  years have been found in freshwater systems (Philippsen, 2013). However, if the glacier extent and chronology of Glacial Stage D is accepted then the FRE at Punta Yartou is required to be in the order of ~6,000  $^{14}\text{C}$  years. Furthermore, the age of  $19,649 \pm 97$   $^{14}\text{C}$  yr BP (c. 23,750 Cal yr BP) is also significantly older than the minimum ages for Glacial Stage D. The radiocarbon sample of

19,649 ± 97 <sup>14</sup>C yr BP was obtained from 15 cm depth above the basal radiocarbon sample, from organic rich mud that did not contain marl, and the age estimate is consistent with the age-depth model (Figure 3.12; Table 3.2). The implications of the Punta Yartou basal ages for understanding deglaciation period in Punta Yartou site are still unclear and are being investigated further. This study simply suggests that the basal period prior to c. 14,700 Cal yr BP is treated with caution (Table 3.3). For the purposes of this study the focus is on the time period after the Vn Reclús tephra layer (c. 14,700 Cal yr BP) and the significance of the pollen record for understanding Late-glacial and Holocene vegetation changes.

The Punta Yartou pollen diagram (Figure 3.16 and 3.17) indicates that the post-glacial environment was characterised by an open vegetation community of heath-grassland Ericaceae, Poaceae and *Acaena*. Ericaceae is present in a wide range of ecosystems. However, it is likely to represent *Empetrum rubrum*, which is a particularly cold-tolerant species and is a typical coloniser of recently deglaciated terrain (Pisano, 1977). The tree-less heath-grassland pollen assemblage also contains other herbs such as Amaranthaceae and wet-land herbs such as *Gunnera*. This latter taxon is consistent with the relatively high percentage of normal pollen grains (~65%), low organic content (<20%) and low rate of sedimentation (~0.01 cm/yr) suggest the continuation of cooler climatic conditions and the limiting of bio-productivity (Figure 3.12 and 4.2). This initial phase of colonisation following deglaciation is replaced by c. 20,580 Cal yr BP with grassland dominated by Poaceae and *Acaena* and a gradual increase in organic content (to ~50%) that suggests an increase in temperatures and relatively wetter conditions, enough to sustain wetland herbs and the presence of a lake on the site. This more humid and less cold period persisted until c. 15,050 Cal yr BP and was similar to environmental conditions following deglaciation after c. 17,700 Cal yr BP identified in other sites at ~53°S which suggest a strong regional climatic signal in Fuego-Patagonia at that time (see Section 4.1.1).

Between c. 15,050 and c. 12,530 Cal yr BP the vegetation was dominated by cold resistant dryland herbs (Poaceae, Asteraceae (Subf. Asteroideae) and *Acaena*). During this period the temperature and humidity conditions were probably lower than the critical limits for the establishment of *Nothofagus* forest (Figure 4.5). This period is coeval with the Antarctic Cold Reversal (Lemieux-Dudon *et al.*, 2010) and provides further evidence for an ecological response to this period of high latitude southern hemisphere cooling. After the nadir of the cooling signal is reached (c. 13,500 Cal yr BP) there is a gradual shift from the dominance of colder-drier tolerant species (Asteraceae (Subf. Asteroideae) towards more mesic vegetation (Poaceae dominance) suggesting a slight increase in effective moisture. This interpretation is supported by an increase in accumulation rates, from ~0.01 cm/yr at c. 15,050 Cal yr BP to ~0.09 cm/yr by c. 13,520 Cal yr BP. At the same time there is a gradual increase in *Myriophyllum* suggesting a return to more favourable climatic conditions at the end of the cooler period (Figure 4.2). There was also an increase in the proportions of *Pediastrum* at the end of this period that suggests the development of more eutrophic lake conditions (Komarek and Jankovska, 2001) (Figure 3.16 and 3.17). The gradual rise in temperature and humidity after c. 13,520 Cal yr BP is also suggested by the transition from grassland to the establishment of *Nothofagus* forest by c. 12,530 Cal yr BP leading to the development of an open-canopy forest by c. 11,870 Cal yr BP. This evidence for the Late-glacial period is highly concordant with the Rio Grande core (see Section 4.1.1).

#### **4.2.2 Early-Holocene period.**

Between c. 12,530 Cal yr BP and c. 11,870 Cal yr BP a continued rise in temperatures and humidity is inferred from the continued increase of *Nothofagus dombeyi* type to ~28% that then plateaued. An increase in the total pollen concentrations was mainly contributed by *Littorella* (Figure 3.21) which is constituent of riparian and lotic environments and so probably indicates an expansion of fen-like water marginal areas at the site as the lake gradually infilled and

shallowed as part of a natural hydrosere succession. At this stage the site is unable to support the aquatic flora such as *Myriophyllum* but the continuous presence of *Pediastrum* suggests that pools of water persisted on the surface of the emergent fen bog. This period of warmer and humid conditions is coeval with, and in contrast to the North Hemisphere Younger Dryas cooling event, registered widely in Greenland ice cores (YD; c. 12,800 - 11,700 yr BP, Rasmussen *et al.*, 2006).

Between c. 11,870 Cal yr BP and c. 9,510 Cal yr BP the terrestrial vegetation is characterised by the appearance of *Drimys* and the expansion of open-canopy *Nothofagus dombeyi* type reaching its highest proportions (~42%) during the Early and Mid Holocene (Figure 3.15 and 4.2) with high proportions of well preserved pollen (Figure 3.24 and 4.2). The expansion and dominance of *Nothofagus* forest probably suggests an increase in temperatures and effective moisture. At c. 11,900 Cal yr BP the stratigraphy indicates the change from lacustrine-mud to peat (80% LOI<sub>550</sub>). However, the aquatic flora and algae finally disappear from the record at c. 10,550 Cal yr BP likely reflecting the persistence of small hollows with water on the surface of the developing mire. Immediately above the Mt Burney 1 micro tephra layer (c. 9,900 Cal yr BP) (Table 3.1) the proportions of Ericaceae increase rapidly and there is a small increase in the concentrations of herb and shrub pollen and a reduction in species diversity (Figure 3.16, 3.17 and 3.24). This likely indicates a short period (~480 yrs) of colonisation of the peat bog by *Empetrum rubrum* heath which continued until c. 9,510 Cal yr BP and was probably encouraged by a large decrease in effective moisture within a period of temperate temperatures during the early-Holocene to mid-Holocene transition. The micro-tephra would only have been a small input of mineral matter into the mire and it is unlikely to have had a significant part in promoting the expansion of heath vegetation across the mire.

After c. 9,510 Cal yr BP until c. 8,220 Cal yr BP the percentages of *Nothofagus dombeyi* type increase to ~40% (Figure 3.24 and 4.2) which may suggest a gradual shift to higher levels of

effective moisture. However, these lines of evidence do not show a clear interval of increased effective moisture identified between c. 9,470 and 8,250 Cal yr BP in the Rio Grande core (see Section 4.1.2).

#### 4.2.3 Mid-Holocene period.

The highest concentrations of charcoal are found between c. 8,220 Cal yr BP and c. 5,170 Cal yr BP (Figure 3.16, 3.27 and 4.2) which coincides with the highest levels of Poaceae, *Acaena* and Cyperaceae and the lowest proportions of *Nothofagus* (~20%) and lower proportions of well preserved pollen (<30%) due to the increase mainly in crumpled, corroded and degraded pollen (Figure 3.24 and 4.2). The contraction of the *Nothofagus* forest and the high presence of charcoal at Punta Yartou are probably related to an intense arid phase leading to an increase in the amount of dry fuel available during the mid-Holocene. The increase in aridity is also contemporary with a similar arid phase recorded at Rio Grande. The intensity of this arid phase is highlighted by the increase in aerobic activity in the mire leading to the increase in deteriorated pollen. This intense arid phase was coeval with an interval of warmer and drier climatic conditions at Rio Grande (see Section 4.1.4).

Between c. 5,170 Cal yr BP and c. 4,960 Cal yr BP there was a peak of the wetland herb *Gunnera*. This expansion of *Gunnera* coincides with the almost absence of charcoal (Figure 3.25 and 4.1). The spread of *Gunnera* is likely to be across the site itself together with the small increase in *Drimys*, *Maytenus* and *Misodendrum* which indicates that the forest was under wetter climatic conditions and under a degree of stress suggesting that this period was relatively wetter and colder climatic conditions (Figure 3.16, 3.17 and 4.1). Between c. 4,960 Cal yr BP and c. 3,440 Cal yr BP open-canopy *Nothofagus* forest continues to be dominant (~40%) around the site. During the middle of this interval at c. 4,265 Cal yr BP there was a second phase of increased fire activity which coincided with the disappearance of *Misodendrum* from which a

small decrease in effective moisture, probably caused by slight increase in temperature, is inferred (Figure 3.27 and 4.2).

#### 4.2.4 Late-Holocene period.

Between c. 3,440 and c. 2,170 Cal yr BP there was a rapid increase in Ericaceae proportions (~53%) and pollen concentrations (Figure 3.16, 3.17 and 4.2) and decreased tree and shrub taxa. This suggests a higher concentration of autochthonous pollen and that the surface of the peat was likely replaced by *Empetrum rubrum* from which a reduction in effective moisture is inferred (Figure 3.18).

After c. 2,170 Cal yr BP and to the near present (c. 870 Cal yr BP) *Nothofagus dombeyi* type achieves near total dominance of the pollen record (~80%) which suggests the establishment of a closed-canopy *Nothofagus* forest and may indicate an increase in effective moisture. However, *Misodendrum* for a short interval reaches its maximum levels (~5%) (Figure 4.2) and there was a corresponding dramatic decrease in well-preserved pollen, mainly contributed by an increase in corroded and degraded pollen grains. The peak in *Misodendrum* (Figure 3.24 and 4.2) suggests a reduction in effective moisture and that the *Nothofagus* forest, although thriving under warmer and wetter conditions for most of the period, likely experienced fluctuating periods of stress between c. 2,170 and the present.

Approximately 85 cm below the surface of the mire there were frequent trunks of wood that were impenetrable to the corer and these probably represent a drier period of short duration when *Nothofagus* trees were able to colonise the bog surface and then subsequently died as wetter conditions returned to the bog. Also, there were small dead stands of *Nothofagus betuloides* on the surface and margins of the peat bog, which suggests colonisation of drier-ground tree species in the recent past (Figure 2.5). The small tree diameter (< 15cm) suggests

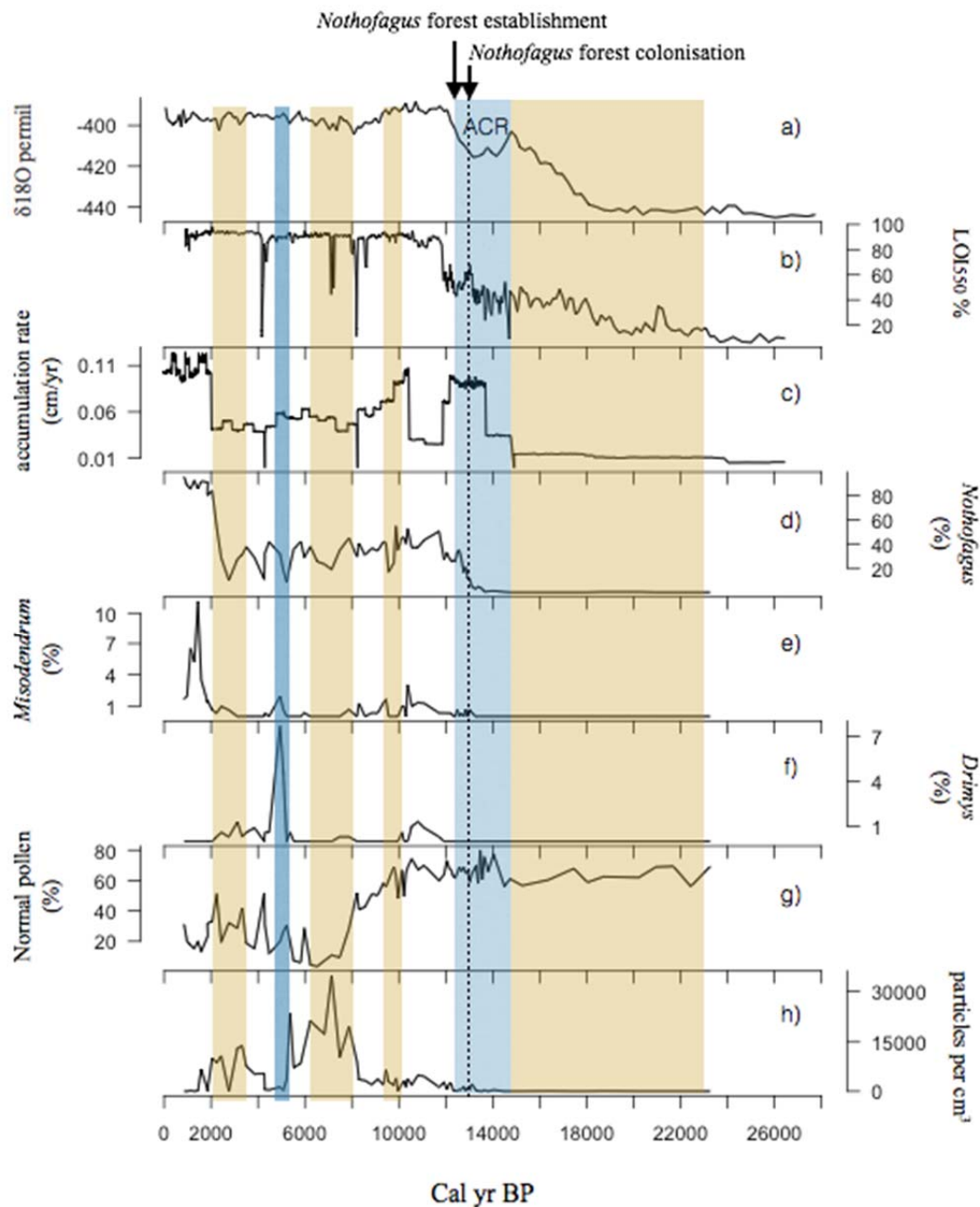


Figure 4.2 Summary of Punta Yartou core. a) deuterium record as temperature proxy from ice core (Dome C) (Lemieux-Dudon *et al.*, 2010); b) organic content; c) accumulation rate; d) percentage *Nothofagus*; e) percentage *Misodendrum*; f) percentage *Drimys*; g) percentage normal pollen preservation; h) charcoal concentrations. Orange coloured shading indicates intervals of warmer / lower effective moisture, light blue shading indicates interval of colder / lower, dark blue shading indicates interval of colder / higher effective moisture.

that the development of the drier phase was relatively short (in the order of decades). These events were not correlated to the pollen core as it was not possible to sample the last 80 cm of the bog due to the unconsolidated nature of the peat. However, the fossil wood just below the surface of the bog and the dead trees on the surface of the bog indicate that in the late-Holocene to very recent past there have been significant fluctuations in effective moisture levels at the site (see Section 4.1.5).

### **4.3 Lago Lynch.**

#### **4.3.1 Late-glacial period.**

An AMS-radiocarbon basal age taken from the contact between the organic lacustrine sediment and the underlying bluish-grey clay/silt glacial sediment from the Lago Lynch core suggests a minimum age of c. 15,610 Cal yr BP for ice retreat (Figure 3.13; Table 3.4). The Lago Lynch core lies within the inner moraines that correspond to Glacial Stage D (Glasser *et al.*, 2008) (Figure 1.3 and 2.7) although to date, the glacial chronology of the Lago Lynch area of Tierra del Fuego has not been the focus of detailed field study.

Between c. 15,610 Cal yr BP and c. 15,010 Cal yr BP the post-glacial vegetation was an open and treeless community dominated by the heath Ericaceae (~54%) and accompanied by Poaceae (~20%) and *Acaena* (~20%) (Figure 3.18 and 3.19). Within the heath-grassland vegetation there were also wetland herbs such as Ranunculaceae, *Gunnera* and *Caltha*. The more humid taxa, the relatively high percentages of well preserved pollen (~62%) and moderately high rate of sedimentation (~0.03 cm/yr) (Figure 3.13), suggest this was a period of relatively high effective moisture and a more favourable climate for the early development of vegetation at the site. Also, the presence of *Myriophyllum* and *Pediastrum* indicate the presence of a relatively eutrophic lake.

Between c. 15,010 Cal yr BP and c. 14,430 Cal yr BP the vegetation was dominated by Ericaceae heath (~66%). A reduction in effective moisture is inferred from the expansion of the heathland and the corresponding decrease in wetland herbs as Ranunculaceae, *Gunnera* and *Caltha*. The shift to drier conditions is further supported by the reduction in the proportion of normal pollen decreases to ~26%, the lowest value in the whole record, and increases in corroded and degraded pollen which suggest the development of more aerobic conditions at the mire surface (Figure 3.25 and 4.3). These inferences are further supported by the increase in abundance of *Myriophyllum* and *Pediastrum* algae which suggest an expansion of the lake habitat suited to shallow rooting aquatic flora and more eutrophic conditions under relatively dry-warmer conditions.

Between c. 14,430 Cal yr BP and 12,710 Cal yr BP the Ericaceae heath was replaced by grassland vegetation. The proportions of wetland taxa such as Ranunculaceae, *Gunnera* and *Caltha* also increased slightly and this vegetation assemblage suggests a decrease in effective moisture. Within this interval *Myriophyllum* and *Pediastrum* also gradually decreased and organic content declined to ~10%. These changes suggest a shift to less eutrophic lake conditions and a reduction in bio-productivity likely driven by climatic cooling. This interval is coeval with the ACR period (c. 14,550 - 12,800 yr BP) (Lemieux-Dudon *et al.*, 2010).

After c. 13,490 Cal yr BP the dryland taxa, such as Poaceae (~41%), Asteraceae (Subf. Asteroideae), *Acaena* and Cyperaceae increased and the wetland taxa *Caltha* and the Ericaceae dwarf shrubs decreased and *Nothofagus dombeyi* type increased to ~7%. The proportion of well preserved pollen also increased to ~53%. This suggests the persistence of steppe vegetation but increasing patches of *Nothofagus* forest in the landscape towards the end of the ACR period from which an increase in effective moisture is inferred and a shift to more mesic conditions

that encouraged the establishment of the forest by c. 12,710 Cal yr BP at Lago Lynch and south-central Tierra del Fuego (Figure 3.18, 3.19 and 4.3).

The Lago Lynch core indicates palaeoenvironmental changes comparable in character and timing to those illustrated in the Antarctic ice cores (Blunier and Brook, 2001; Lemieux *et al.*, 2010). Following deglaciation there was a gradual warming prior to c. 14,430 Cal yr BP then followed by an interval of steppe vegetation until c. 13,600 Cal yr BP during the onset of the Antarctic Cold Reversal (ACR) and then followed by rapid and large scale warming at the start of the Holocene c. 12,710 Cal yr BP. The same timing and nature of palaeoenvironmental changes during the LGIT have been documented in Rio Grande and Punta Yartou cores (see Section 4.1.1 and 4.2.1).

#### **4.3.2 Early-Holocene period.**

From c. 12,710 Cal yr BP to c. 11,020 Cal yr BP the dryland herbs decreased in proportions and *Nothofagus dombeyi* type correspondingly increased to ~50%. *Misodendrum* first appears and well preserved pollen increased to ~70% (Figure 3.25 and 4.3) which suggests the establishment and continued presence of an open-canopy *Nothofagus* forest at Lago Lynch. This marks the transition from the semi-arid steppe conditions of the Late-glacial to the wetter and warmer climatic conditions of the early-Holocene. Within this interval, around c. 12,230 Cal yr BP, charcoal first appears in the core which further indicates a gradual increase in temperature and greater abundance of dry fuel. A key component of the total land pollen at this time is *Galium*, represented by high pollen concentrations (Figure 3.18, 3.19 and 3.22). *Galium* would have expanded across the fen-margins of the site as the lake gradually infilled to form a bog. The low proportions of *Pediastrum*, traces of *Myriophyllum* and the appearance of *Sphagnum* moss reflect the disappearance of the lacustrine environment.

During the period between c. 12,710 Cal yr BP and c. 11,020 Cal yr BP relatively wetter and warmer climatic conditions are inferred from the Lago Lynch pollen and sediment core. Again it is highlighted that this interval takes place during the drier and colder Younger Dryas (YD) glacial event in the Northern Hemisphere (c. 12,800 Cal yr BP to 11,800 Cal yr BP) (Rasmussen *et al.*, 2006).

Between c. 11,020 Cal yr BP and c. 10,340 Cal yr BP, the organic matter increased to around 80% (LOI<sub>550</sub>) and the accumulation rate to ~0.04 cm/yr (Figure 3.13). This moderately high accumulation rate occurs just after a transition from minerogenic-rich lacustrine sediment to organic-rich peat (*Sphagnum*) and so is a reflection of the typical higher growth and accumulation rates of peat. Contemporaneous with the transition from lake to peat bog was a further increase in fire activity by c. 10,870 Cal yr BP (Figure 3.28 and 4.3) suggesting climatic conditions conducive to the creation of drier fuel.

The transitions from lakes to peat-bogs in all the cores sampled by this study (Rio Grande c. 2,610 Cal yr BP; Punta Yartou c. 11,630 Cal yr BP and Lago Lynch c. 10,780 Cal yr BP) do not appear to be synchronous among the sites. Therefore, it is not clear if the switch in the hydrological conditions at each site was due to the more gradual process of infilling and a gradual hydroseral succession (autogenic process) or if it was driven or at least accelerated by a reduction in effective moisture in the region (allogenic). Despite the reduction in effective moisture it was not sufficient for the steppe vegetation to expand, and the vegetation in this interval (between c. 11,020 Cal yr BP and c. 10,340 Cal yr BP) was an open-canopy *Nothofagus* forest with scattered shrubs/trees of *Drimys* that favoured the more local humid areas (Figure 3.18, 3.19 and 4.3).

Between c. 10,340 Cal yr BP and c. 9,870 Cal yr BP the open-canopy mixed *Nothofagus* forest contracted dramatically accompanied by an increase in steppe vegetation dominated by

Poaceae. This period strongly suggests a significant reduction in effective moisture and a corresponding westward migration of the forest/steppe ecotone. A similar longitudinal shift in the forest/steppe ecotone was identified in Rio Grande vegetation core between c. 10,590 Cal yr BP and c. 9,470 Cal yr BP (see Section 4.1.3).

Between c. 9,870 and c. 8,670 Cal yr BP there were high magnitude fluctuations in the extent of the *Nothofagus* forest and Poaceae dominated steppe. These fluctuations are likely due to the sensitivity of the Lago Lynch record owing to its location on the eastern margin of the forest/steppe ecotone and so probably reflect a continued interplay between periods of higher effective moisture driving eastwards and enabling forest expansion, followed by drier periods and forest contraction. The fluctuations in the proportions of Cyperaceae also highlight the extent to which the variations in effective moisture affected the mire surface wetness at the site.

The early-Holocene between c. 8,670 Cal yr BP and c. 8,220 Cal yr BP is characterised by a shift to more mesic conditions inferred from a sustained increase in *Nothofagus* and the well preserved pollen (~55%) (Figure 4.3). This suggests a more sustained period of wetter climatic conditions. This is further supported by the dramatic decrease and virtual absence of charcoal in the record likely associated with the wetter climatic conditions reducing the ready availability of combustible fuel (Figure 3.28 and 4.3). It is unclear if this shift to a wetter environment was driven by an increase in precipitation and/or a lowering of temperature.

#### **4.3.3 Mid-Holocene period.**

Between c. 8,220 Cal yr BP and c. 6,670 Cal yr BP there was a reduction in the extent of *Nothofagus* forest and the presence of *Misodendrum* and a corresponding increase in the extent of grassland. This was also accompanied by an increase in dryland taxa such as Asteraceae (Subf. Asteroideae) and *Acaena*. This change in vegetation indicates the expansion of steppe

and a lowering of effective moisture levels. The decreases in organic matter to ~70% and in the accumulation rate (~0.025 cm/yr) probably reflect a drying of the bog surface and a slowing in the growth and preservation of peat (Figure 3.13). This latter point is also indicated by the very low percentages of normally preserved pollen (<30%) and increase in corroded and degraded (Figure 3.25) at this time which suggests an increase of aerobic activity at the mire surface and in the peat humification. The drying of the mire surface and the increase in fire strongly suggest a prolonged period of intense aridity which led to the contraction of the forest extent both by reduced moisture availability and likely by fire. This is consistent with Rio Grande and Punta Yartou cores (see Section 4.1.4 and 4.2.4).

Between c. 6,670 Cal yr BP and c. 3,790 Cal yr BP there was a gradual increase of *Nothofagus dombeyi* type proportions (~70%) together with an increase in well-preserved pollen and a decrease in charcoal concentrations (Figure 3.25, 3.28 and 4.3). This suggests a change to wetter climatic conditions leading to the eastwards expansion of closed-canopy *Nothofagus* forest in the area. Within this interval (between c. 6,670 Cal yr BP and c. 3,790 Cal yr BP) of expanded *Nothofagus* forest there are two periods characterised by *Nothofagus* forest contraction between c. 5,170 Cal yr BP and c. 4,660 Cal yr BP where there was a decrease in *Sphagnum* and Cyperaceae proportions and also a dramatic decrease in charcoal concentrations (Figure 3.18, 3.19, 3.28 and 4.3). These changes in proportions were in line with an increase in Asteraceae (Suf. Asteroideae) and Ericaceae suggesting drier conditions at the mire surface that permitted the colonisation of the Ericaceae heath and others herbs on the bog likely triggered by decrease in effective moisture. This decrease in effective moisture is consistent with Rio Grande and Punta Yartou cores (see Section 4.1.4 and 4.2.4).

The second period of *Nothofagus* forest contraction was between c. 4,660 Cal yr BP and c. 3,790 Cal yr BP and was likely due to a shift to drier conditions at the peat bog surface that allowed the Ericaceae heath to colonise the peat bog indicated by the dramatic increase in the

pollen concentrations of Ericaceae and Asteraceae (Subf. Asteroideae) (Figure 3.22). Contemporary strands of evidence in the Rio Grande and Punta Yartou records show a similar pattern of climate change (see Section 4.1.3 and 4.2.3).

#### 4.3.4 Late-Holocene period.

Between c. 3,790 Cal yr BP and 2,640 Cal yr BP the proportions of *Nothofagus dombeyi* type reached to ~70%. High proportions of *Nothofagus* are interpreted as the development of closed-canopy *Nothofagus* forest facilitated by relatively high levels of effective moisture. However, the presence of *Misodendrum* and the decrease in well-preserved pollen to ~65% and increase in crumpled pollen (Figure 3.24 and 4.2) suggest the levels of effective moisture were borderline for the maintenance of such closed-canopy *Nothofagus* forest. The relatively high concentration of autochthonous Ericaceae pollen also suggests that the surface of the peat was relatively dry and the drier peat hummocks were likely colonised by *Empetrum rubrum* (Figure 3.21).

The ecosystems operating at each site display differences in the degree of complacency and sensitivity to palaeoclimatic changes. Rio Grande which is located at the western end, and therefore, wetter end of the longitudinal transect presented more complacency in its ecological responses. In contrast the drier sites at Punta Yartou and Lago Lynch displayed higher magnitude and higher frequency in the fluctuations of the forest/steppe ecotone. The climatic inferences obtained from these three records are key to providing more reliable interpretations of sub-millennial changes in the intensity/proximity of the SSWs. In the next chapter a synthesis of the three-palaeoenvironmental core integrates the major findings of this study with those in the literature to produce a new understanding of the sequence of environmental change in Fuego-Patagonia.

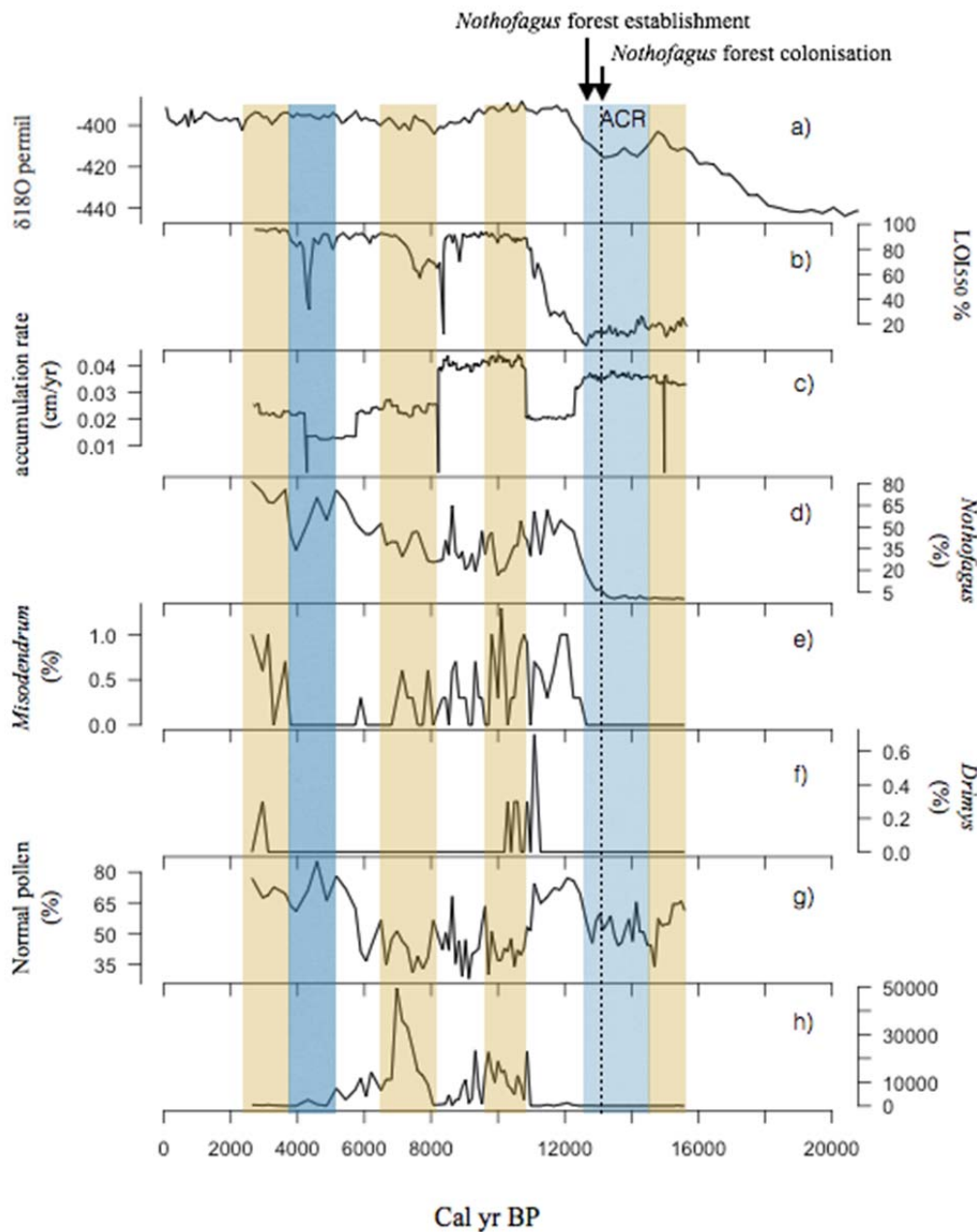


Figure 4.3 Summary of Lago Lynch core. a) deuterium record as temperature proxy from ice core (Dome C) (Lemieux *et al.*, 2010); b) organic content; c) accumulation rate; d) percentage *Nothofagus*; e) percentage *Misodendrum*; f) percentage *Drimys*; g) percentage normal pollen preservation; h) charcoal concentrations. Orange shading indicates intervals of warmer and lower effective moisture, light blue shading indicates interval of colder and lower effective moisture, dark blue shading indicates interval of colder and wetter climatic conditions.

# CHAPTER 5:

## Palaeoenvironmental synthesis

This chapter provides a synthesis of the three-palaeoenvironmental records and integrates the major findings of this study with those in the literature to produce a new understanding of the sequence of environmental change in Fuego-Patagonia. This synthesis provides a new reconstruction of ecological responses to inferred regional climatic changes during the Late-glacial and the Holocene in Fuego-Patagonia and Southern South America (SSA).

This synthesis is organised in three sections, the first section circumscribes the timing and extent of the climate-vegetation linkages operating within the Patagonian forest/steppe ecotone by identifying the natural variability of ecotone-ecosystems and their responses to large-scale controls of the regional climate in terms of the variations in the position and/or intensity of the southern westerlies winds (SWWs) in Fuego-Patagonia at  $\sim 53^{\circ}\text{S}$ , during the Last Glacial/Interglacial Transition (LGIT) and the Holocene. The second section provides evidence for the timing and pattern of the establishment of *Nothofagus* forest across Fuego-Patagonia during the Late-glacial and the Holocene transition and this furthers our understanding about the environmental factors that enabled the spread of forest after the last glaciation. Finally, the third section links the past vegetation changes to variations in past fire activity and large-scale controls of climate during the occupation of Tierra del Fuego by prehistoric peoples.

## **5.1 Palaeoenvironmental reconstruction of Fuego-Patagonia (~53°S) during Last Glacial/Interglacial Transition and Holocene.**

This study has produced a suite of palaeoenvironmental evidence (pollen, stratigraphy, chronology) from three sites along a longitudinal transect at ~53°S. The environmental changes recorded in the three sites display a degree of synchrony in responses to similar large-scale climatic changes during the Late-glacial, mid-Holocene and late-Holocene. However, there is also relative “asynchrony” and/or high centennial-scale differences among the sites during the early Holocene. This relative asynchrony and/or high centennial-scale fluctuations are likely due to the responses of site-specific ecosystem-sensitivities to the climatic changes.

### **5.1.1 Late-glacial period.**

After c. 18,800 Cal yr BP a strong warming of ~8°C occurred in the region at around ~53°S (Caniupán *et al.*, 2011) and this is consistent with the warming trend recorded in Antarctic ice cores (Blunier and Brook, 2001; Lemieux *et al.*, 2010). The climatic warming led to the retreat of the Magellan glaciers after Glacial stage D by c. 17,700 yr BP (McCulloch *et al.*, 2005b). Plant colonisation started immediately after the ice retreat from the study sites, suggesting a minor warming pulse by c. 16,000 Cal yr BP leading to an area free of ice at the Rio Grande and Lago Lynch sites by this time (Figure 3.11 and 3.12).

The Late-glacial vegetation prior to c. 15,000 Cal yr BP at Rio Grande, Punta Yartou and Lago Lynch was treeless and was initially dominated by Ericaceae and heath-grassland. The sites were dominated by wetland vegetation such as the herbs Amaranthaceae, *Caltha*, *Gunnera* and at Rio Grande the cushion bog-forming plant *Drapetes* was also present. High levels of well-preserved pollen were found in all the sites. This evidence indicates relatively wet climatic conditions enough to sustain wetland herbs and the presence of lakes at the three sites. This

evidence suggests a return of the SSWs closer to their present southern position at  $\sim 50^\circ - 55^\circ\text{S}$ . This interpretation of the timing and geographical shift in the SSWs is consistent with other pollen records from Fuego-Patagonia that similarly indicate more humid conditions at this time (McCulloch and Davies, 2001; Markgraf and Huber, 2010; Moreno *et al.*, 2012).

Between c. 15,000 Cal yr BP and c. 14,400 Cal yr BP there was a shift to more mesic conditions and wetland taxa such as *Amaranthaceae*, *Caltha* and *Gunnera* decreased coupled with an increase in grassland taxa such as *Poaceae* and *Acaena* at Rio Grande and Punta Yartou. At Lago Lynch heath vegetation, mainly dominated by *Ericaceae*, reached high proportions ( $\sim 60\%$ ) suggesting a decrease in effective moisture relative to the previous interval. These inferences are further supported by the probable shallowing of lake levels at Rio Grande and Lago Lynch and also the shift to more eutrophic conditions under relatively drier conditions. At Rio Grande and Lago Lynch the accumulation rate continued to be relatively high ( $\sim 0.05\text{cm/yr}$  and  $\sim 0.04\text{cm/yr}$  respectively) and at Punta Yartou the accumulation rate increased to  $\sim 0.05\text{cm/yr}$ . Also, at Rio Grande the organic matter reached a high value  $\sim 50\%$  at the same time as a similar increase in organic content at Punta Yartou. This period between c. 15,000 Cal yr BP and c. 14,400 Cal yr BP of relatively higher organic productivity likely indicates an increase in temperature and/or precipitation. Also, the dramatic increase in corroded and degraded pollen at Rio Grande and Lago Lynch also supports the inference of a shift to relatively drier conditions. Furthermore, the evidence from all three sites suggests that the reduction in effective moisture was caused by an increase in temperature.

The three palaeoenvironmental records reconstructed by this study provide for the first time clear stratigraphical evidence, alongside the vegetation changes demonstrated by the pollen, that supports the inference of a significant shift to warmer interstadial conditions between c. 15,000 Cal yr BP and c. 14,400 Cal yr BP, which suggests the influence of relatively weaker SSWs during that time. The timing and character of the palaeoenvironmental changes during the Late-

glacial in southern Patagonia and Tierra del Fuego at  $\sim 53^{\circ}\text{S}$  does not substantially vary among the three sites. The palaeoenvironmental changes in this study are comparable in their nature and duration with the climatic changes recorded in the Antarctic ice cores (Blunier and Brook 2001; Lemieux-Dudon *et al.*, 2010).

Stratigraphic and vegetation evidence at the Rio Grande and Punta Yartou reveals that between c. 14,400 Cal yr BP and c. 12,500 Cal yr BP the Ericaceae heath vegetation was replaced by cold resistant dryland herbs such as Poaceae and Asteraceae (Subf. Asteroideae) and the *Acaena* and the wetland taxa correspondingly decreased. This evidence indicates a decrease in humidity levels and a return to colder conditions. *Pediastrum* dramatically decreased suggesting less eutrophic lake conditions and decreased bio-productivity. Also, at the Rio Grande site a decrease in organic content and accumulation rate suggests a shift to less favorable climatic conditions, either a decrease in temperature and/or precipitation suggesting lower biological productivity in the lake. This evidence suggests a weaker influence of the SSWs and a reduction in precipitation. At Lago Lynch there was also a near complete replacement of the Ericaceae heath vegetation by cold resistant dryland herbs (Asteraceae-Poaceae). However, the expansion in wetland-taxa suggests that at Lago Lynch the humidity levels appear to have increased although remaining cold. This apparent contradiction between the Rio Grande and Punta Yartou records with the Lago Lynch record may be due to the westward penetration of moisture from south Atlantic air masses. This interplay between the south Atlantic and Pacific moisture sources has also been suggested for some parts of Central Patagonia when the SSWs had a very weak influence on the Pacific west coast (Whitlock *et al.*, 2007). During this period (c. 14,400 Cal yr BP and c. 12,500 Cal yr BP) the temperature and humidity conditions were probably lower than critical limits for *Nothofagus* forest expansion. This period is coeval with the ACR (c. 14,550 – 12,800 Cal yr BP, Lemieux-Dudon *et al.*, 2010) (Figure 5.1) and provides the first compelling evidence for an ecological response to this period of high latitude southern hemisphere cooling.

However, after the nadir of the cooling signal in the Antarctic ice core records (c. 13,500 yr BP) the vegetation at ~53°S began to respond to the onset of further warming that marks the start of the Holocene in Fuego-Patagonia. By c. 13,200 Cal yr BP, at the end of the cooler ACR period, the vegetation changed from the dominance of colder-drier tolerant species (Asteraceae (Subf. Asteroideae)) towards a more mesic vegetation community dominated by Poaceae. More significantly *Nothofagus dombeyi* type increased to ~3% at Punta Yartou and to ~7% at Lago Lynch. The development of steppe with patches of *Nothofagus* forest is interpreted as a shift to more mesic and more temperate conditions, although remaining at this time still colder relative to the Holocene, leading gradually to the spread of more extensive *Nothofagus* forest by c. 12,500 Cal yr BP. The expansion of *Nothofagus* forest and increase in inferred humidity suggests an eastward shift of the forest-steppe ecotone due to the relatively stronger influence of the SSWs after c. 13,500 Cal yr BP. Palaeoenvironmental evidence from Lago Tamar (~52°S) supports the inference of more temperate and moist conditions promoting the expansion of *Nothofagus* forest at c. 13,200 Cal yr BP (Lamy *et al.*, 2010). Also, Putman *et al.*, (2010) reviewed the evidence for glacier advances in New Zealand and South Patagonia during the ACR and they identify that the glacier “resurgence” culminated c. 13,000 yr ago, coinciding with the trend to more warmer and wetter conditions towards the end of the ACR (after c. 13,500 Cal yr BP).

In summary the Late-glacial palaeoenvironmental evidence from the three cores presented by this study suggests relatively drier and warmer climatic conditions between c.15,000 Cal yr BP and c. 14,400 Cal yr BP followed by an interval between c. 14,400 Cal yr BP and 13,200 Cal yr BP when the heath vegetation was replaced by cold resistant dry-herbs. By c. 13,200 Cal yr BP the vegetation changed from the dominance of colder-drier tolerant species towards the expansion of steppe dominated by Poaceae with patches of *Nothofagus* forest is interpreted as

more mesic conditions leading gradually to the establishment of the forest by c. 12,500 Cal yr BP. These palaeoenvironmental changes are comparable in nature and duration, although with a lag of <300 yrs to those recorded in the Antarctic ice cores.

### **5.1.2 Early-Holocene period.**

Between c. 12,500 Cal yr BP and c. 11,700 Cal yr BP a gradual rise in temperatures and more humid conditions are inferred from the early establishment of an open-canopy *Nothofagus* forest at all three sites, marking a transition from the semi-arid steppe conditions of the Late-glacial to the more humid and warmer climatic conditions of the early-Holocene. This environmental reconstruction is coeval with and in contrast to the northern hemisphere Younger Dryas cooling event, registered in the Greenland ice core records (c. 12,800 - 11,700 yr BP) (Rasmussen *et al.*, 2006). This evidence suggests that the core of SWWs storm tracks was either more focused and/or increased in intensity and precipitation reached its maximum at ~53°S by this time. However, the presence of charcoal at c. 12,600 Cal yr BP in Rio Grande, c. 13,640 Cal yr BP in Punta Yartou and at c. 12,230 Cal yr BP in Lago Lynch sites within a period of warmer and wetter conditions at ~53°S (see Section 5.3) appears to be inconsistent. It is likely that this reflects a seasonal pattern of higher winter precipitation and warmer-drier summers coupled with an increase in woodland fuel leading to a moderate increase in fire at this time (Markgraf and Huber, 2010). However, human activity as a source of ignition cannot be excluded (see Section 5.3).

Between c. 11,700 Cal yr BP and c. 10,500 Cal yr BP, higher percentages of *Nothofagus* pollen and the presence of wetland taxa at all three study sites suggests that the relatively high levels of effective moisture continued until c. 10,500 Cal yr BP. During this interval there appears to be higher variability in the magnitude of the levels of effective moisture recorded at the Lago Lynch in comparison to the more stable records from Rio Grande and Punta Yartou. The high

variability at Lago Lynch is probably due to its geographical location on the eastern boundary of the present forest-steppe ecotone and was more likely sensitive to small-scale fluctuations in the proximity and intensity of the SSWs.

Between c. 10,500 Cal yr BP and c. 9,600 Cal yr BP a dramatic decrease in effective moisture is inferred from the contraction of the *Nothofagus* forest and corresponding expansion of steppe, dominated by Poaceae at Rio Grande. A reduction in effective moisture is also inferred from the colonisation of the peat bog by Ericaceae heath coupled with an expansion of grassland vegetation identified at Lago Lynch. However, at Punta Yartou there was a period of time, ~480yrs (between c. 9,990 Cal yr BP and c. 9,510 Cal yr BP) of decreased extent of *Nothofagus* forest and colonisation of the peat bog by Ericaceae heath. This period of decreased effective moisture is likely to be part of a wider regional signal that has been identified elsewhere previously. McCulloch and Davies (2001) inferred an intense arid phase between c. 10,700 Cal yr BP and c. 9,550 Cal yr BP based on pollen and diatom evidence from Puerto del Hambre (~53°S) and this coincides with a dramatic drop at c. 10,000 Cal yr BP in hydrophytic pollen at Gran Campo Nevado ~52°S (Fesq-Martin *et al.*, 2004; Lamy *et al.*, 2010). A synthesis of this evidence suggests a weaker influence of the SSWs leading to a decrease in precipitation. It is probable, given the persistent aridity signal along the southern Andes that the core of the SSWs was then more focused through the Drake Passage (McCulloch *et al.*, 2000). This episode is contemporaneous with an increase in SSTs off the Antarctic peninsula and over-turning of the southern oceans by increased wind speeds.

From c. 9,600 Cal yr BP to c. 8,200 Cal yr BP there was a re-expansion of the *Nothofagus* forest which indicates an increase in effective moisture at Rio Grande and Punta Yartou, while at Lago Lynch there continued to be rapid fluctuations in the forest/steppe ecotone (Figure 5.1) suggesting intervals of small increases in the influence of the SSWs. These small increases in the proximity/intensity of the SSWs can be also seen in the establishment of *Nothofagus* in

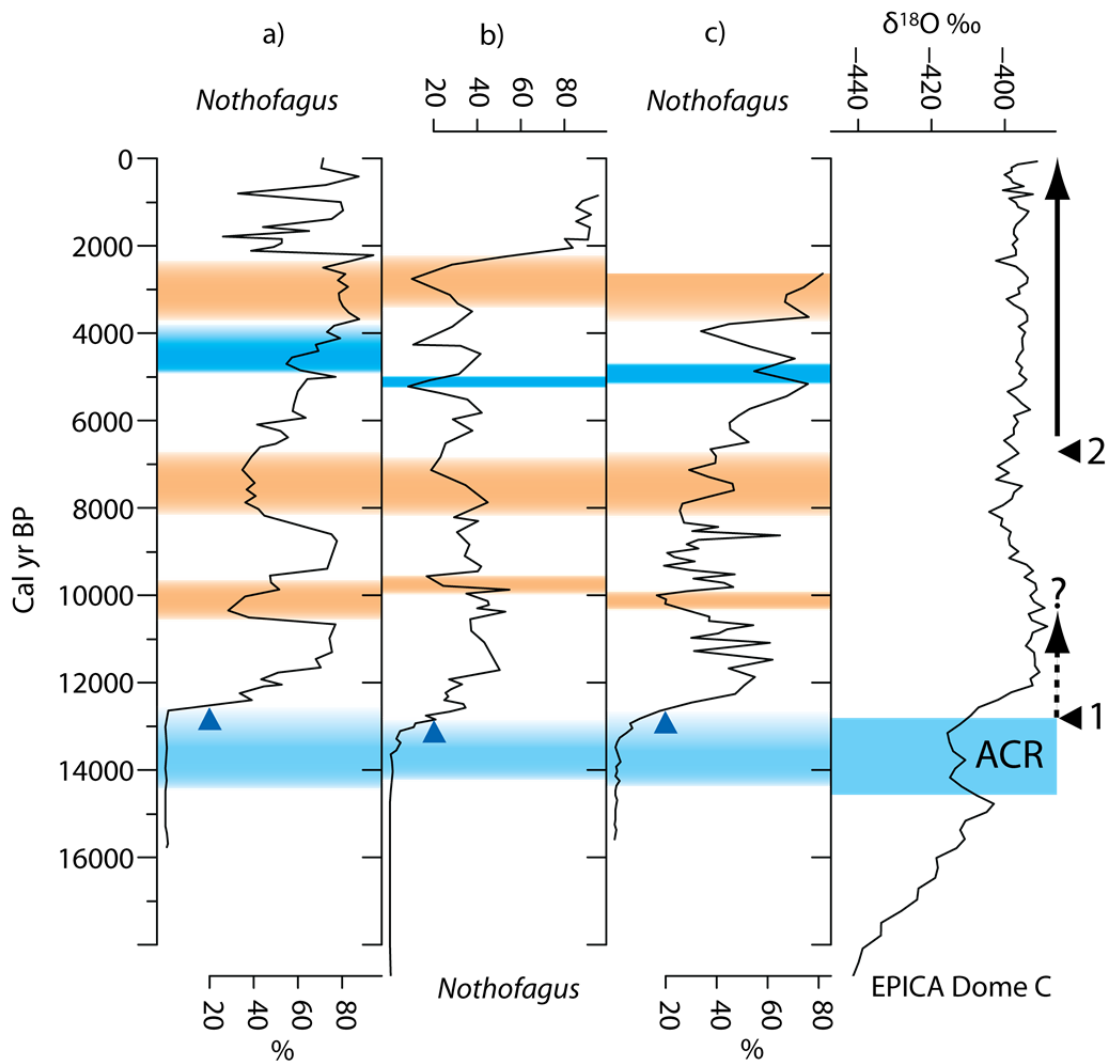


Figure 5.1 *Nothofagus* pollen percentages from a) Rio Grande, b) Punta Yartou and c) Lago Lynch and the EPICA Dome-C deuterium–temperature record (Lemieux *et al.*, 2010). Black triangles (1 and 2) show the first and the second phases of human occupation in Tierra del Fuego, respectively. The question mark indicates the gap of evidence in human occupation in Tierra del Fuego. The blue arrows show the establishment of *Nothofagus* forest ( $\geq 20\%$ ) in each of the study sites. Orange shading indicates intervals of warmer and lower effective moisture, light blue shading indicates interval of colder and lower effective moisture, dark blue shading indicates interval of colder and wetter climatic conditions.

current drier areas of Fuego-Patagonia by c. 8,900 Cal yr BP at Lago Yehuín (~54°) (Markgraf, 1983); c. 8,500 Cal yr BP at Estancia Esmeralda II (~53°) (McCulloch and Davies, 2001).

Furthermore, the evidence suggests that by c. 12,500 Cal yr BP and c. 11,700 Cal yr BP the SWWs were located closer to ~53°S and/or were more intensified and precipitation levels reached their maximum. This was then followed by a general weakening of the SSWs and a decrease in precipitation between c. 10,500 Cal yr BP and c. 9,600 Cal yr BP. Between c. 9,600 Cal yr BP and c. 8,200 Cal yr BP there was a slight increase of SSWs' influence. Contrary to the palaeoenvironmental reconstructions of this study, marine and terrestrial palaeoenvironmental records from Gran Campo Nevado and west side of Estrecho de Magallanes (~52°S-53°S) (Lamy *et al.*, 2010; Harada *et al.*, 2013; Caniupán *et al.*, 2011, 2014) suggest that during the Early-Holocene the core of the SWWs was stronger and more stable between c. 12,500 Cal yr BP and c. 8,500 Cal yr BP. The differences in the climatic conditions inferred from the different records may be due to the different degree of complacency or sensitivity of the different ecosystems to sub-centennial scale fluctuations and instability of the SWWs after c. 11,700 Cal yr BP (Figure 5.1). It is anticipated that the higher geographical resolution of this study provides a better understanding of the different responses of the ecosystems to the regional climatic variability.

### 5.1.3 Mid Holocene Period.

Between c. 8,250 Cal yr BP and c. 5,000 Cal yr BP in the region (~53°S) there was an expansion of grassland steppe and inferred lower levels of effective moisture. Also, there was a corresponding higher presence of charcoal at Punta Yartou and Lago Lynch. Between c. 8,250 Cal yr BP and c. 6,800 Cal yr BP the arid phase became more intense and it probably led to an increase in the amount of dry fuel available during the mid-Holocene in Fuego-Patagonia leading to the highest fire activity promoted by very weak SSWs at this time. This arid phase

was brought to a close after c. 6,800 Cal yr BP by an increase in humidity and inferred intensification of the SSWs.

Between c. 5,000 Cal yr BP and c. 3,500 Cal yr BP at Rio Grande there was a gradual expansion of *Nothofagus* forest which suggests an increase in the levels of effective moisture. However, *Misodendrum* was well represented suggesting that the *Nothofagus* forest was likely under some stress and living near to its critical ecological range. Given that the expansion was probably enabled by an increase in humidity the stress may have been caused by a reduction in temperature during a Neoglacial period (Bentley *et al.*, 2009). However, between c. 5,240 Cal yr BP and c. 4,960 Cal yr BP there was a peak in wetland herbs, most noticeably *Gunnera*. The spread of *Gunnera* is likely to have been across the site itself together with the increase in *Drimys* and *Maytenus*. This expansion of wetland taxa coinciding with the reduction in fire activity during this interval suggests that it was a brief period of wetter and perhaps also cooler climatic conditions. At Lago Lynch there was a marked decrease in *Nothofagus* proportions associated with a dramatic increase in pollen concentrations of Ericaceae and Asteraceae (Subf. Asteroideae) and other wetland taxa, such as *Myrteola* and *Caltha* (Figure 3.19).

Furthermore, based on the different strands of palaeoenvironmental evidence from all three study sites it is inferred that precipitation did not decline at this time, but the stress conditions that affected the *Nothofagus* forest were probably caused by colder conditions. This inference is further supported by a range of different proxies, such as bulk organic geochemistry analysis from ~55°S (Moy *et al.* 2011), palynology from ~55°S (Borromei *et al.*, 2010), palynology and marine molluscs from ~54°S (Candel *et al.*, 2009) and proxy-derived sea surface temperatures from ~53°S (Lamy *et al.*, 2010; Harada *et al.*, 2013; Caniupán *et al.*, 2014). All these climate proxy measures suggest a gradual decline of temperatures between c. 4,500 Cal yr BP and c. 3,800 Cal yr BP.

#### 5.1.4 Late-Holocene Period.

At Rio Grande between c. 3,500 Cal yr BP and c. 2,300 Cal yr BP closed-canopy *Nothofagus* forest developed but higher proportions of *Misodendrum* persisted suggesting that the forest was still under relatively stressed conditions. At the same time, there was an increase in charcoal concentrations and a decrease in well-preserved pollen (increases in corroded and degraded pollen) and a dramatic increase in *Myriophyllum*. This suggests a likely decrease in effective moisture, due to less precipitation and/or an increase in temperature during this interval leading to a shallowing lake conditions. At this time the probable cause of the continued forest stress switched from being cooler temperatures to decreased humidity. At Rio Grande, *Myriophyllum* gradually disappeared by c. 2,610 Cal yr BP at the transition from a lake to a peat bog. This may have been part of an autogenic hydroseral succession but accelerated by drier climatic conditions. While at Punta Yartou there was a substantial increase in pollen concentrations, mainly contributed by Ericaceae (Figure 3.18) as the surface of the peat bog was colonised by *Empetrum rubrum* from which a reduction in effective moisture is inferred. At the same time at Lago Lynch there was an increase in *Nothofagus forest* and a corresponding increase in *Misodendrum* and decline in Ericaceae heath. The evidence for the spread of forest taken separately would suggest a contradictory increase in effective moisture but these pollen changes were also accompanied by an increase in the proportion of corroded and degraded pollen at Lago Lynch which suggests aerobic conditions prevailed at the mire surface during a period of decreased effective moisture. In view of the expansion of *Nothofagus forest* it is probable that the reduction in effective moisture was caused mainly by a lowering in precipitation due to a weakening and/or shifting of the SSWs. This interpretation is supported by the lower humidity between c. 3,500 yr BP and c. 2,500 yr BP recorded in high-resolution stalagmite samples at Gran Campo Nevado (~52°S) (Schimpf *et al.*, 2011) and in the pollen record from Lago Cipresses (~52°S) (Moreno *et al.*, 2009).

On the other hand, peat and pollen records from Lago Fagnano at ~54°S were interpreted to document a cold and dry Neoglacial period from 2,800 Cal yr BP to c. 2,700 Cal yr BP (Van Geel *et al.*, 2000; Chambers *et al.*, 2007) coinciding with the transition from lake to peat bog conditions at Rio Grande by c. 2,610 Cal yr BP, the authors mention that this short interval was probably caused by relatively low solar activity which led to a decrease in temperatures in the northern Hemisphere particularly at mid-high latitudes. Further higher resolution studies for this time period are needed to confirm the relationship between the transition from lake to peat bog conditions in Rio Grande site by c. 2,610 Cal yr BP, and cold and dry Neoglacial period from c. 2,800 Cal yr BP to c. 2,700 Cal yr BP (Van Geel *et al.*, 2000; Chambers *et al.*, 2007).

The period from c. 2,300 Cal yr BP to the present is characterised by rapid and high magnitude fluctuations in levels of effective moisture. At Rio Grande there were significant decreases of *Nothofagus* forest associated with episodes of colonisation of the peat bog by Ericaceae heath likely in response to episodes of decreased effective moisture. In contrast, the periods of *Nothofagus* forest increase, the absence of *Drimys* and *Maytenus* trees, scarce *Misodendrum* and the higher proportions of well-preserved pollen suggest brief episodes of relatively wet climatic conditions until c. 800 Cal yr BP.

At Punta Yartou between c. 2,170 Cal yr BP and c. 870 Cal yr BP there was a closed-canopy forest with higher proportions of *Misodendrum* and a lower diversity of species which suggests relatively high effective moisture. From the depth of ~98 cm (c. 870 Cal yr BP) it is likely that these wetter conditions resulted in the unconsolidated fen peat that could not be effectively sampled. This most recent period of sub-centennial fluctuations in effective moisture has been associated with the Little Ice Age (LIA), Medieval Warm Period (MWP) and human impact recorded in the palaeoenvironmental records from Lago Guanaco (~51°S) (Moy *et al.*, 2008), Lago Cipreses (~51°S) (Moreno *et al.*, 2014), Isla Santa Inés (~53°S) (Fontana and Bennett, 2012), Estrecho de Magallanes (~53°S) (Caniupán *et al.*, 2014), Lago Yehuín (~54°S)

(Markgraf, 1983) Las Cotorras Mire (~54°S) (Borromei *et al.*, 2010) and the Canal Beagle (~55°S) (Obelich *et al.*, 1998).

The sub-centennial variability in effective moisture appears to be a more regional than local climatic signal and which corroborates the strategy of using a longitudinal transect of sites to increase the sensitivity of this study and to increase the potential for inferring regional climate changes at higher resolution rather than relying on single sites within a region which may give misleading local specific climate records.

## **5.2 Early establishment of *Nothofagus* forest at ~53°S.**

During the LGM the glaciers expanded from the Cordillera Darwin and flowed into the lowlands and fjords of Fuego-Patagonia and the larger marine embayment of Bahía Inútil and the Estrecho de Magallanes (Figure 5.2). During the LGM sea levels were lower, ~ -125 m asl. (Fleming *et al.*, 1998), exposing large land areas along the eastern Atlantic coast of Tierra del Fuego and forming a land bridge between the Patagonian mainland and Tierra del Fuego which is today submerged by the sea. During the LGM the vegetation in Tierra del Fuego appears to have been largely treeless and dominated by the cold resistant steppe vegetation of Ericaceae heath, Asteraceae (Subf. Asteroideae) and grassland (Markgraf 1993). Evidence for the local persistence of *Nothofagus* trees and a continuous presence of c. 20–40% *Nothofagus* pollen during an earlier interstadial (>41,000 yr BP) has been recorded from the forest/steppe ecotone near the eastern Atlantic coast (Viamonte 54°11'S-66°21'W, Markgraf 1993) (Figure 5.2). The continued presence of traces of *Nothofagus* in most high latitude pollen records is ambiguous as the peaks appear to be time transgressive and may have been the result of long distance wind transport of pollen from the more northern temperate forests. However, stronger evidence has been provided by molecular genetic studies and ecological niche modeling (Mathiasen and Premoli, 2010; Premoli *et al.*, 2010) that indicates the local persistence and spread from large

and isolated ice-free refugia of *Nothofagus pumilio*, and probably *Drimys* and *Maytenus* trees also, likely located close to the southeastern coastal areas of Tierra del Fuego (Figure 5.2).

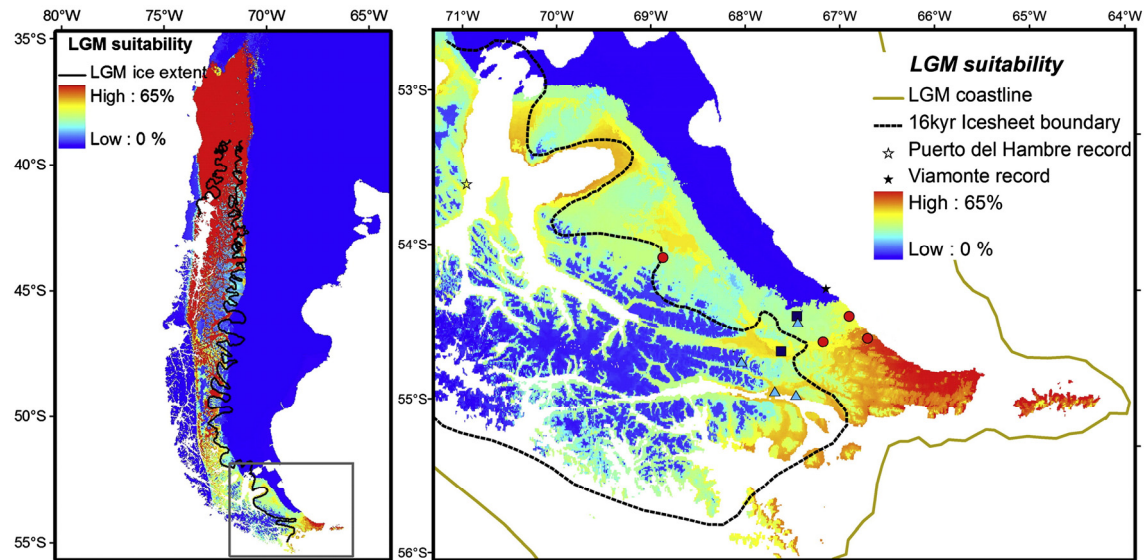


Figure 5.2 Potential distributions of *Nothofagus* during the LGM in southern South America. (from Premoli *et al.*, 2010).

The early and continuous presence of *Nothofagus* pollen (>2%) and also the early expansion of *Nothofagus* pollen (~20%) during the LGIT varies at different latitudinal/longitudinal sites in Fuego-Patagonia. The earliest date for the establishment of *Nothofagus* forest is 12,710 Cal yr BP recorded at Lago Lynch which is the most eastern location which receives the lowest levels of precipitation. The establishment of *Nothofagus* was ~180 years later at Punta Yartou and finally ~230 years later at Rio Grande. The difference in timing of the establishment of the *Nothofagus* forest may be related to the distance from the potential refugia suggested by the molecular genetic evidence (Figure 5.2). The low elevation sites presently located in the mixed evergreen and deciduous *Nothofagus* forest (Lago Lynch, Punta Yartou, Rio Grande, Puerto del Hambre, Ushuaia II and Harberton) (Figure 5.3) were colonised earlier than those sites currently located in drier areas. The deciduous and open deciduous *Nothofagus* forest (Lago Yehuín,

Estancia Esmeralda II, Onamonte) was also earlier than sites currently located in wetter areas, such as in the Magellanic moorland environments (Isla Santa Ines, Isla Clarence) (Figure 5.3). The later arrival of forest in the western wetter areas may have been due to the persistence of ice in the early Holocene. Furthermore, the timing of forest establishment is likely to be closely associated with shifts in the intensity of precipitation/temperature driving eastwards and forming pulses or windows of ideal climatic conditions for *Nothofagus* forest establishment in Fuego-Patagonia along a longitudinal corridor within the precipitation gradient.

The palaeoecological data provided by this study includes the “earliest” evidence for the establishment of subantarctic *Nothofagus* forest during the LGIT in Fuego-Patagonia. *Nothofagus* forest established by c. 12,480 Cal yr BP at Rio Grande, by c. 12,530 at Punta Yartou and by c. 12,710 Cal yr BP at Lago Lynch; c. 1,010 yr, c. 830 yr and c. 780 yr earlier respectively than the “earliest previous” ages for forest establishment in Fuego-Patagonia at 11,700 Cal yr BP at Puerto del Hambre (53°36’S, 70°55’W) (McCulloch and Davies, 2001).

The near-synchronous ecological response among the three study sites at ~53°S infers that these locations in a longitudinal transect were subject to large-scale dramatic shifts towards wetter and warmer climatic conditions by c. 12,500 Cal yr BP. However, the evidence suggests that an increase in warming was likely to be the main factor that enabled the establishment of *Nothofagus* forest at ~53°S. The synthesis of the stratigraphic and vegetation evidence from the three study sites suggests that during the Late-glacial (>14,700 Cal yr BP) the climate in Fuego-Patagonia was relatively humid but remained colder than present but warmer than the previous glacial period. The persistence of *Nothofagus* refugia during the last glaciation indicates that the drier climatic conditions during the LGM were not the main limiting factor for the establishment of forest. It is more likely that the lower temperatures influenced by the Antarctic climate regime prevented the widespread establishment of *Nothofagus* forest until the climatic warming at the end of the Late-glacial/early-Holocene.

The history of *Nothofagus* forest expansion during the LGIT supports the key inference that the core of the SWWs was strengthened and precipitation reached its maximum along  $\sim 53^{\circ}\text{S}$  between c.12,500 Cal yr BP and c. 11,700 Cal yr BP. The increased influence of the core SWWs was likely accompanied by an equivalent southward shift of the Antarctic Circumpolar Current (ACC) coinciding with the onset of warming as evidenced by the deuterium temperature record from Antarctic ice cores (Lemieux- Dudon *et al.*, 2010).

### **5.3 Migration of *Nothofagus* forest, human occupation and past fire activity.**

The expansion of forest at  $\sim 53^{\circ}\text{S}$  during the LGIT was closely followed by the appearance of charcoal at c. 12,600 Cal yr BP in Rio Grande, c. 13,640 Cal yr BP in Punta Yartou and at c. 12,230 Cal yr BP in Lago Lynch (Figure 5.3 and 5.4). The increase in charcoal, and by association the increase in fire activity across Tierra del Fuego was contemporary with the wider spread of forest across Tierra del Fuego by c. 11,000 Cal yrs BP (Borromei, 1995; Quattrocchio and Borromei, 1998; Huber *et al.*, 2004). The coincidence of the increase of fire and the expansion of forest indicates that alongside the climatic conditions the type and availability of woody fuel may also have been an important factor (Huber *et al.*, 2004). However, the near synchronous onset of high fire activity over an extensive area of the “deciduous” and “mixed evergreen–deciduous” forest across Fuego-Patagonia indicates that a large-scale climatic cause was the more likely driving factor. However, in all records the establishment of *Nothofagus* forest has been associated with wetter and warmer climatic conditions. Therefore, it is still unclear why during unfavorable climatic conditions and relatively high fuel moisture content can have led to the ignition and spreading of fire in Tierra del Fuego.

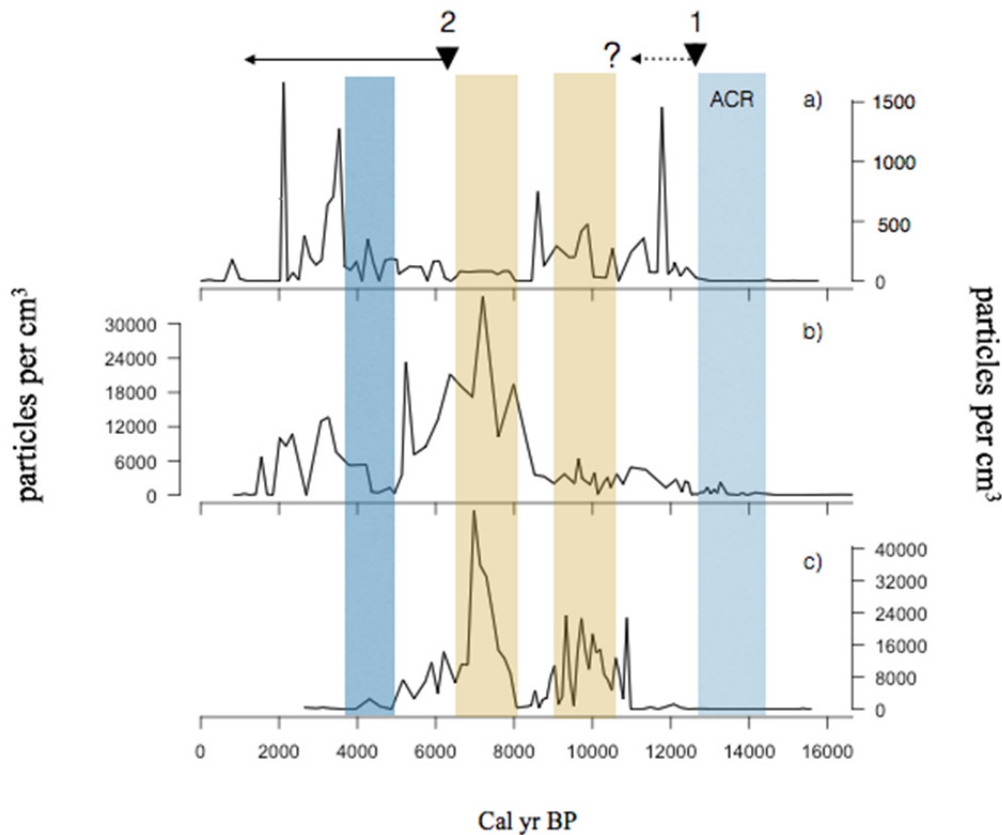


Figure 5.3 Charcoal concentrations from a) Rio Grande, b) Punta Yartou and c) Lago Lynch sites. Black triangle number one and number two show the first and the second phases of human occupation in Tierra del Fuego, respectively. The arrows show the establishment of *Nothofagus* forest ( $\geq 20\%$ ) in each study sites. Yellow shading indicates intervals of warmer and lower effective moisture, light blue shading indicates interval of colder and lower effective moisture, dark blue shading indicates interval of colder and wetter climatic conditions.

Contrary to the timing and pattern of fire activity across Tierra del Fuego the charcoal particle record increased some 1,800 years earlier than the establishment of forest at Puerto del Hambre ( $\sim 53^{\circ}\text{S}$ ) by c. 13,500 Cal yr BP. Puerto del Hambre is located on the mainland in mixed evergreen deciduous forest (McCulloch and Davies, 2001). This increase in fire activity was after the nadir of the of the ACR ( $\sim 13,500$  yr BP), when climatic conditions were still relatively

colder and drier than the present and the vegetation was grassland with a relatively low fuel moisture content (see Section 5.1).

Massone (2004), Morello *et al.*, (2012) and Prieto *et al.*, (2013) have identified two main phases of terrestrial hunter-gatherer occupation in Isla Grande de Tierra del Fuego. The oldest radiocarbon dates for the earliest human occupation of Tierra del Fuego was recorded at the Tres Arroyos rockshelter c. 12,840 - 12,570 Cal yr BP in the central-west of Tierra del Fuego (~53°S). The second pulse of human occupation in north-western Tierra del Fuego has been dated to c. 6,290 - 6,020 Cal yr BP in the vicinity of Bahía Inútil (~53°S) (Figure 1.7).

The palaeoenvironmental conditions in Tierra del Fuego associated with the first phase of human occupation were characterised by a transition from the semi-arid steppe/tundra conditions of the Late-glacial to the wetter and warmer conditions of the early Holocene which promoted the establishment of the forest by c. 12,850 Cal yr BP at Punta Yartou and by c. 12,710 Cal yr BP at Lago Lynch. The first phase of human occupation was relatively coeval with the commencement of the presence of charcoal at c. 12,230 Cal yr BP at Lago Lynch, and with an increase in charcoal concentration at c. 12,400 Cal yr BP at Punta Yartou and (Figure 5.1 and 5.4). The establishment of the forest by c. 12,850 - 12,710 Cal yr BP would have provided an increase in the important woodland resources, for example for firewood, for foraging food and to build shelters (Gusinde, 1937; Piqué and Mansur, 2009) for the first phase of human occupation in Tierra del Fuego (~53°S) by 12,840 – 12,570 Cal yr BP (Massone, 2004; Morello *et al.*, 2012; Prieto *et al.*, 2013).

During the second phase of human occupation in Tierra del Fuego during the mid-Holocene (c. 6,290 - 6,020 Cal yr BP, Massone, 2004; Morello *et al.*, 2012; Prieto *et al.*, 2013) the dominant vegetation was steppe under drier and warmer climatic conditions. These were more favorable conditions for the spreading of fire due to the relatively lower fuel moisture content. This

second pulse of human occupation is contemporary with the highest intervals of past fire activity recorded at Punta Yartou and Lago Lynch sites (Figure 5.1). This suggests that the increase in fire activity may not only have been exacerbated by the drier climatic conditions but also due to human activity and ignition sources.

There is an apparent gap in the record of human occupation between c. 12,840 - 12,570 Cal yr BP and the mid-Holocene c. 6,290 - 6,020 Cal yr BP the reason for which is still unclear. Several hypotheses have been advanced to explain the lack of evidence for human occupation during the early to mid-Holocene, including local extinction or outward-migration of the prehistoric people (Borrero, 1996; Borrero and McEwan, 1997; Prieto *et al.*, 2013). During this apparent gap in human occupation there was a significant decrease in effective moisture levels in the eastern-drier site at Lago Lynch and at Punta Yartou. This shift to drier climatic conditions and the resulting ecological responses at the Lago Lynch and Punta Yartou likely reflect the declining influence of the SSWs around (~53°S) leading to the westward migration of the forest-steppe ecotone (Figure 5.1 and 5.3). From c. 8,250 Cal yr BP to c. 6,800 Cal yr BP there was an intense arid phase that might have led to the highest fire activity in line with the maximum western shift of the forest/steppe ecotone suggesting very weak SSW influence at this time (Figure 5.4). The palaeoenvironmental records from this study point towards the hypothesis that the prehistoric peoples were either driven out from this arid region at the time or they migrated westwards with the steppe/forest ecotone, which was also favored by the camelid Guanacos that were a principal source of food for the terrestrial hunter-gatherers. The later eastward expansion of the forest in the later Holocene may now obscure any evidence for human occupation during the early- to mid-Holocene gap.

The minimal concentrations of charcoal identified in the Rio Grande record are puzzling. It would appear that the neither the periods of evergreen forest or of steppe were significantly affected by fire. The small peaks in charcoal after c. 4,000 Cal yr BP occurred against a

backdrop of wetter conditions and so contrary to the idea of drier favorable conditions leading to the spread of fire. It is probable that the charcoal was either produced by small contained fires controlled by human activity and/or was mainly from larger but more distal fires.

More records are needed to further clarify inter-regional differences in Late Quaternary fire histories. The evidence of this study supports the assertion that large-scale climatic factors were the primary cause behind Late-glacial/early-Holocene fire patterns. The highest fire activity occurred during the mid-Holocene where the large-scale climate patterns were likely the primary control on fire occurrence as also suggested by Markgraf and Anderson (1994).

However, the links between early people moving onto Tierra del Fuego and a higher fire frequency cannot be excluded. More research in the area is necessary to understand the link between the migration of the forest with human occupation in the central and northern sector of Fuego-Patagonia. However, the lack of archaeological evidence renders it difficult to resolve these issues, mainly due to the complex geography and the probability that many of the archaeological sites are now located within the area of closed-forest and so possibly obscuring valuable evidence of human occupation.

The palaeoenvironmental evidence provided by the three study sites show differences in their degree of complacency and sensitivity of the vegetation ecosystems operating at those sites. At the wetter site, Rio Grande demonstrated a greater degree of complacency in ecological responses whereas the drier sites at Punta Yartou and Lago Lynch showed higher variability and large-scale fluctuations from longitudinal shifts in the forest/steppe ecotone. The climatic conditions inferred from these differences provide useful insight into the role of the changes in intensity of the SSWs in driving ecological changes across Fuego-Patagonia during the LGIT and the Holocene.

# CHAPTER 6:

## Conclusions

This study circumscribed the timing and extent of climate-vegetation linkages operating within the Fuego-Patagonia forest/steppe ecotone, identifying the natural variability of ecotone-ecosystems and their responses to the large-scale controls of regional climate in terms of the variations in the intensity of Southern Westerly Winds (SWWs) in Fuego-Patagonia at  $\sim 53^{\circ}\text{S}$ , during the Late-glacial and the Holocene.

The high sensitivity and resolution of the three-palaeoenvironmental cores obtained by this study and the strong positive correlation between the Patagonian precipitation and the SWWs (Garreaud *et al.*, 2013) meant that it was possible to reconstruct the shifts of the forest/steppe ecotone at  $\sim 53^{\circ}\text{S}$ . These three cores provide the highest resolution (temporally) terrestrial palaeoenvironmental record and the oldest continuous reconstruction of vegetation changes for Fuego-Patagonia, inferred from pollen analysis and supported by lithostratigraphy, tephrochronology and radiocarbon dating during the Late-glacial and the Holocene.

One of the contributions of this thesis involved the selection of study sites, for the first time in Patagonia a longitudinal transect ( $\sim 53^{\circ}\text{S}$ ) following a strong west-east precipitation-vegetation gradient has been presented. From the present wetter “mixed evergreen” forest dominated by *Nothofagus betuloides* forest in the west, to the “mixed evergreen-deciduous” forest dominated by *Nothofagus betuloides* in the central part and then “deciduous” forest dominated by *Nothofagus pumilio* in the drier east part of the gradient. The different ecosystems explored in

this study provide an important geographical and ecological dimension to improve our understanding about the different ecological responses to large-scale controls of the regional climate in terms of the changing intensity of SWWs in Fuego-Patagonia at  $\sim 53^{\circ}\text{S}$ .

There were differences in the degree of sensitivity exhibited by the ecosystems reconstructed at each site. At the wetter site, Rio Grande, there was perhaps more complacency in the ecological responses whereas the drier sites at Punta Yartou and Lago Lynch showed higher variability and large fluctuations in the forest/steppe ecotone. The climatic conditions inferred from these differences provide a more reliable and refined interpretation of changes in the intensity of the SWWs at a sub-millennial scale. The synthesis of the palaeoenvironmental records from  $\sim 53^{\circ}\text{S}$  demonstrate a shift to warmer and more humid conditions, with the maximum influence of the SWWs between c. 12,500 Cal yr BP and c. 11,700 Cal yr BP indicated by the expansion of *Nothofagus* forest. This was then followed by a period of relative stability between c. 11,700 Cal yr BP and c. 10,500 Cal yr BP. Between c. 10,500 Cal yr BP and c. 9,600 Cal yr BP there was dramatic change to drier conditions which resulted in a westwards migration of the forest/steppe ecotone. The dry phase was eventually ended by an inferred increase in the intensity of the SWWs. This record of dynamic changes in the behaviour of the SWWs is contrary to the evidence from marine and terrestrial palaeoenvironmental cores from  $\sim 52^{\circ}$  -  $53^{\circ}\text{S}$  (Lamy *et al.*, 2010) which indicates that during the LGIT the core of the westerlies was stronger but more stable (between c. 12,500 Cal yr BP and c. 8,500 Cal yr BP). The records presented by this study provide an improved understanding of the nature of the vegetation changes during the LGIT. They also demonstrate that very careful site selection is necessary to better separate the “local” from the regional climatic signal.

It is acknowledged that this study was focused on high resolution records of the changing intensity of the SWWs at  $\sim 53^{\circ}$  in Fuego-Patagonia during the Late-glacial and the Holocene

rather than identifying the range of latitudinal displacement of the SWWs. The SWWs are a very complex component of the global atmospheric system that governs the climate in South America so, to infer the latitudinal shift of the westerlies would require a larger campaign of palaeoenvironmental coring to reconstruct longitudinal transects following the strong west-east precipitation-vegetation gradient at different latitudinal locations.

Another contribution of this thesis is in terms of the sampling resolution. Data from three high resolution cores has been produced. Punta Yartou, is one of the highest resolution cores and the longest core in Fuego-Patagonia that covers the vegetation changes that provide a reconstruction of the climatic variability during the LGIT and the Holocene leading to a reliable interpretation of the data. A very carefully designed BACON age-depth model was created to calibrate the radiocarbon ages. New tephra layers have been geochemically identified for Fuego-Patagonia and these layers provided chrono-stratigraphic markers between the study sites and provided clear and reliable information for future work in Patagonia. However, there is still a lack of geochemical information for the tephrostratigraphy especially during the Late-glacial and the Holocene and this will need to be investigated further.

The correlation of these high-resolution palaeoenvironmental cores to the deuterium-derived temperature records derived from Antarctic ice cores (Lemieux-Dudon *et al.*, 2010) has helped in our understanding of whether climatic changes within the Antarctic domain provoked ecological responses in the vegetation of Fuego-Patagonia during the Late-glacial and the Holocene. The different lines of palaeoenvironmental evidence demonstrate a high degree of synchrony showing similar large-scale climatic patterns of variability among the three sites located at (~53°S) during the Late-glacial and the Holocene. For first time in Fuego-Patagonia the timing and character of palaeoenvironmental changes during the Last Glacial/Interglacial Transition (LGIT) in southern Patagonia and Tierra del Fuego showed changes comparable in character and duration to those illustrated in Antarctic ice cores. Firstly, the Rio Grande record

has provided clear stratigraphical evidence alongside the pollen record of vegetation change at the study site that supports the inference of a dramatic shift to warmer interstadial conditions between 16,000 and 14,400 Cal yr BP with an onset at c. 14,800 Cal yr BP.

Secondly, during the period coeval with the Antarctic Cold Reversal (c. 14,550 - 12,800 Cal yr BP, Lemieux-Dudon *et al.*, 2010) the stratigraphic and vegetation evidence in the study sites revealed that between c. 14,400 Cal yr BP and c. 12,500 Cal yr BP the open grass-heath and treeless vegetation, mainly dominated by Ericaceae, was replaced by cold resistant dryland herbs such as Poaceae and Asteraceae (Subf. Asteroideae). At the same time *Acaena* and wetland taxa decreased which provides compelling evidence for an ecological response to this period of high latitude southern hemisphere cooling.

After the nadir of the ACR signal in Antarctic records (c. 13,500 yr BP) there was a change from the dominance of colder-drier tolerant species (Asteraceae Subf. Asteroideae) towards the expansion of steppe dominated by Poaceae with patches of *Nothofagus* of the study sites. This vegetation change is interpreted as a response to a shift to more mesic conditions but with relatively colder conditions persisting, leading gradually to the establishment of forest by c. 12,500 Cal yr BP. An eastward shift in the forest-steppe ecotone is inferred due to the increased influence of relatively stronger SWWs after c. 13,500 Cal yr BP. This sequence of vegetation changes and inferred climatic change strongly suggests that Fuego-Patagonia was firmly rooted in the Antarctic domain during the LGIT.

The limited numbers of palaeoecological cores from Fuego-Patagonia provide conflicting evidence for the timing and pattern of *Nothofagus* forest establishment across Fuego-Patagonia during the LGIT and this limits our understanding about the environmental factors that enabled the early establishment of the forest. The new palaeoecological data given in this study includes “earliest” evidence for the establishment of subantarctic *Nothofagus* forest during the LGIT in

Fuego-Patagonia. The forest became established by c. 12,500 Cal yr BP and there was relative synchrony in the timing of forest expansion across the study sites. This synchronous ecological response among the sites around  $\sim 53^{\circ}\text{S}$  provides evidence that the sites were subject to large-scale dramatic shifts toward wetter and warmer climatic conditions by c. 12,500 Cal yr BP provoked by the influence of strong SWWs that reached their maximum along  $\sim 53^{\circ}\text{S}$  between c. 12,500 Cal yr BP and c. 11,700 Cal yr BP. This high influence of the core of the SWWs was probably accompanied by a southward shift of the Antarctic Circumpolar Current (ACC) coinciding with an onset of southern hemisphere warming during the LGIT.

During the Mid-Holocene from c. 8,250 Cal yr BP to c. 6,800 Cal yr BP the arid phase was more intense and it probably led to an increase in the amount of dry fuel available during the mid-Holocene in Fuego-Patagonia leading to the highest fire activity facilitated by the influence of very weak SWWs at this time. This was followed by a slight increase in the intensity of SWWs after c. 6,800 Cal yr BP. Between c. 5,000 Cal yr BP and c. 3,500 Cal yr BP, based on multiple strands of evidence among study sites, it is inferred that climatic conditions were wetter and colder coinciding with a Neoglacial period for Fuego-Patagonia. Between c. 3,500 Cal yr BP and c. 2,300 Cal yr BP there was a period with a decrease in effective moisture that was triggered mainly by a drop in precipitation caused by a weakening of the SWWs with lower humidity being inferred between c. 3,500 yr BP and c. 2,500 yr BP. Between c. 2,300 Cal yr BP and the present, there was rapid sub-centennial effective moisture variability which may be associated with the Little Ice Age (LIA) and Medieval Warm Period (MWP). It is anticipated that an improvement in the temporal resolution of the Rio Grande data during the last millennium will help to identify the cause of the forest/steppe ecotone fluctuations and whether these fluctuations are due to recent climate changes such as the LIA and MWP.

The evidence for the fire history of Fuego-Patagonia provided by this study is consistent with the hypothesis that large-scale climate patterns are the primary controls on the occurrence of

fire. However, the links between early people moving onto Tierra del Fuego and a higher fire frequency cannot be excluded. Also, more research in the area is necessary to confirm and appreciate the link between the migrations of the forest with human occupation in the central north part of Fuego-Patagonia. However, it is difficult to resolve these issues because the archaeological evidence at this moment is scarce and scattered, mainly due to the complex geography and the likelihood that many of the archaeological sites may now be obscured by the closed-*Nothofagus* forest due to the eastwards migration of the forest/steppe ecotone in the later Holocene.

This study has advanced our understanding of the extent of climate-vegetation linkages operating within the Fuego-Patagonia forest/steppe ecotone in Fuego-Patagonia at ~53°S during the LGIT and the Holocene. The nature and extent of the palaeoenvironmental changes are comparable in character and length to those identified in the Antarctic ice core records. Following deglaciation after c. 16,000 Cal yr BP and until c. 12,500 Cal yr BP it is apparent that the Fuego-Patagonia region was more under the influence of the Antarctic domain rather than northern hemisphere palaeoclimatic changes transmitted through the ocean-atmosphere systems. After 12,500 Cal yr BP the ecology of Fuego-Patagonia was more directly influenced by changes in the intensity/proximity of the SWWs. This study provides a base-line, allowing the development of future research that explores the responses of vegetation to climatic changes during the LGIT and the Holocene in Patagonia and the wider southern hemisphere.

## References

- Aceituno, P., Fuenzalida, H., and Rosenblüth, B. (1993) Climate along the extra tropical west coast of South America. In H. A. Mooney, E. R. Fuentes, and B. I. Kronberg, eds., *Earth System Responses to Global Change: Contrasts between North and South America*. San Diego, CA: Academic Press, 61 - 69.
- Aravena, J.C. and Luckman, B.H. (2009) Spatio-temporal rainfall patterns in southern South America. *International Journal of Climatology*. 29, 2106 - 2120.
- Aravena, J.C., Lara, A., Wolodarsky, A., Villalba, R., Cuq, E. (2002) Tree-ring growth patterns and temperature reconstruction from *Nothofagus pumilio* (Fagaceae) forests at the upper treeline of southern Chilean Patagonia. *Revista Chilena De Historia Natural*. 75, 361 - 376.
- Auer, V., Salmi, M., Salminen, K. (1955) Pollen and spore types of Fuego Patagonia. *Annales Academiae Scientiarum Fennicae. Geologica Geographica*. 43, 1 - 14.
- Benn, D.I. and Clapperton, C.M. (2000) Pleistocene glacial tectonic landforms and sediments around central Magellan Strait, southernmost Chile: evidence for fast outlet glaciers with cold-based margins. *Quaternary Science Reviews*. 19 (6), 591 - 612.
- Bennett, K.D. (1996) Determination of the number of zones in a biostratigraphical sequence. *New Phytologist*. 132(1), 155 - 170.
- Bennett, K.D., Willis, K.J. (2001) Pollen. In: Last, W.M., Smol, J.P. (Eds.), *Tracking Environmental Change Using Lake Sediments. Terrestrial, Algal and Siliceous Indicators*, vol. 3. Kluwer Academic Publishers, Dordrecht. 171 - 203.
- Bentley, M.J., Hodgson, D.A., Smith, J.A., Cofaigh, C.Ó., Domack, E.W., Larter, R.D., Roberts, S.J., Brachfeld, S., Leventer, A., Hjort, C., Hillenbrand, C.D., Evans, J. (2009) Mechanisms of Holocene palaeoenvironmental change in the Antarctic Peninsula region. *The Holocene*. 19, 51 - 69.
- Bentley, M.J., Sugden, D.E., McCulloch, R.D., Hulton, N.R.J. (2005) The landforms and pattern of deglaciation in the Strait of Magellan and Bahía Inútil, southernmost South America. *Geografiska Annaler*. 87A (2), 313 - 333.
- Birks, H.J.B., Birks, H.H. (1980) *Quaternary Palaeoecology*. Edward Arnold, London. 289 pp.
- Blaauw, M. and Christen, J.A. (2011) Flexible paleoclimate age-depth models using an autoregressive gamma process. *Bayesian Analysis*. 6, 457 - 474.
- Blaauw, M., (2010) Methods and code for “classical” age-modelling of radiocarbon sequences. *Quaternary Geochronology*. 5(5), 512 - 518.

- Blunier, T. and Brooks, E.J. (2001) Timing of millennial-scale climate change in Antarctica and Greenland during the last glacial period. *Science*. 291(5501), 109 - 12.
- Boelke, O., Moore, D.M., Roig, F.A. (Editors) (1985) *Transecta botánica de la Patagonia Austral*. Cons. Nac. Invest. Cient. Tec., Argentina, Inst. Patagonia, Chile, R. Soc. Great Britain, Buenos Aires, 733.
- Borrero, L. A. (1996) The Pleistocene–Holocene transition in southern South America, in L.G. Straus, B. Eriksen, J. Erlandson & D. Yesner (ed.) *Humans at the end of the Ice Age: the archaeology of the Pleistocene– Holocene transition*. New York: Plenum. 339 - 54.
- Borrero, L.A. (1999) Human dispersal and climatic conditions during Late Pleistocene times in Fuego-Patagonia. *Quaternary International*. 53-54, 93 - 99.
- Borrero, L.A. (2011) The Theory of Evolution, Other Theories, and the Process of Human Colonization of America. *Evolution: Education and Outreach*, 4(2), 218 - 222.
- Borrero, L.A. and McEwan, C. (1997) The peopling of Patagonia: the first human occupation, in C. McEwan, L. Borrero, A. Prieto (ed.) *Patagonia. Natural history, prehistory and ethnography at the uttermost end of the earth: 32–45*. London: British Museum Press.
- Borromei, A., Coronato, A., Franzen, L.G., Ponce, F., López Sáez, J.A., Maidana, N., Rabassa, J., Candel, M.S. (2010) Multiproxy record of Holocene paleoenvironmental change, Tierra del Fuego, Argentina. *Palaeogeography, Palaeoclimatology, Palaeoecology*. 286, 1 - 6.
- Boyd, B., Anderson, J., Wellner, J., Fernández, R. (2008) The sedimentary record of glacial retreat, Marinelli Fjord, Patagonia: regional correlations and climate ties. *Marine Geology*. 255 (3-4), 165 - 178.
- Burru, L.S., Mandri, M.E.T. De., Antoni, H.L.D. (2006) Paleocomunidades vegetales del centro de Tierra Del Fuego durante el Holoceno temprano y tardío. *Revista del Museo Argentino de Ciencias Naturales*. 8(2), 127 - 133.
- Campbell, I. D. (1994) Pollen preservation: experimental wet-dry cycles in saline and desalinated sediments. *Palynology*. 18, 5 - 10.
- Candel, M.S., Borromei, A.M., Martínez, M.A., Gordillo, S., Quattrocchio, M., Rabassa, J. (2009) Middle–Late Holocene palynology and marine mollusks from Archipiélago Cormoranes area, Beagle Channel, southern Tierra del Fuego, Argentina. *Palaeogeography, Palaeoclimatology, Palaeoecology*. 273 (1 - 2).
- Caniupán, A.M., Lamy, F., Lange, C.B., Arz, H.W., Kaiser, J., Kilian, R., León, T., Mollenhauer, G., Pantoja, S., Tiedemann, R., Wellner, J.S. (2014) Holocene sea-surface temperature variability in the Chilean fjord region. *Quaternary Research*. 82, 342 - 353.

- Caniupán, A.M., Lamy, F., Lange, C.B., Kaiser, J., Arz, H., Kilian, R., Baeza, O., Aracena, C., Hebbeln, D., Kissel, C., Laj, C., Mollenhauer, G., Tiedemann, R. (2011) Millennial-scale sea surface temperature and Patagonian Ice Sheet changes off southernmost Chile (53°S) over the past ~60 kyr. *Paleoceanography*. 26, PA3221.
- Chambers, F., Mauquoy, D., Brain, S., Blaauw, M., Daniel, J. (2007) Globally synchronous climate change 2800 years ago: proxy data from peat in South America. *Earth Planetary Science Letters*. 253, 439 - 444.
- Clapperton, C.M., Sugden, D.E., Kauffman, D., McCulloch, R.D. (1995) The last glaciation in central Magellan Strait, southernmost Chile. *Quaternary Research*. 44, 133 - 148.
- Cushing, E.J. (1967) Evidence for differential pollen preservation in Late Quaternary sediments in Minnesota. *Review of Palaeobotany and Palynology*. 4, 87 - 101.
- De Klerk, P., Joosten, H. (2007) The difference between pollen types and plant taxa: *Quaternary Science Journal*. 56(3), 162 - 171.
- Denton, G.H., Anderson, R.F., Toggweiler, J.R., Edwards, R.L., Schaefer, J.M., Putnam, A.E. (2010) The Last Glacial termination. *Science*. 328 (5986), 1652 - 1656.
- Denton, G.H., Lowell, T.V., Heusser, C.J., Moreno, P.I., Andersen, B.G., Heusser, L.E., Schlüchter, C., Marchant, D.R. (1999) Interhemispheric linkage of paleoclimate during the last glaciation. *Geografiska Annaler*. 81A, 107 - 153.
- Douglass, D.C., Singer, B.S., Kaplan, M.R., Ackert, R.P., Mickelson, D.M., Caffee, M.W. (2005) Evidence of early Holocene glacial advances in southern South America from cosmogenic surface-exposure dating. *Geology*. 33, 237 - 240.
- Dugmore, A.J., Larsen, G., Newton, A.J. and Sugden, D.E. (1992) Geochemical stability of fine-grained silicic tephra layers in Iceland and Scotland. *Journal of Quaternary Science*. 7, 173 - 183.
- Fægri, K., Kaland, P.E., Krzywinski, K. (1989) Textbook of Pollen Analysis. 4th edition, Wiley, Chichester. 328 pp.
- Fesq-Martin, M., Friedmann, A., Peters, M., Behrmann, J., Kilian, R. (2004) Late-glacial and Holocene vegetation history of the Magellanic rain forest in southwestern Patagonia, Chile. *Vegetation History and Archaeobotany*. 13 (4), 249 - 255.
- Fleming, K., Johnston, P., Zwart, D., Yokoyama, Y., Lambeck, K. and Chappell, J. (1998) Refining the eustatic sea-level curve since the last glacial maximum using far- and intermediate-field sites. *Earth and Planetary Science Letters*. 163, 327 - 342.
- Fletcher, M.S. and Moreno, P.I. (2011) Zonally symmetric changes in the strength and position of the Southern Westerlies drove atmospheric CO<sub>2</sub> variations over the past 14 k.y. *Geology*. 39 (5), 419 - 422.

- Fontana, S.L. and Bennett, K. (2012) Postglacial vegetation dynamics of western Tierra del Fuego. *The Holocene*. 22(11), 1337 - 1350.
- Fontijn, K., Lachowycz, S.M., Rawson, H., Pyle, D.M., Mathera, T.A., Naranjo, J.A., Moreno-Roa, H. (2014) Late Quaternary tephrostratigraphy of southern Chile and Argentina. *Quaternary Science Reviews*. 89, 70 - 84.
- Garcia, J.L., Kaplan, M.R., Hall, B.I. (2012) Glacier expansion in southern Patagonia throughout the Antarctic cold reversal. *Geology*. 40(9), 859 - 862.
- Garreaud, R., Lopez, P., Minvielle, M., Rojas, M. (2013) Large-Scale Control on the Patagonian Climate. *Journal of Climate*. 26(1), 215 - 230.
- Garreaud, R.D., Vuille, M., Compagnucci, R., Marengo, J. (2009) Present-day South American climate. *Palaeogeography, Palaeoclimatology, Palaeoecology*. 281, 180 - 195.
- Glasser, N.F., Harrison, S., Jansson, K.N., Kleman, J. (2008) The glacial geomorphology and Pleistocene history of southern South America between 38°S and 56°S. *Quaternary Science Reviews*. 27, 365 - 390.
- Glasser, N.F., Harrison, S., Winchester, V., Aniya, M. (2004) Late Pleistocene and Holocene palaeoclimate and glacier fluctuations in Patagonia. *Global and Planetary Change*. 43(1-2), 79 - 101.
- Gosse, J.C. and Phillips, F.M. (2001) Terrestrial in situ cosmogenic nuclides: theory and application. *Quaternary Science Reviews*. 20, 1475 - 1560.
- Grill, S., Borronei, A., Martinez, G., Gutierrez, M.A., Cornou, M.E. & Olivera, D. (2007) Palynofacial analysis in alkaline soils and paleoenvironmental implications: The Paso Otero 5 archaeological site (Necochea district, Buenos Aires province, Argentina). *Journal of South American Earth Sciences*, 24(1), 34 - 47.
- Grimm, E.C. (1987) CONISS; a FORTRAN 77 program for stratigraphically constrained cluster analysis by the method of incremental sum of Squares. *Computers and Geosciences*. 13(1), 13 - 35.
- Grimm, E.C., Blaauw, M., Buck, C.E., Williams, J.W. (2014) Age Models, Chronologies, and Databases Workshop: Complete Report and Recommendations. Queen's University Belfast, Northern Ireland, United Kingdom, 13-16 January 2014.
- Gusinde, M. (1937) Die Feuerland Indianer. T.I: Die Selk'Nam. [1982] Mödlig-Wien. (Translation: Los indios de Tierra del Fuego. I: Los Selk'nam. 2 vols. Buenos Aires: Centro Argentino de Etnología Americana).
- Haberzettl, T., Anselmetti, F.S., Bowen, S.W., Fey, M., Mayr, C., Zolitschka, B., Ariztegui, D., Mauz, B., Ohlendorf, C., Kastner, S., Lücke, A., Schäbitz, F., Wille, M. (2009) Late Pleistocene dust deposition in the Patagonian steppe extending and refining the

- paleoenvironmental and tephrochronological record from Laguna Potrok Aike back to 55 ka. *Quaternary Science Reviews*. 28(25-26), 2927 - 2939.
- Hall, B.L., Porter, C.T., Denton, G.H., Lowell, T.V., Bromley, G.R.M. (2013) Extensive recession of Cordillera Darwin glaciers in southernmost South America during Heinrich Stadial 1. *Quaternary Science Reviews*. 62, 49 - 55.
- Harada, N., Ninnemann, U., Lange, C.B., Marchant, M.E., Sato, M., Ahagon, N., Pantoja, S. (2013) Deglacial–Holocene environmental changes at the Pacific entrance of the Strait of Magellan. *Palaeogeography, Palaeoclimatology, Palaeoecology*. 375, 125 - 135.
- Havinga, A. J. (1984) A 20-year experimental investigation into the decay of pollen and spores in various soil types. *Pollen Spores*. 26, 541 - 558.
- Havinga, A.J. (1964) Investigation into the differential corrosion susceptibility of pollen and spores. *Pollen Spores*. 6, 621 - 635.
- Hayward, C. (2011) High spatial resolution electron probe microanalysis of tephtras and melt inclusions without beam-induced chemical modification. *The Holocene*. 22(1), 119 - 125.
- Henriquez, J.M., Pisano, E., Marticorena, C. (1995) Catálogo de la flora vascular de Magallanes (XII° Región), Chile. *Anales Instituto de la Patagonia, Serie Ciencias Naturales*. 23: 5 – 30.
- Heusser, C.J. (1971) *Pollen and Spores of Chile*. The University of Arizona Press, Tucson, Arizona, 167 pp.
- Heusser, C.J. (1987) Fire history of Fuego-Patagonia. *Quaternary of South America and Antarctic Peninsula*. 5, 93 - 109.
- Heusser, C.J. (1993) Late Quaternary Forest-Steppe contact zone, Isla Grande de Tierra del Fuego, Subantarctic South America. *Quaternary Science Reviews*. 12, 169 - 177.
- Heusser, C.J. (1994) Paleoindians and fire during the late Quaternary in southern South America. *Revista Chilena de Historia Natural*. 67, 435 - 443.
- Heusser, C.J. (1994) Quaternary paleoecology of fuego-patagonia. *Revista do Instituto Geologico, Sao Paulo*. 15(112), 7 - 26.
- Heusser, C.J. (1998) Deglacial paleoclimate of American Sector of the Southern ocean Canal Beagle. *Palaeogeography, Palaeoclimatology, Palaeoecology*. 118, 1 - 24.
- Heusser, C.J. (1999) Human forcing of the vegetation change since the last ice age in southern Chile and Argentina. *Bamberger Geographische Schriften*. 19, 211 - 231.
- Hogg, A.G., Hua, Q., Blackwell, P.G., Niu, M., Buck, C.E., Guilderson, T.P., Heaton, T.J., Palmer, J.G., Reimer, P.J., Reimer, R.W., Turney, C.S.M., Zimmerman, S.R.H. (2013) SHCal13 southern hemisphere calibration, 0-50,000 years cal BP. *Radiocarbon*. 55, 1889-1903.

- Holloway, R. G. (1989) Experimental mechanical pollen degradation and its application to Quaternary age deposits. *Texas Journal of Science*. 41: 131 – 145.
- Huber, U.M., Markgraf, V., Schäbitz, F. (2004) Geographical and temporal trends in Late Quaternary fire histories of Fuego-Patagonia, South America. *Quaternary Science Reviews*. 23(9-10), 1079 - 1097.
- Hulton, N.R.J., Purves, R.S., McCulloch, R.D., Sugden, D.E., Bentley, M.J. (2002) The Last Glacial maximum and deglaciation in southern South America. *Quaternary Science Reviews*. 21(1-3), 233 - 241.
- Jowsey, P.C. (1966) An improved peat sampler. *New Phytologist*. 65, 245 - 248.
- Kalnay, E., Kanamitsu, M., Kistler, R., Collins, W., Deaven, D., Gandin, L., Iredell, M., Saha, D., White, G., Woollen, J., Zhu, Y., Chelliah, M., Ebisuzaki, W., Higgins, W., Janowiak, J., Mo, K.C., Ropelewski, C., Wang, J., Leetma, A., Reynolds, R., Dennis, J. (1996) The NCEP/NCAR 40-years reanalysis project. *Bulletin of the American Meteorological Society*. 77, 437 - 472.
- Kaplan, M.R., Fogwill, C.J., Sugden, S.E., Hulton, N.R.J., Kubik, P. W., Freeman, S.P.H.T. (2008) Southern Patagonian glacial chronology for the Last Glacial period and implications for Southern Ocean climate. *Quaternary Science Reviews*, 27(3-4), 284 - 294.
- Kilian, R. and Lamy, F. (2012) A review of Glacial and Holocene paleoclimate records from southernmost Patagonia (49–55°S). *Quaternary Science Reviews*. 53, 1 - 23.
- Kilian, R., Biester, H., Behrmann, J., Baeza, O., Fesq-Martin, M., Hohner, M., Schimpf, D., Friedmann, A., Mangini, A. (2006) Millennium-scale volcanic impact on a superhumid and pristine ecosystem. *Geology*. 34 (8), 609 - 612.
- Kilian, R., Hohner, M., Biester, H., Wallrabe-Adams, H., Stern, Ch, (2003) Holocene peat and lake sediment tephra record from the southernmost Chilean Andes (53-55°S). *Revista Geológica de Chile*. 30 (1), 47-64.
- Kilian, R., Schneider, C., Koch, J., Fesq-Martin, M., Biester, H., Casassa, G., Arévalo, M., Wendt, G., Baeza, O., Behrmann, J. (2007) Palaeoecological constraint on Late Glacial and Holocene ice retreat in the Southern Andes (53°S). *Global and Planetary Change*. 59 (1-4), 49-66.
- Komárek, J. and Jankovská, V. (2001) Review of the Green Algal Genus *Pediastrum*; Implication for Pollen-Analytical Research. J. Cramer, Stuttgart.
- Lamy, F., Hebbeln, D., Wefer, G. (2010) High-Resolution Marine Record of Climatic Change in Mid-latitude Chile during the Last 28,000 Years Based on Terrigenous Sediment Parameters. *Quaternary Research*. 93(1999), 83–93.

- Lamy, F., Kilian, R., Arz, H., Francois, J., Kaiser, J., Prange, M., Steinke, T. (2010) Holocene changes in the position and intensity of the southern westerly wind belt. *Nature Geoscience*. 3 (10), 695-699.
- Lamy, F., Rühlemann, C., Dierk Hebbeln, D., Wefer, G. (2002) High and low latitude climate control on the position of the southern Peru-Chile Current during the Holocene. *Paleoceanography*. 17 (2).
- Lemieux-Dudon, B., Blayo, E., Petit, J.-R., Waelbroeck, C., Svensson, A., Ritz, C., Barnola, J.-M., Narcisi, B.M., Parrenin, F. (2010) Consistent dating for Antarctic and Greenland ice cores. *Quaternary Science Reviews*. 29 (1-2), 8 - 20.
- Luckman, B.H. and Villalba, R. (2001) Assessing the Synchronicity of Glacier Fluctuations in the Western Cordillera of the Americas During the Last Millennium. In *Interhemispheric climate linkages*. pp. 119 - 140.
- Mancini, M.V. (2009) Holocene vegetation and climate changes from a peat pollen record of the forest-steppe ecotone, southwest of Patagonia (Argentina). *Quaternary Science Reviews*. 28, 1490 - 1497.
- Markgraf, V and D'Antoni HL (1978) Pollen Flora of Argentina. Tuscon AZ: The University of Arizona.
- Markgraf, V. (1983) Late and Postglacial vegetational and palaeoclimatic changes in subantarctic, temperate and arid environments. *Palynology*. 7, 43 - 70.
- Markgraf, V. (1993) Paleoenvironments and paleoclimates in Tierra del Fuego and southernmost Patagonia, South America. *Palaeogeography, Palaeoclimatology, Palaeoecology*. 102 (1-2), 53 - 68.
- Markgraf, V. and Huber, U.M. (2010) Late and postglacial vegetation and fire history in Southern Patagonia and Tierra del Fuego. *Palaeogeography, Palaeoclimatology, Palaeoecology*, 297(2), 351 - 366.
- Markgraf, V., Anderson, L. (1994) Fire history of Patagonia: climate versus human cause. *Revista do Instituto Geologico, Sao Paulo*. 15, 33 - 47.
- Markgraf, V., Webb, R.S., Anderson, K.H., Anderson, L. (2002) Modern pollen/climate calibration for southern South America. *Palaeogeography, Palaeoclimatology, Palaeoecology*. 181, 357 - 397.
- Markgraf, V., Whitlock, C., Haberle, S. (2007) Vegetation and fire history during the last 18,000 cal yr B.P. in Southern Patagonia: Mallín Pollux, Coyhaique, Province Aisén (45°41'30" S, 71°50'30" W, 640 m elevation). *Palaeogeography, Palaeoclimatology, Palaeoecology*. 254(3-4), 492 - 507.

- Massone, M. (2004) Los cazadores despues del hielo. Santiago: Direccion de Bibliotecas, Archivos y Museos.
- Mathiasen, P. and Premoli, A.C. (2010) Out in the cold: genetic variation of *Nothofagus pumilio* (Nothofagaceae) provides evidence for latitudinally distinct evolutionary histories in austral South America. *Molecular ecology*. 19(2), 371 - 85.
- McCulloch, R. and Davies, S. (2001) Late-glacial and Holocene palaeoenvironmental change in the central Strait of Magellan, southern Patagonia. *Palaeogeography, Palaeoclimatology, Palaeoecology*. 173 (3-4), 143 - 173.
- McCulloch, R., Bentley, M., Purves, S., Hulton, N., Sugden, R., Clapperton, Ch. (2000) Climatic inferences from glacial and palaeoecological evidence at the Last Glacial termination, southern South America. *Journal of Quaternary Science*. 15 (4), 409 - 417.
- McCulloch, R., Fogwill, C., Sugden, D., Bentley, M., Kubik, P. (2005a). Chronology of the last glaciation in central Strait of Magellan and Bahía Inútil, southernmost South America. *Geografiska Annaler: Series A, Physical Geography*. 87 (2), 289 - 312.
- McCulloch, R.D. (1994) Palaeoenvironmental evidence for the Late Wisconsin/Holocene transition in the Strait of Magellan, southern Patagonia, unpublished PhD. Thesis, University of Aberdeen.
- McCulloch, R.D. (2010) Westerlies, effect on glaciers. In: Singh, V.P. and Haritashya, U.K. (Eds.) *Encyclopedia of Snow, Ice and Glaciers*, Springer, Dordrecht. The Netherlands. 1253 pp.
- McCulloch, R.D. and Bentley, M.J. (1998) Late glacial ice advances in the Strait of Magellan, southern Chile. *Quaternary Science Reviews*. 17: 775 - 787.
- McCulloch, R.D., Bentley, M.J., Tipping, R.M., Clapperton, C.M. (2005b) Evidence for late-glacial ice dammed lakes in the central Strait of Magellan and Bahia Inutil, southernmost South America. *Geografiska Annaler: Series A, Physical Geography*. 87 (2), 335 - 362.
- McCulloch, R.D., Figuerero Torres, M.J., Mengoni Goñalons, G., Barclay, R., Mansilla, C.A. A Holocene record of environmental changes from Rio Zeballos, Central Patagonia. *The Holocene*. Submitted.
- Meglioli, A. (1992) Glacial Geology of Southernmost Patagonia, the Strait of Magellan and northern Tierra del Fuego, Unpublished PhD Thesis, Lehigh University, USA.
- Moore, B.M. (1983) *Flora of Tierra del Fuego*. Anthony Nelson, Oswestry.
- Moore, P.D., Webb, J.A., Collinson, M.E. (1991) *Pollen Analysis*. Second Edition. Blackwell Scientific Publishers, Oxford. 216 pp.

- Morello, F., Borrero, L., Massone, M., Stern, C.R., García-Herbst, A., Arroyo-Kalin, M. (2012) Tierra del Fuego peopling during the Holocene: discussing colonization, biogeographic barriers and interactions in southernmost Patagonia, Chile. *Antiquity*. 86, 71 - 87.
- Morello, F., Orello, F., Borrero, L., Torres, J., Massone, M., Arroyo-Kalin, M., McCulloch, R.D., Calas, E., Lucero, M., Martinez, I., Bahamonde, G. (2009) Evaluando el registro arqueológico de Tierra del Fuego durante el Holoceno temprano y medio, in M. Salemme, F. Santiago, M. Alvarez, E. Piana, M. Vazquez & M.E. Mansur (ed.) *Arqueología de Patagonia: una mirada desde el último confin. 1075 - 1092*. Ushuaia: Editorial Utopías.
- Moreno, P.I., François, J.P., Villa-Martínez, R.P., Moy, C.M. (2009) Millennial-scale variability in Southern Hemisphere westerly wind activity over the last 5000 years in SW Patagonia. *Quaternary Science Review*. 28, 25 - 38.
- Moreno, P.I., Vilanova, I., Villa-Martínez, R., Garreaud, R.D., Rojas, M., De Pol-Holz, R. (2014) Southern Annular Mode-like changes in southwestern Patagonia at centennial timescales over the last three millennia. *Nature communications*. 5, 4375.
- Moreno, P.I., Villa-Martínez, R., Cardenas, M.L., Sagredo, E.A. (2012) Deglacial changes of the southern margin of the southern westerly winds revealed by terrestrial records from SW Patagonia (52°S). *Quaternary Science Reviews*. 41, 1 - 21.
- Moy, C.M., Dunbar, R.B., Guilderson, T.P., Waldmann, N., Mucciarone, D.A., Recasens, C., Ariztegui, D., Austin Jr., J.A., Anselmetti, F.S. (2011) A geochemical and sedimentary record of high southern latitude Holocene climate evolution from Lago Fagnano, Tierra del Fuego. *Earth Planet. Science Letters*. 302 (1–2), 1 - 13.
- Myster, R. W. (editor) (2012) *Ecotones between forest and grassland*. Springer, Dordrecht London. 327 pp.
- Obelic, B., Alvarez, A., Argullo, J., Piana, E.L. (1998) Determination of water palaeotemperature in the Beagle Channel (Argentina) during the last 6000 years through stable isotope composition of *Mytilus edulis* shells. *Quaternary of South America & Antarctic Peninsula*. 11, 47 - 71.
- Piqué, R. and Mansur, M.E. (2009) Between the Forest and the Sea: Hunter-Gatherer Occupations in the Subantarctic Forests in Tierra del Fuego, Argentina. *Arctic Anthropology*. 46(1 - 2), 144 - 157.
- Pisano, E. (1977) Fitogeografía de Fuego-Patagonia chilena I. Comunidades vegetales entre las latitudes 52° y 56°S. *Anales del Instituto de la Patagonia*. 8, 121 - 250.
- Premoli, A.C., Mathiasen, P., Kitzberger, T. (2010) Southern-most Nothofagus trees enduring ice ages: Genetic evidence and ecological niche retrodiction reveal high latitude (54°S)

- glacial refugia. *Palaeogeography, Palaeoclimatology, Palaeoecology*. 298(3-4), 247 - 256.
- Prieto, A., Stern, C.R., Estévez, J.E. (2013) The peopling of the Fuego-Patagonian fjords by littoral hunter-gatherers after the mid-Holocene H1 eruption of Hudson Volcano. *Quaternary International*. 317, 3 - 13.
- Rabassa, J. (2008) Late Cenozoic glaciations in Patagonia and Tierra del Fuego. In: Rabassa, J. (ed.), "Late Cenozoic of Patagonia and Tierra del Fuego". *Developments in Quaternary Sciences*. 11, Chapter 8, 151–204. Elsevier, Amsterdam.
- Ramsey, C.B. (2009) Bayesian analysis of radiocarbon dates. *Radiocarbon*. 51 (1).
- Rasmussen, S.O., Andersen, K.K., Svensson, A.M., Steffensen, J.P., Vinther, B.M., Clausen, H.B., Siggaard-Andersen, M.L., Johnsen, S.J., Larsen, L.B., Dahl-Jensen, D., Bigler, M., Röthlisberger, R., Fischer, H., Goto-Azuma, K., Hansson, M.E., Ruth, U. (2006) A new Greenland ice core chronology for the last glacial termination. *Journal of Geophysical Research*. 111, D06102.
- Rojas, M., Moreno, P., Kageyama, M., Crucifix, M., Hewitt, C., Abe-Ouchi, A., Ohgaito, R., Brady, E.C., Hope, P. (2009) The SouthernWesterlies during the Last Glacial Maximum in PMIP2 simulations. *Climate Dynamics*. 32 (4), 525 - 548.
- Sagredo, E., Moreno, P.I., Villa-Martinez, R., Kaplan, M.R., Kubik, P.W., Stern, C.R. (2011) Fluctuations of the Última Esperanza ice lobe (52°S), Chilean Patagonia, during the last glacial maximum and termination 1. *Geomorphology*. 125(1), 92 - 108.
- Schimpf, D., Kilian, R., Kronzb, A., Simon, K., Spötl, C., Wörnerb, G., Deininger, M., Mangini, A. (2011) The significance of chemical, isotopic, and detrital components in three coeval stalagmites from the superhumid southernmost Andes (53°S) as high-resolution palaeo-climate proxies. *Quaternary Science Reviews*. 30(3-4), 443 - 459.
- Schneider, C., Kilian, R., Santana, A., Butorovic, N., Casassa, G. (2003) Weather observations across the southern Andes at 53°S. *Physical Geography*. 24 (2), 97 - 119.
- Sime, L.C., Kohfeld, K.E., Le Quéré, C., Wolff, E.W., DeBoer, A.M., Graham, R.M., Bopp, L. (2013) Southern Hemisphere westerly wind changes during the Last Glacial Maximum: model-data comparison. *Quaternary Science Reviews*. 64, 104 - 120.
- Steele, D., Engwell, S. (2009) Preparation of tephra samples for electron microprobe analysis. School of GeoSciences. The University of Edinburgh. 3pp.
- Stern, C.R. (2008) Holocene tephrochronology record of large explosive eruptions in the southernmost Patagonia Andes. *Bulletin of Volcanology*. 70 (4), 435 - 454.
- Stern, C.R., Moreno, P.I., Henriquez, W.I., Villa-Martínez, R., Sagredo, E.A., Aravena, L.C. Tephrochronology in the area around Cochrane (~47°S), southern Chile. Submitted.

- Stern, C.R., Moreno, P.I., Villa-Martínez, R., Sagredo, E.A., Prieto, A., Labarca, R. (2011) Evolution of ice-dammed proglacial lakes in Última Esperanza, Chile: implications from the late-glacial R1 eruption of Reclús volcano, Andean Austral Volcanic Zone. *Andean Geology*. 38 (1), 82 - 97.
- Stockmarr, J. (1971) Tablets with spores used in absolute pollen analysis. *Pollen et Spores*. 13, 615 - 621.
- Sugden, D., Bentley, M., Fogwill, M., Hulton, N., McCulloch, R., Purves, R. (2005) Late-glacial glacier events in southernmost South America: a blend of 'northern' and 'southern' hemispheric climatic signals?. *Geografiska Annaler: Series A, Physical Geography*. 87 (2), 273 - 288.
- Sugden, D.E., McCulloch, R.D., Bory, A.J.M., Hein, A.S. (2009) Influence of Patagonian glaciers on Antarctic dust deposition during the Last Glacial period. *Nature Geoscience*. 2 (4), 281 - 285.
- Tell, G., Izaguirre, I. & Allende, L. (2011) Diversity and geographic distribution of Chlorococcales (Chlorophyceae) in contrasting lakes along a latitudinal transect in Argentinean Patagonia. *Biodiversity Conservation*.
- Tipping, T. (1987) The origins of corroded pollen grains at five early postglacial pollen sites in western Scotland. *Review of Palaeobotany and Palynology*, 53, 151 - 161.
- Toggweiler, J.R., Russell, J.L. & Carson, S.R. (2006) Midlatitude westerlies, atmospheric CO<sub>2</sub>, and climate change during the ice ages. *Paleoceanography*, 21(2), PA2005.
- Trivi, M.E. and Burry, L.S. (2006) Dispersión-depositación del polen actual en Tierra del Fuego, Argentina. *Revista Mexicana de Biodiversidad*, 77, 89 - 95.
- Tuhkanen, S. (1990) The climate of Tierra del Fuego from a vegetation geographical point of view and its ecoclimatic counterparts elsewhere. *Acta Botanica Fennica*. 125, 4 - 17.
- Tweddle, J.C. & Edwards, K.J. (2010) Pollen preservation zones as an interpretative tool in Holocene palynology. *Review of Palaeobotany and Palynology*. 161(1-2), 59 - 76.
- Van Geel, B., Heusser, C.J., Renssen, H., Schuurmans, C.J.E. (2000) Climatic change in Chile at around 2700 BP and global evidence for solar forcing: a hypothesis. *The Holocene*. 10, 659 - 664.
- Veblen, T.T., Hill, R.S., Read, J. (1996) *The Ecology and Biogeography of Nothofagus Forests*. Yale University Press, Newhaven and London, pp403
- Villa-Martínez, R. and Moreno, P.I. (2007) Pollen evidence for variations in the southern margin of the westerly winds in SW Patagonia over the last 12,600 years. *Quaternary Research*. 68(3), 400 - 409.

- Villa-Martínez, R., Moreno, P.I., Valenzuela, M. (2012) Deglacial and postglacial vegetation changes on the eastern slopes of the central Patagonian Andes (47°S). *Quaternary Science Reviews*, 32, 86 - 99.
- Villagrán, C. (1980) Vegetationsgeschichtliche und pflanzensoziologische Untersuchungen im Vicente Pérez Rosales Nationalpark (Chile): Vaduz: J. Cramer.
- Von Post, L. (1929) Die Zeichenschrift der Pollenstatistik. *Geologiska Föreningens i Stockholm. Föreläsningar (GFF)* 51, 543 - 565.
- Waldmann, N., Borromei, A.M., Recasens, C., Olivera, D., Martínez, M.A., Maidana, N.I., Ariztegui, D., Austin, J.A., Anselmetti, F.S., Moy, C. (2014) Integrated reconstruction of Holocene millennial-scale environmental changes in Tierra del Fuego, southernmost South America. *Palaeogeography, Palaeoclimatology, Palaeoecology*. 399, 294 - 309.
- Whitlock, C. and Larsen, C. (2001) Charcoal as a fire proxy. In: Last, W.M., Smol, J.P. (Eds.), *Tracking Environmental Change Using Lake Sediments. Terrestrial, Algal and Siliceous Indicators*, vol. 3. Kluwer Academic Publishers, Dordrecht.
- Wille M, Maidana NI, Schäbitz F, Fey M, Haberzettl T, Janssen S, Lücke A, Mayr C, Ohlendorf C, Schleser GH & Zolitschka B. (2007) Vegetation and climate dynamics in southern South America: The microfossil record of Laguna Potrok Aike, Santa Cruz, Argentina. *Review of Palaeobotany and Palynology*. 146(1-4), 234 - 246.
- Wingenroth, M. and Heusser, C.J. (1984) Polen en la Alta Cordillera: Quebrada Benjamin Matienzo Andes Centrales, Mendoza Argentina. Instituto Argentino de Nivología y Glaciología.

Appendix:

Geochemical composition of the  
tephra layers.

## Mt Buney (B2)

### Rio Grande

B2 (V) - RG

	Na2O	MgO	Al2O3	K2O	CaO	FeO	SiO2	P2O5	TiO2	MnO	Total
1	4.5896	0.2840	12.2260	1.6055	1.6676	1.1569	78.0683	0.0318	0.2009	0.0382	99.9
2	4.2950	0.2911	12.2971	1.6510	1.5942	1.3963	76.9207	0.0264	0.2094	0.0400	98.7
3	4.3522	0.2860	11.9690	1.5344	1.5178	1.2415	76.5031	0.0330	0.2115	0.0305	97.7
4	4.2454	0.2837	11.9451	1.6330	1.6188	1.3888	74.7348	0.0225	0.2270	0.0349	96.1
5	4.6279	0.3409	12.7326	1.4549	1.7379	1.4012	76.4141	0.0288	0.2090	0.0428	99.0
6	4.4065	0.2790	11.9986	1.6400	1.4480	1.1252	77.1269	0.0259	0.1922	0.0304	98.3
7	4.2960	0.2448	11.6263	1.7259	1.4620	1.2738	75.4245	0.0286	0.1914	0.0364	96.3
8	4.5603	0.3406	12.1518	1.6481	1.6268	1.2042	75.9034	0.0272	0.2277	0.0410	97.7
9	4.5566	0.2843	12.6190	1.6527	1.6085	1.2472	78.1572	0.0326	0.2191	0.0476	100.4
10	4.4465	0.2772	12.0811	1.7535	1.5101	1.2308	78.0863	0.0178	0.2037	0.0414	99.6

### Punta Yartou

B2 (V) - PY

	Na2O	MgO	Al2O3	K2O	CaO	FeO	SiO2	P2O5	TiO2	MnO	Total
1	4.5965	0.2784	12.3122	1.6212	1.5706	1.1613	77.5853	0.0234	0.1985	0.0390	99.4
2	4.6453	0.3142	12.1707	1.5783	1.7331	1.3570	77.3404	0.0295	0.2259	0.0351	99.4
3	4.5511	0.3354	12.2334	1.6107	1.6171	1.2185	76.9140	0.0349	0.2109	0.0398	98.8
4	4.5131	0.3037	12.1667	1.6461	1.5927	1.2411	77.2980	0.0392	0.2055	0.0341	99.0
5	4.3048	0.3131	12.1204	1.6165	1.4345	1.1624	77.2212	0.0364	0.2050	0.0300	98.4
6	4.4978	0.2723	12.3647	1.6841	1.5065	1.2764	76.8605	0.0347	0.2052	0.0398	98.7
7	4.4035	0.2665	11.8112	1.6990	1.4666	1.1167	77.9962	0.0258	0.1881	0.0298	99.0
8	4.5805	0.3098	12.7837	1.6065	1.5875	1.4179	77.4897	0.0366	0.2118	0.0345	100.1
9	4.5227	0.2992	12.2667	1.5564	1.5825	1.2579	76.7852	0.0349	0.2137	0.0453	98.6

### Lago Lynch

B2 (V)-LL

	Na2O	MgO	Al2O3	K2O	CaO	FeO	SiO2	P2O5	TiO2	MnO	Total
1	4.5894	0.3647	12.6249	1.6629	1.8445	1.5148	76.6255	0.0226	0.2563	0.0449	99.6
2	4.3873	0.2657	12.0648	1.6834	1.5619	1.2711	77.3267	0.0263	0.2163	0.0414	98.8
3	4.2599	0.2729	11.6585	1.6787	1.3701	1.0632	75.8773	0.0267	0.1914	0.0357	96.4
4	4.4492	0.2804	11.9777	1.6697	1.3850	1.1610	75.1926	0.0192	0.1904	0.0254	96.4
5	4.2543	0.2434	11.5883	1.6404	1.4317	1.1618	75.3578	0.0365	0.1841	0.0269	95.9
6	4.4787	0.3165	12.1905	1.5446	1.6165	1.2340	77.0130	0.0322	0.2274	0.0488	98.7
7	4.4578	0.3072	11.8071	1.6663	1.5217	1.3832	76.0120	0.0258	0.2112	0.0402	97.4
8	4.6012	0.2823	12.6156	1.7131	1.6716	1.3830	78.1302	0.0274	0.2193	0.0490	100.7
9	4.7766	0.3812	12.3533	1.5678	1.8336	1.5701	75.9103	0.0359	0.2516	0.0362	98.7
10	4.5389	0.2529	12.0607	1.6928	1.5317	1.2232	78.0572	0.0222	0.1931	0.0370	99.6

# Mt Boney (B1)

## Punta Yartou

B1 (M)-PY

	Na2O	MgO	Al2O3	K2O	CaO	FeO	SiO2	P2O5	TiO2	MnO	Total
1	4.4695	0.2444	11.8112	1.7864	1.3084	1.0365	76.7831	0.0276	0.1714	0.0340	97.7
2	4.2197	0.3012	12.0680	1.5999	1.3757	1.2900	77.9736	0.0379	0.1821	0.0307	99.1
3	4.4455	0.2845	11.5105	1.6455	1.3363	1.0181	75.6414	0.0376	0.1489	0.0389	96.1
4	4.5167	0.2708	11.7737	1.5922	1.2914	1.1312	75.0755	0.0369	0.1421	0.0350	95.9
5	4.4895	0.2655	12.1851	1.7768	1.3296	0.9825	76.0788	0.0358	0.1390	0.0334	97.3
6	4.6024	0.2401	11.6785	1.6109	1.3264	0.9798	74.8558	0.0277	0.1392	0.0354	95.5
7	4.3289	0.2448	12.6317	1.6155	1.5216	0.9938	75.6888	0.0382	0.1708	0.0460	97.3
8	4.4463	0.2954	11.8056	1.5476	1.4293	1.0316	75.7570	0.0414	0.1771	0.0349	96.6
9	4.5070	0.2928	11.8967	1.6087	1.3786	0.8839	77.2843	0.0370	0.1520	0.0445	98.1

## Lago Lynch

B1(M)-LL

	Na2O	MgO	Al2O3	K2O	CaO	FeO	SiO2	P2O5	TiO2	MnO	Total
1	4.2092	0.2587	12.1205	1.8116	1.1245	0.8847	74.8334	0.0382	0.1297	0.0402	95.5
2	4.4104	0.2460	11.9499	1.7390	1.3167	0.9360	75.5526	0.0378	0.1479	0.0360	96.4
3	4.2981	0.2395	11.8299	2.2407	1.1108	1.0359	74.8403	0.0440	0.1395	0.0351	95.8
4	4.5069	0.2434	12.6848	1.8341	1.3278	1.0214	77.0403	0.0282	0.1495	0.0339	98.9
5	4.4594	0.2626	11.9621	1.5063	1.3911	1.2439	76.3603	0.0331	0.1911	0.0402	97.5
6	4.3367	0.2450	11.8448	1.5943	1.2616	1.0077	76.2836	0.0195	0.1604	0.0363	96.8
7	4.5332	0.2624	12.1911	1.6195	1.3040	0.9020	77.4106	0.0275	0.1470	0.0445	98.4
8	4.4360	0.2512	12.3619	1.8485	1.2184	1.0011	76.6490	0.0306	0.1539	0.0326	98.0
9	4.2638	0.2715	11.8884	1.6616	1.4131	1.0479	76.0628	0.0309	0.1765	0.0327	96.8

## Volcán Hudson (Hb)

### Lago Lynch

Hb (M)-LL

	Na2O	MgO	Al2O3	K2O	CaO	FeO	SiO2	P2O5	TiO2	MnO	Total
1	5.8950	1.5129	15.7091	2.8689	2.9738	5.1464	64.1762	0.3708	1.3418	0.1710	100.1659
2	5.7270	1.5698	15.7217	2.8805	3.4396	4.8891	65.4212	0.2923	1.2409	0.1491	101.3312
3	6.3146	1.4368	14.8247	2.8361	2.6713	4.5847	62.1342	0.3397	1.2123	0.1502	96.5046
4	6.3141	1.2557	15.4621	2.9063	2.5239	4.6618	64.8961	0.2640	1.1304	0.1539	99.5683
5	6.1279	1.4510	15.5792	2.9979	2.7913	4.7543	64.9065	0.3128	1.1859	0.1564	100.2632
6	5.8403	1.7732	15.8491	2.7875	3.6490	5.2748	64.3274	0.3395	1.2205	0.1705	101.2318
7	6.1408	1.3654	15.9152	2.9624	2.8327	5.1044	64.3996	0.2944	1.1884	0.1590	100.3623
8	5.7971	1.7050	15.3139	2.9261	3.3182	5.1101	63.6419	0.3563	1.2133	0.1554	99.5373
9	6.2017	1.5953	14.8222	2.6571	3.2082	5.0960	61.6121	0.3752	1.2982	0.1632	97.0292
10	6.3162	1.1261	15.4565	2.9922	2.4754	4.1406	65.3124	0.2719	1.0903	0.1360	99.3176
11	5.9412	1.4490	15.6624	2.8067	3.0370	5.1119	65.2137	0.3197	1.2293	0.1713	100.9422
12	5.2028	1.3991	15.3537	4.6571	2.9386	4.8383	64.4259	0.3296	1.2088	0.1395	100.4934

## Volcán Hudson (Ha)

### Punta Yartou

Ha (M)-PY

	Na2O	MgO	Al2O3	K2O	CaO	FeO	SiO2	P2O5	TiO2	MnO	Total
1	5.7739	1.6250	15.8801	2.7829	3.3830	5.2456	64.3226	0.3651	1.2655	0.1519	100.7956
2	5.9244	1.7631	15.0265	2.6675	3.6416	5.3069	63.7118	0.3431	1.2523	0.1734	99.8106
3	5.7414	1.7637	15.1724	2.6433	3.5149	5.0490	64.1031	0.3471	1.2369	0.1566	99.7284
4	5.8206	1.6948	15.8663	2.7023	3.5329	5.0308	63.5173	0.3601	1.2190	0.1608	99.9049
5	5.8132	1.1899	15.4815	3.0046	2.5971	4.4114	65.1605	0.2704	1.1074	0.1553	99.1913
6	5.9947	1.7015	15.5625	2.8407	3.4511	4.8641	64.5136	0.3298	1.2114	0.1567	100.6261
7	5.7344	1.3223	14.0464	2.4933	2.7810	4.7073	59.7971	0.3345	1.1582	0.1406	92.5151
8	5.8401	1.4088	15.4013	2.8601	3.0221	4.5410	64.5225	0.3459	1.2023	0.1531	99.2972
9	5.7291	1.3250	15.1632	2.8678	2.6500	4.6028	63.3794	0.3249	1.1737	0.1498	97.3657

# Volcán Hudson (H1)

## Rio Grande

H1 (V)-RG

	Na2O	MgO	Al2O3	K2O	CaO	FeO	SiO2	P2O5	TiO2	MnO	Total
1	6.1110	1.2051	15.3731	3.0406	2.7065	4.6116	65.8666	0.2458	1.1557	0.1498	100.4658
2	5.8764	1.6150	15.6978	2.7338	3.3317	4.9898	64.8211	0.3239	1.3116	0.1660	100.8671
3	5.7492	1.1792	15.0271	3.0665	2.4652	4.2917	64.6234	0.2138	1.1092	0.1491	97.8744
4	5.6565	1.2435	15.1374	2.9787	2.5733	4.5394	65.4707	0.2687	1.1893	0.1535	99.2110
5	5.8367	1.2445	15.5486	2.9696	2.6763	4.5168	65.8425	0.2596	1.1744	0.1431	100.2121
6	5.5434	1.5994	14.8848	2.6785	3.2398	5.4860	63.1832	0.3457	1.3315	0.1714	98.4637
7	5.7118	1.3695	15.4993	2.8548	2.9694	4.9676	64.5720	0.3019	1.2423	0.1546	99.6432
8	5.8624	1.4464	15.7090	2.8579	3.3402	4.8588	64.1722	0.2793	1.2059	0.1636	99.8957
9	5.3551	1.4664	14.7793	2.5859	3.1555	4.9304	61.6417	0.3496	1.2564	0.1615	95.6818
10	5.7478	1.5021	15.5792	2.7332	3.1068	5.0296	63.3939	0.3376	1.3435	0.1686	98.9423
11	5.7633	1.3527	15.1423	2.8595	3.0685	4.6800	63.6309	0.2714	1.2020	0.1377	98.1083

## Punta Yartou

H1 (V)-PY

	Na2O	MgO	Al2O3	K2O	CaO	FeO	SiO2	P2O5	TiO2	MnO	Total
1	6.2177	1.2766	15.1281	2.8913	2.5758	4.2722	65.0658	0.2574	1.1751	0.1431	99.0031
2	5.9252	1.2095	15.7765	2.9786	2.5156	4.6420	66.4788	0.2290	1.1762	0.1406	101.0720
3	5.8967	1.1975	14.9463	2.9471	2.4801	4.4799	65.6290	0.2577	1.1400	0.1481	99.1224
4	5.7565	1.0909	15.8274	3.1849	2.3828	4.0925	66.3070	0.2771	1.2000	0.1364	100.2555
5	5.8673	1.5251	15.8366	2.7523	3.3745	5.1419	63.7936	0.3115	1.2749	0.1634	100.0411
6	5.8025	1.1934	15.0892	3.0766	2.4387	4.5685	65.6455	0.2522	1.1404	0.1521	99.3591
7	5.8264	1.9395	15.8850	2.6502	3.7377	5.4216	63.0747	0.3064	1.2357	0.1594	100.2366
8	5.7777	1.4254	15.5888	2.9039	2.9029	4.9075	64.9753	0.2838	1.2175	0.1614	100.1442
9	5.2660	1.8177	14.9859	2.6122	3.4774	4.8589	61.6408	0.3014	1.2268	0.1446	96.3317
10	5.7804	1.4824	15.4648	2.8511	3.1760	4.9577	64.5638	0.3532	1.3212	0.1607	100.1113
11	5.3143	1.5700	15.4720	2.7369	3.3694	4.9695	65.0099	0.3323	1.2674	0.1484	100.1901
12	5.3896	1.3191	15.4389	2.9538	2.7173	4.6032	66.2312	0.2634	1.1682	0.1402	100.2249
13	5.7763	1.4891	15.6725	3.0427	3.0650	4.6166	64.7932	0.3255	1.2636	0.1460	100.1905

# Volcán Hudson (H1)

## Lago Lynch

H1 (V)-LL

	Na2O	MgO	Al2O3	K2O	CaO	FeO	SiO2	P2O5	TiO2	MnO	Total
1	5.9518	1.4574	15.2234	2.7946	2.9599	4.9871	64.7976	0.2950	1.2375	0.1461	99.8504
2	5.9748	1.4083	15.4245	2.7106	3.0141	4.5296	64.5864	0.3012	1.2276	0.1599	99.3370
3	5.7416	1.5276	15.4225	2.6560	3.0554	5.6709	64.7051	0.3585	1.3779	0.1584	100.6739
4	5.8743	1.2386	15.7087	2.7354	2.9142	4.4083	64.9063	0.2802	1.2476	0.1454	99.4590
5	5.5405	1.6191	15.7984	2.7927	3.4607	5.3390	64.4774	0.2871	1.2404	0.1457	100.7010
6	5.9780	1.5668	15.5533	2.8292	3.1224	4.8704	64.6337	0.3004	1.2638	0.1590	100.2770
7	5.4795	1.5072	15.4831	2.7955	3.0242	4.9167	65.4296	0.2844	1.2260	0.1497	100.2959
8	5.9907	1.6424	15.4033	2.6398	3.4580	5.1116	63.2363	0.3204	1.3161	0.1536	99.2722
9	5.4076	2.2585	15.7027	2.4765	4.2384	5.6164	62.6645	0.3012	1.2757	0.1505	100.0920
10	5.5458	2.1501	16.0561	2.4509	4.6117	5.7175	62.0009	0.2662	1.0787	0.1302	100.0081
11	5.6102	1.6795	15.5059	2.6694	3.3673	5.1672	63.0239	0.3227	1.3104	0.1522	98.8087
12	6.0601	1.8354	15.3356	2.6263	3.6065	5.4168	62.9899	0.3161	1.2624	0.1670	99.6161

# Volcán Reclús (R1)

## Rio Grande

R1 (V)-RG											
	Na2O	MgO	Al2O3	K2O	CaO	FeO	SiO2	P2O5	TiO2	MnO	Total
1	4.1313	0.2276	12.1811	2.4871	1.4428	1.2056	75.9345	0.0306	0.1079	0.0459	97.7944
2	3.7535	0.2001	12.2253	2.4189	1.5525	1.2505	73.9568	0.0326	0.1074	0.049	95.5466
3	3.9379	0.1861	12.1903	2.71	1.5425	1.1731	75.5825	0.0231	0.1124	0.0441	97.502
4	3.9062	0.2262	12.2552	2.6699	1.5159	1.2156	75.4141	0.0182	0.1095	0.0452	97.376
5	3.9761	0.217	11.9806	2.4401	1.5581	1.307	75.8736	0.0294	0.1081	0.0426	97.5326
6	4.0481	0.2044	12.5129	2.7696	1.4886	1.1866	76.9507	0.0167	0.1011	0.0455	99.3242
7	3.7621	0.2201	12.3512	2.5991	1.4403	1.1787	75.1874	0.026	0.1041	0.0436	96.9126
8	3.6051	0.1795	12.1496	2.5581	1.4225	1.277	74.856	0.0156	0.101	0.0397	96.2041
9	3.7779	0.204	12.371	2.5463	1.5431	1.0628	74.8408	0.0323	0.1002	0.0473	96.5257
10	3.8971	0.1941	12.4244	2.4907	1.4808	1.319	75.259	0.0254	0.1043	0.0462	97.241
11	3.7001	0.205	12.0026	2.7112	1.3862	1.146	75.014	0.0261	0.1079	0.0472	96.3463
12	3.9051	0.2055	12.4879	2.3263	1.5582	1.2161	76.2445	0.0258	0.1113	0.0432	98.1239
13	3.78	0.2107	12.3097	2.5554	1.5395	1.2298	75.9727	0.0228	0.1034	0.0381	97.7621
14	3.9757	0.1742	12.1457	2.4408	1.5132	1.045	75.9594	0.0324	0.1114	0.0466	97.4444

## Punta Yartou

R1 (V)-PY											
	Na2O	MgO	Al2O3	K2O	CaO	FeO	SiO2	P2O5	TiO2	MnO	Total
1	4.0011	0.2061	12.753	2.7191	1.4626	1.2651	75.5975	0.0306	0.1073	0.0501	98.1925
2	3.8844	0.2041	12.5978	2.6188	1.3763	1.221	75.1205	0.0259	0.1068	0.0423	97.1979
3	3.8548	0.2174	12.1426	2.5363	1.4219	1.216	75.2317	0.0351	0.1067	0.0303	96.7928
4	3.8254	0.2143	12.3518	2.4521	1.4936	1.2706	74.8511	0.0226	0.1082	0.0359	96.6256
5	3.8465	0.2238	11.8787	2.5736	1.5041	1.3153	75.1683	0.0231	0.1049	0.0388	96.6771
6	3.8249	0.2008	12.28	2.3516	1.6872	1.1359	74.9278	0.0339	0.1179	0.0377	96.5977
7	3.7276	0.2351	12.0662	2.5587	1.5312	1.2907	75.0238	0.0449	0.1023	0.0405	96.621
8	3.9634	0.2242	12.3568	2.5324	1.514	1.1668	74.76	0.0289	0.1152	0.0379	96.6996
9	3.7705	0.2556	11.9771	2.4673	1.4866	1.0832	74.3014	0.0338	0.111	0.0442	95.5307
10	3.7962	0.2087	11.9416	2.6082	1.4263	1.2359	74.6075	0.0222	0.1182	0.0436	96.0084

## Volcán Reclús (R1)

### Lago Lynch

---

R1 (V)-LL

	Na2O	MgO	Al2O3	K2O	CaO	FeO	SiO2	P2O5	TiO2	MnO	Total
1	3.7862	0.2347	12.3805	2.5184	1.4675	1.164	75.1186	0.0292	0.1065	0.0407	96.8463
2	3.7887	0.244	12.5982	2.5856	1.5613	1.2239	76.1761	0.0255	0.11	0.0359	98.3492
3	4.0572	0.2148	12.1382	2.5273	1.4352	1.1732	75.4988	0.028	0.1016	0.0366	97.2109
4	3.706	0.2107	12.4759	2.5827	1.499	1.1718	75.7097	0.0384	0.1024	0.0454	97.542
5	3.797	0.2073	12.3464	2.651	1.5704	1.2665	74.6115	0.0327	0.1038	0.0323	96.6189
6	3.9677	0.2078	12.3035	2.5397	1.5579	1.176	74.678	0.0333	0.1084	0.0439	96.6162
7	3.5502	0.2072	12.3151	2.56	1.4516	1.2717	74.6529	0.0311	0.111	0.0406	96.1914
8	3.8937	0.1965	12.2277	2.5329	1.486	1.1815	75.6671	0.0402	0.1063	0.0385	97.3704
9	3.8233	0.1892	12.1281	2.5684	1.451	1.1316	75.4763	0.022	0.1026	0.0452	96.9377
10	3.857	0.2059	11.9979	2.5818	1.4473	1.26	75.6078	0.0369	0.1101	0.0368	97.1415

---

COPY OF FOLD-OUT FIGURES (in pocket at back of thesis)

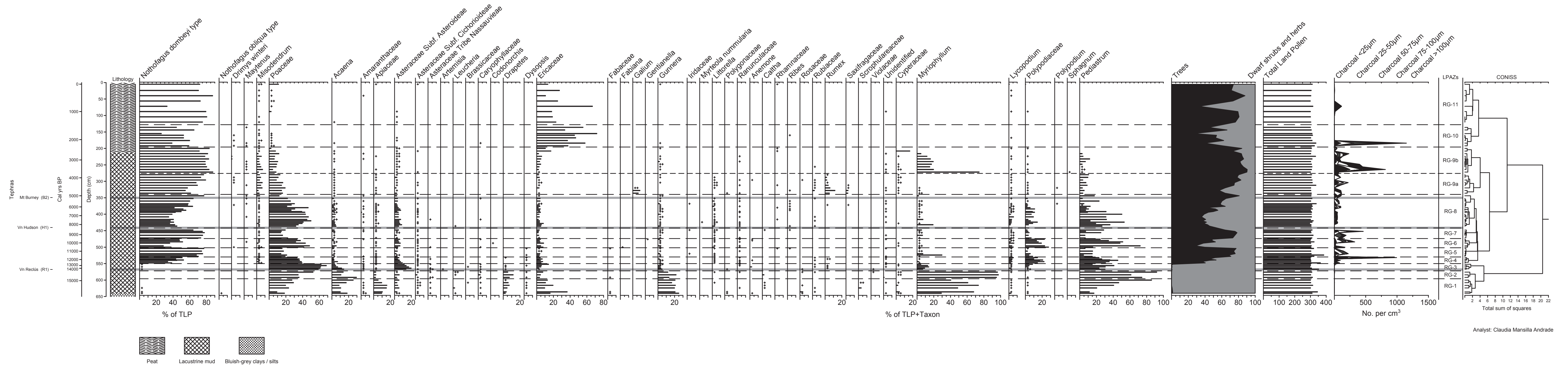


Figure 3.14 Rio Grande: percentage pollen diagram and charcoal concentrations.

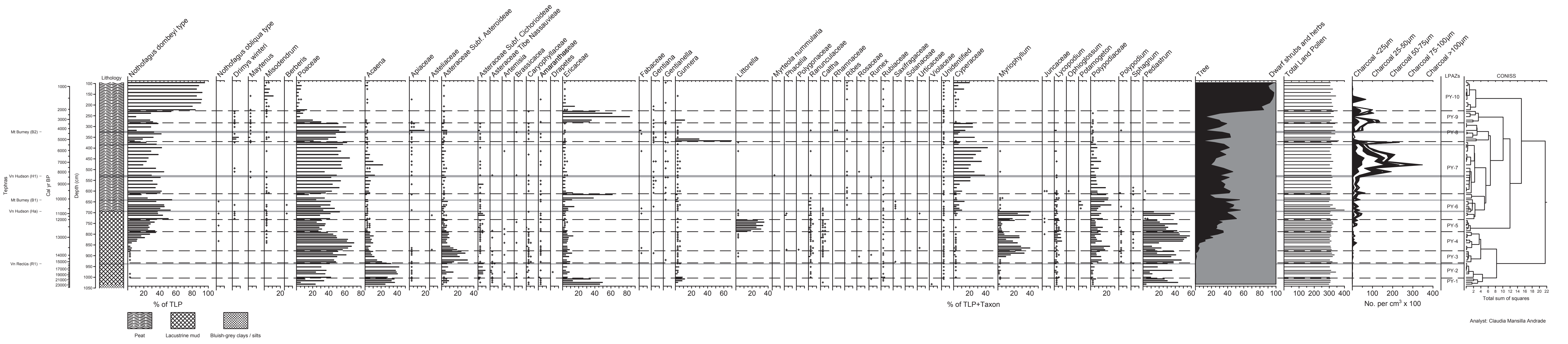


Figure 3.16 Punta Yartou: percentage pollen diagram and charcoal concentrations.

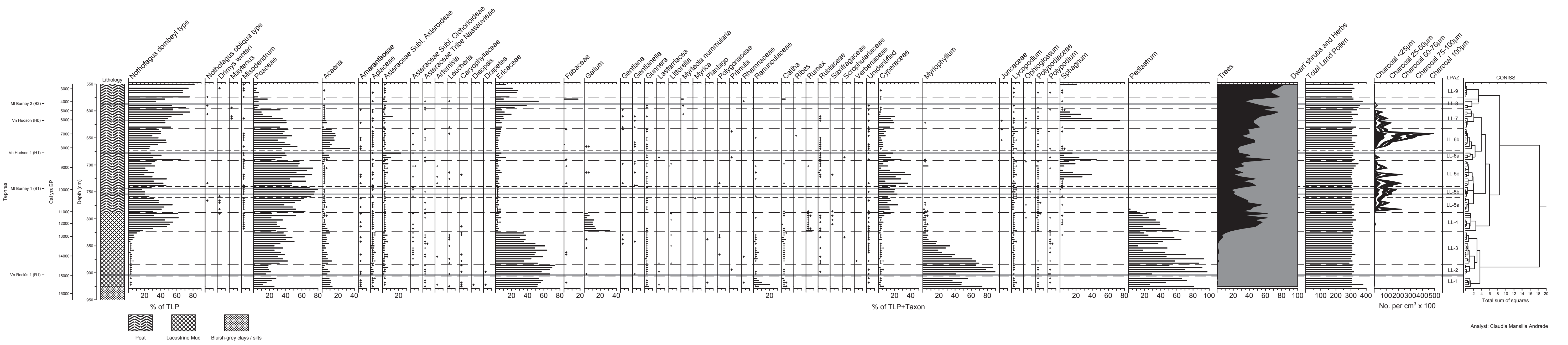


Figure 3.18 Lago Lynch: percentage pollen diagram and charcoal concentrations.

COPY OF FOLD-OUT FIGURES (in pocket at back of thesis)

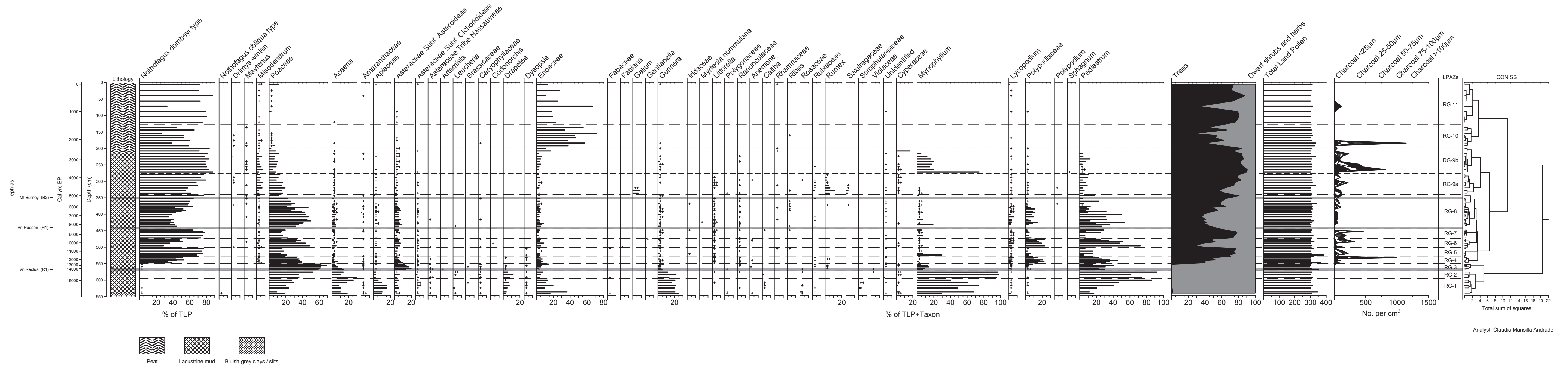


Figure 3.14 Rio Grande: percentage pollen diagram and charcoal concentrations.

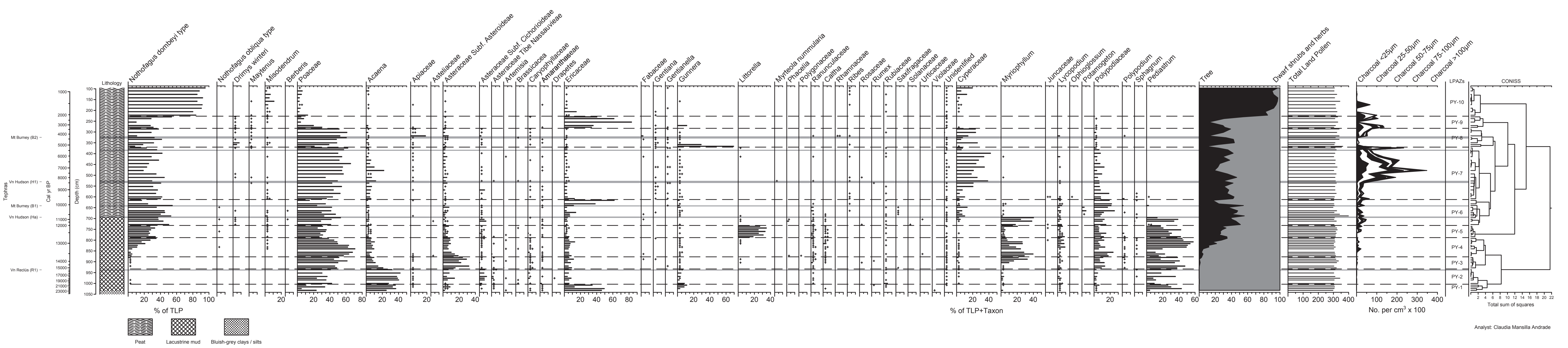


Figure 3.16 Punta Yartou: percentage pollen diagram and charcoal concentrations.

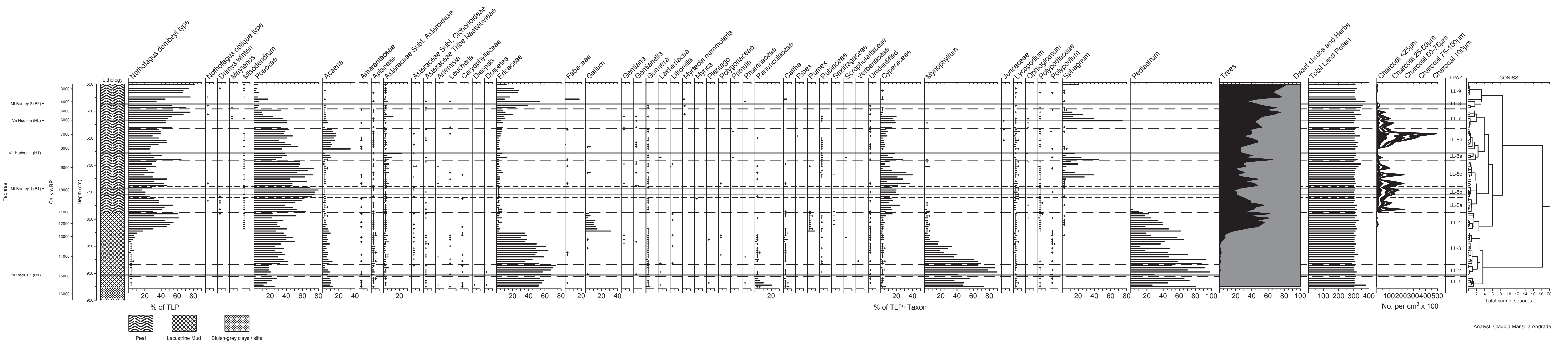


Figure 3.18 Lago Lynch: percentage pollen diagram and charcoal concentrations.